

**HOST-GUEST COMPLEXATION BASED ON
CUCURBITURILS**

by

LINA YUAN

A thesis submitted to the Department of Chemistry
in conformity with the requirements for
the degree of Doctor of Philosophy

Queen's University

Kingston, Ontario, Canada

January 2008

Copyright © Lina Yuan, 2008

DEDICATION

This thesis is dedicated to Ruibing Wang and the love we used to have. Thanks to him for always being here for me and that he truly cares about me no matter what. With all the gratitude I can have, I wish him all the best in the future.

ABSTRACT

This thesis deals with the effects of host-guest complexation, based on cucurbit[*n*]uril (CB[*n*], *n* = 6, 7 and 8) host molecule, on the chemical, electrochemical and spectroscopic properties of the included guests. Both CB[6] and CB[7] form 1:1 complexes with $[\text{CH}_3\text{bpy}(\text{CH}_2)_6\text{bpyCH}_3]^{4+}$, encapsulating the central hexamethylene chain. With its relatively larger cavity, a second CB[7] host will include one of the viologen units, forcing, through steric and electronic repulsions, the first CB[7] to abandon the inclusion of the central chain and move to the other viologen unit, thus forming a [3]pseudorotaxane. The inclusion of the two enantiomers of protonated N-benzyl-1-(1-naphthyl)ethylamine in the achiral CB[7] results in a five-fold increase in the molar optical rotation of $\{\text{BNEAH}\cdot\text{CB}[7]\}^+$ and significant changes in the longer wavelength band in the circular dichroism spectra, attributed to a restricted rotation of the naphthyl group about the chiral center upon inclusion of the benzyl portion of the guest in the CB[7] cavity.

The effects of host-guest complexation of the (trimethylammonio)-methylferrocene(+/2+) couple ($\text{FcTMA}^{+/2+}$) by CB[7] on the kinetics of its electron self-exchange and electron transfer reactions were investigated. The slow exchange of the ferrocene guest, allows for the simultaneous monitoring of the ^1H NMR line-broadening for both the FcTMA^+ and $\{\text{FcTMA}\cdot\text{CB}[7]\}^+$ species in the presence of the paramagnetic FcTMA^{2+} ; The electron self-exchange rate constant increases moderately upon inclusion

of both reduced and oxidized species, while the rate constants for the oxidation of ferrocenes by the bis(2,6-pyridinedicarboxylato)cobaltate(III) ion (which does not bind to CB[7]), were significantly reduced a result of reduced thermodynamic driving forces and steric hindrance to close approach of the oxidant to the encapsulated ferrocenes. This work was extended to investigations of the inclusion of bis(ferrocene) guests, demonstrating that a sufficiently long linker is required to accommodate a CB[7] host on each ferrocene unit. The formation of stable host-guest complexes of the bent titanocene, $\text{TiCp}_2(\text{H}_2\text{O})_2^{2+}$, with both CB[7] and CB[8] were characterized in aqueous solution. The CB[8] formed a more stable complex than CB[7], contrary to the order observed with ferrocene guests, attributable to the larger radius of the bent titanocene guest.

ACKNOWLEDGEMENT

This thesis would not have been possible without the kindest support, encouragement, consideration and the remarkable patience of my supervisor, Prof. Donal H. Macartney. As my supervisor and mentor, he has taught me more than I can give him credit for here, as he has shown me, by his example, what a good scientist and person should be. He is the best supervisor one can ever have and imagine. I cannot thank him enough. I just simply wish him and his family all the best in the future.

Professors Suning Wang and Philip Jessop deserve special thanks as my thesis committee members and advisors for their advice and guidance for my research projects. I am indebted to Dr. François Sauriol for her help on the topic of NMR spectroscopy, and to Dr. Bernd Keller and Jessie Sui for their time and discussion of the MS characterization. I am also grateful to Prof. Natalie Cann and Shihao Wang for their help with the computational calculations of the energy-minimized structures.

I also would like to express my appreciation to all of those with whom I have had the pleasure to work with in the past four years. First, my special and deepest gratitude goes to Ruibing Wang for his love, support and sincere care. I wouldn't be who I am without him. I wish he can always have what he wants and live a happy and healthy life. Second, I would like to thank Ian Wyman, the nicest person I have ever met, for his unbelievable kindness and knowledgeable advices. I also thank Saroja Hettiarachchi for her fellowship in the lab.

Nobody has been more important to me in the world than my family. There is no word to express my gratitude to my parents for their endless support, love and the faith they always have in me. They are always there for me and genuinely love me no matter what. I wish them a happy and healthy life.

Last, but not the least, the generous support from Queen's University and NSERC Canada is greatly appreciated.

STATEMENT OF ORIGINALITY

All work presented herein was performed by the author under the supervision of Professor Donal H. Macartney at Queen's University, except for the kinetic measurements on the (trimethylammonio)methylferrocene cation, in the absence and in the presence of cucurbit[7]uril (CB[7]) host molecules, and the cyclic voltammetry experiments of titanocene with and without CB[7] host, which were carried out by the author, Dr. Ruibing Wang and Dr. Donal H. Macartney, and the energy-minimized structures calculations which were carried out with the assistance of Shihao Wang.

TABLE OF CONTENTS

ABSTRACT	iii
ACKNOWLEDGEMENT	v
STATEMENT OF ORIGINALITY	vii
TABLE OF CONTENTS	viii
LIST OF TABLES	xv
LIST OF FIGURES	xvi
LIST OF ABBREVIATIONS.....	xxii
Chapter 1 INTRODUCTION	1
1.1 Supramolecular Chemistry.....	1
1.1.1 Definition and Development.....	1
1.1.2 Nature of Supramolecular Interactions.....	2
1.1.2.1 Electrostatic Interactions.....	2
1.1.2.2 Hydrogen Bonding.....	3
1.1.2.3 π - π Stacking Interactions.....	4
1.1.2.4 van der Waals Forces.....	5
1.1.2.5 Hydrophobic Interactions.....	6
1.1.3 Concepts in Supramolecular Chemistry.....	7
1.1.3.1 Molecular Self-assembly.....	7
1.1.3.2 Molecular Recognition.....	8

1.1.3.3	Host-guest Chemistry.....	8
1.1.3.4	Mechanically-interlocked Molecular Architectures.....	9
1.1.3.5	Dynamic Covalent Chemistry.....	9
1.1.4	Characterizing Supramolecular Systems.....	10
1.1.4.1	Structural Information.....	10
1.1.4.2	Kinetics of Complexation.....	12
1.1.4.3	Thermodynamic Information.....	14
1.1.5	Summary.....	14
1.2.	Inclusion Complexes and Host-Guest Chemistry.....	15
1.2.1	Introduction.....	15
1.2.2	Design Principles and Complementarity and Preorganization.....	15
1.2.3	Dynamic Character of Inclusion Complexes.....	16
1.2.4	Classification of Supramolecular Host-Guest Compounds.....	18
1.2.5	Macrocyclic Hosts and Their Application.....	20
1.2.5.1	Crown Ethers and Cryptands.....	20
1.2.5.2	Calixarenes.....	22
1.2.5.3	Porphyryns.....	24
1.2.5.4	Cyclodextrins.....	25
1.2.5.5	Cucurbiturils.....	27
1.3	Cucurbiturils.....	28
1.3.1	Synthesis of Cucurbiturils.....	28

1.3.2 Structures and Physical Properties.....	29
1.3.3 Host-Guest Chemistry of Cucurbit[6]uril.....	31
1.3.3.1 Comparison of the Thermodynamics of Complexation.....	31
1.3.3.2 Host-Guest Complexation of CB[6].....	32
1.3.3.3 Binding Selectivity of CB[6].....	35
1.3.3.4 Thermodynamics and Kinetics of the Complexation of CB[6].....	36
1.3.4 Host-Guest Chemistry of Cucurbit[n]uril Homologues.....	38
1.3.4.1 Host-Guest Complexation of Cucurbit[7]uril.....	40
1.3.4.2 Host-Guest Complexation of CB[5], CB[8] and CB[10].....	41
1.3.5 Applications of Cucurbituril Family.....	44
1.3.5.1 Reaction Mediators.....	44
1.3.5.2 Molecular Machines and Switches.....	46
1.3.5.3 Drug Delivery and Gene Transfection.....	50
1.3.5.4 Waste-Stream Remediation.....	51
1.3.6 Cucurbit[n]uril Derivatives.....	52
1.3.6.1 Synthesis of Cucurbit[n]uril Derivatives.....	52
1.3.6.2 Applications of Cucurbit[n]uril Derivatives.....	54
1.3.7 Summary and Perspectives.....	55
1.4 Research Aims.....	56
References.....	58

Chapter 2	HOST-GUEST COMPLEXATION BETWEEN CUCURBITU[6]RIL AND CUCURBITU[7]RIL WITH A TETRACATIONIC BIS(VIOLOGEN) GUEST.....	69
2.1	Introduction.....	70
2.2	Experimental.....	73
2.2.1	Materials Preparation.....	73
2.2.2	Methods and Instrumentation.....	75
2.2.3	Determination of the Host-Guest Stability Constants.....	76
2.3	Results and Discussion.....	79
2.3.1	Binding Between CB[6] and $[\text{CH}_3\text{bpy}(\text{CH}_2)_6\text{bpyCH}_3]^{4+}$	79
2.3.2	Binding Between CB[7] and $[\text{CH}_3\text{bpy}(\text{CH}_2)_6\text{bpyCH}_3]^{4+}$	81
2.4	Summary.....	86
	References.....	87
Chapter 3	HOST-GUEST COMPLEXATION BETWEEN THE ACHIRAL CUCURBITU[7]RIL HOST AND CHIRAL GUEST MOLECULES.....	90
3.1	Introduction.....	90
3.2	Experimental.....	92
3.2.1	Materials Preparation.....	92
3.2.2	Methods and Instruments.....	94
3.2.3	Determination of the Binding Stoichiometry and Stability Constant.....	95
3.2.4	Energy-Minimization Calculations.....	100

3.3 Results and Discussion.....	100
3.3.1 Host-Guest Complexes.....	100
3.3.2 Effect of Inclusion on the Chiroptic Behaviour.....	102
3.4 Summary.....	107
References.....	109

Chapter 4 HOST-GUEST COMPLEXATION OF CUCURBIT[7]URIL WITH (TRIMETHYLAMMONIO)METHYLFERROCENE IN AQUEOUS SOLUTION.....113

4.1 Introduction.....	114
4.2 Experimental.....	117
4.2.1 Materials Preparation.....	117
4.2.1.1 (Trimethylammonio)methylferrocene Iodide ([FcTMA]I).....	118
4.2.1.2 (Trimethylammonio)methylferrocene tetrafluoroborate ([FcTMA]BF ₄).....	118
4.2.1.3 (Trimethylammonio)methylferrocenium tetrafluoroborate {[FcTMA](BF ₄) ₂ }	119
4.2.1.4 Ammonium bis(2,6-pyridinedicarboxylato)cobaltate(III).....	119
4.2.2 Methods and Instruments.....	120
4.2.2.1 Kinetic Measurements.....	120
4.2.2.2 ¹ H NMR Line Broadening Experiment.....	120
4.2.2.3 Cyclic Voltammetry.....	121
4.2.2.4 UV-Visible Spectroscopy.....	121

4.3 Results and Discussion.....	121
4.3.1 Complexation Between CB[7] and FcTMA ⁺	121
4.3.2 Electron Self-Exchange Kinetics.....	124
4.3.2.1 Determination of the Self-Exchange Rate Constants.....	124
4.3.2.2 Determinations of k_{12} and k_{21}	129
4.3.2.3 Comparison with Other Hosts.....	133
4.3.2.4 Increase in the Electron Self-Exchange Rate Constant upon Guest Inclusion	134
4.3.3 Electron Transfer Kinetics.....	136
4.4 Summary.....	140
References.....	142

Chaper 5 **HOST-GUEST COMPLEXATION OF CURCUBITURILS WITH
BIS(FERROCENE) COMPLEXES AND DIAQUATITANOCENE**.....147

5.1 Introduction.....	149
5.2 Experimental.....	152
5.2.1 Materials Preparation.....	152
5.2.1.1 Synthesis of compound [1]Br.....	153
5.2.1.2 Synthesis of compound [2]I ₂	154
5.2.1.3 Assembly of Host-Guest Complexes in Solution.....	154
5.2.2 Methods and Characterization.....	155

5.3 Results and Discussion.....	157
5.3.1 Complexation of Bis(ferrocenes) with CB[7].....	157
5.3.2 Complexation of Diaquatitanocene with CB[7].....	163
5.3.3 Complexation of Titanocene with CB[8].....	169
5.3.4 Comparison of the Effects of Complexation with CB[7] and CB[8].....	172
5.4 Summary.....	173
References.....	175
Chapter 6 CONCLUSIONS AND SUGGESTIONS FOR FUTURE WORK.....	177
6.1 Conclusions.....	177
6.2 Suggestions for Future Work.....	180
References.....	183

LIST OF TABLES

Table 1.1	Binding constants of a series of amines with CB[6].	34
Table 3.1	Solution composition (mL) for the UV-visible Job's plot measurements.	97
Table 3.2	Optical rotation changes upon the formation of 1:1 inclusion complexes between (<i>R</i>)- and (<i>S</i>)- <i>N</i> -benzyl-1-(1-naphthyl)ethylamine hydrochloride and CB[7] in aqueous solution.	103
Table 3.3	Structure information obtained from HF/3-21G** Gaussian calculation for (<i>R</i>)-/(<i>S</i>)- (BNEAH ⁺) before and after complexation with CB[7].	106
Table 4.1	Rate constants (25 °C) for the self-exchange reactions of the FcTMA ^{+ /2+} couple (k_{11} , k_{12} , k_{21} , and k_{22}) and the electron-transfer reaction of FcTMA ⁺ with Co(dipic) ₂ ⁻ (k_{Co}^0 and k_{Co}^{host}) in the presence of CB[7], β-CD, or p-SO ₃ CX[6] in aqueous solution.	134
Table 4.2	Rate constants for the oxidation of FcTMA ⁺ or Fc(CH ₂ OH) (0.20 mM) by [Co(dipic) ₂] ⁻ (2 mM) in the absence and presence of CB[7] at 25 °C and I = 0.10 M (NaCl).	138

LIST OF FIGURES

Figure 1.1	A schematic representation of the relationships between molecular and supramolecular chemistry.....	2
Figure 1.2	Main types of hydrogen bond geometry.....	4
Figure 1.3	Two types of π - π stacking interactions.....	5
Figure 1.4	Schematic illustrations of the enthalpic hydrophobic effect and the entropic hydrophobic effect.....	7
Figure 1.5	Examples of mechanically-interlocked molecular architectures.....	9
Figure 1.6	An example of a reaction sequence demonstrating dynamic covalent chemistry.....	10
Figure 1.7	A sample of a UV-Vis Job's plot curve showing the formation of a 1:1 host-guest complex.....	11
Figure 1.8	NMR titration plot for fast exchange equilibration on the NMR time scale and schematic NMR spectra for fast and slow equilibria.....	13
Figure 1.9	Schematic illustration of the difference between a cavitate and clathrate.....	19
Figure 1.10	Three examples of the crown ether family of host molecules.....	21
Figure 1.11	The structures of the [2,2,2] and [2,2,1]cryptands.....	22
Figure 1.12	Typical structure and multiple potential binding sites of calixarenes.....	23
Figure 1.13	Four conformations of calixarenes.....	24
Figure 1.14	The structure of porphine, showing the carbon substitution positions.....	25
Figure 1.15	Structures of α -, β - and γ -cyclodextrin.....	26
Figure 1.16	The methods for the synthesis of cucurbit[n]urils.....	28

Figure 1.17 Structural parameters of CB[n] homologues.....	29
Figure 1.18 Comparison of electrostatic potential surfaces of CB[7] and β -CD.....	31
Figure 1.19 Comprehensive mechanistic scheme for molecular recognition by CB[6] ...	33
Figure 1.20 Proposed binding mechanism of CB[6] with neutral and ammonium guests.	38
Figure 1.21 The binding preference of CB homologues.....	39
Figure 1.22 Charge-transfer (CT) complexes formed in CB[8] and two comparative crystal structures	43
Figure 1.23 CB[6] functions as a “chamber” to catalyze the 1,3-dipolar addition reaction between azide and alkyene.....	45
Figure 1.24 One example of a molecular switch based on CB[6]	48
Figure 1.25 Formation of a binary complex, based on CB[8], acting as a detector to sense catechol and dopamine by forming ternary complexes.	49
Figure 1.26 CB[6] can be delivered to DNA through non-covalent self-assembly.....	51
Figure 1.27 Three ways to introduce functional groups at the periphery of cucubiturils.	53
Figure 2.1 Schematic illustration of different binding modes of CB[6] and CB[7] with the tetracationic bis(viologen) guest $[\text{CH}_3\text{bpy}(\text{CH}_2)_6\text{bpyCH}_3]^{4+}$	72
Figure 2.2 ^1H NMR spectrum of $[\text{CH}_3\text{bpy}(\text{CH}_2)_6\text{bpyCH}_3]_4\text{I}_4$ in $\text{DMSO-}d_6$ obtained at 400 MHz at 25°C	74
Figure 2.3 ^{13}C NMR spectrum of $[\text{CH}_3\text{bpy}(\text{CH}_2)_6\text{bpyCH}_3]_4\text{I}_4$ in $\text{DMSO-}d_6$ obtained at 100 MHz at 25°C	75
Figure 2.4 ^1H NMR spectra of $[\text{CH}_3\text{bpy}(\text{CH}_2)_6\text{bpyCH}_3]^{4+}$ (1,0 mM) in the absence and in the presence of 0.6, 1.1 and 1.9 equivalents of CB[6] at 25 °C in 0.10 M NaCl/D ₂ O after 24 h incubation in a 50 °C water bath	80

Figure 2.5	^1H NMR spectra of $[\text{CH}_3\text{bpy}(\text{CH}_2)_6\text{bpyCH}_3]^{4+}$ (1.0 mM) in the absence and in the presence of 0.3, 0.6, 0.9, 1.1, 1.4, 1.6, 1.8, 2.1 and 2.5 equivalents of CB[7] at 25 °C in 0.10 M NaCl/D ₂ O.....	82
Figure 2.6	Chemical shift change of H3/H3' protons of the $[\text{CH}_3\text{bpy}(\text{CH}_2)_6\text{bpyCH}_3]^{4+}$ guest upon addition of CB[7]. Inset: a plot of $[\text{CB}[7]]/\Delta\delta_{\text{obs}}$ against $[\text{L}]_t + [\text{CB}[7]]_t + ([\text{L}]_t\Delta\delta_{\text{obs}}/\Delta\delta_{\text{lim}})$ from which the value of $K_{2\text{CB}[7]}$ was determined.....	85
Figure 3.1	Formation of a host-guest complex between cucurbit[7]uril and (<i>R</i>)- <i>N</i> -benzyl-1-(1-naphthyl)ethylamine.....	92
Figure 3.2	The structure of the guests (<i>S</i>)- and (<i>R</i>)-BNEAH ⁺	93
Figure 3.3	UV-visible spectra for the Job's plot titration curve with CB[7] and (<i>R</i>)-BNEAH ⁺	96
Figure 3.4	Job's plot curve of UV absorbance change (at 305 nm) of (<i>R</i>)-BNEAH ⁺ upon the addition of CB[7], indicating the formation of 1:1 host-guest complex.....	96
Figure 3.5	Plot of the chemical shift of the guest phenyl H2' proton as a function of the concentration of CB[7] (up to 2.6 mM), with (<i>R</i>)-BNEAH ⁺ at 1mM.....	98
Figure 3.6	^1H NMR spectrum of CB[7] (0.516 mM) with (<i>R</i>)-BNEAH ⁺ (3.36 mM) and TSP (1.68 mM) in D ₂ O at 25 °C, after 30 minutes incubation.....	98
Figure 3.7	^1H NMR spectra of the (<i>R</i>)-BNEAH ⁺ in the absence and the presence of CB[7] in D ₂ O.....	101
Figure 3.8	Molar rotation versus ratio of CB[7] to [(<i>R</i>)- or (<i>S</i>)-BNEAH ⁺] in aqueous solution.....	104

Figure 3.9	The energy-minimized gas-phase structures for (<i>R</i>)- and (<i>S</i>)-BNEAH ⁺ guests and the 1:1 host–guest complexes with CB[7], suggesting the considerable change in the conformations of the substituents about the chiral center.....	105
Figure 3.10	Circular dichroism spectra for (<i>R</i>)-BNEAH ⁺ , {(<i>R</i>)-BNEAH•CB[7]} ⁺ , (<i>S</i>)-BNEAH ⁺ and (<i>S</i>)-BNEAH•CB[7]} ⁺	107
Figure 4.1	The structure of the (trimethylammonio)methylferrocene (FcTMA ⁺²⁺) couple	117
Figure 4.2	¹ H NMR spectra of FcTMA ⁺ (1.0 mM) in the absence and presence of cucurbit[7]uril in D ₂ O at 25 °C	123
Figure 4.3	¹ H NMR line broadening spectra of FcTMA ⁺ (1.0 mM) in the presence of 0.21 mM CB[7] with increasing concentrations of total FcTMA ²⁺	125
Figure 4.4	Linear dependences of W _{DP} - W _D on [FcTMA ²⁺] _{total} for the Cp ring proton resonance of FcTMA ⁺ (4.24 ppm) or {FcTMA•CB[7]} ⁺ (3.52 ppm) at various concentrations of CB[7] at 25 °C.....	126
Figure 4.5	The possible pathways of electron self-exchange reactions for the FcTMA ⁺²⁺ couple in the absence and presence of CB[7]	127
Figure 4.6	Plots of log k _{ex} against CB[7] concentration derived from the observed line broadening in the resonances for the FcTMA ⁺ and {FcTMA•CB[7]} ⁺ species.....	129
Figure 4.7	Cyclic voltammogram of FcTMA ^{2+/+} (1.0 mM) in the absence and presence of CB[7] host molecule (1.2 equivalent) without added electrolyte at 25 °C ..	130
Figure 4.8	Plots of the electron transfer rate constant, k _{et} , against the [CB[7]]/[ferrocene] ratio for the oxidation of FcTMA ⁺ , Fc(CH ₂ OH), and FcMPE ⁺ by Co(dipic) ₂ ⁻ in aqueous solution (I = 0.10 M (NaCl)) at 25.0 °C	139

Figure 5.1	Structure of the bent metallocene, titanocene dichloride	150
Figure 5.2	The structure of two cationic bis(ferrocene) complexes 1 and 2	153
Figure 5.3	¹ H NMR spectra (400 MHz) of compound 1 (1.0 mM) in the absence and presence of a different amount of CB[7] in D ₂ O at 25 °C	158
Figure 5.4	¹ H NMR spectra (400 MHz) of the solution containing compound 1 (1.0 mM), FcTMA ⁺ (3.0 mM) and CB[7] (1.0 mM) in D ₂ O at 25 °C, which was used to determined the inclusion constant of compound 1 into CB[7]	159
Figure 5.5	¹ H NMR spectra (400 MHz) of compound 2 (1mM) in the absence and presence of different amount of CB[7] in D ₂ O at 25 °C	161
Figure 5.6	Cyclic voltammograms of compound 1 (1.0 mM) in the absence and presence of 0.8 and 1.6 mM CB[7] in 0.10 M NaCl aqueous solution at 25 °C	162
Figure 5.7	Cyclic voltammograms of compound 2 (1.0 mM) in the absence and presence of 0.8 and 1.6 mM CB[7] in 0.1.0 M NaCl aqueous solution at 25 °C	163
Figure 5.8	¹ H NMR spectra (400 MHz) of TiCp ₂ (D ₂ O) ₂ ²⁺ (1.0 mM) in the absence and presence of different amount of CB[7] in D ₂ O at 25 °C	165
Figure 5.9	Plot of Δδ _{obs} against the host/guest ratio for the inclusion of CB[7] by the TiCp ₂ (D ₂ O) ₂ ²⁺ complex in D ₂ O	166
Figure 5.10	¹ H NMR spectra (400 MHz) of the solution containing TiCp ₂ (D ₂ O) ₂ ²⁺ , the competitor and CB[7] in a ratio of 3.2:1.4:1 in D ₂ O at 25 °C, which was used to determine the inclusion constant of diaquatitanocene with CB[7], by a competition method	167

Figure 5.11 Cyclic voltammograms of $\text{TiCp}_2(\text{H}_2\text{O})_2^{2+}$ (1.0 mM) in the absence and presence of 1.2 mM CB[7] in aqueous solution (containing 0.10 M NaNO_3) at room temperature	168
Figure 5.12 ^1H NMR spectra (400 MHz) of $\text{TiCp}_2(\text{D}_2\text{O})_2^{2+}$ (1mM) in the absence and presence of different amount of CB[8] in D_2O at 25 °C.....	170
Figure 5.13 ^1H NMR spectra (400 MHz) of the solution containing $\text{TiCp}_2(\text{D}_2\text{O})_2^{2+}$, the protonated 1-aminoadamantane competitor and CB[8] in a ratio of 1:1:1 in D_2O at 25 °C, used to determined the inclusion constant of $\text{TiCp}_2(\text{D}_2\text{O})_2^{2+}$ with CB[8] by the NMR competition method	171
Figure 5.14 The energy-minimized gas-phase structure of the $\{\text{TiCp}_2(\text{H}_2\text{O})_2\cdot\text{CB}[7]\}^{2+}$ and $\{\text{TiCp}_2(\text{H}_2\text{O})_2\cdot\text{CB}[8]\}^{2+}$ host-guest complex (HF/3-21G** basis set).....	172
Figure 6.1 Structures of the $\text{CH}_3\text{bpe}(\text{CH}_2)_6\text{bpeCH}_3^{4+}$ tetracation and the proposed $\{\text{CH}_3\text{bpe}(\text{CH}_2)_6\text{bpeCH}_3\cdot 3\text{CB}[7]\}^{4+}$ complex	181
Figure 6.2 Two examples of chiral substituted titanocene dichloride complexes.....	182

LIST OF ABBREVIATIONS

α	optical rotation
β_{mn}	overall stability constant
Φ	molar optical rotation
δ	chemical shift
δ_{obs}	observed chemical shift
δ_{lim}	chemical shift at equilibrium
ϵ	molar absorptivity coefficient
κ_{el}	electronic transmission coefficient
ν_n	nuclear frequency factor
k_B	Boltzmann constant
ΔA	absorbance change
\AA	Angstrom
A	absorbance or acceptor
BNEAH ⁺	protonated N-benzyl-1-(1-naphthyl)ethylamine
bpy	4,4'-bipyridine
CB[n]	cucurbit[n]uril
CD	cyclodextrin or circular dichroism
Cp ⁻	cyclopentadienyl anion
CT	charge transfer
CV	cyclic voltammetry
d	doublet

dd	doublet of doublets
D	donor
dipic ²⁻	2,6-pyridinedicarboxylate
DMF	dimethylformamide
dmol	decimole
DMSO	dimethyl sulfoxide
DNA	Deoxyribonucleic acid
$E_{1/2}$	half-wave potential
(<i>E</i>)-FcMPE ⁺	(<i>E</i>)-1-ferrocenyl-2-(1-methyl-4-pyridinium)ethylene
ESI-MS	Electrospray Ionization Mass Spectrometry
ESP	electrostatic potential
<i>f</i>	fractional occupancy or nonlinear correction term
F	Faraday constant
FcCH ₂ OH	hydroxymethylferrocene
FcTMA ⁺	(trimethylammonio)methylferrocene
FcX	ferrocene derivatives
ΔG	Gibbs free energy
ΔG^*_{in}	inner-sphere reorganizational energy
ΔG^*_{out}	solvent reorganizational energy
G	guest
ΔH°	enthalpy
H	host
HPLC	High Performance Liquid Chromatography

HPVCL	High Performance Virtual Computing Laboratory
hr	hour
Hz	hertz
I	proton integration or ionic strength
IR	Infrared
<i>J</i>	coupling constant
J	Joule
K	Kelvin
K_p	the effective equilibrium constant
L	Liter
L^{4+}	$[\text{CH}_3\text{bpy}(\text{CH}_2)_6\text{bpyCH}_3]^{4+}$
λ	wavelength
m	multiplet
M	Molar (mole/liter) and Molecular ion
MALDI-TOF	Matrix-Assisted Laser Desorption Time-of-Flight
mmol	millimole
mM	millimolar
<i>m/z</i>	mass to charge ratio
$\text{Me}_{10}\text{CB}[5]$	decamethylcucurbit[5]uril
$\text{Me}_4\text{CB}[6]$	tetramethylcucurbit[6]uril
$\text{Me}_6\text{CB}[6]$	hexamethylcucurbit[6]uril
mg	milligram
MHz	megahertz

mL	milliliter
MS	Mass Spectroscopy
mV	millivolt
MV ²⁺	methylviologen (1,1'-dimethyl-4,4'-bipyridinium)
NHE	Normal Hydrogen Electrode
NMR	Nuclear Magnetic Resonance
NOESY	Nuclear Overhauser Effect Spectroscopy
P	population
ppm	parts per million
q	quartet
r	radius
R	gas constant
RVR ²⁺	dialkylviologen
ΔS°	entropy
s	singlet or second
<i>p</i> -SO ₃ CX[6]	<i>para</i> -sulfonated calix[6]arene
t	triplet
TSP	3-(trimethylsilyl)propionic-2,2,3,3- <i>d</i> ₄ acid
μ M	micromolar
UV	ultraviolet
<i>W</i>	work term
W	line width at half-maximum height

Chapter 1

INTRODUCTION

1.1 Supramolecular Chemistry

1.1.1 Definition and Development

Supramolecular chemistry refers to chemistry which focuses on non-covalent interactions of molecules, and is a highly interdisciplinary field covering aspects of chemistry, physics, and biochemistry. It has been defined as “chemistry beyond the molecule” by one of its founding fathers, Jean-Marie Lehn, who won the Nobel Prize in chemistry with Charles Pedersen and Donald Cram in 1987 for their significant contributions to molecular recognition.^{1,2} Unlike traditional organic synthesis, which usually involves the making and breaking of covalent bonds to get the desired molecules, supramolecular chemistry mostly utilizes noncovalent interactions, such as hydrogen bonding, van der Waals interactions, ionic interactions and hydrophobic interactions, to hold molecules together to form supramolecular complexes. The relationship between molecular and supramolecular chemistry in terms of both structures and interactions is illustrated schematically below (Figure 1.1).³

Supramolecular chemistry is a relatively young discipline, dating back to the late 1960s and early 1970s. However, its roots and many simple supramolecular chemical systems may be traced back almost to the beginnings of modern chemistry.^{3,4} It has drawn considerable attention in the recent decades as a new emerging and fast-growing domain lying amidst chemistry, physics, material science and biochemistry.

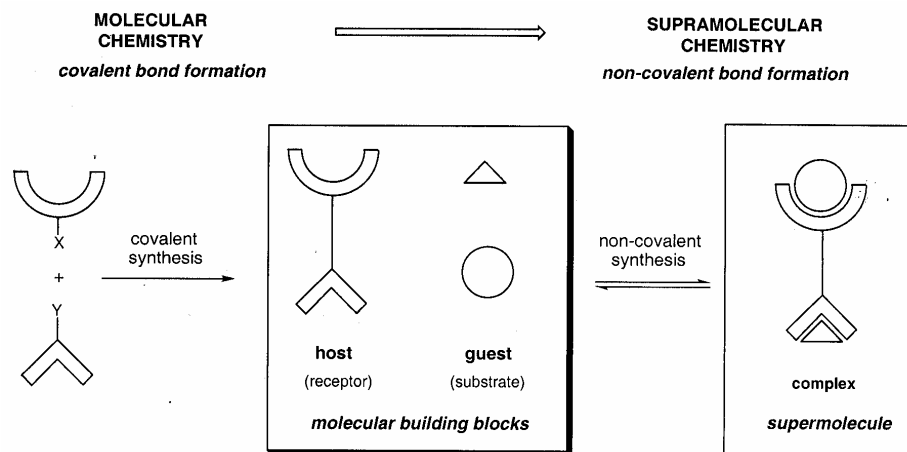


Figure 1.1 A schematic representation of the relationships between molecular and supramolecular chemistry.³

1.1.2 Nature of Supramolecular Interactions

In general, noncovalent interactions, which do not involve the sharing of electron pairs, encompass an enormous range of attractive and repulsive forces. They play an important role in supramolecular systems, in which all of these interactions and their effects usually interplay together on both the host and the guest, as well as on their surroundings. The most prevalent interactions, along with their estimated energies, are illustrated below.

1.1.2.1 Electrostatic Interactions

Electrostatic interactions (50-350 kJ/mol) are the interactions between charged molecules (ion-ion interactions) and charged molecules with dipolar molecules (ion-dipole interactions), with energies (V) determined by Coulomb's Law:

$$V = \frac{q_i q_j}{4\pi\epsilon_0\epsilon_r r_{ij}} \quad (1.1)$$

where q_i and q_j are the magnitude of the charges, r_{ij} is the distance between these two charges, ϵ_0 is the permittivity of free space and ϵ_r is the relative dielectric constant of the medium in which the charges exist.

From equation 1.1, it is easy to understand that the interaction can be either attractive or repulsive, depending on the two interacting charges. The dielectric constant of the medium (ϵ_r) also can have a significant effect on the strength of particular electrostatic interactions. As with van der Waals interactions, in polar media the magnitude of electrostatic interaction also tend to be attenuated. The electrostatic interaction is probably the strongest interaction among all kinds of noncovalent interactions,³ and plays a very important role in supramolecular complexations.

1.1.2.2 Hydrogen Bonding

The hydrogen bond (4-120 kJ/mol) is defined by Pimentel and McClellan⁵ as the interaction between a functional group A-H (usually called a hydrogen bond donor) and an atom or a group of atoms B (hydrogen bond acceptor) in the same (intramolecular hydrogen bond) or a different molecule (intermolecular hydrogen bond). As both atoms A and B are electronegative, they tend to share the hydrogen atom using their electron pairs. It is a special type of electrostatic interaction involving the formation of bonds to hydrogen.

The hydrogen bond has been widely investigated by spectroscopic tools such as IR and NMR spectroscopy and neutron/X-ray diffraction. Figure 1.2 shows the main types of hydrogen bonds which have been characterized.⁴ The strength of a hydrogen bond can vary from the weakest (~ 4 kJ/mol) to the strongest (~ 120 kJ/mol) in intermolecular noncovalent interactions, depending on the interaction direction. Usually it is weaker than electrostatic

interactions, but stronger than van der Waals interactions. The inherent directionality of hydrogen bonds make them ideal in supramolecular self-assembly and molecular recognition systems.

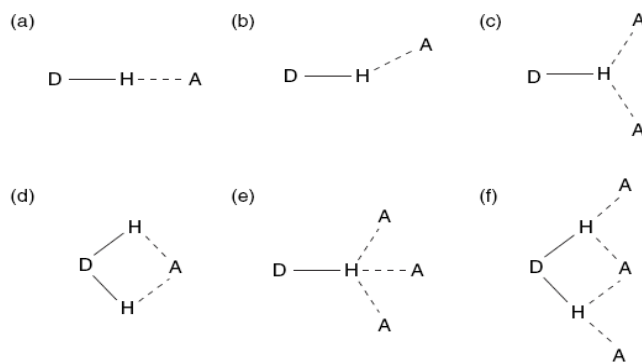


Figure 1.2 Main types of hydrogen bond geometry: (a) linear; (b) bent; (c) donating bifurcated; (d) accepting bifurcated; (e) trifurcated; (f) three-centre bifurcated.³

1.1.2.3 π - π Stacking Interactions

The weak π - π stacking interactions (0-50 kJ/mol), which usually occur between aromatic rings in which one ring is relatively electron rich and the other is electron poor, are caused by intermolecular overlapping of p-orbitals in π -conjugated systems. Therefore, the strength of the interaction increases with the number of π electrons. They can be generally divided into two types: face-to-face and edge-to-face π - π stacking interactions, as shown in Figure 1.3.⁴ Face-to-face π - π stacking interactions are responsible for the slippery feel and lubrication properties of graphite and play an important role in stabilizing the DNA double helix. Edge-to-face π - π stacking interactions, which can be regarded as a form of weak hydrogen bonding between electron deficient hydrogen atoms of one aromatic ring and the delocalized π -electrons of another aromatic ring, are believed to be the reason for the characteristic herringbone packing of many small aromatic hydrocarbons in the solid state.

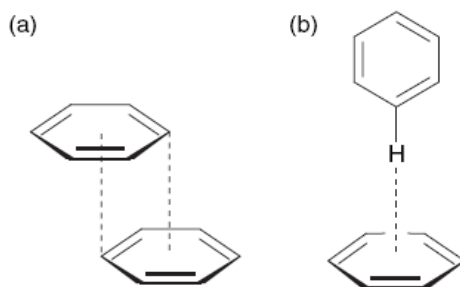


Figure 1.3 Two types of π - π stacking interactions: (a) face-to-face and (b) edge-to-face.³

The nature of π - π stacking interactions is still under heated debate. It has been proposed, by Sanders and Hunter,³ to be a competition between electrostatic and van der Waals interactions. Wilcox and co-workers,³ however, suggest that the importance of van der Waals interactions might outweigh that of electrostatic interactions in explaining the effects of π - π stacking interactions. Despite the lack of clarity in their origins, π - π stacking interactions, which are sometimes stronger than other noncovalent interactions, also play an important role in various aspects of supramolecular chemistry.

1.1.2.4 van der Waals Forces

The van der Waals interactions (< 5 kJ/mol) are a collective group of long range inductive and dispersive intermolecular forces between uncharged molecules, which act at a distance which is generally larger than the size of their electron clouds. These forces arise because the uncharged molecules are usually electric dipoles, and tend to align with each other to induce further polarization of neighbouring molecules, so forming an attractive net. Inductive forces can be divided into two types: permanent dipole-dipole interactions and induced dipole-dipole interactions. Dispersion forces, also called London Forces, are just the

result of momentary fluctuations of the electron density within the electron cloud of the molecules.^{3,4,6} The van der Waals interactions are usually weak, but the additive effects can be significant. Similar to other electrostatic forces, the strength of van der Waals interactions are strongly dependent on the interacting distance and the medium. Polar media tend to undermine the inductive interactions; however dispersive interactions will generally be enhanced under such conditions.

1.1.2.5 Hydrophobic Interactions

In water or other protic media, the non-polar regions of molecules tend to associate together to reach the most stable hydrogen-bonded status. The force which drives this process to occur is called a hydrophobic interaction (combined hydrophobic effects is a more proper term for it). Usually water is the most favourable solvent for the association of non-polar species, but for the complexations which involve hydrogen bonding, the host-guest inclusion process can be attenuated in this solvent system. Since in this process the non-polar solutes need to exclude water or protic media to come together, it is easy to understand that host-guest complexation will involve partial or full desolvation of the host and guest, and the solvation effects play a crucial role in mediating the stability of formed complexes.^{3,4}

Hydrophobic interactions are certainly of great importance in both the folding and recognition behaviour of large biomolecules, as well as in supramolecular complexations. It is especially of crucial importance for the inclusion of non-polar guests by hydrophobic cavities of cyclic hosts such as cyclodextrins, cucurbiturils and calixarenes in aqueous solution. In these cases, the hydrophobic effects can be divided into two energetic components, enthalpic and entropic.⁴ Enthalpic effects refer to the stabilization of water

molecules expelled from the cavity of the host. The cavity of the host, which is usually hydrophobic, tends to expel the polar water molecules and include a non-polar guest. The release of original intracavity water molecules into the bulk solvent will lower the energy of the whole system, thus making the process enthalpically favourable (Figure 1.4a). Entropic effects come from the fact that before the binding of the guest into the cavity, both the guest and host are disrupting the bulk water system, and the inclusion of guest into the cavity will reduce this disruption and hence create an entropic gain, as shown in Figure 1.4b.

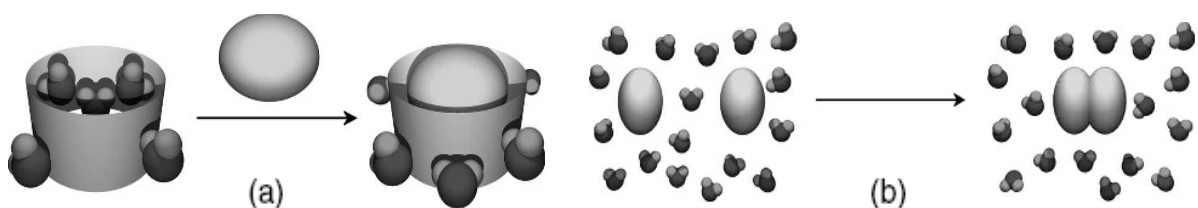


Figure 1.4 (a) The displacement of water molecules from a hydrophobic cavity is responsible for the enthalpic hydrophobic effect, and (b) two organic molecules creating a hole within an aqueous phase, giving rise to the entropic hydrophobic effect.⁶

1.1.3 Concepts in Supramolecular Chemistry

1.1.3.1 Molecular Self-assembly

Molecular self-assembly is the spontaneous assembly of molecules without guidance or forces from outside. There are basically two types of self-assemblies, intermolecular self-assembly and intramolecular self-assembly.³ Intermolecular self-assembly is more common in the supramolecular complexation systems focussed on in this thesis. Intramolecular self-assembly is quite important in the polymer and biochemistry fields and, for example, complex polymers can self-assemble to form a well-defined stable structure from a random

coil, and the self-folding of proteins to form more favourable secondary or tertiary structures is a typical example of intramolecular self-assembly in biological systems.

1.1.3.2 Molecular Recognition

In general, molecular recognition refers to the specific binding of a guest molecule to a complementary host molecule through noncovalent interactions. The two molecules have the ability to identify each other and fit together in an optimum manner.⁷ Weak intermolecular forces that act over a short distance, such as hydrogen bonding and electrostatic interactions, play an important role in this process. The research into molecular recognition in organic and supramolecular chemistry is inspired by the recognition behaviour in nature, such as replication of nucleic acids, immune response with antibodies, signal transduction in receptors, and regulation in enzymes.⁷ One of the earliest examples is crown ethers, which have the ability to recognize specific cations. A great number of artificial examples have been established since then and Moore and coworkers,⁸ for example, have demonstrated the molecular recognition between two isophthalic acids and one host molecule through multiple hydrogen bonds.

1.1.3.3 Host-guest Chemistry

Host-guest chemistry is an important subdivision of supramolecular chemistry, in which usually two or more molecules or ions are held together to form a complex in a unique structural relationship through intermolecular forces.^{3,4} The host molecule is defined as an organic molecule or ion with convergent binding sites in the complex, while the guest molecule is referred to as any molecule or ion with divergent binding sites in the complex,

such as antibodies (the host) and antigens (the guest) in immunology. Host-guest behaviour is commonly observed in compounds such as inclusion and intercalation complexes, clathrates, cryptands, and molecular tweezers.

1.1.3.4 Mechanically-interlocked Molecular Architectures

As the analogues to the key and the key chain loop, mechanically-interlocked molecular architectures refer to those molecules which are connected not through traditional covalent bonds, but as the consequence of their topology.⁹ The molecules are not connected directly, but significant bond distortion is involved in order to separate them. There are a great number of these architectures, such as catenanes, rotaxanes, molecular knots, and molecular Borromean rings, as shown in Figure 1.5.⁹ These architectures are quite important for the development of molecular machines.

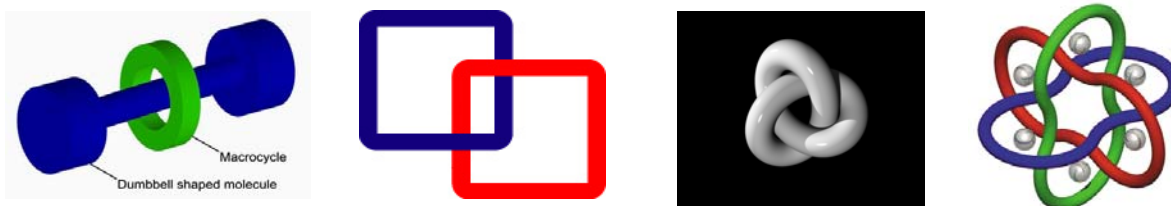


Figure 1.5 Examples of mechanically-interlocked molecular architectures (from left to right): rotaxanes, catenanes, molecular knots and molecular Borromean rings.⁹

1.1.3.5 Dynamic Covalent Chemistry

Dynamic covalent chemistry is a chemical strategy in which covalent bonds are broken and then directed by noncovalent interactions to form a structure with the lowest energy, reversibly.¹⁰ An example is shown in Figure 1.6, in which the formation of polyacetal macrocycles by a series of reactions was demonstrated.¹¹

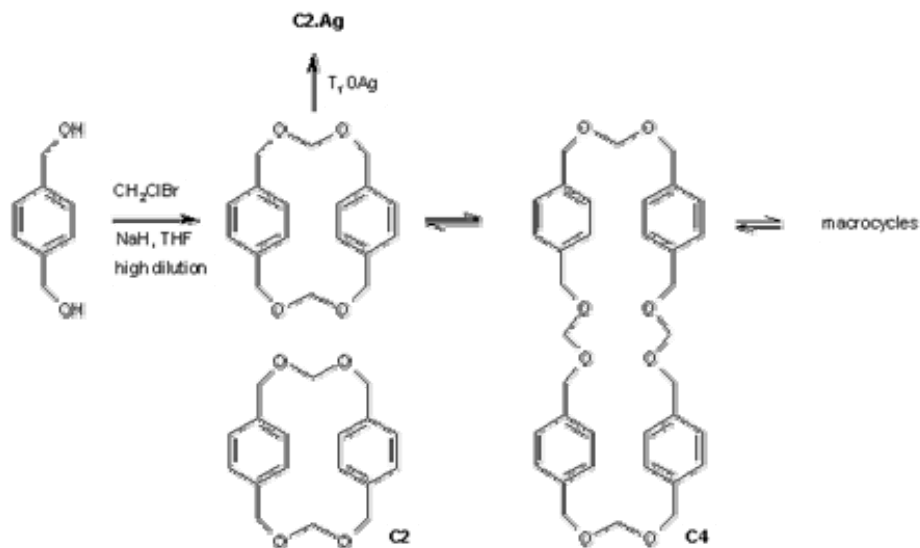


Figure 1.6 An example of a reaction sequence demonstrating dynamic covalent chemistry.⁹

1.1.4 Characterizing Supramolecular Systems

1.1.4.1 Structural Information

Once the design and synthesis have been achieved, the supramolecular system which is held together by non-covalent interactions must be characterized to obtain the information about the formed structure and the kinetics and thermodynamics of the binding process. The most convincing method is X-ray crystallography, as it can provide a direct vision of the structure of formed complex and give a straightforward picture of the binding sites, by which the information about the interactions that hold the guest in place can be obtained. However, the crystal information can only be obtained for the solid state, which might be different from the molecular properties in solution.^{12,13}

To understand the system in solution, alternative methods are used, such as nuclear magnetic resonance (NMR), which is a sensitive technique for monitoring the interactions between molecules.¹⁴ A typical NMR titration experiment is usually performed to obtain

binding information, in which the spectrum of the host/guest in a deuterated solvent is first measured, and then the guest/host is added in small aliquots. If binding occurs, the electronic environments of host and guest will perturb each other and by monitoring the signals of host or guest proton resonances, the structural conformation(s) of the complex can be deduced. It is often used to determine the stoichiometry of binding by a continuous variation method (Job's plot), in which stoichiometry can be determined by the position of highest point. As shown in Figure 1.7, for example, the stoichiometry of the host-guest complex is indicated to be 1:1.

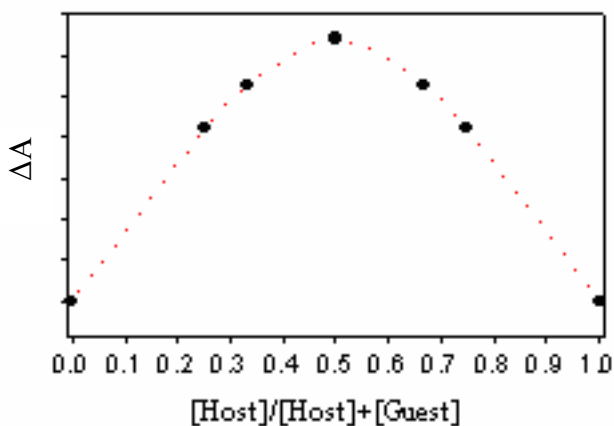


Figure 1.7 A sample of a UV-visible Job's plot curve showing the formation of a 1:1 host-guest complex.⁶

Nuclear Overhauser Effect Spectroscopy (NOESY), which provides an NMR spectrum correlating resonances that are physically close together, has been widely used to determine the geometry of the complexation between host and guest molecules. It is especially useful for more complicated systems such as helices.

Mass spectrometry (MS), especially using electrospray ionization (ESI-MS), has also been recognized as a useful method for supramolecular systems in the past decade. Because electrospray ionization is soft enough to keep the complexes intact through the measurement, by analyzing the mass values and isotopic patterns, information about the binding stoichiometry and mass information for the complexes can be obtained.^{15,16} In addition, UV-visible spectroscopy is also quite useful to study the interactions between host and guest molecules, and is especially effective for investigating complexes containing π -electron systems or transition metals.¹⁷

1.1.4.2 Kinetics of Complexation

Host-guest complexation is a dynamic exchange between the bound and unbound host and guest species. By analyzing the NMR spectra of mixtures of the host and guest, information about the binding kinetics between the host and guest molecules can often be obtained.¹⁸⁻²³

When the exchange process is faster than the frequency separation of the free and bound species, the NMR resonances of the host/guest are observed as an average peak, as shown in Figure 1.8b. With the addition of guest, the average peak shifts continuously until the receptor is saturated, and then the titration curve can be extracted by plotting the chemical shift as a function of the concentration of the guest, as shown in Figure 1.8a. As we can see, at the beginning the resonance of the host is perturbed significantly by the addition of guest. The host eventually becomes saturated by the guest and the resonance finally reaches an equilibrium position. However, if the exchange is slow on NMR timescale, instead of an

average resonance, two separate peaks, which represent the free and bound species, will be observed, as shown in Figure 1.8b.

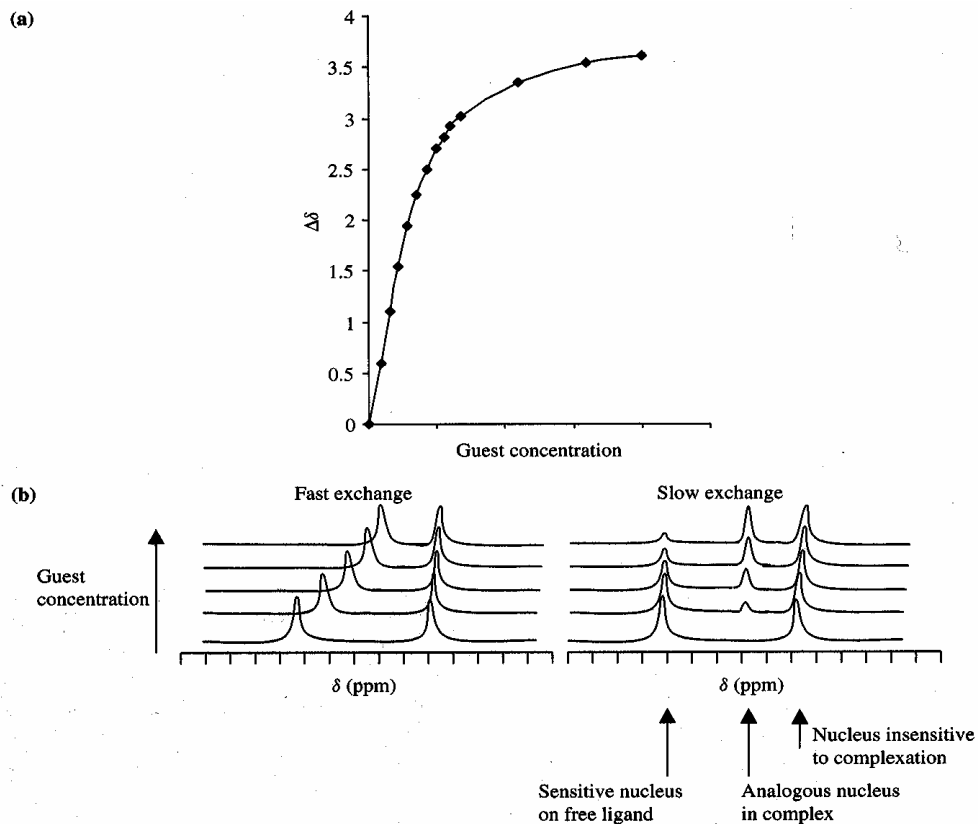


Figure 1.8 (a) ^1H NMR titration plot for fast exchange equilibration on the NMR time scale; (b) Schematic NMR spectra for fast and slow guest exchange equilibria.⁶

UV-visible spectroscopy has also been used to investigate the kinetics of the formation and dissociation of host-guest complexes. Since the lifetime of the technique is typically 10^{-15} s (greater than rate-limiting diffusion of the host and guest), all of the exchange processes would be slow in this timescale and the formation of the host-guest from

the individual species may result in a change in the UV-visible spectrum, whose time-dependence may be monitored.

1.1.4.3 Thermodynamic Information

Thermodynamic data, such as the host-guest stability constant, can be obtained from titration experiments as well. With NMR spectroscopy as an example, if the binding is kinetically slow, the complexation constant can be calculated from the relative integrations of the bound and unbound resonances. If the binding is kinetically fast, binding constant can be deduced from the titration curve of the complexation-induced shifts (as shown in Figure 1.8a), by applying a non-linear least-squares procedure to fit a theoretical model of the complexation process to the experimental data. The enthalpy (ΔH°) and entropy (ΔS°) of the binding equilibrium can be calculated from the different binding constants obtained by performing the titration experiments at different temperatures.²⁴

1.1.5 Summary

Supramolecular chemistry is one of the most important new areas in inorganic, organic and biochemistry to develop in the past few decades. It introduced a new approach in chemistry, which utilizes many non-covalent forces instead of traditional covalent bonds to hold molecules together. In this portion of the Introduction, the basic concepts and classifications of supramolecular chemistry have been illustrated. Several main types of non-covalent interactions, the key to supramolecular chemistry, have also been expounded upon. Methods used to characterize supramolecular system have been introduced as well. The next

section of the Introduction will focus on host-guest chemistry, which is the mainstay of the research projects described in this thesis.

1.2 Inclusion Complexes and Host-Guest Chemistry

1.2.1 Introduction

The discovery of a by-product in the preparation of bis[2-(*o*-hydroxyphenoxy)ethyl] by Pederson, 2,3,11,12-dibenzo-1,4,7,10,13,16-hexaoxacyclooctadeca-2,11-diene, marked the beginning of his Nobel Prize winning research in host-guest (or inclusion) chemistry.²⁵ As has been illustrated in section 1.1.3.3, host-guest chemistry describes one kind of supramolecular chemistry, in which the formed complexes are composed of two or more molecules held together by non-covalent intermolecular forces. In this section, the basic concept of preorganization and complementarity will be illustrated, followed by a discussion of the dynamic character of inclusion complexes, and a simple classification system for supramolecular host-guest compounds. Following this, the supramolecular chemistry of several types of macrocyclic host molecules and their applications will be described.

1.2.2 Design Principles of Complementarity and Preorganization

In order to bind guest molecules, a host must have binding sites which are complementary to those of the guest(s), both in their intrinsic properties (hydrogen bond donor/acceptor ability, hardness or softness, etc.) and relative spatial positions (possible distances and conformations for them to bind to each other). This feature is known as complementarity, which is a concept of great importance in supramolecular complexation processes.

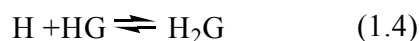
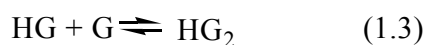
In some cases, a host whose structure is preorganized does not undergo a significant conformational change upon binding with the guest. This host preorganization has a great contribution to the overall free energy of the complexation, because the process of host-guest binding can be considered to occur in two stages. In the first step, the host will readjust itself in order to arrange its binding sites in a way that is most complementary to the guest and, at the same time, minimize the unfavourable interactions between one binding site and another. This process is energetically unfavourable. Following this rearrangement, the energetically favourable binding process will occur in the second step. The overall free energy of the complexation refers to the sum of these two processes. Thus, if the host is preorganized, the energy used for this rearrangement will be small and hence the overall free energy will be increased. However, compared to conformationally mobile hosts, which can adjust rapidly to changing conditions, and thus both association and dissociation processes are relatively fast, preorganized hosts tend to have slower guest binding kinetics because they may have difficulty in passing through the complexation transition state.

Overall, complementarity and preorganization are two important concepts in the study of supramolecular complexation, the principles of which have been widely used to guide the design of the molecular architectures of macrocyclic hosts.

1.2.3 Dynamic Character of Inclusion Complexes

Supramolecular complexes, as has been illustrated in section 1.1, are held together by weaker forces than those maintaining the molecular integrity and thus are not structurally rigid. In solution, therefore, there is equilibrium between the host-guest inclusion complex (HG) and its constituent host (H) and guest (G) components.

The free energy difference between the free and complex species, ΔG° , and the rate of the complexation and dissociation of the inclusion complex are two factors which characterize the equilibrium. In a bimolecular complexation process, the following equilibria show the simplest complexations, with 1:1 (equation 1.2), 1:2 (equation 1.3), and 2:1 (equation 1.4) host-to-guest stoichiometries, respectively.



The binding constant K , also known as an association constant K_a , a stability constant K_s , or a formation constant K_f , can be expressed as follows, respectively, for the three host-guest stoichiometries given in equation 1.2 to 1.4, where the brackets denote molar concentrations.

$$K_{11} = [HG]/([H][G]) \quad (1.5)$$

$$K_{12} = [HG_2]/([HG][G]) \quad (1.6)$$

$$K_{21} = [H_2G]/([H][HG]) \quad (1.7)$$

In a general form, the overall binding constant of the equilibrium in equation 1.8 can be written as given in equation 1.9



$$\beta_{mn} = [H_mG_n]/([H]^m[G]^n) \quad (1.9)$$

In most measurements, instead of stepwise binding constants, only the value of overall binding constant can be obtained. The overall binding constant is related to the free energy difference of the system ΔG and temperature T by equation 1.10, where k is the Boltzmann constant.

$$K = e^{(-\Delta G/kT)} \quad (1.10)$$

Thus the value of ΔG can be deduced by the equation above. According to the Gibbs-Helmholtz equation (eq 1.11), the enthalpy (ΔH) and entropy change ($T\Delta S$) upon complexation can be obtained by performing measurements of the complexation at different temperatures.

$$\Delta G = \Delta H - T\Delta S \quad (1.11)$$

Investigation of the dynamic character of inclusion compounds allows supramolecular architects to have a clearer view about the binding process. Numerous research papers and reviews have been published concerning studies of the dynamics of a variety of supramolecular systems.²⁶

1.2.4 Classification of Supramolecular Host-Guest Compounds

According to the relative topological relationship between the guest and the host, host-guest compounds can be divided into two types, cavitates and clathrates, which are formed by host molecules called cavitands and clathrands, respectively. A cavitand refers to a host molecule with intramolecular cavities both in solution and in the solid state.^{27,28} Examples of this type of host molecule are cyclodextrins, crown ethers and cucurbiturils, which will be

described in more detail in section 1.2.5. Usually the structures of cavitands are preorganized and rigid, such that they can form complexes with guests who have complementary shapes and electronic properties, with quite good stability and selectivity.

The concept of the clathrate was first proposed by Powell in 1984 and he defined the term “clathrate”^{29,30} as one kind of inclusion complex “in which two or more components are associated without ordinary chemical union, but through complete enclosure of one set of molecules in a suitable structure formed by another”. The host molecules which can form clathrates are called clathrands and they possess extramolecular cavities, with gaps between two or more hosts. A clathrate thus consists of a lattice of clathrands with the guests trapped in the lattice. A clathrate is therefore usually only found in the solid state, which has limited its prevalence in supramolecular chemistry. The distinction between cavitands and clathrands is shown in Figure 1.9.⁴

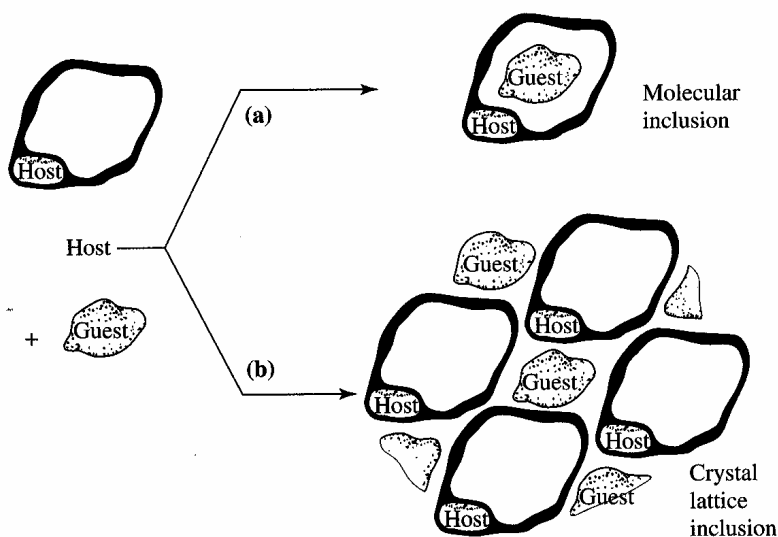


Figure 1.9 Schematic illustration of the difference between a cavitate and clathrate.⁴

1.2.5 Macrocyclic Hosts and Their Applications

As illustrated in section 1.1.3.3, the host is generally defined as a large molecule or aggregate possessing convergent binding sites. The term macrocyclic host refers to those which possess sizeable central holes or cavities. In this section, several important macrocyclic hosts, such as crown ethers, cryptands, calixarenes, porphyrins, cyclodextrins and cucurbiturils will be described in detail.

1.2.5.1 Crown ethers and Cryptands

The synthesis of crown ethers was first patented in Britain by Stewart, Wadden and Borrows in the mid 1950s.³¹ These authors, who were not interested in complexation of the cyclic molecules, failed to further investigate the potential of their findings. This postponed the development of host-guest chemistry until 1976 when Charles Pederson accidentally isolated a small amount of by-product from an organic reaction.²⁵ The solubility behaviour and high degree of crystallinity stimulated Pederson's interest. It was observed that the solubility of this compound in methanol was significantly enhanced when alkali metal salts were added. He eventually concluded that the alkali metal ion had become included in the hole of the molecule. This initial hypothesis was soon proved to be correct and gained Pederson a share of the 1987 Nobel Prize for Chemistry. Crown ethers, as named by Pederson, rapidly became a popular research subject in cation complexation chemistry.

The essential repeating unit of any simple crown ether is the ethyleneoxy group, $-\text{CH}_2\text{CH}_2\text{O}-$, as demonstrated below. The perfectly positioned electronegative oxygen atoms are ideal for the binding with a cation, which can be included within the cyclic host. In addition, the exterior of the host is hydrophobic. The binding process that results means that a hydrophilic cation can be dissolved in hydrophobic solvents. The size of the interior of the

crown ether determines which alkali metal ions will be preferred. The [18]crown-6 (the 18 refers to the total number of atoms in the ring and the 6 refers to the number of oxygen heteroatoms in the ring) has highest affinity for the potassium cation, while the smaller [15]crown-5 prefers the sodium cation (Figure 1.10).³²

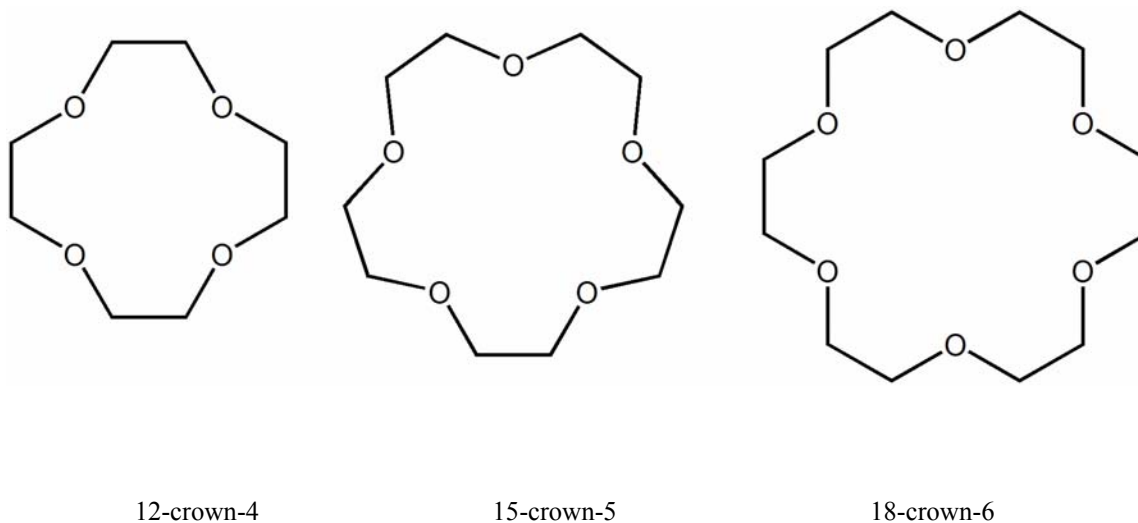


Figure 1.10 Three examples of the crown ether family of host molecules

Shortly after the remarkable finding of Pederson, Jean-Marie Lehn designed and synthesized a series of three-dimensional analogues of the crown ethers, which are known as cryptands.³³ These bicyclic analogues can encapsulate metal ions entirely, thus increasing the cation selectivity and affinity (Figure 1.11). The first and most important member of this family was the [2,2,2]cryptand (the numbers refer to the number of oxygen heteroatoms in the linkers between the bridging nitrogens), which is the analogue of [18]crown-6 and also exhibits high selectivity for the potassium cation over other alkali metal ions, but with almost 10^4 times stronger binding. Similarly, as the analogue of [15]crown-5, the [2,2,1]cryptand selectively binds to the sodium cation with stronger affinity.³⁴

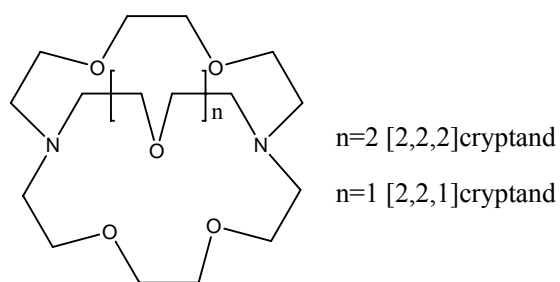


Figure 1.11. The structures of the [2,2,2]- ($n = 2$) and [2,2,1]cryptands ($n = 1$).³⁴

As illustrated, Pedersen and Lehn built the foundations of this burgeoning and promising research field, which was followed by the design and syntheses of thousands of such molecules varying in size and substituents, and containing not only oxygen and nitrogen atoms but also sulfur atoms and aromatic rings.³⁵

1.2.3.1 Calixarenes

The calixarenes, a popular and versatile class of macrocyclic host molecules, are the hydroxyalkylation product of a substituted phenol and an aldehyde.³⁶ The descriptive name “calixarene” was coined by David Gutsche because the shape of the molecule resembles a Greek vase called a “calix” and the other part of the name “arene” refers to the aromatic building block.³⁷ Between these two parts, there is a number in square brackets which represents the number of phenolic residues. Therefore, the most common family member, as shown here in Figure 1.12, is named as *p*-tertbutyl-calix[4]arene.

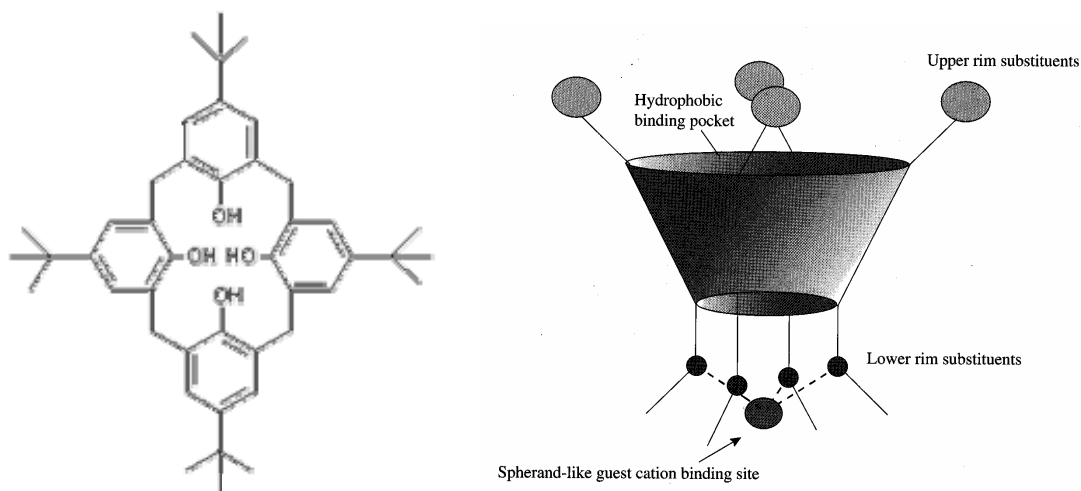


Figure 1.12 Typical structure and multiple potential binding sites of calixarenes.⁶

The anatomy of the structure reveals the multiple potential binding sites of calixarenes. As shown in Figure 1.12, calixarenes possess a hydrophobic cavity with a narrower rim of phenolic oxygen atoms at the bottom and a wide rim of hydrophobic substituents on the top. As a result of the flexibility of the methylene connections between each unit, calixarenes exist in different conformations. Figure 1.13 shows the four conformers of calix[4]arene, existing in solution under a dynamic equilibrium.^{3,36}

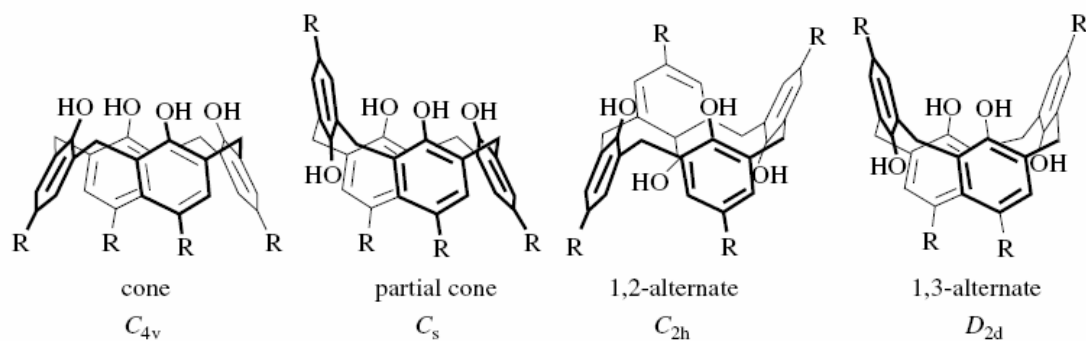


Figure 1.13. Four conformations of calixarenes.³⁶

Due to the versatile binding behaviours, calixarenes have been widely used as enzyme mimetics, ion sensitive electrodes or sensors, selective membranes, in non-linear optics materials and in HPLC stationary phases.^{37,39-42} In addition, given the high selectivity towards sodium over other cations, calixarenes are known as efficient sodium ionophores and are applied as such in chemical sensors. They are commercially used as sodium selective electrodes for the measurement of sodium levels in blood.³⁹

1.2.5.3 Porphyrins

Porphyrin, named after the Greek word “*purple*”, is derived from a heterocyclic compound consisting of four pyrrole-like subunits connected to each other via their α carbon atoms through methine (=CH-) bridges. Many porphyrins are found in nature, such as in green leaves and red blood cells. Laboratory syntheses of porphyrins usually involve the reaction of pyrrole and substituted aldehydes under an acidic environment, as developed by Rothmund.^{43,44}

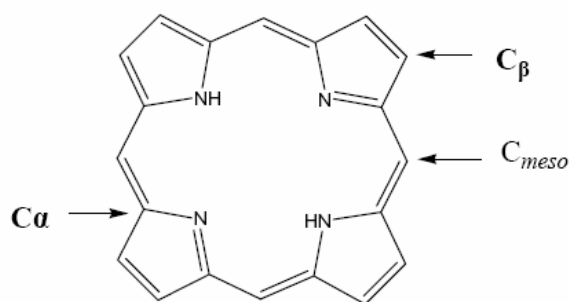


Figure 1.14 The structure of porphine, showing the carbon substitution positions.

The structure of porphine, the simplest porphyrin, is shown above in Figure 1.14. It is a highly conjugated system with 22 π -electrons. Two of the nitrogen atoms are of the pyrrole type, with an electron lone pair pointing inside the macrocycle. When both N-H groups are deprotonated, there will be four electron lone pairs pointing inside the ring. This dianion system will be ideal for binding proper sized cations.⁴⁵ Porphyrins and metalloporphyrins are widely applied in the construction of artificial antenna systems,⁴⁶ photosynthetic center mimics,⁴⁷ gates and redox switches, and in the fabrication of smart devices and machines.⁴⁸

1.2.5.4 Cyclodextrins

Cyclodextrins (abbreviated CD) are macrocyclic oligosaccharides built of α -D-glucopyranoside units linked by α -(1,4) bonds. While they were first described by Villiers in 1891, the structure and chemical properties of natural cyclodextrins were not fully characterized until the mid 1970s.⁴⁹ Ever since, research about cyclodextrins has rapidly

developed and has become an important branch of host-guest chemistry because of their numerous practical applications.⁵⁰

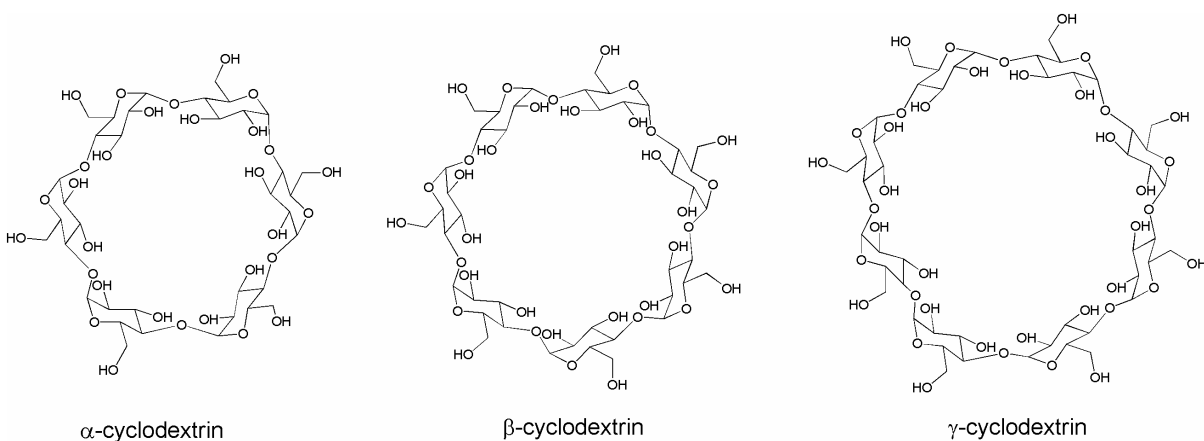


Figure 1.15 Structures of α -, β - and γ -cyclodextrin.

Figure 1.15 shows the structures of the most common CD members; α -, β - and γ -CD, which include 6, 7 and 8 repeating glucopyranoside units, respectively. The connection of glucopyranoside units in such a cyclic manner offers a typical conical structure with a relatively hydrophobic interior and two hydrophilic hydroxyl-rimmed openings. This structural property imparts cyclodextrins their high water solubility and the ability to accommodate appropriately sized guests, such as nonpolar organic molecules, polar amines and acids,⁵¹ ferrocenes⁵² and other organometallic compounds,⁵³ through noncovalent interactions such as hydrogen bonding, hydrophobic interactions, and electrostatic interactions.⁵⁴

Due to their excellent host-guest complexation abilities, CDs have been used in a wide array of fields, such as fabrication of pseudorotaxanes, rotaxanes and other types of molecular machines^{55,56} and catalysts in organic synthesis.⁵⁷ In addition, in the

pharmaceutical industry CDs are used for drug delivery because the inclusion of insoluble, hydrophobic drugs into the cavity of CDs will enable them to penetrate body tissues and then become released afterwards under specific conditions.⁵⁸ They are also employed in environmental protection by immobilizing toxic compounds in their cavities, in food industry for preparing cholesterol free products, and many other applications in a wide array of fields.⁵⁹

1.2.5.5 Cucurbiturils

Cucurbit[*n*]urils (CB[*n*]) are a family of cyclic oligomers of *n* glycoluril units self-assembled from an acid-catalyzed condensation reaction of glycoluril and formaldehyde.⁶⁰⁻⁶⁴ The most studied member, CB[6], was first synthesized and recrystallized by Behrend *et al.* in 1905 and became known as Behrend's polymer.⁶⁵ The constitution of this substance remained unclear until 1981 when Mock and coworkers revealed the remarkable macrocyclic structure, which consists of six glycoluril units bridged by twelve methylene groups, in a pumpkin shape.⁶⁶ Interest in the cucurbit[*n*]uril family of host molecules has been significantly increased by the successful preparation of four new CB[*n*] homologues, CB[5], CB[7], CB[8] and CB[10], by the research groups of Kim and Day.⁶⁷⁻⁶⁹ Nowadays, research into the behaviour of cucurbiturils have overcome most of the early problems such as poor solubility, a lack of a homologous series of different sized host, and methods for preparing substituted cucurbiturils and has provided an outstanding platform for fundamental and applied molecular recognition and self-assembly studies. As shown by its title, this thesis is focused on the host-guest complexation of cucurbiturils. More details about cucurbiturils, in

terms of their structural nature and host-guest binding properties will be described in the following section of the thesis.

1.3 Cucurbit[n]urils

1.3.1 Syntheses of Cucurbit[n]urils

Similar to the synthesis of CB[6], as illustrated in Section 1.2.5.5, other CB[n] hosts are obtained by the condensation of glycoluril and formaldehyde in concentrated HCl or 9M H₂SO₄ solution at 75-90°C rather than >110°C (conventional reaction temperature for CB[6]). The key is the relatively lower temperature, which allowed the formation of significant amounts of CB[n] homologues in addition to CB[6], as schematically illustrated below (Figure 1.16).⁶² The formation and typical content of the mixture is confirmed by NMR and ESI-MS to be ~10-15% CB[5], ~50-60% CB[6], ~20-25% CB[7], and ~10-15% CB[8].

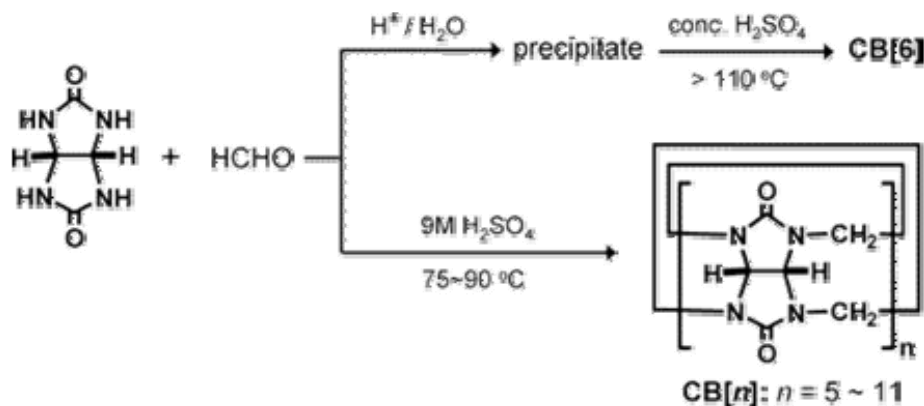
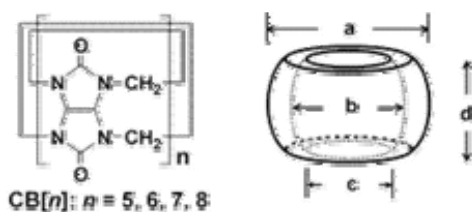


Figure 1.16 The methods for the synthesis of cucurbit[n]urils.⁶²

The mixture can be separated in pure form by fractional crystallization and dissolution,⁶⁷ or chromatography.⁷¹ In order to optimize the yield of individual CB[n] homologues, Day and coworkers examined different reaction conditions and have investigated the cyclization mechanism for the formation of cucurbiturils.⁷¹ More recently, Kim and coworkers have developed a microwave method,⁷² providing a faster and more efficient way of producing a CB[n] mixture, which may be valuable for the production of cucurbiturils on an industrial scale.

1.3.2 Structures and Physical Properties

The cucurbit[n]urils are cyclic oligomers whose shape resembles a pumpkin, with a hydrophobic cavity guarded by two carbonyl-laced portals.⁶⁰⁻⁶⁴ Figure 1.17 shows the structural parameters of the most common CB[n] homologues.



		CB[5]	CB[6]	CB[7]	CB[8]
outer diameter (Å)	a	13.1	14.4	16.0	17.5
cavity (Å)	b	4.4	5.8	7.3	8.8
	c	2.4	3.9	5.4	6.9
height (Å)	d	9.1	9.1	9.1	9.1
cavity volume (Å ³)	-	82	164	279	479

Figure 1.17 Structural parameters of CB[n] homologues.⁶²

Although these hosts possess the same total depth (9.1 Å), their widths at various depths (a, b and c) and cavity volumes increase with the number of glycoluril subunits. Generally, the diameter of the portals (c) is approximately 2 Å narrower than that of the cavity itself (b), which provides significant steric barriers to guest association and dissociation. The CB[6], CB[7] and CB[8] hosts are the analogues of the α -, β - and γ -cyclodextrins, respectively, in term of cavity size. The CB[n] homologues can be distinguished by ^1H and ^{13}C NMR, which is the main characteristic tool to investigate their binding behaviours. The resonances of the methylene and methine protons of CB[n] move downfield with increasing number of glycoluril units.

The solubility of CB[n] homologues is relatively low ($< 10^{-5}$ M) in both water and organic solvent, except for CB[5] and CB[7], which possess moderate solubility in water (up to $2\text{-}3 \times 10^{-2}$ M).⁶⁰⁻⁶⁴ However, due to the weak basicity of the carbonyl portals and their affinity for cations, all CB[n] homologues have greater solubility in acidic solution or solutions containing alkali metal ions, explaining why most studies of host-guest binding of CB[6] were conducted originally in formic acid-water (1:1) solutions. In general, the solubility of CB[n] is lower than that of the cyclodextrins, but show an opposite trend among the homologues, with CB[6] and CB[8] being less soluble than CB[7], while α -CD and γ -CD are more soluble than β -CD.

One of the valuable features of CB[n] homologues is their high thermal stability in the solid state, with no decomposition being observed in thermal gravimetric analysis up to 420 °C for all homologues except CB[7], which starts decomposing at a slightly lower temperature (370 °C).⁶⁰⁻⁶⁴

1.3.3 Host-Guest Chemistry of Cucurbit[n]urils

1.3.3.1 Comparisons of the Thermodynamics of Complexation

As discussed previously, CB[n] is the analogue of CDs in term of cavity size and they bind similar guests of varying sizes. However, these two families have fundamental differences in molecular recognition interactions due to the different functional groups lacing the cavity entrances. In CDs, the OH functional groups can form hydrogen bonds with guests, which is the main driving force of the binding process. However, the carbonyl groups decorating the cavity entrances of cucurbiturils can form both hydrogen bonds and ion-dipole or dipole-dipole interactions, and coordinate to metal ions as well. Figure 1.18 demonstrates the pronounced difference between calculated electrostatic potential (ESP) of CB[7] and β -CD, in which CB[7] displays more negative electrostatic potential at both of the portals and the central cavity regions, compared to β -CD.⁶²

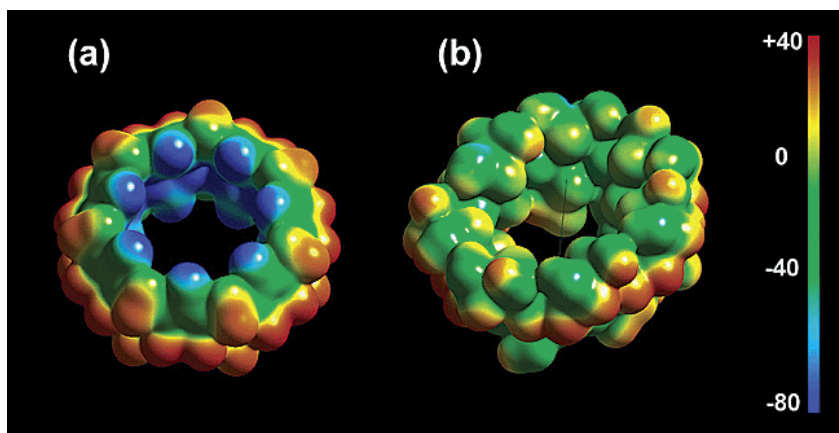


Figure 1.18 Comparison of electrostatic potential surfaces of (a) CB[7] and (b) β -CD.⁶²

The electrostatic effects of the host molecules play an important role in molecular recognition processes in both aqueous and organic solutions.⁷³ Thus, this difference in the electrostatic potentials contributes significantly to the host binding preferences. Cucurbiturils prefer to form inclusion complexes with cationic guests, whereas cyclodextrins preferentially bind to neutral or anionic guests.

Mock and Shih⁷⁴ investigated and compared the binding affinity of α -CD and CB[6] toward a series of alcohols, which are moderately strongly bound guests for both hosts. Despite the fact that cucurbiturils have a preference to bind with positively charged species, CB[6] showed higher affinity and higher selectivity toward all of the studied alcohol guests. A similar comparison has been conducted between CB[6] and [18]crown-6, indicating that CB[6] shows higher affinity than [18]crown-6 toward all cations except Ba^{2+} , which has a preference for [18]crown-6 due to the perfect size match. These examples indicate that cucurbiturils have equal or better binding affinities and selectivities comparing to other well-known host molecules. The high structural rigidity might be playing an important role in the higher binding selectivity toward all guests.

1.3.3.2 Host-Guest Complexation of CB[6]

The CB[6], the first member of the family to be prepared, has been known for a hundred years and studied in detail since 1981. The supramolecular chemistry properties of CB[6], which will be illustrated in this section, can hypothetically be transferred to other CB[n] homologues. Figure 1.19⁶⁴ shows a comprehensive mechanism for the interaction of CB[6] with its common guests including protons, metal ions, amines and ammonium ions.

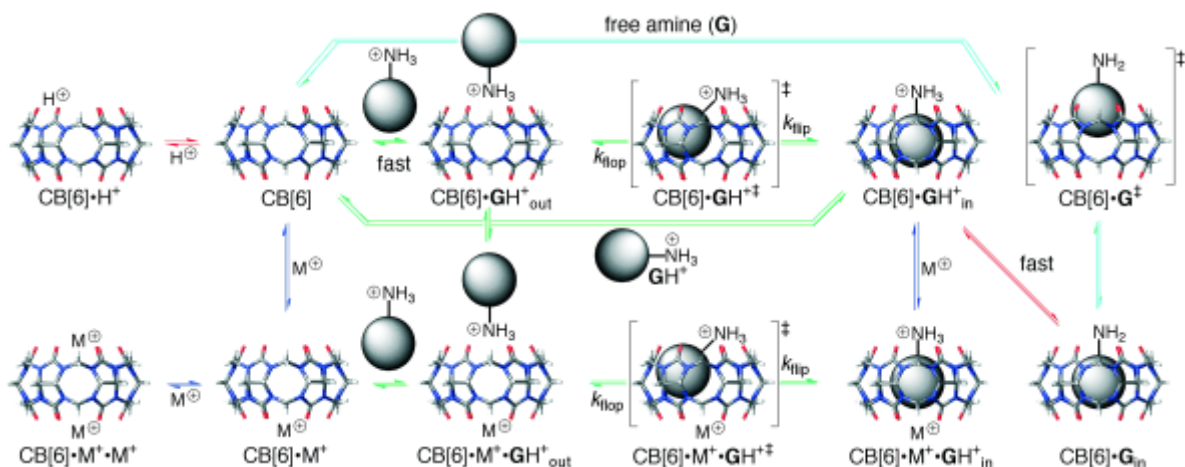


Figure 1.19 Comprehensive mechanistic scheme for molecular recognition by CB[6]. Red arrow: protonation. Blue arrow: cation binding. Green arrow: ammonium ion binding. Light blue arrow: amine binding.⁶⁴

Cucurbit[6]uril, which possesses twelve ureido carbonyl groups in its structure, has been shown to be a weak base, with the pK_a of the conjugated acid of CB[6] measured as 3.02.⁶⁴ It can be protonated in a moderate acidic environment, as shown in Figure 1.19 (red equilibria). Thus, binding events conducted in acidic solution must take the competition of H^+ with the guests into account.

The blue equilibria in Figure 1.19 show the binding of CB[6] with positively charged metal ions, such as alkali-metal, alkaline-earth, transition-metal, and lanthanide cations. There is also a competition between H^+ and metal ions. With an increase in the acidity of the solution, the observed stability constants ($\log K$ values) for guests are decreased.^{75,76}

As illustrated in section 1.3.2, the cavity of CB[6] is analogous to that of α -CD, which is appropriately sized to form inclusion complexes with linear alkyl guests. Given that cucurbiturils prefer to bind with positively charged organic guests due to the negative

electrostatic potential of the portals, Mock and coworkers have investigated the binding behaviour between CB[6] and a series of alkylammonium and alkyldiammonium cations, measuring the stability constants (K_a) by ^1H NMR experiments, as depicted in Table 1.1.^{66,74,77-79}

Table 1.1 Binding constants of a series of protonated amines with CB[6]⁸⁰

Entry	Amine	K_a [M^{-1}]
1	NH_3	83
2	$\text{H}_2\text{N}(\text{CH}_2)_6\text{H}$	2300
3	$\text{H}_2\text{N}(\text{CH}_2)_6\text{OH}$	1200
4	$\text{H}_2\text{N}(\text{CH}_2)_6\text{NH}_2$	2800000
5	$\text{c}-(\text{CH}_2)_2\text{CHCH}_2\text{NH}_2$	15000
6	$\text{c}-(\text{CH}_2)_3\text{CHCH}_2\text{NH}_2$	370000
7	$\text{c}-(\text{CH}_2)_4\text{CHCH}_2\text{NH}_2$	330000
8	$\text{c}-(\text{CH}_2)_5\text{CHCH}_2\text{NH}_2$	80
9	4-MeC ₆ H ₄ CH ₂ NH ₂	320
10	3-MeC ₆ H ₄ CH ₂ NH ₂	n.d.
11	2-MeC ₆ H ₄ CH ₂ NH ₂	n.d.
12	$\text{H}_2\text{N}(\text{CH}_2)_5\text{NH}_2$	2400000
13	$\text{H}_2\text{N}(\text{CH}_2)_2\text{S}(\text{CH}_2)_2\text{NH}_2$	420000
14	$\text{H}_2\text{N}(\text{CH}_2)_2\text{O}(\text{CH}_2)_2\text{NH}_2$	5300

Based on these results, Mock and Shih have concluded that the binding with CB[6] will result in the shielding of guest proton resonances by about 1 ppm for the region which is included in the cavity, whereas the proton signals for the portion of the guest outside the cavity are slightly deshielded by the carbonyl portals. In addition, the dynamic exchange processes between free and bound species are observed to be usually slow on the ^1H NMR timescale, which allows for the direct calculations of the binding constants from integrations of the resonances of the bound and free guests. By comparing the relative binding affinity of entries **2-4** with CB[6], Mock and Shih confirmed that the ion-dipole interactions play a more

important role in the binding process than hydrogen bonds. The replacement of H by NH₂ group increases the binding constant significantly from $2.3 \times 10^3 \text{ M}^{-1}$ to $2.8 \times 10^6 \text{ M}^{-1}$; however, replacing the H by OH, which can also form hydrogen bonds, does not increase the binding affinity at all. Hence, it is easy to understand that the positive charge has given the ammonium ions high specificity for the binding with CB[6].

1.3.3.3 Binding Selectivity of CB[6]

As described in section 1.3.2.1, cucbiturils have relatively high binding selectivity compared to other well-known host molecules. This high selectivity will be useful in the construction of molecular switches, which will be discussed later in the section 1.3.5.2.^{138,139} It has been reported that with a relatively rigid structure and the two close binding regions, the carbonyl portals, which favour positively charged groups, and the hydrophobic cavity, which prefers hydrophobic residues, impart this special feature to the CB[n] family. As discussed above, CB[6] preferentially forms stable complexes with linear alkyl compounds with positive charges, such as protonated diaminoalkanes.

Using the compounds studied in Table 1.1 as examples, the selectivity of CB[6] will be discussed in several aspects. First, Mock and coworkers found that alkyl amines and alkane diamines show *alkyl chainlength-selectivity* when binding with CB[6]. For alkyl amines, CB[6] binds to butylamine more strongly than with propylamine (8-fold) or pentylamine (4-fold). However, in the case of diamines, pentanediamine and hexanediamine have much higher affinities for CB[6] relative to butanediamine and heptanediamine. This can be attributed to the alkyl chainlength match to the cavity depth, by which pentanediamine and hexanediamine can place two ammonium groups adjacent to the carbonyl portals,

optimizing the ion-dipole interactions. Secondly, the binding between CB[6] and guests are also size-selective. As shown in Table 1.1, CB[6] selectively binds to the compounds in entries **6** and **7**, whereas for the three and six-membered ring analogues, it shows much weaker binding affinities. In addition, the binding is also affected by the shape of guests.⁸⁰ For example, compound **7** has a much higher binding affinity when compared to compound **9**, which has a similar size. However, for compounds **10** and **11**, which are the *ortho* and *meta* isomers of **9**, respectively, no binding with CB[6] is detected at all. Finally, the functional groups in guest molecules also play an important role in the binding process, as the binding of compound **13** to CB[6], for example, is much weaker than that of **12**, but stronger when compared with **14**. This can be explained by the solvation effect on the unbound guests. A methylene group is more hydrophobic than a thioether bond, and oxygen has higher hydrophilicity than sulfur.⁷⁴

1.3.3.4 Thermodynamics and Kinetics of Complexation

As discussed previously, CB[6] offers a hydrophobic cavity which is 5.8 Å wide and 9.1 Å high, accessible by two ureido carbonyl-rimmed portals. These portals are approximately 2 Å narrower in diameter than the cavity, which can lead to a constrictive binding property for the host. In addition, the binding events of CB[6] with guests are usually conducted in acidic or saline environment due to the poor solubility of the host.⁶⁰⁻⁶⁴ Therefore, the H⁺ or metal cations function as “lids” to seal the portals, competing with guests binding. Accordingly, unlike cyclodextrins and calixarenes, which allow a fast exchange of the guest due to their relatively flexible openings, the members of the CB[n] family usually display slower kinetics of guest association and dissociation and slow guest

exchange on the NMR time scale. Two separate sets of signals for both complexed and free species can be observed, by which the binding constants can be directly extracted. From the temperature dependence of the binding constant and rate constants, the enthalpy and entropy of the complexation can be deduced ($-RT\ln K = \Delta H - T\Delta S$).

Although considerable attention has been drawn to host-guest complexation processes of CB[n] family and their applications, relatively little has been investigated about the complexation mechanisms and the factors controlling the kinetics and mechanistic aspects of their recognition behaviours. Thermodynamic and kinetics studies are of principle importance to develop further applications of cucubiturils. However, to date, only the complexation kinetics and thermodynamics of CB[6] with a series of alkyl- and cycloalkylammonium cations have been studied by Nau and coworkers,^{80,81} by which the complexation mechanism were proposed as shown in Figure 1.20.

The mechanism shown in Figure 1.20a applies to small uncharged guest molecules, in which the uncharged guests can enter the cavity directly with alkali cations or protons forming “lids” on both carbonyl rims. The mechanism in Figure 1.20b, however, is more reasonable for the binding with organic ammonium cations of a suitable size. First, the organic ammonium cation will coordinate with the carbonyl portal and then flip-flop to enter the hydrophobic cavity in a second step. After investigating the binding thermodynamics and kinetics of CB[6] with a series of organic ammonium cations in solutions at different pH and with different types and concentrations of alkali cations, Nau and coworkers concluded that the binding constants and the ingress rate constants decreased with the increase of the cations or proton concentrations.^{80,81} The egress rate constants, however, remain almost unaffected.

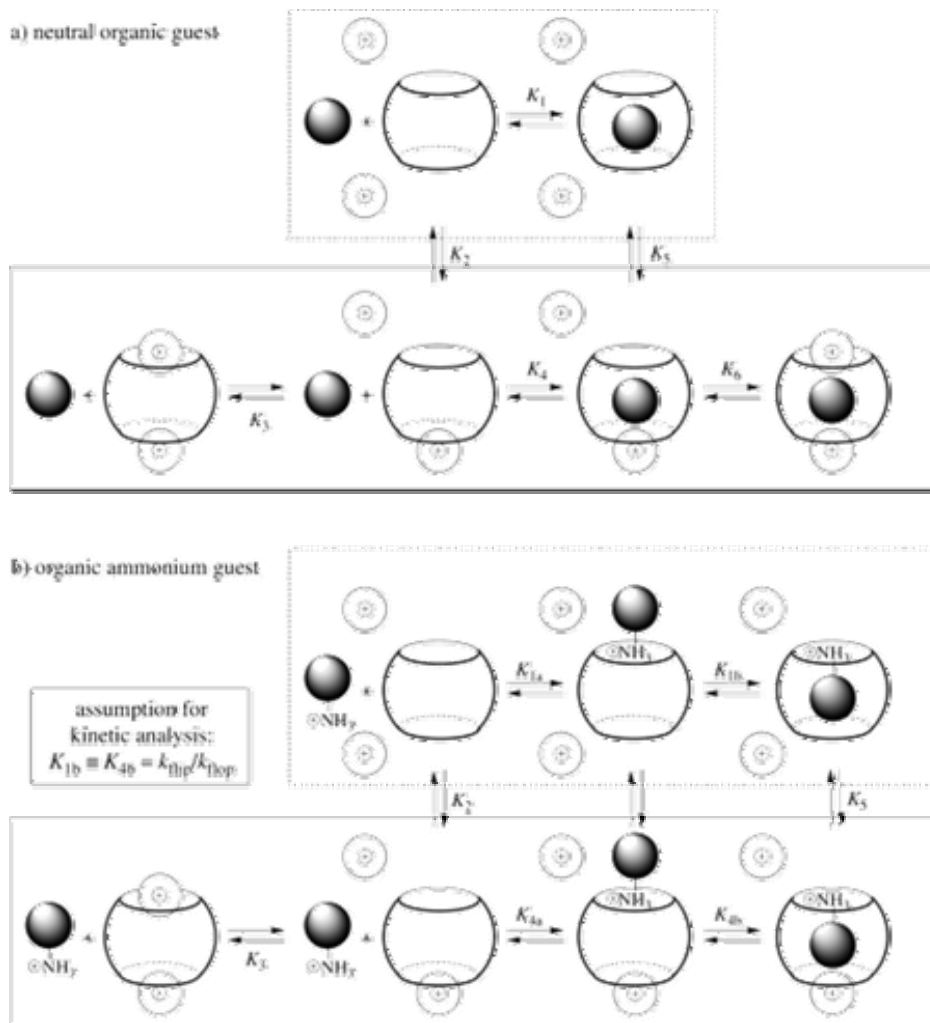


Figure 1.20 Proposed binding mechanism of CB[6] with (a) neutral and (b) ammonium guests.⁸⁰

1.3.4 Host-Guest Chemistry of Cucurbit[n]uril Homologues

Compared to CB[6], which has been developed for about one hundred years, the supramolecular chemistry of other members of CB[n] family such as CB[5], CB[7], CB[8] and CB[10], which were only isolated seven years ago, remains relatively unexplored.^{62,64}

As interpreted previously, the basic principles and lessons learned from CB[6] can be generally transferred to the whole CB[n] family. However, due to their varying cavity and portal sizes, the CB[n] members show remarkable differences in molecular recognition properties when compared to CB[6],⁶² even though they share the same characteristic features of a hydrophobic cavity and two hydrophilic carbonyl-rimmed portals. As shown in Figure 1.21, CB[6] is known to be able to form very stable complexes with protonated alkylammonium cations and modestly stable complexes with some arylammonium ions, such as *p*-methylbenzylamine ion, as discussed in Section 1.3.3.2.

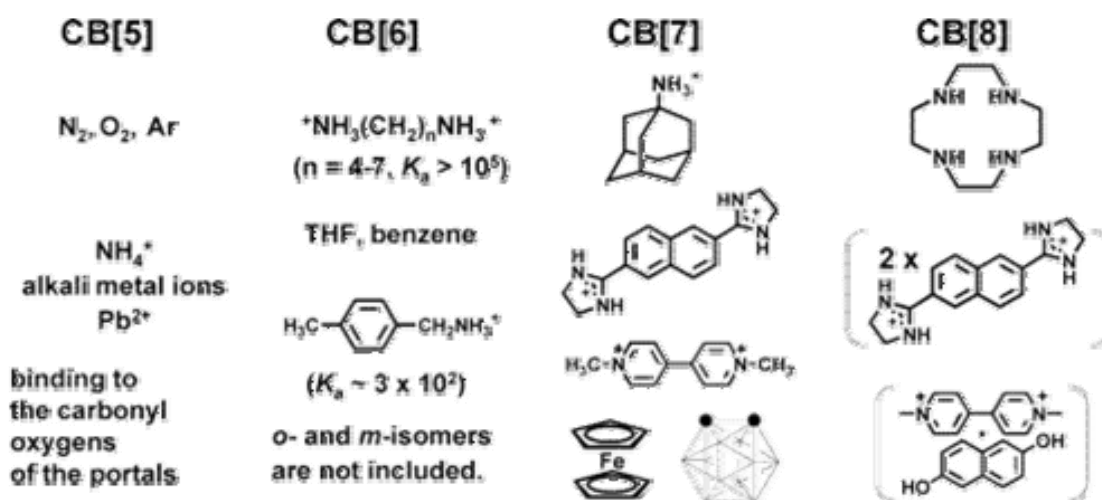


Figure 1.21 The binding preference of CB[n] homologues.⁶²

The CB[5] host, due to its limited cavity and portal size, tends to bind protons as well as metal and ammonium ions at its portals instead of binding organic guests in the cavity. The CB[7], an increasingly popular member of the family, has been proven to have a high affinity for positively charged aromatic and cyclic compounds, and metal compounds such as ferrocene derivatives as well. The CB[8], as shown in Figure 1.21, can form inclusion

complexes with even larger molecules, including cyclen and cyclam. The cavity is also large enough to include two same or different aromatic molecules to form 1:2 or 1:1:1 complexes.

1.3.4.1 Host-Guest Complexation of Cucurbit[7]uril

The cucurbit[7]uril host molecule has attracted considerable attention in recent years as a result of its superior water solubility relative to the others.^{61,62,64} The CB[7], which shares the characteristic features of CB[6], but with larger cavity and portal sizes, is even slightly more voluminous than β -CD and thus can form stable complexes with relatively larger molecules. The guest molecules which have been reported to bind with CB[7] are a variety of positively charged compounds such as viologen dications and tetracations^{82,83} stilbenes,⁸⁴ naphthalenes,^{85,86} protonated aminoadamantanes,⁸⁷ imidazolium cations,⁸⁸ chiral N-benzyl-1-(1-naphthyl)ethylamines⁸⁹ and pyridinium derivatives,⁹⁰ and neutral guests including adamantanes and bicyclooctanes^{62,91-93}, o-carborane,⁹⁴ fullerene⁹⁵ and ferrocene and cobaltocene derivatives,⁹⁶⁻⁹⁸ among others.^{99,100}

As illustrated previously, the basic principles and lessons learned from CB[6] chemistry can be applied to others in the CB[n] family. Kaifer and coworkers have demonstrated that many of the binding properties of CB[6] are retained by CB[7]. For example, Ong and Kaifer investigated the binding of CB[7] with a series of guests with a suitable size in the presence of Na^+ and Ca^{2+} ions. The competition of Na^+ and Ca^{2+} with these guests reduced the K_a values significantly,¹⁰¹ similar to what have been observed for CB[6]. Kaifer and coworkers also demonstrated that CB[7] can reside on different locations when the guest molecule has more than one active binding site,^{102,103} which indicates the same high binding selectivity as observed with CB[6]. Nau and coworkers have shown the

low polarizability of the CB[7] cavity by investigating the binding behaviour of 2,3-diazabicyclo[2,2,2]oct-2-ene with CB[7].^{104,105} This study also allows one to distinguish an alternative mechanism in fluorescence-quenching studies. The fluorescence enhancement of anilinonaphthalenesulfonates upon the inclusion by CB[7] was observed by Wagner and coworkers.⁸⁵ The stabilization of fluorescent species and the H/D exchange of guest molecules has been investigated and reported by our research group.^{88,97} More applications based on CB[7] binding behaviours have also been reported, such as separating positional isomers using CB[7] as an additive,¹⁰⁶ and immobilizing proteins on a solid surface through a non-covalent strategy.¹⁰⁷ More binding events and applications based on CB[7] will be demonstrated in detail in the following sections.

1.3.4.2 Host-Guest Complexation of CB[5], CB[8] and CB[10]

The other three members in the family, CB[5], CB[8] and CB[10], are relatively less developed as they have only been isolated for a couple of years. These CB[n] homologues, however, exhibit promising properties for future investigations in supramolecular chemistry.

Long before the isolation of CB[5],^{70,108} its derivative decamethylcucurbit[5]uril (Me₁₀CB[5]) was synthesized in 1992,¹⁰⁹ and its supramolecular chemistry properties have also been investigated. Bradshaw, Izatt, and coworkers have discovered that Me₁₀CB[5] displays remarkable selectivity for Pb²⁺ ions,¹¹⁰ while CB[5] does not seem to possess the same property. Other than this, CB[5] and Me₁₀CB[5] are expected to have the similar complexation properties, considering the almost identical physical parameters. The supramolecular chemistries of both CB[5] and Me₁₀CB[5] have been limited to the binding of small guest molecules, such as protons and metal ions. In addition, due to the constriction

of the small sized portals, the binding events mostly happen to occur at the portals, rather than in the cavity.^{110,111} It is reported that they both can form weak host-guest complexes with α -, β -, γ -cyclodextrins.¹¹² The most distinguishing property of these two is that they can bind gases such as Kr, Xe, N₂, O₂, Ar, N₂O, NO, CO, CO₂ and NH₃ and small solvent molecules like CH₃OH and CH₃CN.¹¹³⁻¹¹⁵ Miryahara and coworkers demonstrated the reversible sorption and desorption of gases such as N₂O by solid Me₁₀CB[5], indicating the application potentials of CB[5] and Me₁₀CB[5] in reducing NO_x gases levels from the air.^{116,117}

Compared to CB[5], CB[6] and CB[7], the CB[8] possesses a larger cavity, which opens more possibilities in molecular recognition processes. The cavity of CB[8] is similar to γ -cyclodextrin in terms of volume, but is less conformationally flexible. Similar to other CB[n] analogues, CB[8] can selectively bind to larger positively charged guests such as adamantane and methylviologen derivatives,¹¹⁸⁻¹²⁰ by ion-dipole interactions and also prefer to encapsulate large compounds such as fullerene,¹²¹ which can fit perfectly in its cavity. One striking recognition property of CB[8], which is superior to other homologues at this point, is that it is capable of encapsulating two aromatic guests simultaneously into its cavity to form a 1:2 or 1:1:1 host-guest complexes through hydrophobic and π - π stacking interactions.¹²²⁻¹²⁶ This property has attracted considerable attention because it provides unique opportunities in the study of bimolecular reactions,¹²⁷ and molecular recognition¹²⁸ in microenvironments. Kaifer and coworkers demonstrated that the charge-transfer interaction between two aromatic guests has been significantly enhanced upon the inclusion into the cavity of CB[8], as shown in Figure 1.22.¹²⁹ The formation of a 1:1:1 complex has been characterized by X-ray crystallography, indicating that inclusion into the same cavity brought

two molecules close to each other, thus facilitating the charge-transfer process. The cavity of CB[8] is even large enough to include cyclen and cyclam, and more interesting is that the cyclen and cyclam in CB[8] cavity can further coordinate with Cu(II) and Zn(II) to form metal macrocycle compounds within macrocycle complexes.¹³⁰

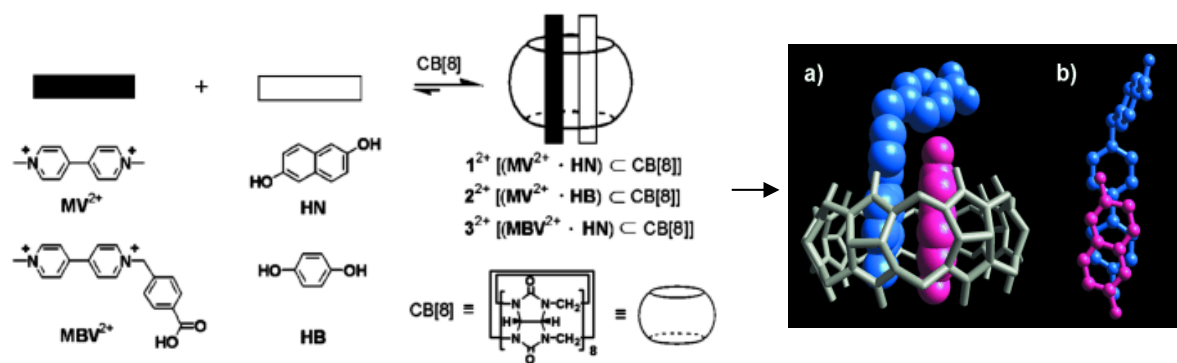


Figure 1.22 Charge-transfer (CT) complexes formed in CB[8] and two comparative crystal structures.¹²⁹ (On the right: crystal structures of (a) $MBV^{2+} \cdot HN$ in CB[8] and (b) $MBV^{2+} \cdot HN$)

The CB[10], discovered as its $CB[5]@CB[10]$ (CB[5] is included in CB[10] cavity) complex a couple of years ago,⁶⁹ was recently isolated by Isaacs and coworkers.⁸⁷ Similar to other family members, CB[10] retains the property of forming stable complexes with a series of guest molecules. However, like CB[8], with the large cavity size, CB[10] shows more novel binding opportunities and application potential. With its vast cavity (870 \AA^3 in volume), CB[10] can especially bind to some important chemical and biochemical substances, such as dyes, fluorophores and peptides, which provides the possible applications in drug delivery and peptides sensing, etc. The cavity size of CB[10] is also large enough for the

encapsulation of some host molecules such as cyclodextrins and calixarenes, by which the combination of utilizing the beneficial features of both hosts will be possible. However, initial studies indicate that only one calix[4]arene derivative can be included into the CB[10] cavity, and after inclusion it can further bind with adamantane derivatives to form a termolecular complex. The interesting part is this calix[4]arene derivative alone does not form complexes with any adamantane derivatives. The formation of termolecular complexes provides CB[10] with broad applications such as in chiral recognition and efficient allosteric control of macromolecular geometries. The preliminary research results foreshow the promising future of CB[10], which might become competitive with CB[8] in the field of molecular machines and biomimetic systems.

1.3.5 Applications of the Cucurbituril Family

As was discussed previously, the unique structures and the outstanding host-guest complexation and molecular recognition properties of the CB[n] family impart them with a variety of applications in a wide range of fields, some of which will be highlighted briefly in this section.

1.3.5.1 Reaction Mediators

In chemical reactions, if two active reactants can be positioned in specific distance and geometry, the reaction between them can be catalyzed in a stereoselective manner. Cucurbit[n]urils, as a result of their unique cavities, can encapsulate two molecules to form 1:1:1 or 1:2 complexes through various non-covalent interactions. Therefore, the cavities of cucurbiturils can function as a reaction “chamber” to mediate chemical reactions. The CB[6]

was first utilized for this purpose by Mock and coworkers, to catalyze the 1,3-dipolar addition reaction between azide and alkyne,¹³¹ as shown in Figure 1.23. The result indicated that the reaction was accelerated by a factor of 5.5×10^4 in the presence of CB[6]. Meanwhile, the high regioselectivity was maintained, which assures that only 1,4-disubstituted triazole was formed as single product. This striking function of CB[6] has subsequently been employed for the preparation of catalytically self-threading rotaxanes,¹³² pseudorotaxanes¹³³ and polyrotaxanes^{134,135} by Steinke and coworkers.

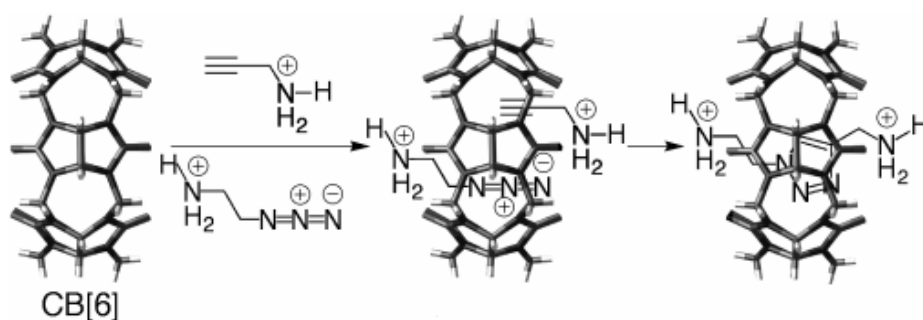


Figure 1.23 CB[6] functions as a “chamber” to catalyze the 1,3-dipolar addition reaction between azide and alkyne.¹³¹

Recently, Kim *et al.* reported the highly stereoselective [2+2] photoreaction of *trans*-diaminostilbene dihydrochloride catalyzed by CB[8] in aqueous solution.¹²⁴ In the 1:2 complexes that are formed, the two guest molecules are held within the cavity of CB[8], where the olefinic groups of the two guests are positioned in a parallel orientation in close proximity, offering high stereoselectivity for the reaction. Based on the same “chamber” effect, the Ramamurthy group and our research group simultaneously demonstrated the CB[8]-promoted photodimerization of *trans*-1,2-bis(4-pyridyl)ethylene and *trans*-N-stilbazoles, which leads to the *syn* dimer in high yield.¹³⁶ Our research group recently

reported that CB[7] can also function as a reaction mediator.⁹⁰ The photodimerization of protonated 2-aminopyridine in aqueous solution yield exclusively the *anti-trans* dimer, which is stabilized upon inclusion, under the direction of CB[7] as a template.

Other than accelerating the reactions and increasing the stereoselectivity between two reactants, CB[n] can also act as a reaction inhibitor, protecting guest molecules from degeneration by encapsulating them into cavities. Recently, our group has reported that the encapsulation of (*E*)-1-ferrocenyl-2-(1-methyl-4-pyridinium)ethylene cation into CB[7] cavity protected it from (*E*) to (*Z*) photoisomerization in aqueous solution to a great extent.⁹⁷ Nau and coworkers demonstrated that the photobleaching and aggregation processes of dye molecule rhodamine 6G is significantly inhibited by complexation with CB[7].¹³⁷ More recently, our research group reported that the inclusion of the α,α' -bis(3-(1-methylimidazolium))-*p*-xylene dication ion into the cavity of CB[7] remarkably inhibits the H/D exchange of the α -carbon proton, due to the formation of hydrogen bonds between the α -carbon protons and oxygen atoms of the carbonyl portals.⁸⁸

All of these examples illustrate that the unique cavity of the CB[n] host can function as a chamber for proper sized guests to either accelerate bimolecular reactions with high regio- and stereoselectivity or protect the guests by inclusion, mediating reactions in a desired manner.

1.3.5.2 Molecular Machines and Switches

A molecular machine is a device on the molecular scale in which the components can display reversible relative position changes upon stimulation by external factors, such as light, electrical energy and chemical energy. This reversible change usually leads to a change in

the physical or chemical properties of the supramolecular system, thus resulting in the change in “output” signals, which can be used to monitor the operation of the molecular machine. The reversibility, by which it is possible to bring the system back to the initial situation by applying an opposite stimulus, is an essential feature for molecular machines. The term “molecular machine” was first coined in late 1980s, and the interest in it has grown exponentially since, such that now it has received considerable attention and research interest.¹³⁸ The CB[n] family, popular host molecules with ready availability and exquisite selectivity, have been explored for building molecular machines.

The first example of CB[n] being employed as a component of molecular machine was reported by Mock and coworkers in 1990.¹³⁹ In their work, a pseudorotaxane of CB[6] and $\text{PhNH}(\text{CH}_2)_6\text{NH}(\text{CH}_2)_4\text{NH}_2$ was formed and introduced as a molecular switch, a type of molecular machines. The CB[6] acts as a shuttle between two alkyl sites along the linear “string” upon a change of the pH value of the system. When the pH is below 6.7, at which point the aniline can be protonated, CB[6] will reside on the hexyldiammonium site with the two positively charged $-\text{NH}_2^+$ groups interacting with the two carbonyl portals. When the pH is increased higher than 6.7, at which point the anilinium will be deprotonated, the CB[6] will vacate the monoprotonated hexyl part and move to the butyldiammonium site with two $-\text{NH}_2^+$ groups optimizing the interactions, as shown in Figure 1.24. Kim and coworkers demonstrated a similar reversible fluorescent molecular switch based on a pseudorotaxane containing a CB[6] bead and a fluorenyltriamine string.¹⁴⁰ The shuttling of inclusion between different locations on the guest molecule, induced by pH changes, can be easily observed by the colour and fluorescence changes. A kinetically controlled molecular switch has also been designed and reported by the same research group, in which the binding

locations of CB[6] on the guest were both thermodynamically controlled and pH dependent.¹⁴¹ A large number of papers about CB[n]-based pH-dependant molecular switches have been published since this pioneering work, such as a pH-controlled on/off molecular shuttle¹⁴² and a polymeric switch based on pseudo-polyrotaxanes.¹⁴³

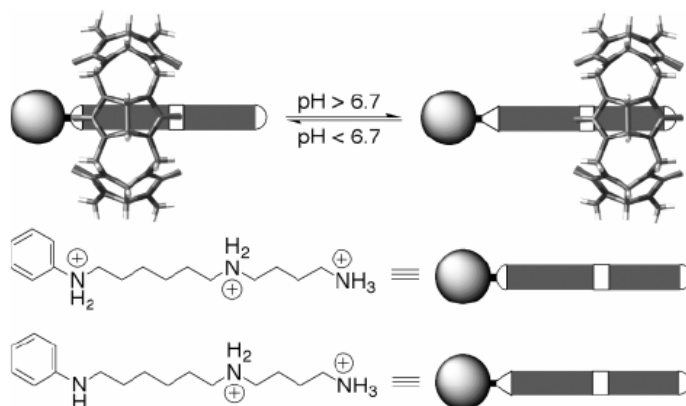


Figure 1.24 One example of a molecular switch based on CB[6].¹³⁹

Other than being actuated by a pH change, many molecular machines are based on stimuli such as photochemical or electrochemical factors.¹⁴⁴⁻¹⁴⁶ Kim's research group first designed and reported a novel [2]pseudorotaxane-based molecular machine, in which the guest can reversibly form a molecular loop with the CB[8] cavity upon electrochemical and photochemical stimuli. Kaifer and coworkers, extending this work, recently reported the redox-switchable dendrimers¹⁴⁷ and pH- or redox-driven molecular switches based on a pseudorotaxane containing CB[7].¹⁴² More work concerning the applications of CB[n] in fluorescent switches has been undertaken and reported by Wagner,^{85,148,149} Nau,¹⁰⁴ and our research group.^{122,151}

Inspired by the fact that molecular machines display a change in the “output” signal

upon stimuli, these machines were further specifically designed and used as molecular detectors. Kaifer and coworkers first designed and constructed a CB[8]-based molecular sensor,¹⁵² in which a binary inclusion complex between CB[8] and the 2,7-dimethyldiazapyrenium dication ($\text{Me}_2\text{DAP}^{2+}$) was formed, and then used to detect the presence of electron-rich aromatic guests such as catechol or dopamine, according to the fact that the further binding of the complex with these electron-rich guests will result in the quenching of the fluorescence of $\text{Me}_2\text{DAP}^{2+}$, as shown in Figure 1.25.

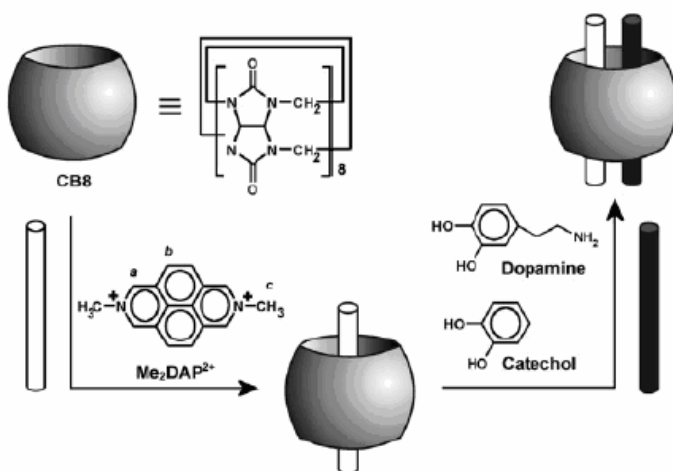


Figure 1.25 Formation of a binary complex, based on CB[8], acting as a detector to sense catechol and dopamine by forming ternary complexes.¹⁵²

The molecular recognition of peptides and proteins in aqueous solution has become a hot topic recently, with broad potential applications in the chemical and biochemical sciences.¹⁵³ Urbach and coworkers reported a novel molecular sensor for the recognition of N-terminal tryptophan in aqueous solution by the synthetic host CB[8], which is known to be capable of forming a 1:1:1 heteroternary complex with aromatic guests.¹⁵⁴ In their

investigation, a complex of CB[8] and methyl viologen (MV^{2+}) was used to further bind with three tryptophan-containing tripeptides. The $\{CB[8]\cdot MV\}^{2+}$ was determined to bind the N-terminal tryptophan with a much higher binding affinity, relative to internal or C-terminal tryptophans. In addition, the formation of a charge-transfer stabilized ternary complex is accompanied by an increase in the charge transfer band and fluorescence quenching of the indole moiety in the peptides. The high binding selectivity and induced change in optical properties makes $\{CB[8]\cdot MV\}^{2+}$ a promising molecular sensor for the detection and separation of peptides with a specific sequence.

1.3.5.3 Drug Delivery and Gene Transfection

Given the characteristic properties such as a hydrophobic cavity and two hydrophilic entrances at the upper and lower portions, the CB[n] family can form very stable non-covalent linkages, in particular, with compounds having an amino or carboxyl functional groups. As a result, numerous studies about the development of drug delivery systems using CB[n] have been conducted in recent years. It has been reported that CB[n] can form stable complexes with some platinum compounds,^{99,100} which have the potential to be used as anticancer drugs. In addition, it was observed that the toxicity of these platinum compounds is significantly reduced upon their complexation with CB[n]. Therefore, CB[n] can function as a drug carrier, stabilizing and carrying the drug through the body and then releasing it where the infection is, thus avoiding the unwanted side effects caused by the binding of hydrolysed platinum drugs to proteins.

Nakamura, Kim and coworkers reported that CB[6] can be selectively delivered to DNA by a mediator through a non-covalent self-assembly process.¹⁴⁵ A guest molecule

containing an acridine unit and tetramine regions, which can be intercalated into DNA and bind with CB[6], respectively, has been designed and employed for this delivery process. The CB[6] and DNA do not bind to each other alone, however in the presence of the guest molecule a ternary complex containing CB[6], the linker and DNA were formed, as shown in Figure 1.26. The formation of this termolecular complex partially protects the DNA from cleavage by the restriction enzyme BanII. Similarly, Kim and coworkers recently demonstrated that a series of dendrimers containing diaminobutane moieties can form ternary complexes with CB[6] and DNA, functioning as an efficient gene delivery carrier.¹⁵⁵

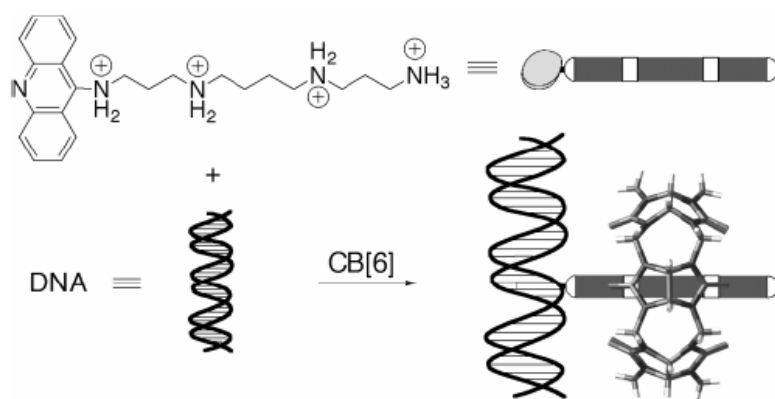


Figure 1.26 CB[6] can be delivered to DNA through a non-covalent self-assembly.¹⁴⁵

1.3.5.4 Waste-Stream Remediation

Behrend and coworkers first reported the complexation of indicator dyes such as Congo red and methylene blue with CB[6] in 1905,^{64,65} which opened the gate for CB[n] being employed for the treatment of waste streams. Research carried out by the Dantz and Buschmann groups^{156,157} suggested that CB[n] could function as a sorbent for water treatment by removing aromatic compounds from contaminated water sources, and dyes from textile wastewater. However in 2001, Karcher *et al.*¹⁵⁸⁻¹⁶⁰ investigated the influence of parameters

such as pH, temperature and salt concentrations on the sorption of these guests by CB[n], revealing that CB[n] is not actually feasible as a sorbent in wastewater treatment due to their poor solubility unless they are covalently fixed onto suitable supporting materials which could reduce the dissolution problem. The fixation of CB[n] on a supporting carrier such as silica has been developed, however the regeneration of CB[n] is still a major issue. Therefore, to date the practical application of CB[n] for wastewater treatment remains unlikely for economic reasons.

1.3.6 Cucurbit[n]uril Derivatives

Despite the wide range of applications of the CB[n] family in molecular recognition, self-assembly and nanotechnology, described in the previous sections, the major limitations such as poor solubility in both aqueous and organic solutions and the difficulty in introducing functional groups on their surface, have blocked further expansion of their possible applications. Therefore, numerous attempts to prepare CB[n] derivatives to overcome these main shortcomings have been carried out over the past several years.

1.3.6.1 Synthesis of Cucurbit[n]uril Derivatives

In principle, there are three potential pathways to introduce functional groups at the periphery of CB[n], as shown in Figure 1.27.⁷⁰ The condensation of substituted glycolurils with formaldehyde (route 1) and the direct functionalization at the “bridging” position or at methylene linkers (route 3) turn out to be effective and are now widely used for the preparation of CB[n] derivatives. Attempts with route 2, however, using substituted aldehydes, have never shown a trace of success, despite the numerous efforts.

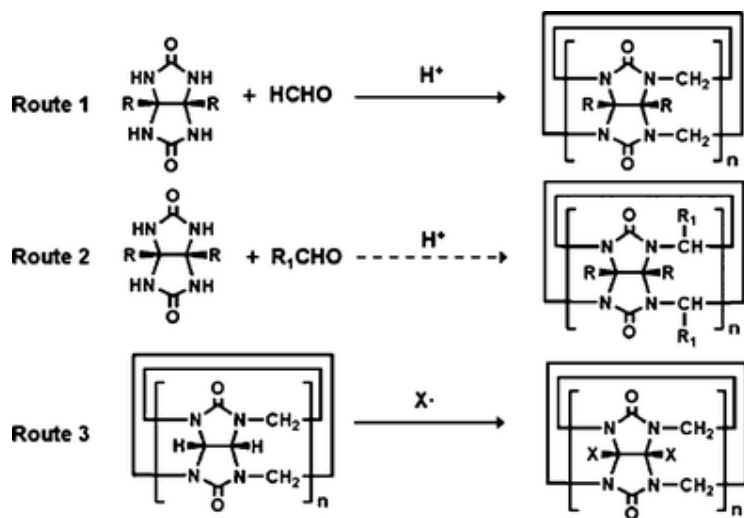


Figure 1.27 Three ways to introduce functional groups at the periphery of cucbiturils.⁷⁰

The first reported work, by Stoddart and coworkers in 1992, was the successful synthesis of Me₁₀CB[5] from dimethylglycoluril and formaldehyde through route 1 under acidic conditions.¹⁰⁹ However, it turns out that the introduction of methyl groups does not improve the solubility of CB[n] in common solvents. Later on, Kim and coworkers demonstrated that the formation of CB[n] derivatives with fused cyclohexyl rings on the “equator” position increased the solubility significantly in both water and organic solvents, such as DMF.¹⁶¹ The limitation of this method is that only small homolog (mainly CB[5]) derivatives are formed due to relatively large steric hindrance in the cyclization process. Nakamura and coworkers reported the synthesis of partially substituted CB[n] by condensation between a mixture of glycoluril and a substituted glycoluril, in specific ratios, and formaldehyde.¹⁶² The formation and separation of Me₄CB[6] and Me₆CB[6] were

reported by Day and coworkers by employing glycoluril and dimethylglycoluril bis(cyclic ether), as the equivalent of dimethylglycoluril, with formaldehyde in the condensation reaction.¹⁶³ Recently, partially substituted CB[6] derivatives with reactive functional groups including *m*- and *p*-diaminophenyl were synthesized and reported by the Kim group.⁷⁰ The solubilities of *m*- and *p*-diaminophenylCB[6] in water have been determined to be fairly good, which allows for the further purification of crude products by gel permeation chromatography and opens up new opportunities in applications.

Route 3, referred to as direct functionalization of CB[n], was thought unlikely for a long time because of the high chemical stability of the CB[n] themselves. However, Kim and coworkers have recently developed the first direct functionalization method, in which K₂S₂O₈ was employed as an oxidant for CB[n] in aqueous solution, to yield hydroxyl derivatives of CB[n] in moderate yield. Optimizations of the reaction condition are still in progress and partial hydroxylation of CB[n] was also proven to be possible, however a complex mixture of hydroxylated products is formed. The high solubility of hydroxyl CB[n] derivatives in DMSO and DMF makes the further functionalization via conventional organic transformation methods such as acylation or alkylation possible.

1.3.6.2 Applications of Cucurbit[n]uril Derivatives

Ions channels are of great importance in controlling ion transportation across membranes, which are usually too hydrophobic for the ion to pass alone. Given the resemblance of the carbonyl portals to the selectivity filter for the K⁺ channel, alkylated CB[n] compounds, such as [CH₃(CH₂)₇S(CH₂)₃O]_{2n}CB[n] (n = 5, 6) were synthesized and incorporated into a unilamellar vesicle by Kim and coworkers, functioning as a ion channel

for proton and alkali metal ions with high selectivity.¹⁶⁴

Kim's group recently reported a new amphiphilic CB[6] derivative $(\text{CH}_3(\text{OCH}_2\text{CH}_2)_3\text{S}(\text{CH}_2)_3\text{O})_{12}\text{CB}[6]$, which can form a vesicle upon sonication with water for 30 minutes.¹⁶⁵ The easily accessible cavity at the vesicle surface and their strong affinity toward polyamines make further modification of the vesicle fairly easy through noncovalent host-guest interactions instead of conventional covalent bonds, which usually requires multi-step synthesis and ends up with low yields. This novel feature will lead to more broad practical applications, such as use in targeted drug/gene delivery systems and in the development of nanostructural materials.

More applications of CB[n] derivatives in a wide range of fields have been reported.^{166,167} For example, the use of $(\text{allyloxy})_{12}\text{CB}[6]$ in the formation of and further functionalization of 2D polymers was investigated, and the immobilization of CB[n] derivatives on a solid surface, functioning as molecular sensors, was also demonstrated by the Kim group.⁷⁰ Recently, CB[n]-anchored silica gel with high separation efficiency for alkaloids was reported by the Kim^{70,72} and Liu⁸⁷ research groups, independently. In addition, the usage of CB[n] derivatives in constructing ion selective electrodes and in the field of antibiotics is under development.¹⁶⁸

1.3.7 Summary and Perspectives

Although the first member in the CB[n] family, CB[6], was synthesized over one hundred years ago, the supramolecular chemistry of this family has just begun to blossom due to the major shortcomings such as poor solubility and inability of further modification. Despite these drawbacks, as novel host molecules with a pumpkins shape, CB[n] still draw

considerable attention in the studies of molecular recognition and host-guest chemistry. Because of their unique and rigid structures, with a hydrophobic cavity accessible from two carbonyl-lined portals, the CB[n] family displays remarkable binding affinity to alkanediammonium ions with high size, shape and functional-group selectivity and usually slow exchange kinetics. To date, the study for binding kinetics and mechanism has been limited to investigations between CB[6] and alkanediammonium ions, which were mainly reported by Nau and coworkers.^{80,81} With the synthesis and isolation CB[n] homologues such as CB[5], CB[7] and CB[8] by the Day^{68,69} and Kim⁶⁷ research groups, the applications of CB[n] family have been expanded dramatically in the many areas such as the catalysis of chemical reactions, development of molecular machines and sensors, waste stream purifications, and drug and gene delivery. Recently, the functionalization of CB[n] brought their chemistry into another dynamic stage, in which the earlier problems are fully or partially solved and more practical applications in chemistry, physics, biochemistry and material science are likely to be developed. The unique structure and novel complexation properties suggest that CB[n] family will challenge other well-known host molecules like cyclodextrins and crown ethers as a molecular recognition platform and become important components in molecular machines, sensors and nanotechnology.

1.4 Research Aims

Given the novel structural and binding properties of the CB[n] family and inspiration from the research of other groups worldwide, my research has been focused on investigations of the host-guest complexation of CB[n] with a series of guest molecules whose physical, chemical or electrochemical properties will change upon the inclusion into the CB[n] cavity,

and can be monitored and spectroscopically characterized by techniques such as NMR, UV-visible, and circular dichroism spectroscopy, mass spectrometry, cyclic voltammetry, and polarimetry. The specific aims are as follows:

1. To investigate the different binding behaviours of CB[6] and CB[7] towards a tetracationic bis(viologen) guest molecule, $[\text{CH}_3\text{bpy}(\text{CH}_2)_6\text{bpyCH}_3]^{4+}$ (bpy = 4,4'-bipyridinium), exploring the possibility of the formation of pseudorotaxanes.
2. To study the chirotopic behaviour of chiral molecules (*S*- and *R*-N-benzyl-1-(1-naphthyl)ethylamine (BNEAH⁺) upon the complexation with the achiral CB[7] in aqueous solution.
3. To investigate the kinetics of the electron self-exchange and electron-transfer reactions of the (trimethylammonio)methylferrocene (FcTMA⁺) host-guest complex with cucurbit[7]uril in aqueous solution.
4. To extend the investigations of CB[7] and CB[8] complexes of ferrocenes to other metallocenes, such as bis(ferrocene) and titanocene guest molecules.

References

1. Lehn, J. M. *Pure Appl. Chem.* **1978**, *50*, 871.
2. Lehn, J. M. *Angew. Chem. Int. Ed. Engl.* **1988**, *27*, 89.
3. Steed, J. W.; Atwood, J. L. *Supramolecular Chemistry*, Wiley: New York, **2000**.
4. Lindoy, L. F.; Atkinson, I. M. *Self-assembly in Supramolecular Systems* The Royal Society of Chemistry: Cambridge, **2000**.
5. Pimentel, G. C.; McClellan, A. L. *The Hydrogen Bond*, Freeman: San Francisco, **1960**.
6. Beer, P. D.; Gale, P. A.; Smith, D. K. *Supramolecular Chemistry*, Oxford University Press, Oxford, **1999**.
7. Gellman, S. H. *Chem. Rev.* **1997**, *97*, 1231.
8. Bielawski, C.; Chen, Y. S. *Chem. Commun.* **1998**, 1313.
9. Breault, G. A.; Hunter, C. A.; Mayers, P. C. *Tetrahedron* **1999**, *55*, 5265.
10. Rowan, S. J.; Cantrill, S. J.; Cousins, G. R.; Sanders, J. K.; Stoddart J. F. *Angew. Chem., Int. Ed.* **2002**, *41*, 898.
11. Cacciapaglia, R.; Di Stefano, S.; Mandolini, L. *J. Am. Chem. Soc.* **2005**, *39*, 13666.
12. Atwood, J. L. *Math. Phys. Sci.* **1996**, *480*, 1
13. Rissanen, K. *Anal. Meth. Supramol. Chem.* **2007**, 305.
14. Tsukube, H.; Furuta, H.; Odani, A.; Takeda, Y.; Kudo, Y.; Inoue, Y.; Liu, Y.; Sakamoto, H.; Kimura, K., In *Comprehensive Supramolecular Chemistry*, Volume 8, J. L. Atwood, J. E. D. Davies, D. D. MacNicol, F. Vögtle, Eds., Elsevier, Oxford, **1996**, 425.
15. Kogej, M.; Schalley, C. A. *Anal. Meth. Supramol. Chem.* **2007**, 104.
16. Baytekin, B.; Baytekin, H. T.; Schalley, C. A. *Org. Biomol. Chem.* **2006**, *4*, 2825.

17. Johnston, L. J.; Wagner, B. D. In *Comprehensive Supramolecular Chemistry*, Volume 8, J. L. Atwood, J. E. D. Davies, D. D. MacNicol, F. Vögtle, Eds., Elsevier, Oxford, **1996**, 537.
18. Yuan, L.; Wang, R.; Macartney, D. H. *J. Org. Chem.* **2007**, *72*, 4539.
19. Smith, A. C.; Macartney, D. H. *J. Org. Chem.* **1998**, *63*, 9243.
20. Macartney, D. H. *J. Chem. Soc., Perkin Trans. 2*, **1996**, *12*, 2775.
21. Macartney, D. H.; Waddling, C. A. *Inorg. Chem.* **1994**, *33*, 5912
22. Wylie, R. S.; Macartney, D. H. *J. Am. Chem. Soc.*, **1992**, *114*, 3136.
23. Hettiarachchi, D. S. N.; Macartney, D. H. *Can. J. Chem.* **2006**, *84*, 905.
24. Lyon, A. P.; Macartney, D. H. *Inorg. Chem.* **1997**, *36*, 729.
25. Pedersen, C. J. *J. Am. Chem. Soc.* **1967**, *89*, 7071
26. Connors, K. A. *Binding Constants: The Measurement of Molecular Complex Stability*, Wiley, Chichester, UK, **1987**.
27. Cram, D. J.; Cram, J. M. *Container Molecules and Their Guests*; The Royal Society of Chemistry: Cambridge, **1994**.
28. Moran, J. R.; Karbach, S.; Cram, D. J. *J. Am. Chem. Soc.* **1982**, *104*, 5826.
29. MacNicol, D. D.; McKendrick, J. J.; Wilson, D. R. *Chem. Soc. Rev.* **1978**, *7*, 65.
30. Tsoucaris, G.; Knossow, M.; Green, B. S.; Arad-Yellin, R. *Mol. Cryst. Liq. Cryst.* **1983**, *96*, 181.
31. Bradshaw, J. S.; Izatt, R. M.; Bordunov V.; Zhu, C. Y.; Hathaway, J. K. In *Comprehensive Supramolecular Chemistry*, G. W. Gokel, Ed., **1996**.
32. (a) Bradshaw, J. S.; Izatt, R. M. *Acc. Chem. Res.* **1997**, *30*, 338; (b) Gokel, G. W.; Leevy, W. M.; Weber, M. E. *Chem. Rev.* **2004**, *104*, 2723.

33. (a) Graf, E.; Lehn, J.-M. *J. Am. Chem. Soc.* **1976**, *98*, 6403; (b) Dietrich, B. In *Comprehensive Supramolecular Chemistry*, Volume 10, J. L. Atwood, J. E. D. Davies, D. D. MacNicol, F. Vögtle, Eds., Elsevier, Oxford, **1996**, 361.
34. Arnaud-Neu, F.; Loufouilou, E. L.; Schwing-Weill, M. J. *J. Chem. Soc., Dalton Trans.* **1986**, 2629.
35. Dalley, N. K.; Smith, J. S.; Larsen, S. B.; Matheson, K. L.; Christensen, J. J.; Izatt, R. *M. J. Chem. Soc., Chem. Commun.* **1975**, 84.
36. Gutsche, C. D. *Calixarenes*; The Royal Society of Chemistry: Cambridge, 1989.
37. Mandolini, L.; Ungaro, R. *Calixarenes in Action*; Imperial College Press: London, **2000**.
38. Boehmer, V. In *Chemistry of Phenols*; Rappoport, Z., Ed.; Wiley: Chichester, **2003**.
39. Gutsche, C. D. *Acc. Chem. Res.* **1983**, *16*, 161.
40. Lhotak, P.; Shinkai, S. *J. Phys. Org. Chem.* **1997**, *10*, 273.
41. Lhotak, P. *Top. Curr. Chem.* **2005**, *255*, 65.
42. Casnati, A.; Sansone, F.; Ungaro, R. *Adv. in Supramol. Chem.* **2003**, *9*, 163.
43. Rothmund P. *J. Am. Chem. Soc.* **1936**, *58*, 625.
44. Rothmund P. *J. Am. Chem. Soc.* **1935**, *57*, 2010.
45. Smith, K. M. *Porphyrins and Metalloporphyrins*; Elsevier: Amsterdam, 1976.
46. Balaban, T. S. *Acc. Chem. Res.* **2005**, *38*, 612.
47. Maruyama, K.; Osuka, A. *Pure Appl. Chem.* **1990**, *62*, 1511.
48. Hush, N. S.; Reimers, J. R.; Hall, L. E.; Johnston, L. A.; Crossley, M. J. *Ann. New York Acad. Sci.* **1998**, *852*, 1.
49. Hedges, A. R. *Chem. Rev.* **1998**, *98*, 2035.
50. Szejtli, J. *J. Mater. Chem.* **1997**, *7*, 575.

51. Harada, A. In *Large Ring Molecules*; Semlyen, J. A., Ed.; Wiley: Chichester, **1996**.
52. Harada, A.; Takahashi, S. *J. Chem. Soc., Chem. Commun.* **1984**, 645.
53. Hapiot, F.; Tilloy, S.; Monflier, E. *Chem. Rev.* **2006**, *106*, 767.
54. Rekharsky, M. V.; Inoue, Y. *Chem. Rev.* **1998**, *98*, 1875.
55. Harada, A. *Acc. Chem. Res.* **2001**, *34*, 456.
56. Wenz, G.; Han, B.-H.; Muller, A. *Chem. Rev.* **2006**, *106*, 782.
57. Takahashi, K. *Chem. Rev.* **1998**, *98*, 2013.
58. Uekama, K.; Hirayama, F.; Irie, T. *Chem. Rev.* **1998**, *98*, 2045.
59. Hedges, A. R. *Chem. Rev.* **1998**, 2035.
60. Mock, W. L. *Top. Curr. Chem.* **1995**, *175*, 1
61. Kim, K. *Chem. Soc. Rev.* **2002**, *31*, 96.
62. Lee, J. W.; Samal, S.; Kim, H.-J.; Kim, K. *Acc. Chem. Res.* **2003**, *36*, 621.
63. Gerasko, O. A.; Samsonenko, D. G.; Fedin, V. P. *Russ. Chem. Rev.* **2002**, *71*, 741.
64. Lagona, J.; Mukhopadhyay, P.; Chakrabarti, S.; Isaacs, L. *Angew. Chem., Int. Ed.* **2005**, *44*, 4844.
65. Behrend, R.; Meyer, E.; Rusche, F. *Justus Liebigs Ann. Chem.* **1905**, 339, 1.
66. Freeman, W. A.; Mock, W. L.; Shih, N.Y. *J. Am. Chem. Soc.* **1981**, *103*, 7367.
67. Kim, J.; Jung, I. S.; Kim, S.Y.; Lee, E.; Kang, J.K.; Sakamoto, S.; Yamaguchi, K.; Kim, K. *J. Am. Chem. Soc.* **2000**, *122*, 540.
68. Day, A. I.; Arnold, A. P.; Blanch, R. J. *Molecules*, **2003**, *8*, 74.
69. Day, A. I.; Blanch, R. J.; Arnold, A. P.; Lorenzo, S.; Lewis, G. R.; Dance, I. *Angew. Chem., Int. Ed.* **2002**, *41*, 275.

70. Kim, K.; Selvapalam, N.; Ko, Y. H.; Park, K. M.; Kim, D.; Kim, J. *Chem. Soc. Rev.* **2007**, *36*, 267.
71. Day, A. I.; Arnold, A. P.; Blanch, R. J.; Snushall, B. *J. Org. Chem.* **2001**, *66*, 8094.
72. Kim, K.; Samal, S.; Kumar, R. N.; Selvapalam, N.; Oh, D. H. *PCT, WO05/103053*, **2005**.
73. Honig, B.; Nicholls, A. *Science* **1995**, *268*, 1144.
74. Mock, W. L.; Shih, N. Y. *J. Org. Chem.* **1986**, *51*, 4440
75. Buschmann, H.J.; Jansen, K.; Meschke, C.; Schollmeyer, E. *J. Solution Chem.* **1998**, *27*, 135.
76. Izatt, R. M.; Terry, R. E.; Haymore, B. L.; Hansen, L. D.; Dalley, N. K.; Avondet, A. G.; Christensen, J. J. *J. Am. Chem. Soc.* **1976**, *98*, 7620.
77. Mock, W. L.; Shih, N. Y. *J. Org. Chem.* **1983**, *48*, 3618.
78. Mock, W. L.; Shih, N. Y. *J. Am. Chem. Soc.* **1988**, *110*, 4706.
79. Mock, W. L.; Shih, N. Y. *J. Am. Chem. Soc.* **1989**, *111*, 2697.
80. Marquez, C.; Hudgins, R. R.; Nau, W. M. *J. Am. Chem. Soc.* **2004**, *126*, 5806.
81. Marquez, C.; Nau, W. M. *Angew. Chem., Int. Ed.* **2001**, *40*, 3155.
82. Kim, H. J.; Jeon, W. S.; Ko, Y. H.; Kim, K. *Proc. Natl. Acad. Sci. USA* **2002**, *99*, 5007.
83. Ong, W.; Gomez-Kaifer, M.; Kaifer, A. E. *Org. Lett.* **2002**, *4*, 1791.
84. Choi, S.; Park, S. H.; Ziganshina, A. Y.; Ko, Y. H.; Lee, J. W.; Kim, K. *Chem. Commun.* **2003**, 2176.
85. Wagner, B. D.; Stojanovic, N.; Day, A. I.; Blanch, R. J. *J. Phys. Chem. B* **2003**, *107*, 10741.
86. Zhang, K.C.; Mu, T.W.; Liu, L.; Guo, Q. X. *Chin. J. Chem.* **2001**, *19*, 558.

87. Liu, S. M.; Ruspic, C.; Mukhopadhyay, P.; Chakrabarti, S.; Zavalij, P. Y.; Isaacs, L. J. *Am. Chem. Soc.* **2005**, *127*, 15959.
88. Wang, R. B.; Yuan, L. N.; Macartney, D. H. *Chem. Commun.* **2006**, 2908.
89. Yuan, L.; Wang, R.; Macartney, D. H. *Tetrahedron: Asymmetry* **2007**, *18*, 483.
90. Wang, R.; Yuan, L.; Macartney, D. H. *J. Org. Chem.* **2006**, *71*, 1237.
91. Shen, Y.; Xue, S.; Zhao, Y.; Zhu, Q.; Tao, Z. *Chin. Sci. Bull.* **2003**, *48*, 2694.
92. Mukhopadhyay, P.; Wu, A.; Isaacs, L. *J. Org. Chem.* **2004**, *69*, 6157.
93. Ma, P.; Dong, J.; Xiang, S.; Xue, S.; Zhu, Q.; Tao, Z.; Zhang, J.; Zhou, X. *Sci. China Ser. B* **2004**, *47*, 301.
94. Blanch, R. J.; Sleeman, A. J.; White, T. J.; Arnold, A. P.; Day, A. I. *Nano Lett.* **2002**, *2*, 147.
95. Constabel, F.; Geckeler, K. E. *Fuller. Nanotub. Carbon Nanostruct.* **2004**, *12*, 811.
96. Jeon, W. S.; Moon, K.; Park, S. H.; Chun, H.; Ko, Y. H.; Lee, J. Y.; Lee, E. S.; Samal, S.; Selvapalam, N.; Rekharsky, M. V.; Sindelar, V.; Sobransingh, D.; Inoue, Y.; Kaifer, A. E.; Kim, K. *J. Am. Chem. Soc.* **2005**, *127*, 12984.
97. Wang, R.; Yuan, L.; Macartney, D. H. *Organometallics* **2006**, *25*, 1820.
98. Ong, W.; Kaifer, A. E. *Organometallics* **2003**, *22*, 4181.
99. Jeon, Y. J.; Kim, S. Y.; Ko, Y. H.; Sakamoto, S.; Yamaguchi, K.; Kim, K. *Org. Biomol. Chem.* **2005**, *3*, 2122.
100. Wheate, N. J.; Day, A. I.; Blanch, R. J.; Arnold, A. P.; Cullinane, C.; Collins, J. G. *Chem. Commun.* **2004**, 1424.
101. Ong, W.; Kaifer, A. E. *J. Org. Chem.* **2004**, *69*, 1383.
102. Moon, K.; Kaifer, A. E. *Org. Lett.* **2004**, *6*, 185.

103. Sindelar, V.; Moon, K.; Kaifer, A. E. *Org. Lett.* **2004**, *6*, 2665.
104. Marquez, C.; Nau, W. M. *Angew. Chem. Int. Ed.* **2001**, *40*, 4387.
105. Mohanty, J.; Nau, W. M. *Photochem. Photobiol. Sci.* **2004**, *3*, 1026.
106. Xu, L.; Liu, S. M.; Wu, C. T.; Feng, Y.Q. *Electrophoresis* 2004, *25*, 3300.
107. Hwang, I.; Baek, K.; Jung, M.; Kim, Y.; Park, K. M.; Lee, D.-W.; Selvapalam, N.; Kim, K. *J. Am. Chem. Soc.* **2007**, *129*, 4170.
108. Jansen, K.; Buschmann, H. J.; Wego, A.; Dopp, D.; Mayer, C.; Drexler, H. J.; Holdt, H. J.; Schollmeyer, E. *J. Incl. Phenom. Macrocycl. Chem.* **2001**, *39*, 357.
109. Flinn, A.; Hough, G. C.; Stoddart, J. F.; Williams, D. J. *Angew. Chem. Int. Ed. Engl.* **1992**, *31*, 1475.
110. Buschmann, H. J.; Cleve, E.; Jansen, K.; Schollmeyer, E. *Anal. Chim. Acta* **2001**, *437*, 157.
111. Zhang, X. X.; Krakowiak, K. E.; Xue, G.; Bradshaw, J. S.; Izatt, R. M. *Ind. Eng. Chem. Res.* **2000**, *39*, 3516.
112. Buschmann, H. J.; Cleve, E.; Jansen, K.; Wego, A.; Schollmeyer, E. *Mater. Sci. Eng. C* **2001**, *114*, 35.
113. Rudkevich, D. M. *Angew. Chem., Int. Ed.* **2004**, *43*, 558.
114. Kellersberger, K. A.; Anderson, J. D.; Ward, S. M.; Krakowiak, K. E.; Dearden, D. V. *J. Am. Chem. Soc.* **2001**, *123*, 11316.
115. Rockwood, A. L.; Van Orman, J. R.; Dearden, D. V. *J. Am. Soc. Mass Spectrom.* **2004**, *15*, 12.
116. Miyahara, Y. JP2003212877, 2001 [*Chem. Abstr.* **2001**, *135*, 6819].
117. Miyahara, Y.; Abe, K.; Inazu, T. *Angew. Chem. Int. Ed.* **2002**, *41*, 3020.

118. Yang, S. L.; Xue, S. F.; Zhu, Q. J.; Tao, Z.; Zhang, J. X.; Zhou, X. *Chin. J. Org. Chem.* **2005**, *25*, 427.
119. Jeon, W. S.; Kim, H. J.; Lee, C.; Kim, K. *Chem. Commun.* **2002**, 1828.
120. Sun, S. G.; Zhang, R.; Andersson, S.; Pan, J. X.; Akermark, B.; Sun, L. C. *Chem. Commun.* **2006**, 4195.
121. Jiang, G. C.; Li, G. T. *J. Photochem. Photobiol. B-Biol.* **2006**, *85*, 223.
122. Wang, R.; Yuan, L.; Ihmels, H.; Macartney, D. H. *Chem. Eur. J.* **2007**, *13*, 6468.
123. Ziganshina, A. Y.; Ko, Y. H.; Jeon, W. S.; Kim, K. *Chem. Commun.* **2004**, 806.
124. Jon, S. Y.; Ko, Y. H.; Park, S. H.; Kim, H. J.; Kim, K. *Chem. Commun.* **2001**, 1938.
125. Pattabiraman, M.; Kaanumalle, L. S.; Natarajan, A.; Ramamurthy, V. *Langmuir* **2006**, *22*, 7605.
126. Pattabiraman, M.; Natarajan, A.; Kaanumalle, L. S.; Ramamurthy, V. *Org. Lett.* **2005**, *7*, 529.
- 127.(a) Kang, J.; Rebek, J., Jr., *Nature* **1997**, *385*, 50; (b) Yoshizawa, M.; Kusukawa, T.; Fujita, M.; Yamaguchi, K. *J. Am. Chem. Soc.* **2000**, *122*, 6311.
- 128.(a) Fujita, M.; Oguro, D.; Miyazawa, M.; Oka, H.; Yamaguchi, K.; Ogura, K. *Nature* **1995**, *378*, 469; (b) Kusukawa, T.; Fujita, M. *Angew. Chem., Int. Ed.* **1998**, *37*, 3142.
129. Kim, H. J.; Heo, J.; Jeon, W. S.; Lee, E.; Kim, J.; Sakamoto, S.; Yamaguchi, K.; Kim, K. *Angew. Chem., Int. Ed.* **2001**, *40*, 1526.
130. Kim, S. Y.; Jung, I. S.; Lee, E.; Kim, J.; Sakamoto, S.; Yamaguchi, K.; Kim, K. *Angew. Chem., Int. Ed.* **2001**, *40*, 2119.
131. Mock, W. L.; Irra, T. A.; Wepsiec, J. P.; Manimaran, T. L. *J. Org. Chem.* **1983**, *48*, 3619.

132. Tuncel, D.; Steinke, J. H. G. *Chem. Commun.* **2002**, 496.
133. Tuncel, D.; Steinke, J. H. G. *Chem. Commun.* **2001**, 253.
134. Tuncel, D.; Steinke, J. H. G. *Chem. Commun.* **1999**, 1509.
135. Tuncel, D.; Steinke, J. H. G. *Macromolecules* **2004**, *37*, 288.
136. Pattabiraman, M.; Natarajan, A.; Kaliappan, R.; Mague, J. T.; Ramamurthy, V. *Chem. Commun.* **2005**, 4542.
137. Mohanty, J.; Nau, W. M. *Angew. Chem., Int. Ed.* **2005**, *44*, 3750.
138. (a) Benniston, A. C. *Chem. Soc. Rev.* **1996**, *25*, 427; (b) Sauvage, J. P. *Chem. Eur. J.* **1998**, *31*, 611; (c) Piotrowiak, P. *Chem. Soc. Rev.* **1999**, *28*, 143.
139. Mock, W. L.; Pierpont, J. J. *Chem. Soc. Chem. Commun.* **1990**, 1509.
140. Jun, S. I.; Lee, J. W.; Sakamoto, S.; Yamaguchi, K.; Kim, K. *Tetrahedron Lett.* **2000**, *41*, 471.
141. Lee, J. W.; Kim, K. P.; Kim, K. *Chem. Commun.* **2001**, 1042.
142. Sindelar, V.; Silvi, S.; Kaifer, A. E. *Chem. Commun.* **2006**, 2185.
143. Tuncel, D.; Tiftik, H. B.; Salih, B. *J. Mater. Chem.* **2006**, *16*, 3291.
144. Jeon, W. S.; Kim, E.; Ko, Y. H.; Hwang, I. H.; Lee, J. W.; Kim, S. Y.; Kim, H. J.; Kim, K. *Angew. Chem. Int. Ed.* **2005**, *44*, 87.
145. Jeon, W. S.; Ziganshina, A. Y.; Lee, J. W.; Ko, Y. H.; Kang, J. K.; Lee, C.; Kim, K. *Angew. Chem., Int. Ed.* **2003**, *42*, 4097.
146. Sobransingh, D.; Kaifer, A. E. *Org. Lett.* **2006**, *8*, 3247.
147. Moon, K.; Grindstaff, J.; Sobransingh, D.; Kaifer, A. E. *Angew. Chem., Int. Ed.* **2004**, *43*, 5496.

148. Wagner, B. D.; Fitzpatrick, S. J.; Gill, M. A.; MacRae, A. I.; Stojanovic, N. *Can. J. Chem.* **2001**, *79*, 1101.
149. Rankin, M. A.; Wagner, B. D. *Supramol. Chem.* **2004**, *16*, 513.
150. Marquez, C.; Nau, W. M. *Angew. Chem., Int. Ed.* **2001**, *40*, 4387.
151. Wang, R.; Yuan, L.; Macartney, D. H. *Chem. Commun.* **2005**, 5867.
152. Sindelar, V.; Cejas, M. A.; Raymo, F. M.; Chen, W. Z.; Parker, S. E.; Kaifer, A. E. *Chem. Eur. J.* **2005**, *11*, 7054.
153. Peczuh, M. W.; Hamilton, A. D. *Chem. Rev.* **2000**, *100*, 2479.
154. Bush, M. E.; Bouley, N. D.; Urbach, A. R. *J. Am. Chem. Soc.* **2005**, *127*, 14511.
155. Lim, Y. B.; Kim, T.; Lee, J. W.; Kim, S. M.; Kim, H. J.; Kim, K.; Park, J. S. *Bioconjugate Chem.* **2002**, *13*, 1181.
156. Buschmann, H.J.; Schollmeyer, E. *J. Incl. Phenom. Mol. Recognit. Chem.* **1992**, *14*, 91.
157. Dantz, D. A.; Meschke, C.; Buschmann, H. J.; Schollmeyer, E. *Supramol. Chem.* **1998**, *9*, 79.
158. Karcher, S.; Kornmuller, A.; Jekel, M. *Water Sci. Technol.* **1999**, *40*, 425.
159. Karcher, S.; Kornmuller, A.; Jekel, M. *Water Res.* **2001**, *35*, 3309.
160. Kornmuller, A.; Karcher, S.; Jekel, M. *Water Res.* **2001**, *35*, 3317.
161. Day, A. I.; Arnold, A. P.; Blanch R. J. WO2000068232, 2000 [*Chem. Abstr.* **2000**, *133*, 362775].
162. Kim, K.; Kim, J.; Jung, I. S.; Kim, S. Y.; Lee, E.; Kang J. K., EP1094065, 2001 [*Chem. Abstr.* **2001**, *134*, 326547].
163. Kim, K.; Kim, J.; Jung, I. S.; Kim, S. Y.; Lee, E.; Kang, J. K., US6365734B1, 2002 [*Chem. Abstr.* **2001**, *134*, 326547z].

164. Jeon, Y. J.; Kim, H.; Jon, S.; Selvapalam, N.; Oh, D. H.; Seo, I.; Park, C. S.; Jung, S. R.; Koh, D. S.; Kim, K. *J. Am. Chem. Soc.* **2004**, *126*, 15944.
165. Lee, H. K.; Park, K. M.; Jeon, Y. J.; Kim, D.; Oh, D. H.; Kim, H. S.; Park, C. K.; Kim, K. *J. Am. Chem. Soc.* **2005**, *127*, 5006.
166. Kim, K.; Jeon, W. S.; Kim, D.; Oh, D. H.; Jon, S. Y. *PCT,WO05/103125*, **2005**.
167. Kim, K.; Balaji, R.; Oh, D. H.; Ko, Y. H.; Jon, S. Y. *PCT,WO04/072151*, **2004**.
168. Zhao, J.; Kim, H. J.; Oh, J.; Kim, S. Y.; Lee, J. W.; Sakamoto, S.; Yamaguchi, K.; Kim, K. *Angew. Chem., Int. Ed.* **2001**, *40*, 4233.

Chapter 2

HOST-GUEST COMPLEXATION BETWEEN CUCURBIT[6]URIL AND CUCURBIT[7]URIL WITH A TETRACATIONIC BIS(VIOLOGEN) GUEST

It has been demonstrated in Chapter 1 that CB[6] and CB[7] show different binding preferences due to different cavity sizes. In this chapter, a tetracationic bis(viologen) guest molecule has been synthesized and employed to investigate the different binding behaviours of CB[6] and CB[7] in aqueous solution by ^1H NMR titrations and mass spectrometry. The formation constants for the [2]pseudorotaxanes and the [3]pseudorotaxane based on CB[6] and CB[7] were determined by different methods to be $K_{\text{CB}[6]} = (8 \pm 2) \times 10^3 \text{ M}^{-1}$, $K_{\text{CB}[7]} = (6 \pm 2) \times 10^3 \text{ M}^{-1}$ and $K_{2\text{CB}[7]} = (6.8 \pm 0.5) \times 10^2 \text{ M}^{-1}$, respectively, which are in good agreement with the values reported for the formation of complexes with similar guests. The effect of the [Host]/[Guest] stoichiometry on the binding modes was studied as well. For CB[6], only a [2]pseudorotaxane was formed with CB[6] residing on the central aliphatic chain, even with a large excess of CB[6] (up to 1.9 equivalents). However, in the case of CB[7], a [2]pseudorotaxane with CB[7] including the central hexamethylene chain was formed when the CB[7] is insufficient (less than 1.0 equivalent). With an increase in the concentration of CB[7], the [2]pseudorotaxane was converted into a [3]pseudorotaxane with two CB[7] encapsulating the two viologens, which can be monitored by the changes in the chemical

shifts of the guest proton resonances in the ^1H NMR spectra. With the encapsulation of one of the viologen groups by a second CB[7], the first CB[7] was forced to abandon its inclusion of central aliphatic chain and move on the other viologen group due to the repulsive interaction between carbonyl portals of CB[7] molecules, thus forming the [3]pseudorotaxane. The formation of these pseudorotaxanes is further confirmed by MALDI-TOF-MS spectrometry. For the first time, a cucurbituril molecular machine which is controlled by the host-guest stoichiometry was demonstrated, opening up new potential applications of CB[n] host molecules in the construction of molecular shuttles and switches.

2.1 Introduction

Due to the different cavity sizes, CB[6] and CB[7] have different binding preferences. CB[6] tends to form stable complexes with aliphatic alkanes, while CB[7] shows high affinity for aromatic moieties, such as pyridines and viologens.¹⁻⁵ Among the guest molecules that have demonstrated specific molecular recognition in their binding modes with the CB[6], CB[7], and CB[8] hosts, the N-alkylated viologen cations have perhaps received the most attention.⁶⁻¹⁷ Kim and coworkers have reported the formation of polypseudorotaxanes based on CB[6] and polyviologens with decamethylene spacers between the viologen groups,⁸ with the CB[6] host residing on the decamethylene chains, rather than the viologen units. Kaifer and coworkers have demonstrated that while the parent methyl viologen dication can form a very stable guest-host complex with CB[7] ($K_{\text{CB}[7]} = 10^5 \text{ M}^{-1}$),^{6,7} it hardly binds to the smaller CB[6] host ($K_{\text{CB}[6]} = 21 \text{ M}^{-1}$). Recently, Kaifer and coworkers have reported that the $\{\text{RVR}\cdot\text{CB}[7]\}^{2+}$ binding mode changes with the length of the aliphatic chains (R) on the viologen (V).^{10,11} When the aliphatic chain on the viologens are

shorter than three carbons, the CB[7] host tends to include the aromatic part of the viologens. For viologens with an aliphatic chain which is longer than three carbons, however, the CB[7] will reside on the aliphatic chain due to the favourable hydrophobic interactions between the CB[7]'s inner cavity and the terminal aliphatic chain. A simple pH controlled molecular shuttle in which the alkyl substituents (penta- and hexamethylene) of the thread are terminated by carboxylic acid groups was designed and constructed based on this binding behaviour change.¹⁴ When the carboxylate groups become protonated at low pH, the CB[7] bead will reside over the alkyl groups. Upon the deprotonation of the carboxylate groups, the CB[7] will switch to residing over the bipyridinium core to optimize the electrostatic interactions. Tuncel and co-workers¹⁶ have recently reported on pH controlled molecular switches based on a CB[6] rotaxane where the binding modes are dictated by acid-base chemistry or heat stimuli. Liu and co-workers have shown that CB[7] resides on one of the octyl chains on the *N,N'*-dioctyl-4,4'-bipyridinium dication, but that it can be moved to the bipyridinium moiety by addition of α -cyclodextrin.¹⁷

This chapter describes an investigation of the binding modes of the tetracationic bis(viologen) guest $[\text{CH}_3\text{bpy}(\text{CH}_2)_6\text{bpyCH}_3]^{4+}$ (L^{4+}) with CB[6] and CB[7]. The host-guest complexes were investigated by ¹H NMR spectroscopy as a function of the CB[n] to guest ratio, revealing that the CB[n]/guest stoichiometry has a significant effect on the binding mode of CB[7], whereas no effect on the binding mode of CB[6] was observed. As shown in Scheme 2.1, only the [2]pseudorotaxane was formed, with CB[6] residing on the central hexamethylene chain, even with host/guest ratios up to 1.9. In the case of CB[7], when the host/guest ratio is lower than one, the formation of a 1:1 complex was observed with CB[7] encapsulating the aliphatic chain, similar to the one with CB[6]. When the ratio of host/guest

is increased beyond one, the binding of the second CB[7] with one of the viologen units will force the first CB[7] to vacate from the central chain and move on to the other viologen unit due to the repulsive dipole-dipole electrostatic interactions between the carbonyl portals of two CB[7] hosts, thus forming the CB[7] [3]pseudorotaxane.

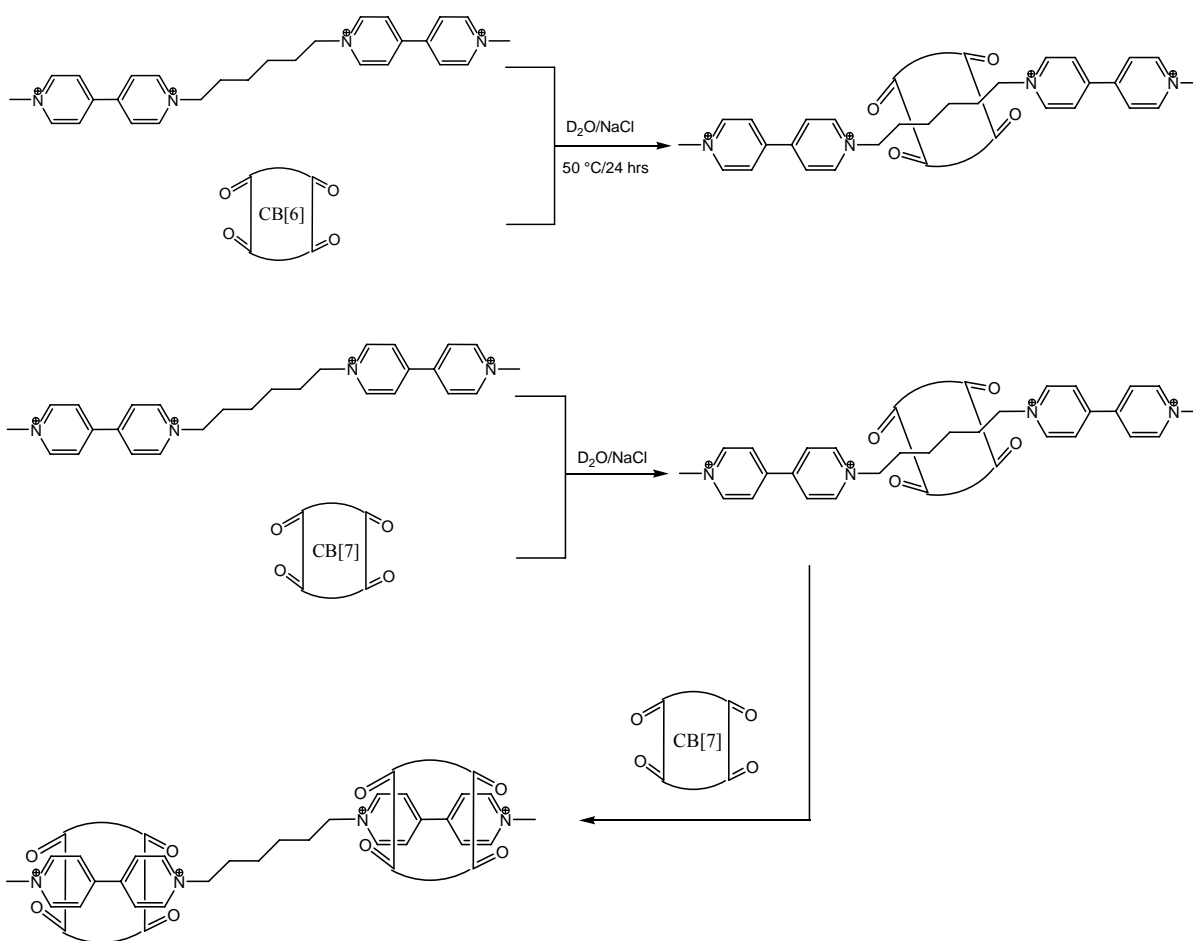


Figure 2.1 Schematic illustration of different binding modes of CB[6] and CB[7] with the tetracationic bis(viologen) guest $[CH_3bpy(CH_2)_6bpyCH_3]^{4+}$.

2.2 Experimental

2.2.1 Material Preparation

Cucurbit[7]uril was used as received (Aldrich), while the cucurbit[6]uril was synthesized by the method developed by Mock and co-workers¹⁸ and characterized by ¹H NMR spectroscopy and mass spectrometry. To a 50 mL three neck flask with 5.68 g glycoluril (40 mmol) in 20 mL 9 M sulfuric acid, 7 mL formaldehyde (in water) was added at 70 °C, and then the mixture heated to 90 °C and kept at this temperature for 36 hours. The reaction mixture was then poured into 200 ml water, followed by the addition of 1.0 L of acetone to produce a precipitate. After 15 minutes, the supernatant was removed by filtration and the resulting solid was further washed with a mixture of water and acetone in a 1:4 ratio (1.0 L) twice and then transferred to a 1:1 mixture of water/acetone (200 mL) and stirred for 20 minutes. The final solid was collected by filtration and washed with water (100 mL) and dried under vacuum. Yield: 45%. ¹H NMR (in D₂O) δ 5.63 (d, *J* = 15.6 Hz, 14H), 5.44 (s, 14H), 4.20 (d, *J* = 15.6 Hz, 14 H) ppm. TOF-MS (in H₂O): *m/z* = 1019.6 (theoretically 1019.3) for [M+Na]⁺.

The bis(viologen) ligand [CH₃bpy(CH₂)₆bpyCH₃]₂I₄ was prepared by adapting a literature procedure.¹⁹ To a solution of 4,4'-bipyridine (8 mmol) in 3 mL of DMF was added 1,6-diiodohexane (2 mmol) in 15 mL of DMF dropwise over a period of 26 h while the temperature of the reaction mixture was maintained at 70 °C. After cooling, diethyl ether was added to produce a yellow precipitate of [bpy(CH₂)₆bpy]₂I₂. This compound was subsequently treated with 3 equivalents of iodomethane in 5 mL of DMF and heated at 90 °C for 10 h. The resulting red precipitate was filtered and dried under vacuum to give [CH₃bpy(CH₂)₆bpyCH₃]₂I₄. Yield: 70%. Mp: 244-246 °C (decomposed). ¹H NMR (DMSO-

d_6), as shown in Figure 2.2, δ 9.42 (d, $J = 6.4$ Hz, 4H), 9.29 (d, $J = 6.8$ Hz, 4H), 8.81 (d, $J = 6.4$ Hz, 4H), 8.77 (d, $J = 6.8$ Hz, 4H), 4.71 (t, $J = 7.4$ Hz, 4H), 4.44 (s, 6H), 2.00 (m, 4H), and 1.40 (m, 4H) ppm. ^{13}C NMR (DMSO- d_6) (Figure 2.3): δ 148.5, 148.0, 146.6, 145.7, 126.5, 126.1, 60.6, 48.1, 30.4, 24.9 ppm. MS (MALDI-TOF-MS): $m/z = 806.9947$ ($[\text{M} - \text{I}]^+$); calculated 806.9917.

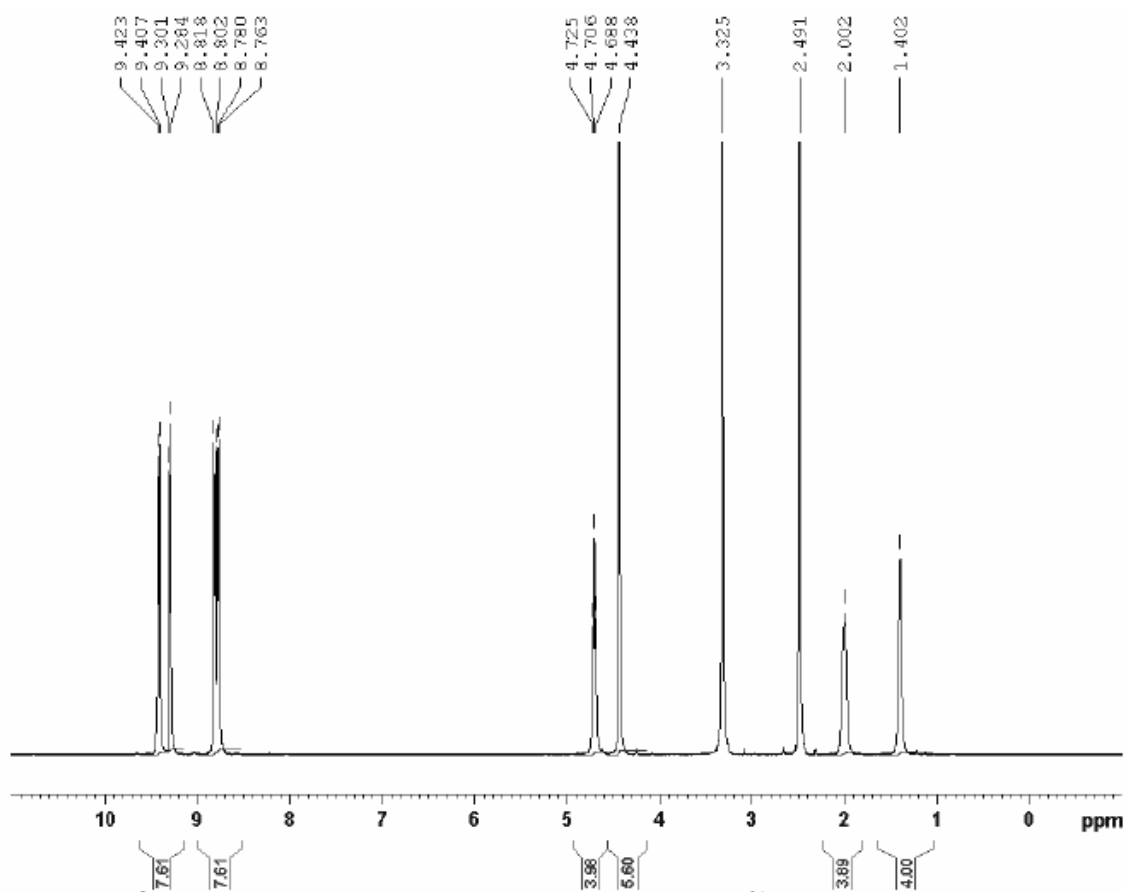


Figure 2.2 ^1H NMR spectrum of $[\text{CH}_3\text{bpy}(\text{CH}_2)_6\text{bpyCH}_3]\text{I}_4$ in DMSO- d_6 obtained at 400 MHz at 25°C.

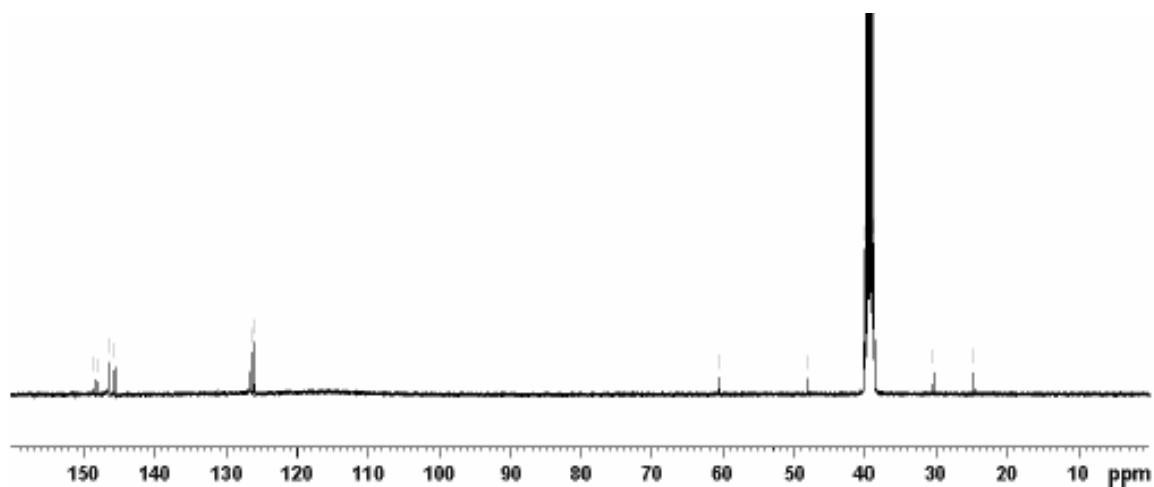


Figure 2.3 ^{13}C NMR spectrum of $[\text{CH}_3\text{bpy}(\text{CH}_2)_6\text{bpyCH}_3]\text{I}_4$ in $\text{DMSO-}d_6$ obtained at 100 MHz at 25°C .

2.2.2 Methods and Instruments

The ^1H NMR and ^{13}C NMR spectra were measured on a Bruker AV-400MHz NMR spectrometer. The ^1H NMR titration data was obtained by preparing 1.0 mM of the guest molecule in D_2O in the absence and presence of varied concentrations of $\text{CB}[n]$ (up to 2.5 equivalents). The solutions were thoroughly mixed and allowed to equilibrate for several minutes in the probe (25°C) before the spectrum was acquired.

The mass spectroscopy measurement was carried out on a Voyager DE-STR matrix assisted laser desorption ionization time-of-flight (MALDI-TOF) mass spectrometer (Applied Biosystems, Foster City, CA) equipped with a UV laser (337 nm). The sample was mixed with the matrix of 2,5-dihydroxybenzoic acid (DHB) on a MALDI target and dried at room temperature, and then analyzed at positive ionization mode. The MALDI-TOF

instrument was operated in reflectron mode with the accelerating voltage of 20 kV. The acquired data were processed using the software Data Explorer version 4.0 (Applied Biosystems).

2.2.3 Determination of the Host-Guest Stability Constants

^1H NMR titration experiments were performed to determine the binding constants of CB[6] and CB[7] with $[\text{CH}_3\text{bpy}(\text{CH}_2)_6\text{bpyCH}_3]^{4+}$ in D_2O . Mixtures of 1.0 mM solutions of $[\text{CH}_3\text{bpy}(\text{CH}_2)_6\text{bpyCH}_3]^{4+}$ with different amounts of CB[7] (up to 2.5 mM) were prepared in D_2O with $I = 0.1 \text{ M NaCl}$, and sonicated to completely dissolve the solutes before performing the NMR measurements.

When the binding between host (CB) and guest (G) is kinetically slow on the ^1H NMR timescale,²⁰⁻²² it is applicable to determine the proton resonance integrations for both bound (I_{bound}) and free species (I_{free}) separately, which can then be used to determine the binding constant by the following equation:



Given: $[\text{CB} \cdot \text{G}] + [\text{CB}]_{\text{free}} = [\text{CB}]_{\text{total}} \quad (2.2)$

$$[\text{CB} \cdot \text{G}] + [\text{G}]_{\text{free}} = [\text{G}]_{\text{total}} \quad (2.3)$$

And: $[\text{G}]_{\text{free}}/[\text{CB} \cdot \text{G}] = I_{\text{free}}/I_{\text{bound}} \quad (2.4)$

The binding constant K_{CB} can be interpreted as:

$$K_{CB} = \frac{[CB \cdot G]}{\{[CB]_{total} - [CB \cdot G]\}[G]_{free}} \quad (2.5)$$

In equations 2.3 and 2.4, the values of $[G]_{total}$ and $[CB]_{total}$ are known, the value of I_{free}/I_{bound} can be calculated from the 1H NMR spectrum, and therefore the values of $[CB \cdot G]$ and $[G]_{free}$ can be calculated. The value of the binding constant K_{CB} can thus be determined by equation 2.5.

However, when the exchange between free and bound species is fast on the 1H NMR timescale,²³⁻³⁴ the signal observed in the NMR spectra will have the average chemical shift of both species. In this case, the complexation constant can be determined by a quantitative 1H NMR titration method. For the 1:1 complex formed in solution, the observed chemical shift δ_{obs} for the guest is the average of the chemical shifts of the nucleus in free and complexed guest. Given the chemical shift of free guest (δ_G) and the limiting chemical shift for complex (δ_{lim}), the observed chemical shift δ_{obs} can be expressed by the following equation:

$$\delta_{obs} = f_{10} \delta_G + f_{11} \delta_{lim} \quad (2.6)$$

in which f_{10} and f_{11} represent the corresponding fractional occupancies of the free and bound states of the guest, respectively. Since $f_{10} + f_{11} = 1$, equation 2.6 can be written as:

$$\delta_{obs} = f_{11} (\delta_{lim} - \delta_G) + \delta_G \quad (2.7)$$

The chemical shift differences are defined by:

$$\Delta\delta_{\text{obs}} = \delta_{\text{obs}} - \delta_{\text{G}} \quad (2.8a)$$

$$\Delta\delta_{\text{lim}} = \delta_{\text{lim}} - \delta_{\text{G}} \quad (2.8b)$$

which will make equation 2.9:

$$\Delta\delta_{\text{obs}} = f_{11} \Delta\delta_{\text{lim}} \quad (2.9)$$

The total concentration of guest is defined as $[G]_t$, and given $f_{11} = \Delta\delta_{\text{obs}}/\Delta\delta_{\text{lim}} = [\text{CB} \cdot \text{G}]/[G]_t$, thus the binding constant for 1:1 complex can be written as:

$$K_{11} = \frac{[\text{CB} \cdot \text{G}]}{[\text{CB}][\text{G}]} = \frac{f_{11}}{[1 - f_{11}][\text{CB}]} \quad (2.10)$$

Combined with equation 2.9, the following equation can be deduced:

$$\frac{1}{\Delta\delta_{\text{obs}}} = \frac{1}{\Delta\delta_{\text{lim}} K_{11} [\text{CB}]} + \frac{1}{\Delta\delta_{\text{lim}}} \quad (2.11)$$

That is:

$$\frac{[\text{CB}]}{\Delta\delta_{\text{obs}}} = \frac{1}{\Delta\delta_{\text{lim}} K_{11}} + \frac{[\text{CB}]}{\Delta\delta_{\text{lim}}} \quad (2.12)$$

Since: $[\text{CB}] = [\text{CB}]_t - [\text{CB} \cdot \text{G}]$, equation 2.12 can be rearranged as:

$$\frac{[\text{CB}]_t}{\Delta\delta_{\text{obs}}} = \frac{[\text{CB}]_t + [G]_t - [G]_t \Delta\delta_{\text{obs}}/\Delta\delta_{\text{lim}}}{\Delta\delta_{\text{lim}}} + \frac{1}{\Delta\delta_{\text{lim}} K_{11}} \quad (2.13)$$

Nakano *et al.*³⁵ developed a graphical technique to determine binding constant when the concentrations of host and guest are comparable, in which a plot of $[CB]_t/\Delta\delta_{\text{obs}}$ against $[CB]_t + [G]_t$ was made at first based on the ^1H NMR titration data to give an estimate value for $\Delta\delta_{\text{lim}}$. This value of $\Delta\delta_{\text{lim}}$ is used to calculate $[CB\cdot G]$, based on $f_{11} = \Delta\delta_{\text{obs}}/\Delta\delta_{\text{lim}} = [CB\cdot G]/[G]_t$, and then a plot is made according to equation 2.13. Iterations are carried out until the plots converge. The value of $\Delta\delta_{\text{lim}}$ can be calculated from the slope of the curve, and combined with the value of intercept of the curve, the value of K_{11} can be determined.

2.3 Results and Discussion

2.3.1 Binding Between CB[6] and $[\text{CH}_3\text{bpy}(\text{CH}_2)_6\text{bpyCH}_3]^{4+}$

The binding behaviour of $[\text{CH}_3\text{bpy}(\text{CH}_2)_6\text{bpyCH}_3]^{4+}$ with CB[6] was investigated first. The ^1H NMR spectra of $\text{CH}_3\text{bpy}(\text{CH}_2)_6\text{bpyCH}_3^{4+}$ in the absence and in the presence of 0.6, 1.1 and 1.9 equiv. of CB[6] in 0.1 M NaCl/D₂O (recorded after 24 h incubation in a 50 °C water bath) are shown in Figure 2.4. With the addition of CB[6], significant upfield shifts for the H β , and H γ methylene protons are observed. Meanwhile, for the aromatic protons, the H2' and H3' protons, which are near to the central aliphatic chain, experience downfield shifts of 0.53 and 0.05 ppm, respectively, while the aromatic H2 and H3 resonances and the methyl resonance remain essentially unchanged. Given the fact that upfield complexation-induced chemical shifts of the resonance are associated with the inclusion of the guest into the interior cavity of cucurbiturils and the downfield shifts are observed for the protons which are located near to the carbonyl portals,³⁶⁻³⁸ the resonance changes of the guest upon the inclusion reveal the formation of a [2]pseudorotaxane with the CB[6] residing on the

central hexamethylene chain, with two positively charged nitrogen atoms interacting with the carbonyl oxygen atoms of the CB[6] portals. No inclusion of CB[6] over the aromatic moieties is observed even with 1.9 equivalents of CB[6], which can be explained by the low binding constant of CB[6] with the methylviologen cation ($K = 21 \pm 2 \text{ M}^{-1}$), reported by Kaifer and coworkers.⁷

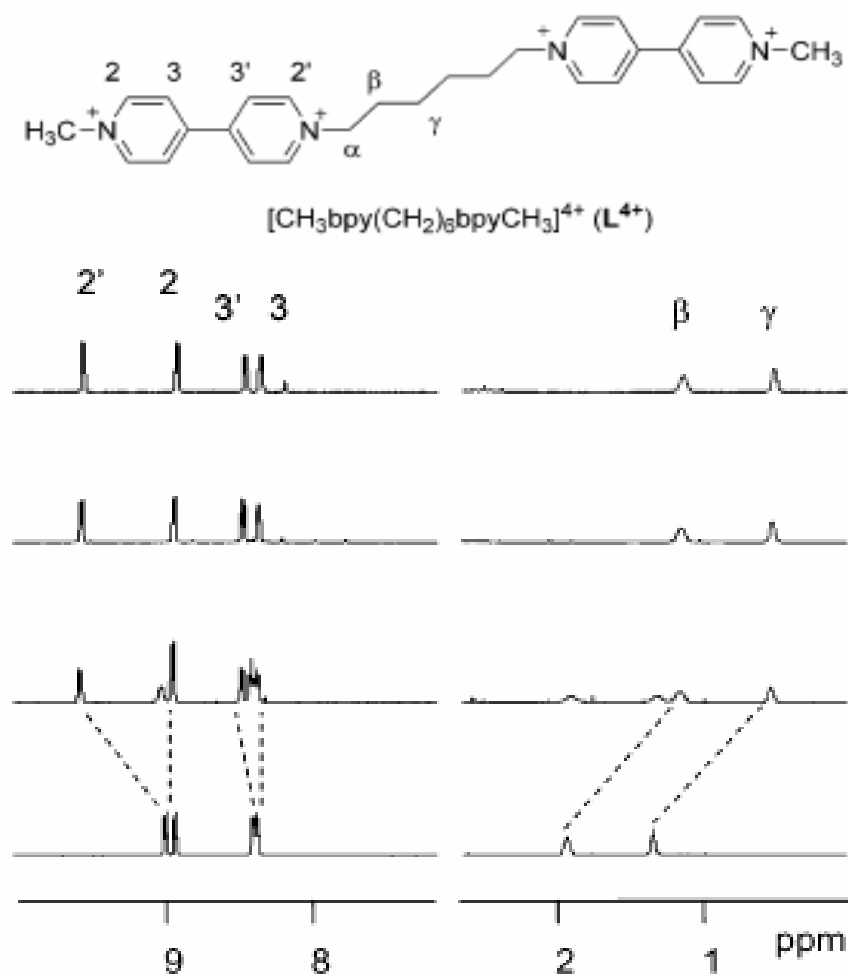


Figure 2.4 ^1H NMR spectra of $[\text{CH}_3\text{bpy}(\text{CH}_2)_6\text{bpyCH}_3]^{4+}$ (1 mM) in the absence and in the presence of 0.6, 1.1 and 1.9 equivalents of CB[6] (from bottom to top) at 25 °C in 0.1 M NaCl/D₂O after 24 h incubation in a 50 °C water bath.

The formation of a 1:1 complex is confirmed by the result of the MALDI-TOF mass spectrum with peaks at $m/z = 355$ for $[\mathbf{L}+\text{CB}[6]]^{4+}$, 474 for $[\mathbf{L}+\text{CB}[6]\text{H}^+]^{3+}$, 711 for $[\mathbf{L}+\text{CB}[6]-2\text{H}^+]^{2+}$, and 774 for $[\mathbf{L}+\text{CB}[6]+\text{I}^-\text{H}^+]^{2+}$. Since the exchange between the free and bound species is slow on the NMR scale, as indicated by the separate resonances corresponding to respective protons of the free and bound guest, the stability constant for the formation of the [2]pseudorotaxane was determined by a ^1H NMR titration (based on Equation 2.5, as illustrated in Section 2.2.3) to be $K_{\text{CB}[6]} = (8 \pm 2) \times 10^3 \text{ M}^{-1}$, which is in good agreement with the value of $2.5 \times 10^4 \text{ M}^{-1}$ reported by Buschmann and co-workers for the 1:1 complex between $[\text{bpy}(\text{CH}_2)_6\text{bpy}]^{2+}$ and $\text{CB}[6]$.³⁹ The complex is thermodynamically stable, with no dissociation being observed from NMR experiments up to 65 °C.

2.3.2 Binding Between CB[7] and $[\text{CH}_3\text{bpy}(\text{CH}_2)_6\text{bpyCH}_3]^{4+}$

As has been discussed previously, CB[7] has attracted considerable attention as a host molecule in recent years in part due to its superior water solubility relative to other homologues. The CB[7], which shares the characteristic features of CB[6], but with a larger cavity and portal sizes, is even slightly more voluminous than β -cyclodextrin and thus can form stable complexes with relatively larger molecules, such as viologens, stilbenes, protonated aminoadamantanes, ferrocene and cobaltocene derivatives.⁴⁰⁻⁴⁶ The complexation of CB[7] with the $[\text{CH}_3\text{bpy}(\text{CH}_2)_6\text{bpyCH}_3]^{4+}$ tetracation was conducted in 0.10 M NaCl/D₂O and monitored by ^1H NMR spectroscopy. Two different binding behaviours are revealed by the NMR titration result. As shown in Figure 2.5, when the ratio of CB[7] to the guest is lower than 1.1, the resonances of the aliphatic H β and H γ resonances move upfield by 0.75 ppm, and the H2, H3, and H3' aromatic protons are observed to be slightly

downfield-shifted. This is similar to what was observed for CB[6], indicating the formation of a [2]pseudorotaxane with CB[7] residing on the central hexamethylene chain. The resonance for the aromatic H₂' proton is found to be slightly upfield-shifted, which is different from the case with CB[6], where a downfield shift in proton H₂' is observed, suggesting that larger bound host has a greater range of motion along the chain.

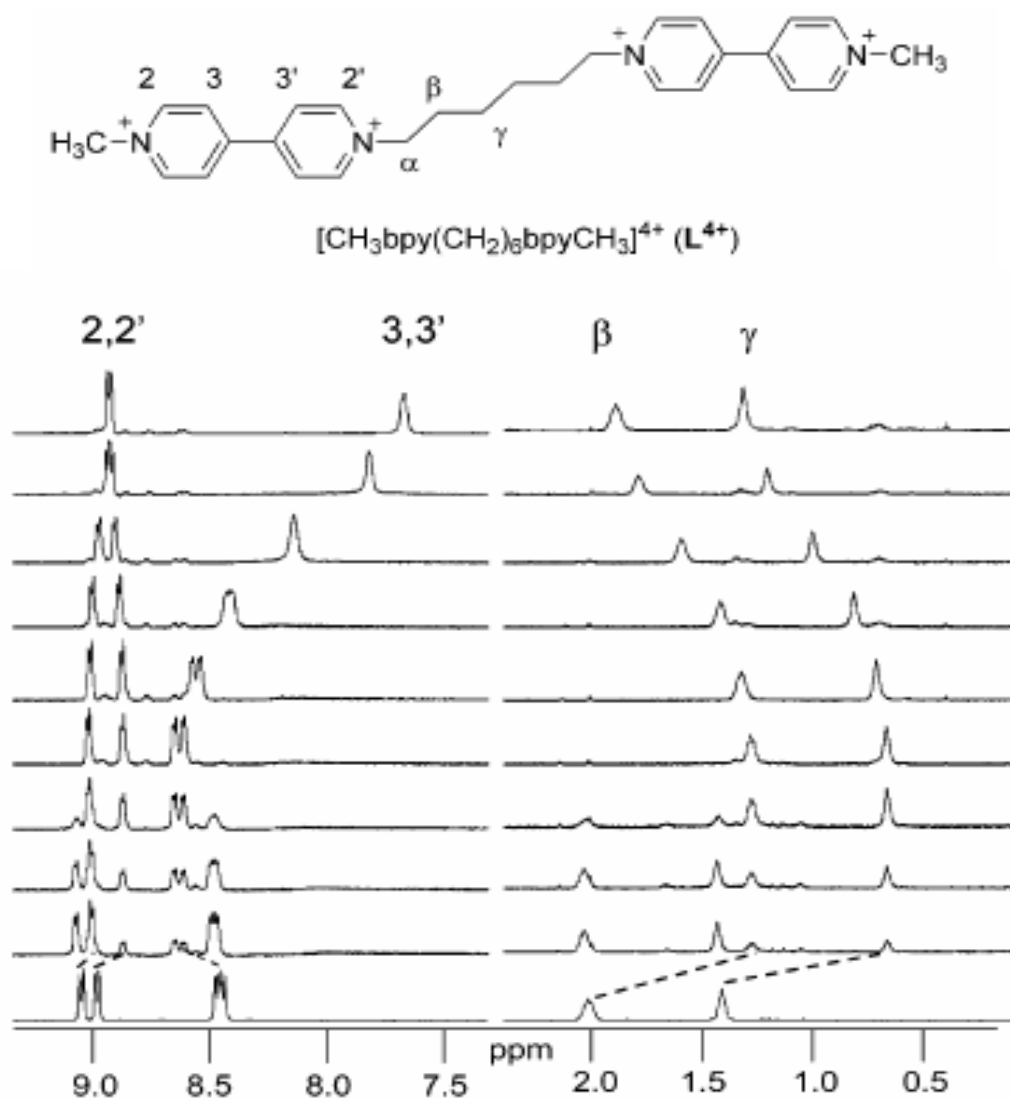


Figure 2.5 ^1H NMR spectra of $[\text{CH}_3\text{bpy}(\text{CH}_2)_6\text{bpyCH}_3]^{4+}$ (1 mM) in the absence and in the presence of 0.3, 0.6, 0.9, 1.1, 1.4, 1.6, 1.8, 2.1 and 2.5 equivalents of CB[7] (from bottom to top) at 25 °C in 0.1 M NaCl/D₂O.

The formation of this 1:1 complex can be confirmed by the result of mass spectrometry, with peak at $m/z = 397$ for $[L+CB[7]]^{4+}$ and 857 for $[L+CB[7]-H]^{2+}$. The exchange between the free and bound species of this CB[7] [2]pseudorotaxane is slow on the 1H NMR timescale, such that two sets of peaks are observed in the 1H NMR spectra, similar to the case of CB[6]. The equilibrium constant is determined to be $K_{CB[7]} = (6 \pm 2) \times 10^3 M^{-1}$ ($\Delta G^\circ = -5.3 \text{ kcal mol}^{-1}$) from the integrations of the free and bound guest species using equation 2.5.

As the ratio of CB[7] to guest is increased beyond one, the resonances of aromatic H3 and H3' protons undergo a considerable upfield shift from 8.6 ppm for the [2]pseudorotaxane to a limiting shift of 7.1 ppm for the [3]pseudorotaxane (shown in Figure 2.5), similar to what was observed for these protons in CB[7] complexes of other symmetrical RVR²⁺ viologens.¹⁹ Meanwhile, the resonances of the aliphatic H β and H γ protons move downfield toward the original chemical shifts observed in the free guest, suggesting that the [2]pseudorotaxane is converted into a [3]pseudorotaxane by the inclusion of the tetracationic thread by a second CB[7] host. In the presence of a second CB[7] molecule, the original host molecule is forced to abandon its inclusion of the hexamethylene chain in favour of the unoccupied viologen group. The simultaneous inclusion of the hexamethylene chain and an adjacent viologen group is less stable because of electrostatic and steric interactions between the hosts in these locations. The polar carbonyl-rimmed portals would result in significant repulsive dipole-dipole electrostatic interactions between two CB[7] hosts when placed over neighbouring regions of the guest. With the two CB[7] encapsulating the two viologen groups, each portal of the host is adjacent to its own set of positive charges, maximizing the number of ion-dipole interactions between the guest and hosts. In addition, because of the

bend in the long axis of the guest between the viologen and hexamethylene sections of the guest, there would be some unfavourable steric interactions between two hosts on adjacent sections of the guest.

The formation of the 2:1 complex can be further confirmed by the result of mass spectrometry, in which a peak at $m/z = 688$ for $[L + 2CB[7]]^{4+}$ is observed. The exchange between the free and bound guest molecules are observed to be fast on the 1H NMR timescale, as indicated by the average resonances for the free and bound species in Figure 2.6 when the ratio of $[CB[7]]$ to $[L^{4+}]$ is higher than one.

A plot of chemical shift changes for protons H3/H3' of L^{4+} as a function of the concentration of $CB[7]$ was made, as shown in Figure 2.6, to determine the stability constant for the binding of the second $CB[7]$ to L^{4+} to form $\{L \cdot 2CB[7]\}^{4+}$ using equation 2.13, although equation 2.13 is designed for the determination of binding constant for 1:1 complex with fast exchange on the 1H NMR timescale. The exchange between free and bound species is slow when the first equivalent of $CB[7]$ is added, and then the process becomes a fast exchange when the second $CB[7]$ is added and the first $CB[7]$ is forced to move along the guest from the central chain to the other viologen group. Technically, as only one $CB[7]$ was introduced to the whole system, the process can be considered as the formation of a 1:1 complex between $\{L \cdot CB[7]\}^{4+}$ and $CB[7]$. Therefore, by plotting the values of $[CB]_t / \Delta\delta_{obs}$ against $[CB]_t + [L^{4+}]_t - [\{L \cdot 2CB[7]\}^{4+}]_t$, based on equation 2.13 (the inset of Figure 2.6), the value of $K_{2CB[7]}$ was determined to be $(6.8 \pm 0.5) \times 10^2 M^{-1}$ ($\Delta G^\circ = -3.9 \text{ kcal mol}^{-1}$) from the ratio of the slope to the intercept.

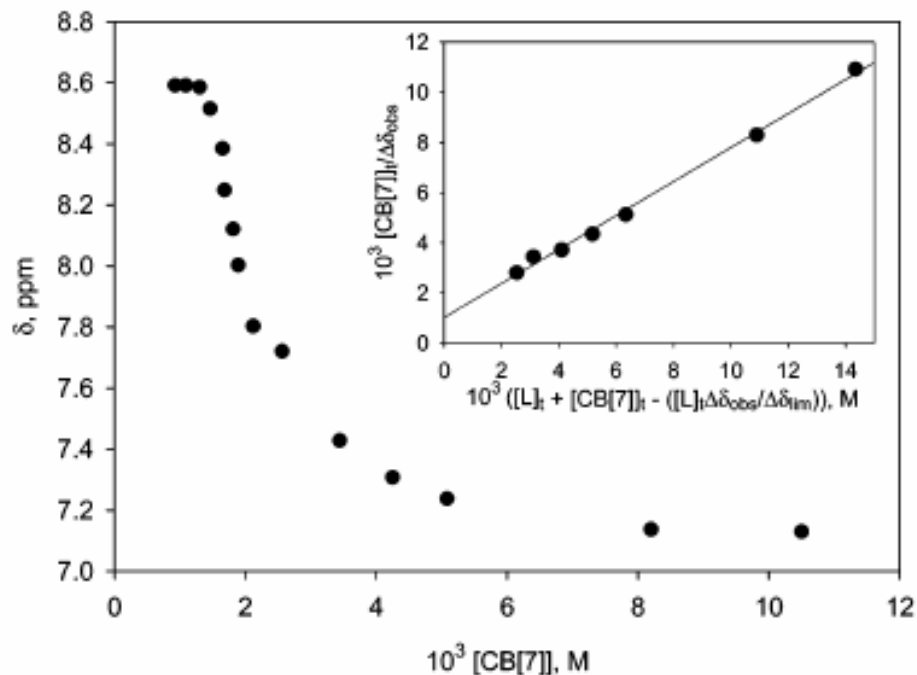


Figure 2.6 Chemical shift change of H3/H3' protons of the $[CH_3bpy(CH_2)_6bpyCH_3]^{4+}$ guest upon addition of CB[7]. Inset: a plot of $[CB[7]]/\Delta\delta_{obs}$ against $[L]_t + [CB[7]]_t + ([L]_t\Delta\delta_{obs}/\Delta\delta_{lim})$ from which the value of $K_{2CB[7]}$ was determined.

This value is substantially smaller than the binding constant for a 1:1 complex reported for the inclusion of dialkylviologen dications with CB[7] (10^4 - 10^6 M^{-1}),¹⁹ indicating that the extra process of shifting the original CB[7] bound to the hexamethylene chain over to the viologen unit makes the adding of the second CB[7] less favourable. The overall favourability of including two viologen units ($2\Delta G^\circ = -7.8$ $kcal\ mol^{-1}$), as opposed to having a free CB[7] residing on the hexamethylene chain ($\Delta G^\circ = -5.3$ $kcal\ mol^{-1}$), provided the driving force for the formation of the [3]pseudorotaxane.

2.4 Summary

In this chapter, the binding behaviours of CB[6] and CB[7] with a tetracationic bis(viologen) guest molecule $[\text{CH}_3\text{bpy}(\text{CH}_2)_6\text{bpyCH}_3]^{4+}$ were investigated by ^1H NMR and MALDI-TOF-MS experiments. Both CB[6] and CB[7] formed [2]pseudorotaxanes with the guest, with the CB[n] residing on the central hexamethylene chain, while CB[7] can also form a [3]pseudorotaxane with two host molecules located on the two viologen groups. When more than one equivalent of CB[7] was introduced to the system, the initial CB[7] host which was on the central chain will vacate the inclusion of the hexamethylene chain as a result of the electrostatic and steric repulsions that would arise in simultaneous binding of adjacent aliphatic and aromatic portions of the guest. The significant effect of the stoichiometry of the CB[7]/guest ratio on the binding behaviour suggest its potential applications in the construction of stoichiometry-controlled molecular machines. Very recently, combinations of cucurbiturils and cyclodextrin have been used to make new examples of pseudorotaxanes, in which the different binding behaviours of the two types of host were used to create novel supramolecular complexes.^{47,48} In one study,⁴⁷ a [3]pseudorotaxane was prepared with one equivalent each of CB[7] and β -CD on a $\text{Ru}(\text{bpy})_3$ -terminated viologen-naphthalene guest in which the CB[7] was positioned initially over the viologen group. The addition of the β -CD, which bound over the linker between the viologen and the naphthalene units, pushed the CB[7] to the linker between the $\text{Ru}(\text{bpy})_3$ and viologen units. The authors described it as a “tightened nut on bolt” structural mode.⁴⁷

References

1. Lagona, J.; Mukhopadhyay, P.; Chakrabarti, S.; Isaacs, L. *Angew. Chem., Int. Ed.* **2005**, *44*, 4844.
2. Kim, K. *Chem. Soc. Rev.* **2002**, *31*, 96.
3. Gerasko, O. A.; Samsonenko, D. G.; Fedin, V. P. *Russ. Chem. Rev.* **2002**, *71*, 741.
4. Kim, K.; Selvapalam, N.; Oh, D. H. *J. Incl. Phenom. Macro. Chem.* **2004**, *50*, 31.
5. Lee, J. W.; Samal, S.; Selvapalam, N.; Kim, H. J.; Kim, K. *Acc. Chem. Res.* **2003**, *36*, 621.
6. Kim, H.-J.; Jeon, W. S.; Ko, Y. H.; Kim, K. *Proc. Natl. Acad. Sci. USA* **2002**, *99*, 5007.
7. Ong, W.; Gomez-Kaifer, M.; Kaifer, A. E. *Org. Lett.* **2002**, *4*, 1791.
8. Choi, S.; Lee, J. W.; Ho, Y. H.; Kim, K. *Macromolecules* **2002**, *35*, 3526.
9. Ong, W.; Kaifer, A. E. *J. Org. Chem.* **2004**, *69*, 1383.
10. Moon, K.; Kaifer, A. E. *Org. Lett.* **2004**, *6*, 185.
11. Sindelar, V.; Moon, K.; Kaifer, A. E. *Org. Lett.* **2004**, *6*, 2665.
12. Jeon, W. S.; Ziganshina, A. Y.; Lee, J. W.; Ko, Y. H.; Kang, J.-K.; Lee, C.; Kim, K. *Angew. Chem., Int. Ed.* **2003**, *42*, 4097.
13. Ong, W.; Kaifer, A. E. *Angew. Chem., Int. Ed.* **2003**, *42*, 2164.
14. Sindelar, V.; Silvi, S.; Kaifer, A. E. *Chem. Commun.* **2006**, 2185.
15. Moon, K.; Grindstaff, J.; Sobransingh, D.; Kaifer, A. E. *Angew. Chem., Int. Ed.* **2004**, *43*, 5496.
16. Tuncel, D.; Ozsar, O.; Tiftik, H. B.; Salih, B. *Chem. Commun.* **2007**, 1369.
17. Liu, Y.; Li, X.-Y.; Zhang, H.-Y.; Li, C.-J.; Ding, F. *J. Org. Chem.* **2007**, *72*, 3640.
18. Freeman, W. A.; Mock, W. L.; Shih, N.-Y. *J. Am. Chem. Soc.* **1981**, *103*, 7367.

19. Lee, S. K.; Shin, S. Y.; Lee, S.; Lee, C.; Park, J. W. *J. Chem. Soc., Perkin Trans. 2* **2001**, 1983.
20. Wang, R.; Yuan, L.; Macartney, D. H. *Chem. Commun.* **2006**, 2908.
21. Hettiarachchi, D. S. N.; Macartney, D. H. *Can. J. Chem.* **2006**, *84*, 905.
22. Yuan, L.; Macartney, D. H. *J. Phys. Chem. B* **2007**, *111*, 6949.
23. Hanna, M. W.; Ashbaugh, A. L. *J. Phys. Chem.* **1964**, *68*, 811.
24. Foster, R.; Fyfe, C. A. *J. Chem. Soc. B* **1966**, 926.
25. Carper, W. R.; Buess, C. M.; Hipp, G. R. *J. Phys. Chem.* **1970**, *74*, 4229.
26. Wachter, H. N.; Fried, V. *J. Chem. Ed.* **1974**, *51*, 798.
27. Wong, K. F.; Ng, S. *Spectrochim. Acta*, **1976**, *32A*, 455.
28. Seal, B. K.; Mukherjee, A. K.; Mukherjee, D. C.; Farell, P. G.; Westwood, J. V. *J. Magn. Reson.* **1983**, *51*, 318.
29. Mathur, R.; Becker, E. D.; Bradley, R. B.; Li, N. C. *J. Phys. Chem.* **1963**, *67*, 2190.
30. Huggins, C. M.; Pimentel, G. C.; Shoolery, J. N. *J. Chem. Phys.* **1955**, *23*, 1244.
31. Creswell, C. J.; Allred, A. L. *J. Phys. Chem.* **1962**, *66*, 1469.
32. Connors, K. A.; Mollica, J. A. *J. Pharm. Sci.* **1966**, *55*, 772.
33. Sahai, R.; Loper, G. L.; Lin, S. H.; Eyring, H. *Proc. Nat. Acad. Sci. USA*, **1974**, *71*, 1499.
34. Foster, R.; Fyfe, C. A. *Prog. NMR Spectrosc.* **1969**, *4*, 1.
35. Nakano, M.; Nakano, N. I.; Higuchi, T. *J. Phys. Chem.* **1967**, *71*, 3954.
36. Mock, W. L. *Top. Curr. Chem.* **1995**, *175*, 1.
37. Mock, W. L. In *Comprehensive Supramolecular Chemistry*; Vogtle, F., Ed.; Pergamon: Oxford, **1996**; Vol. 2, pp. 477-493.

38. Mock, W. L.; Shin, N. Y. *J. Org. Chem.* **1986**, *51*, 4440.
39. Buschmann, H.-J.; Meschke, C.; Schollmeyer, E. *An. Quim. Int. Ed.* **1998**, *94*, 241.
40. Kim, H. J.; Jeon, W. S.; Ko, Y. H.; Kim, K. *Proc. Natl. Acad. Sci. USA* **2002**, *99*, 5007.
41. Ong, W.; Gomez-Kaifer, M.; Kaifer, A. E. *Org. Lett.* **2002**, *4*, 1791.
42. Choi, S.; Park, S. H.; Ziganshina, A. Y.; Ko, Y. H.; Lee, J. W.; Kim, K. *Chem. Commun.* **2003**, 2176.
43. Wagner, B. D.; Stojanovic, N.; Day, A. I.; Blanch, R. J. *J. Phys. Chem. B* **2003**, *107*, 10741.
44. Yuan, L.; Wang, R.; Macartney, D. H. *Tetrahedron: Asymmetry* **2007**, *18*, 483.
45. Wang, R.; Yuan, L.; Macartney, D. H. *J. Org. Chem.* **2006**, *71*, 1237.
46. Jeon, W. S.; Moon, K.; Park, S. H.; Chun, H.; Ko, Y. H.; Lee, J. Y.; Lee, E. S.; Samal, S.; Selvapalam, N.; Rekharsky, M. V.; Sindelar, V.; Sobransingh, D.; Inoue, Y.; Kaifer, A. E.; Kim, K. *J. Am. Chem. Soc.* **2005**, *127*, 12984.
47. Zou, D.; Andersson, S.; Zhang, R.; Sun, S.; Akermark, B.; Sun, L. *Chem. Commun.* **2007**, 4734.
48. Yang, C.; Ko, Y. K.; Selvapalam, N.; Oginane, Y.; Mori, T.; Wada, T.; Kim, K.; Inoue, Y. *Org. Lett.* **2007**, *9*, 4789.

Chapter 3

HOST-GUEST COMPLEXATION BETWEEN AN ACHIRAL CUCURBIT[7]URIL HOST AND CHIRAL GUEST MOLECULES

The effects of cucurbit[n]uril encapsulation on the chemical, optical and electrochemical properties of guest molecules have been widely investigated. In this chapter, the chiroptic behaviours of one set of chiral molecules (*S*)- and (*R*)-*N*-benzyl-1-(1-naphthyl)ethylamine (BNEAH⁺) upon the inclusion in the hydrophobic cavity of CB[7] in aqueous solution have been investigated by ¹H NMR, UV-visible and circular dichroism spectroscopy, polarimetry and electrospray mass spectrometry. The binding stoichiometry was determined by a Job's plot and a ¹H NMR titration and the stability constant was calculated to be $(1.2 \pm 0.4) \times 10^8 \text{ M}^{-1}$ by ¹H NMR competitive binding method. The chiroptic behaviour of the guests upon inclusion in the CB[7] cavity in aqueous solution was investigated by polarimetry and circular dichroism spectrometry and will be discussed in the terms of the configurations of the substituents about the chiral center.

3.1 Introduction

As the most popular member of the CB[n] family, CB[7] has drawn more recent attention than other homologues as the result of its comparatively superior solubility in aqueous solution. As with β -cyclodextrin,^{1,2} the cavity of CB[7] can accommodate aromatic molecules, with a portal diameter of 5.4 Å and an internal cavity diameter of 7.3 Å.³ The binding between CB[7] and a variety of hydrophobic cationic guest molecules,⁴⁻⁹ such as viologens,¹⁰ metallocene cations (with $K_{\text{CB[7]}} > 10^{12} \text{ M}^{-1}$),¹¹⁻¹³ has been investigated.

Cucurbit[n]urils, especially CB[7], have been widely used to modify the chemical and spectroscopic properties of guest molecules.¹⁴⁻¹⁸ This has included photodimerization reactions,¹⁹⁻²⁴ stabilizations of dyes and other guest molecules,²⁵⁻²⁸ and fluorescence switches.²⁹

The formations of supramolecular guest–host complexes involving chiral components have been widely investigated.³⁰⁻³¹ Chiral selectivity in guest–host molecular recognition has been employed in chiral separations and asymmetric synthesis and catalysis. Amongst the chiral cyclic host molecules available, the cyclodextrins have perhaps received the greatest attention.³²⁻³⁴ Achiral host molecules, which are induced-fit type receptors, such as crown ethers,³⁵⁻³⁷ calixarenes and resorcarenes,^{38,39} and porphyrin tweezers,⁴⁰⁻⁴⁴ are found to be capable of forming chiral host–guest complexes by including chiral guests. Unlike the chiral cyclodextrin host molecules, the achiral host molecules such as cyclic cucurbituril hosts should not exhibit any chiral selectivity in guest–host molecular recognition. Rekharsky *et al.*,⁴⁵ however, have recently shown that enantiomeric host–guest complexes composed of CB[6] with (*R*)- or (*S*)-2-methylpiperazine provide 95% enantioselectivity towards binding of a second chiral guest, (*S*)-2-methylbutylamine. In research described in this chapter, the chiroptic behaviour of the guest–host complexes composed of the optical isomers of protonated (*R*)/(*S*)-*N*-benzyl-1-(1-naphthyl)ethylamine (BNEAH⁺) in an achiral cucurbit[7]uril host cavity was investigated, as shown schematically below in Figure 3.1.

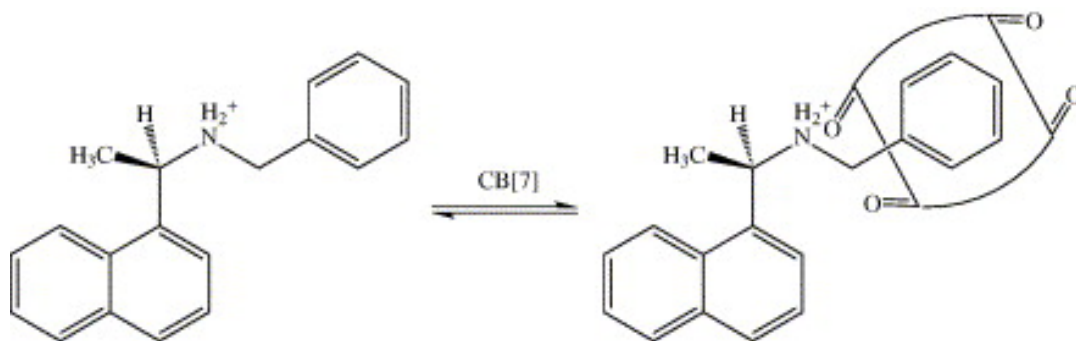


Figure 3.1 Formation of a host-guest complex between cucurbit[7]uril and (*R*)-*N*-benzyl-1-(1-naphthyl)ethylamine.

3.2 Experimental

3.2.1 Material Preparation

The hydrochloride salts of (*R*)/(*S*)-*N*-benzyl-1-(1-naphthyl)ethylamine ((*R*)- and (*S*)-BNEAH⁺) were used as received from Aldrich (structures are as shown in Figure 3.2). ¹H NMR (400 MHz, D₂O) δ = 1.73 (d, 3H), 4.03 (d, H), 4.18 (d, H), 5.27 (q, H), 7.21 (m, 2H), 7.33 (m, 3H), 7.55 (m, 3H), 7.59 (d, H), 7.69 (m, H), 7.83 (d, 2H) ppm; ESI-MS: *m/z* = 262.5 (*S*) and 262.6 (*R*) for [M-Cl]⁺ (theoretically 262.2)

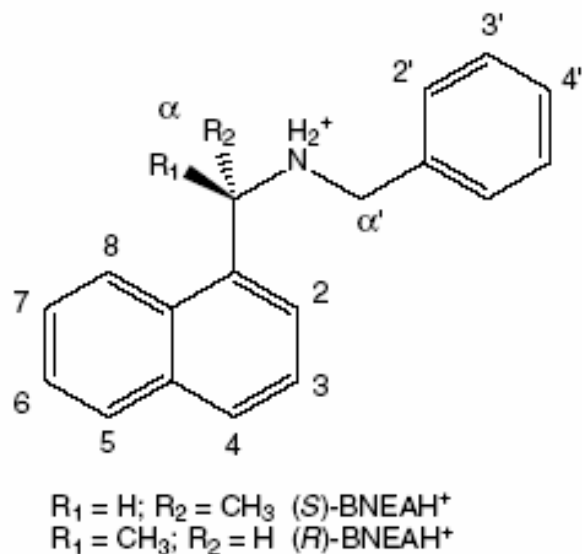


Figure 3.2 The structure of the guests (*S*)- and (*R*)-BNEAH⁺.

Cucurbit[7]uril was prepared by the method developed by Day and coworkers as follows.⁴⁶ Finely powdered glycoluril (10 g, 70 mmol) and powdered paraformaldehyde (4.22 g, 140 mmol) were added together in a mortar and thoroughly mixed as dry powders, and then transferred to a 50 mL three-neck round bottom flask. Ice-cold concentrated HCl (14.2 mL) was added to the dry powder while stirring rapidly until the mixture set as a gel. After standing for 30 minutes, the gel was heated at 100 °C for 18 h. The mixture was cooled and then filtered to collect the first crop of colourless crystals. The filtrate was then evaporated to one-fourth of the original volume. Water (5 mL) was added to produce a colourless crystalline suspension, which was removed by filtration. The filtrate was then reduced to 12 mL by rotary evaporation and poured into 35 mL of MeOH. After 18 h, the off-white precipitate was collected by filtration and dissolved by hot 20% aqueous glycerol while stirring and heating. Methanol was then added dropwise to produce a white precipitate,

which was filtrated and further washed with MeOH three times to remove extra glycerol. The product was dried at 60 °C for 12 h to give the final cucurbit[7]uril as an off-white solid. Yield: 30%. ¹H NMR (400 MHz, D₂O) δ 4.00 (d, 2H, *J* = 15.5 Hz, CH₂), 5.18 (d, 2H, *J* = 15.5 Hz, CH₂), 5.28 (s, 2H, CH) ppm; ¹³C NMR (100 MHz, D₂O) δ 53.5 (CH₂), 72.0 (CH), 157.5 (CO) ppm. TOF-MS: *m/z* = 1186.1 for [CB[7] + Na]⁺.

The host-guest complex was formed by sonicating an equal molar solution (1.0 mM) of CB[7] and the chiral guest molecule for 10 minutes. ¹H NMR (400 MHz, D₂O) δ = 1.85 (d, 3H), 3.76 (d, 1H), 4.19 (d, 1H), 6.63 (m, 4H), 6.85 (m, 1H), 7.61 (m, 3H), 7.83 (d, H), 7.93 (dd, 2H), 8.39 (d, 1H); the peaks at δ = 4.11, 5.41 and 5.65 can be assigned to the CB[7]; ESI-MS: *m/z* = 1424.2 for [(*S*)-BNEAH+CB[7]-Cl]⁺ (theoretically 1424.5) and 1424.5 for [(*R*)-BNEAH+CB[7]-Cl]⁺ (theoretically 1424.5).

3.2.2 Methods and Instruments

The UV-visible spectra were all recorded on a Hewlett Packard 8452A diode array spectrometer using quartz cells with a 1.00 cm path length. The ¹H NMR spectra were measured in D₂O using a Bruker AV-400 spectrometer, employing the residual HDO signal as an internal reference, with guests (1 mM) in the absence and presence of different concentrations of CB[7] (up to 2.6 mM).

The optical rotation data were obtained on AUTOPOL V polarimeter with λ = 589 nm at *T* = 25.3 °C. Samples were prepared at a concentration of 5 mM for the guest molecule, with varying concentrations of CB[7] up to 7.5 mM in acidic aqueous solution, and measured in a 10 mm cell. The circular dichroism spectra were recorded using a Jasco J-715

spectrometer at room temperature with a cell of 1.0 cm pathlength. The concentrations of (*R*)/(*S*)-BNEAH⁺ and CB[7] were 0.10 and 0.15 mM, respectively, in aqueous solution.

The electrospray ionization mass spectra (ESI-MS) were acquired on a Waters 2Q Single Quadrupole MS spectrometer equipped with an ESI/APCI multiprobe to confirm the formation of 1:1 complexes between both enantiomers with CB[7]. Solutions of 0.10 mM guests with 0.12 mM CB[7] were prepared, and the measurements was performed after one hour incubation at room temperature.

3.2.3 Determination of the Binding Stoichiometry and Stability Constant

The stoichiometry of the host/guest complex was determined by UV-visible Job's plot of the absorbance changes at 305 nm in the mixtures of (*R*)-BNEAH⁺ with CB[7]. From two stock solutions of 0.10 mM CB[7] and (*R*)-BNEAH⁺ in water, a series of solutions were prepared in which the sum of the number of moles of CB[7] and (*R*)-BNEAH⁺ was kept constant, but the relative amount of these two was systematically varied, as shown in Table 3.1. The UV-visible spectrum was obtained with each of the solution in the table (shown in Figure 3.3), and a plot of the change of absorbance at wavelength of 305 nm (from that of an equal concentration of free guest) as a function of $\frac{[\text{BNEAH}^+]}{([\text{BNEAH}^+] + [\text{CB}[7]])}$ was made. As shown in Figure 3.4, the maximum is reached when the value of $\frac{[\text{BNEAH}^+]}{([\text{BNEAH}^+] + [\text{CB}[7]])}$ is 0.50, suggesting the formation of a 1:1 host:guest complex.

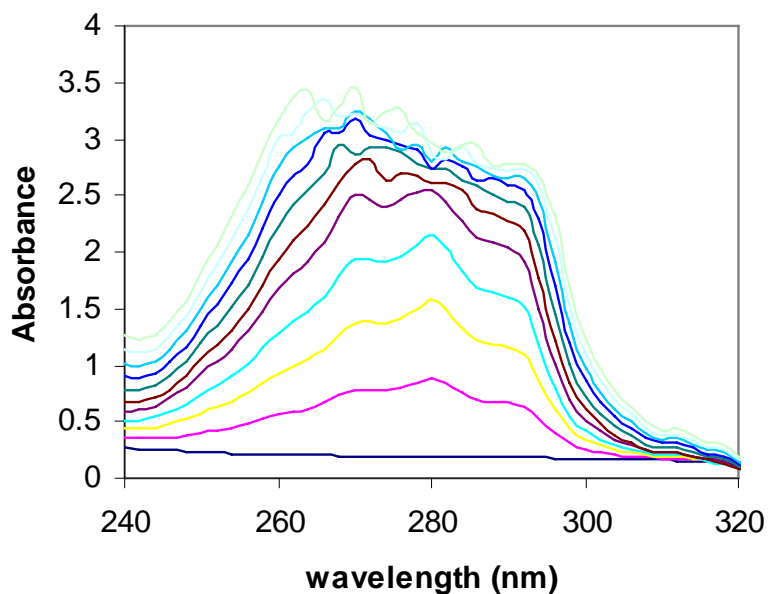


Figure 3.3 UV-visible spectra for the Job's plot titration curve with CB[7] and (R)-BNEAH⁺. From bottom to top, the value of $[BNEAH^+]/([BNEAH^+]+[CB[7]])$ increase from 0.0 to 1.0 in increments of 0.10.

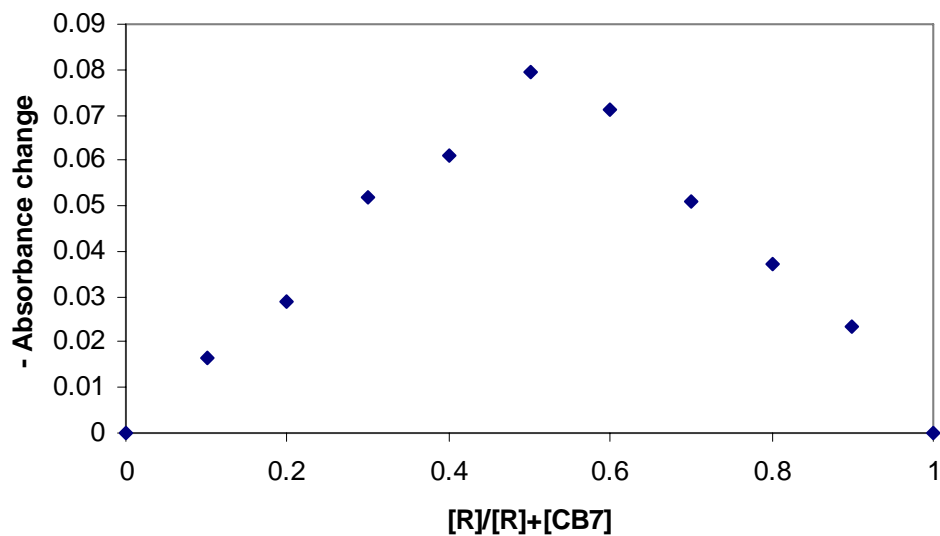


Figure 3.4 Job's plot curve of UV absorbance change (on 305 nm) of (R)-BNEAH⁺ upon the addition of CB[7], indicating the formation of 1:1 host-guest complex (maximum at 0.50).

Table 3.1 Solution composition (ml) for the UV-visible Job's plot measurements (Total volume is 3.00 ml).

Solution	0.10mM CB[7] (ml)	0.10 mM (R)-BNEAH ⁺ (ml)	[Guest]/([Guest]+[Host])
1	3.00	0	0
2	2.70	0.30	0.10
3	2.40	0.60	0.20
4	2.10	0.90	0.30
5	1.80	1.20	0.40
6	1.50	1.50	0.50
7	1.20	1.80	0.60
8	0.90	2.10	0.70
9	0.60	2.40	0.80
10	0.30	2.70	0.90
11	0	3.00	1.00

The 1:1 binding stoichiometry was also confirmed by the ¹H NMR spectral titrations and polarimetry titrations. Figure 3.5 shows the ¹H NMR titration curve with CB[7] and (R)-BNEAH⁺. Equilibrium is reached when the host/guest ratio is approximately one, indicating the formation of 1:1 complex. Since the ¹H NMR spectra of the two enantiomers are the same, only the (R)-BNEAH⁺ is shown as an example. The steep slope indicates the high binding constant, which can not be calculated by conventional titration measurements. Instead, the guest–host stability constant had to be determined by a ¹H NMR competition method, using 3-(trimethylsilyl)propionic-2,2,3,3-*d*₄ acid ($K_{\text{CB}[7]} = (1.82 \pm 0.22) \times 10^7 \text{ M}^{-1}$)⁴ as the competing guest, according to the following procedure.

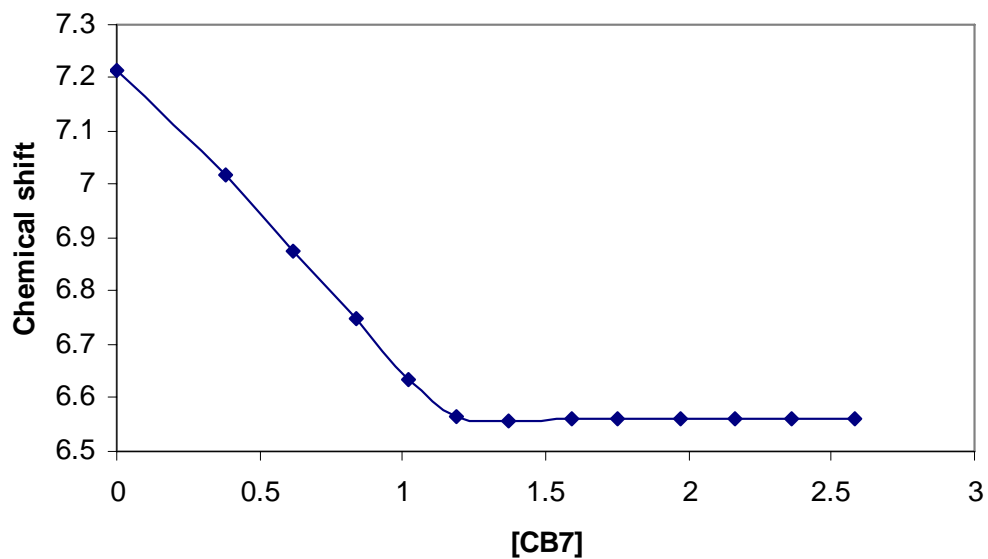


Figure 3.5 Plot of the chemical shift of the guest phenyl H2' proton as a function of the concentration of CB[7] (up to 2.6 mM), with (R)-BNEAH⁺ at 1mM.

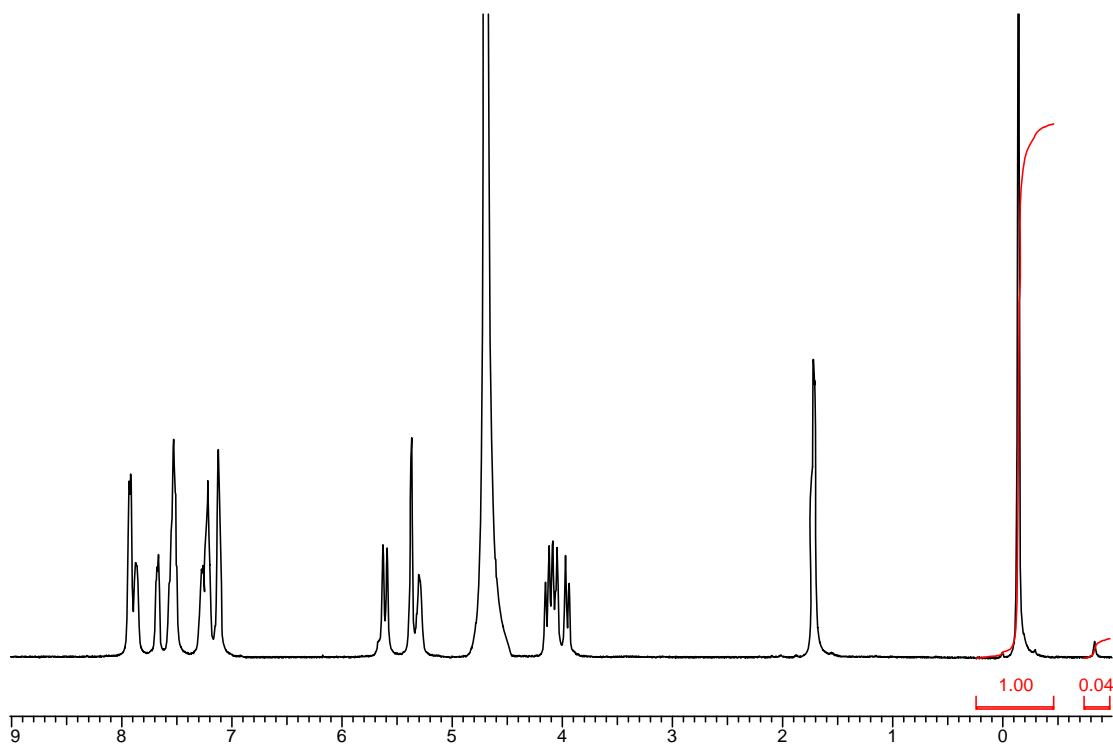


Figure 3.6 ¹H NMR spectrum of CB[7] (0.516 mM) with (R)-BNEAH⁺ (3.36 mM) and TSP (1.68 mM) in D₂O at 25 °C, after 30 minutes incubation.

A solution containing CB[7] (0.516 mM), 3-(trimethylsilyl)propionic-2,2,3,3- d_4 acid (TSP, 1.68 mM) and (*R*)-*N*-benzyl-1-(1-naphthyl)ethylamine hydrochloride (3.36 mM) was mixed and allowed to reach equilibrium, as shown in the ^1H NMR spectrum in Figure 3.6. Given that $[\text{CB}[7]]_t = 0.516 \text{ mM}$, $[\text{TSP}]_t = 1.68 \text{ mM}$, and $[\text{BNEAH}^+]_t = 3.36 \text{ mM}$, and using the integrations of the proton resonances at -0.142 and -0.832 ppm, which are the methyl resonances of the free and bound TSP species, respectively, the following concentrations may be calculated:

$$[\text{TSP}\cdot\text{CB}[7]] = [0.04/(0.04 + 1.54)] \times 1.68 \text{ mM} = 0.04 \text{ mM}$$

$$[\text{TSP}]_{\text{free}} = 1.68 - 0.04 = 1.64 \text{ mM}$$

$$[\text{CB}[7]]_t = [\text{TSP}\cdot\text{CB}[7]] + [\text{BNEAH}\cdot\text{CB}[7]^+] = 0.516 \text{ mM}$$

Thus:
$$[\text{BNEAH}\cdot\text{CB}[7]^+] = 0.516 - 0.04 = 0.476 \text{ mM}$$

Also:
$$\begin{aligned} [\text{BNEAH}^+]_{\text{free}} &= [\text{BNEAH}^+]_t - [\text{BNEAH}\cdot\text{CB}[7]^+] \\ &= 3.36 - 0.476 = 2.89 \text{ mM} \end{aligned}$$

Thus:

$$\begin{aligned} K_{\text{relative}} &= \frac{K_{\text{TSP}}}{K_{\text{BNEAH}}} = \frac{[\text{TSP}\cdot\text{CB}[7]][\text{BNEAH}^+]_{\text{free}}}{[\text{BNEAH}\cdot\text{CB}[7]^+][\text{TSP}]_{\text{free}}} \quad (3.1) \\ &= \frac{0.04 \times 2.89}{0.476 \times 1.64} = 0.148 \end{aligned}$$

The binding constant between 3-(trimethylsilyl)propionic-2,2,3,3- d_4 acid and CB[7] (K_{TSP}) is reported to be $(1.82 \pm 0.22) \times 10^7 \text{ M}^{-1}$. Therefore, K_{BNEAH} can be calculated by equation 3.1 to be $(1.2 \pm 0.4) \times 10^8 \text{ M}^{-1}$.

3.2.4 Energy-Minimization Calculations

The structures of the BNEAH⁺ cations and the {BNEAH·CB[7]}⁺ guest–host complexes in the gas phase were computed by energy minimizations using Gaussian 03, Revision C.02, programs⁴⁷ run on the computing facilities of the High Performance Virtual Computing Laboratory (HPVCL) at Queen’s University. The structure of the complex was originally constructed using ChemDraw and Chem 3D (ChemOffice 7.0, CambridgeSoft) programs and imported into Gaussian 03. The basis set used for the calculations was HF/3-21G**.

3.3 Results and Discussion

3.3.1 Host-Guest Complexes

The formation of 1:1 guest–host complexes of conjugate acids of the chiral molecules (*S*)- and (*R*)-*N*-benzyl-1-(1-naphthyl)ethylamine (BNEAH⁺) with cucurbit[7]uril were investigated by ¹H NMR titrations, as shown in Figure 3.7. With the addition of CB[7], the resonances for phenyl moiety (labeled by *) are shifted upfield from the positions of the free guest and the H7 and H8 protons of the naphthyl group experience a modest downfield shift, while the other resonances for the majority of the aromatic naphthyl protons exhibit no shifts. This suggests the inclusion of phenyl group (rather than the naphthyl group) into the CB[7] hydrophobic cavity with carbonyl portals pointing to the H7 and H8 protons on naphthyl group.

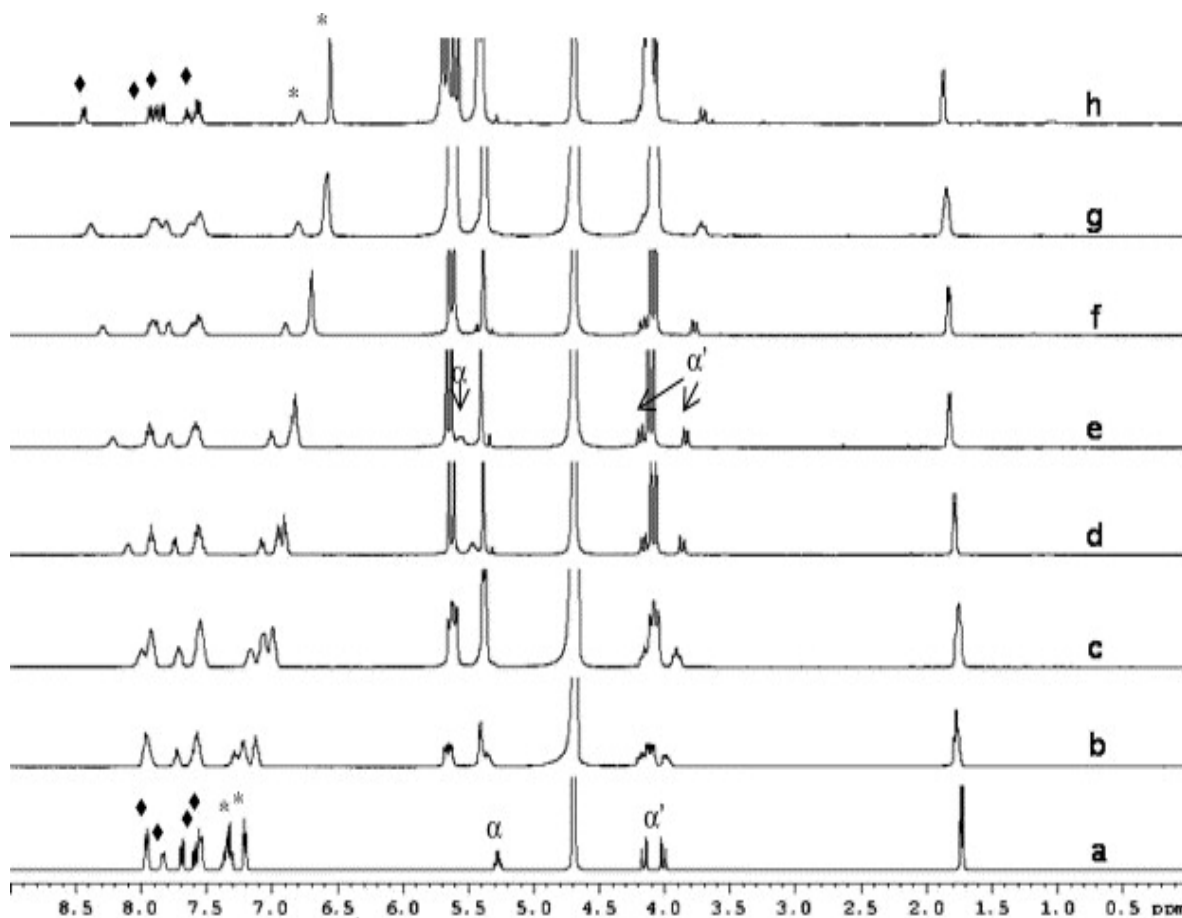


Figure 3.7 ^1H NMR spectra of the $(R)\text{-BNEAH}^+$ in the (a) absence and (b–h) presence of CB[7] in D_2O . The ratios of $[\text{CB}[7]]/[(R)\text{-BNEAH}^+]$ are (b) 0.17, (c) 0.33, (d) 0.50, (e) 0.66, (f) 0.85, (g) 1.05 and (h) 2.01. The symbols (*) and (♦) are for the aromatic phenyl and naphthyl protons, respectively. The α - and α' -protons are adjacent to the naphthyl and phenyl rings, respectively.

The binding stoichiometry was determined by a UV-visible Job's plot measurement and a ^1H NMR titration to be a 1:1 host-guest ratio, which was confirmed by an electrospray mass spectrum, with peaks at m/z at 1424.2 for $[\text{S-BNEAH}+\text{CB}[7]\text{-Cl}]^+$ and 1424.5 for $[\text{R-BNEAH}+\text{CB}[7]\text{-Cl}]^+$. These results are in good agreement of the theoretical value of $m/z = 1424.5$. The stability constant was determined by a ^1H NMR competitive titration, due to the

host-guest high affinity, to be $K_{\text{CB}[7]} = (1.2 \pm 0.4) \times 10^8 \text{ M}^{-1}$ by employing 3-(trimethylsilyl)propionic-2,2,3,3- d_4 acid ($K_{\text{CB}[7]} = (1.82 \pm 0.22) \times 10^7 \text{ M}^{-1}$)⁴ as the competing guest. This calculated stability constant is in good agreement with the values reported for similar compounds such as α,α' -diamino-*p*-xylene ($K_{\text{CB}[7]} = 1.84 \times 10^9 \text{ M}^{-1}$),⁴ and 1,4-bis(4,5-dihydro-1*H*-imidazol-2-yl)benzene ($K_{\text{CB}[7]} = 5.2 \times 10^9 \text{ M}^{-1}$)⁹ with CB[7].

The energy-minimized gas-phase structures of the guest and guest-host complexes were calculated by Gaussian 03 software, indicating the considerable preference of CB[7] for the benzyl ring rather than the ethylnaphthyl moiety of the guest molecules (Figure 3.9). In addition, despite the fact that CB[7] has relatively strong affinity for naphthyl group alone ($K_{\text{CB}[7]} = 3.0 \times 10^3 \text{ M}^{-1}$),⁴⁸ no binding between CB[7] and ethylnaphthyl group of the guest molecule is observed since the binding of one CB[7] over the benzyl portion sterically inhibits the further binding of a second CB[7] to the naphthyl group. Electrostatic repulsions between the carbonyl-lined portals of the CB[7] would also likely inhibit the close approach of two CB[7] hosts on one molecule (as described in the previous chapter).

3.3.2 Effect of Inclusion on the Chiroptic Behaviour

The chiroptic behaviour of the two enantiomeric guest molecules upon binding with CB[7] were investigated by polarimetry, in terms of the molar optical rotation. The inclusions of the enantiomers of the *N*-benzyl-1-(1-naphthyl)ethylammonium cation (BNEAH⁺) in CB[7] result in considerable increases in the magnitudes of their optical rotation. As shown in Table 3.2, the molar optical rotation for the *R* isomer increases from $-208 \text{ deg cm}^2 \text{ dmol}^{-1}$ for the free guest to $-940 \text{ deg cm}^2 \text{ dmol}^{-1}$ for the guest–host complex,

while a corresponding change from +208 to +940 deg cm² dmol⁻¹ was observed for the *S* isomer.

The titration curves were plotted based on the data in Table 3.2, as shown in Figure 3.8. The equilibrium is reached when the ratio of CB[7] to guests is approximately one, which also confirms the formation of a 1:1 ratio host/guest complex. The sharp linear increase in the molar rotation with CB[7] concentration in the titration curve are consistent with the high binding constants of the inclusion complexes which are formed.

Table 3.2 Optical rotation changes upon the formation of 1:1 inclusion complexes between (*R*)- and (*S*)-*N*-benzyl-1-(1-naphthyl)ethylamine hydrochloride and CB[7] in aqueous solution.

[CB[7]]/[R/S]	α_R (degree)	Molar rotation $[\Phi]_R$	α_S (degree)	Molar rotation $[\Phi]_S$
0	-0.0520	-208.0	0.0520	208.0
0.2	-0.0845	-338.0	0.0895	358.0
0.4	-0.1176	-470.4	0.1227	490.8
0.6	-0.1508	-603.2	0.1578	631.2
0.8	-0.1823	-729.2	0.1887	754.8
1.0	-0.2115	-846.0	0.2218	887.2
1.2	-0.2333	-933.2	0.2403	961.2
1.4	-0.2348	-939.2	0.2362	944.8
1.6	-0.2343	-937.2	0.2307	922.8
1.8	-0.2365	-946.0	0.2325	930.0

† The data were obtained with $T = 25.3^\circ\text{C}$, $\lambda = 589 \text{ nm}$, $l = 1 \text{ dm}$, [guest] was kept constant at 2.5 mM throughout the measurement .

$$[\Phi] = \frac{\alpha}{c l} \frac{3}{n^2 + 2} \frac{M}{100}$$
 where c is concentration of optically active component (g/mL); l is the length of cell (dm); n is the refractive index, for water = 1; M is the molecular weight of optically active substance.

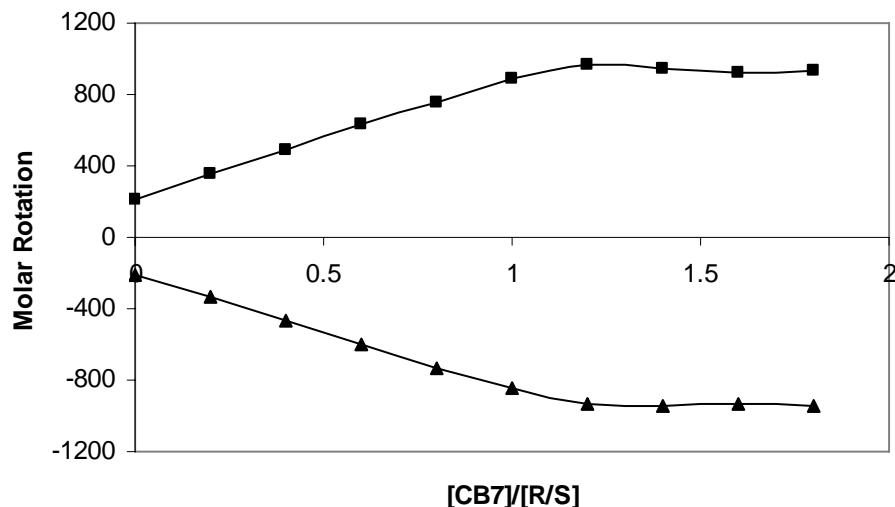


Figure 3.8 Molar rotation versus ratio of CB[7] to [(R) or (S)-BNEAH⁺] in aqueous solution: (■) (S)-BNEAH⁺ and (▲) (R)-BNEAH⁺.

It is well known and understandable that solvent has a significant effect on the value of optical rotation of chiral molecules in solution.⁴⁹ Recently, Wiberg and Vaccaro *et al.* have reported that the calculated optical rotation magnitude of (R)-(-)-3-chloro-1-butene has a remarkably large dependence on the C=C-C-C torsional angle.⁵⁰ The changes observed in the optical rotation of (R)- and (S)-N-benzyl-1-(1-naphthyl)ethylamine hydrochloride are believed to be most likely a combination of conformational and solvational effects.

From the gas-phase energy-minimized structures, as shown in Figure 3.9, 75–80° changes in the torsional angles between the C^{*}-CH₃ or C-NH₂⁺ bonds and the plane of the naphthyl ring upon binding of (S)-BNEAH⁺ to CB[7] were observed, and the torsion angles between the C^{*}-CH₃ or C^{*}-C1 bonds and the NH₂⁺-CH₂ bond change by 25–30° for the (R)-isomer (as summarized in Table 3.3). While there is free rotation of the naphthyl ring in the free guest, it is clearly restricted in its rotation with respect to the chiral centre by virtue of the cucurbit[7]uril binding of the benzyl portion of the guests.

Although the protonated (*R*)- and (*S*)- α -methylbenzylammonium cations, which lack the naphthyl chromophore, bind strongly to CB[7], there is no observed change in their optical rotations upon complexation to the host molecule.

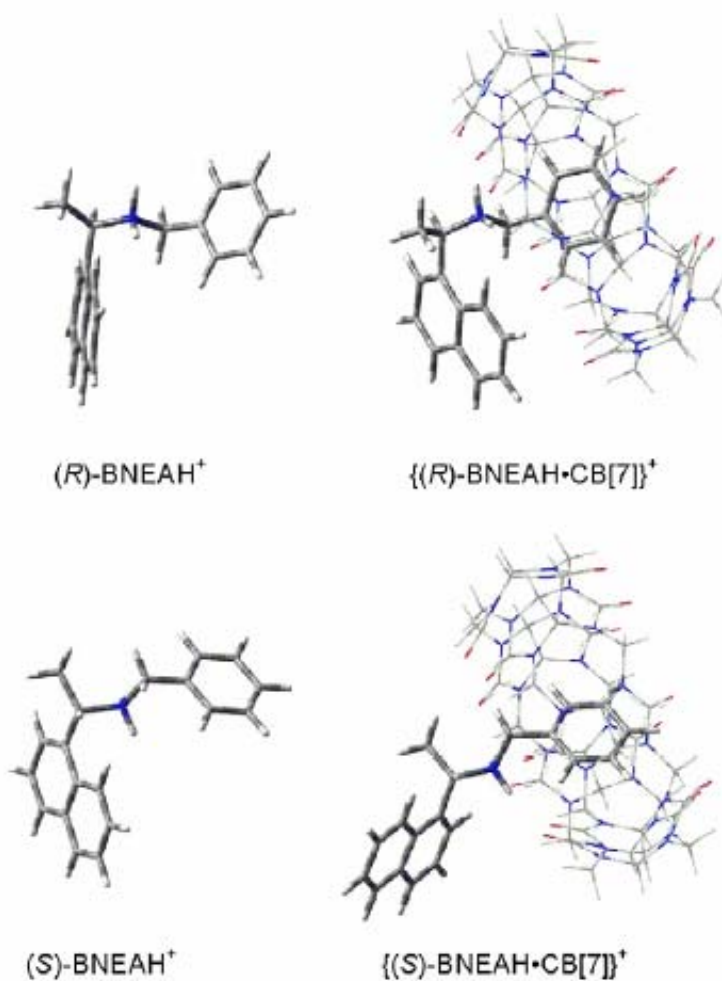


Figure 3.9 The energy-minimized gas-phase structures for (*R*)- and (*S*)-BNEAH⁺ guests and the 1:1 host–guest complexes with CB[7], suggesting the considerable change in the conformations of the substituents about the chiral center.

Table 3.3 Structure information obtained from HF/3-21G** Gaussian calculation for (R)-/(S)-(BNEAH⁺) before and after complexation with CB[7].

Torsional angles	R	R•CB[7]	S	S•CB[7]
N-C* & naphthyl plane	60.20	53.37	73.22	150.04
C*-CH ₃ & naphthyl plane	-65.22	-71.91	-166.27	-87.51
CH ₂ -N & C*-C1	67.90	41.64	-166.41	-164.19
CH ₂ -N & C*-CH ₃	-163.56	169.29	68.20	72.36

The circular dichroism (CD) spectra of the BNEAH⁺ isomers and their CB[7] host-guest complexes were determined in aqueous solution. As shown in Figure 3.10, the main features in these mirror image spectra are peaks in the 225–230 nm and 275–285 nm regions, which correspond to the ¹B_b and ¹L_a transitions, respectively. For the [BNEAH]⁺ isomers, the two peaks are of opposite signs, with the (R)-isomer negative and the (S)-isomer positive for the 225–230 nm peak and the opposite for the 275–285 nm. Upon inclusion in the CB[7], the CD spectra exhibit a decrease in the magnitude of the peak at 225–230 nm, with a slight hypsochromic shift. There is a reversal of the sign and an increase in the magnitude of the 275–285 nm peaks, which exhibits a bathochromic shift. The inclusion of the benzyl group in the CB[7] cavity restricts the motion of the naphthyl chromophore of the guest, thus causing the significant changes in circular dichroic behaviour of the guest.

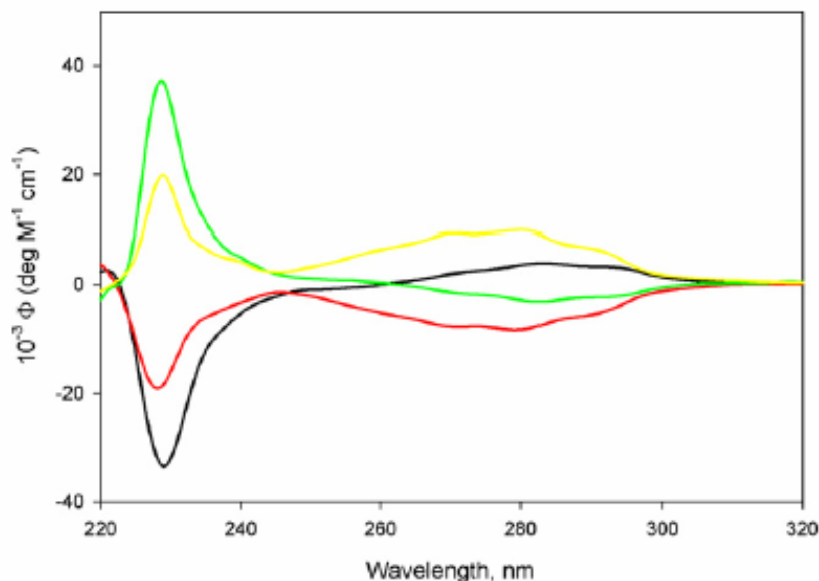


Figure 3.10 Circular dichroism spectra for (R) -BNEAH⁺ (black), $\{(R)\text{-BNEAH}\cdot\text{CB}[7]\}^+$ (red), (S) -[BNEAH⁺ (green), and $(S)\text{-BNEAH}\cdot\text{CB}[7]\}^+$ (yellow). The concentrations of BNEAH⁺ and CB[7] are 0.10 and 0.15 mM, respectively, in aqueous solution.

3.4 Summary

In this chapter, the profound effects of specific ion-dipole and H-bonding interactions between a chiral guest and an achiral host molecule on the optical properties of optical isomers through complexation induced geometric changes have been investigated using (R) - and (S) -N-benzyl-1-(1-naphthyl)ethylamine hydrochloride and CB[7] as examples. The formations of 1:1 host-guest complexes was confirmed by a UV-visible Job's plot, ESI-MS spectrometry, and ¹H NMR spectral and molar optical rotation titrations. The binding constant between these two enantiomers and CB[7] is determined to be $(1.2 \pm 0.4) \times 10^8 \text{ M}^{-1}$ by employing 3-(trimethylsilyl)propionic-2,2,3,3-*d*₄ acid as a competitor guest for ¹H NMR binding measurements. Upon the inclusion of benzyl moiety into the hydrophobic cavity, the

rotation of the naphthyl chromophore of the guest was restricted to some degree, which results in the five-fold increase in molar optical rotation and significant changes in the circular dichroism spectra. The significant change in optical properties of the guests is explained by the considerable change in the preferred conformations of the substituents about the chiral center, which was revealed by the energy minimization calculations using Gaussian 03.

This work has shown that even though the cucurbit[7]uril is an achiral host molecule, it can affect the chiroptic properties of chiral guest molecules upon encapsulation of a portion of the guest molecule into CB[7] cavity. In the free guests, the observed optical rotation is an average of the values for all of the conformations of the molecules, as a result of free rotations about the bonds to the chiral center. The strong binding of the chiral guest serves to sterically restrict the rotation of the ethylnaphthyl group, holding it in conformations which have higher optical rotations. Isaacs and coworkers⁵¹ have prepared a derivative of cucurbit[6]uril, (\pm)-bis-nor-seco-CB[6], and demonstrated diastereoselective molecular recognitions with guests such as amino acids. With the stability and selectivity of the molecular recognition of cucurbit[7]urils towards a variety of guest molecules, chiral molecular recognition research with CB[n] hosts likely has an important future.

References

1. Szejtli, J. *Chem. Rev.* **1998**, *98*, 1743.
2. Connors, K. A. *Chem. Rev.* **1997**, *97*, 1325.
3. Lagona, J.; Mukhopadhyay, P.; Chakrabarti, S.; Isaacs, L. *Angew. Chem., Int. Ed.* **2005**, *44*, 4844.
4. Liu, S.; Ruspic, C.; Mukhopadhyay, P.; Chakrabarti, S.; Zavalij, P. Y.; Isaacs, L. *J. Am. Chem. Soc.* **2005**, *127*, 15959.
5. Kim, H.-J.; Jeon, W. S.; Ko, Y. H.; Kim, K. *Proc. Nat. Acad. Sci. USA* **2002**, *99*, 5007.
6. Ong, W.; Kaifer, A. E. *J. Org. Chem.* **2004**, *69*, 1383.
7. Sindelar, V.; Cejas, M. A.; Raymo, F. M.; Kaifer, A. E. *New J. Chem.* **2005**, *29*, 280.
8. Sindelar, V.; Cejas, M. A.; Raymo, F. M.; Chen, W.; Parker, S. E.; Kaifer, A. E. *Chem. Eur. J.* **2005**, *11*, 7054.
9. Hettiarachchi, D. S. N.; Macartney, D. H. *Can. J. Chem.* **2006**, *84*, 905.
10. Ong, W.; Gomez-Kaifer, M.; Kaifer, A. E. *Org. Lett.* **2002**, *4*, 1791.
11. Ong, W.; Kaifer, A. E. *Organometallics* **2003**, *22*, 4181.
12. Jeon, W. S.; Moon, K.; Park, S. H.; Chun, H.; Ho, Y. K.; Lee, J. Y.; Lee, S. E.; Samal, S.; Selvapalm, N.; Rekharsky, M. V.; Sindelar, V.; Sobransingh, D.; Inoue, Y.; Kaifer, A. E.; Kim, K. *J. Am. Chem. Soc.* **2005**, *127*, 12984.
13. Wang, R.; Yuan, L.; Macartney, D. H. *Organometallics* **2006**, *25*, 1820.
14. Mock, W. L. *Top. Curr. Chem.* **1995**, *175*, 1.
15. Mock, W. L. *In Comprehensive Supramolecular Chemistry*; Vogtle, F., Ed.; Pergamon: Oxford, **1996**; Vol. 2, pp 477–493.
16. Kim, K. *Chem. Soc. Rev.* **2002**, *31*, 96.

17. Lee, J. W.; Samal, S.; Kim, H.-J.; Kim, K. *Acc. Chem. Res.* **2003**, *36*, 621.
18. Gerasko, O. A.; Samsonenko, D. G.; Fedin, V. P. *Russ. Chem. Rev.* **2002**, *71*, 741.
19. Kim, H.-J.; Heo, J.; Jeon, W. S.; Lee, E.; Kim, J.; Sakamoto, S.; Yamaguchi, K.; Kim, K. *Angew. Chem., Int. Ed.* **2001**, *40*, 1526.
20. Jon, S. Y.; Ko, Y. H.; Park, S. H.; Kim, H.-J.; Kim, K. *Chem. Commun.* **2001**, 1938.
21. Pattabiraman, M.; Natarajan, A.; Kaanumalle, L. S.; Ramamurthy, V. *Org. Lett.* **2004**, *7*, 529.
22. Pattabiraman, M.; Natarajan, A.; Kaliappan, R.; Mague, J. T.; Ramamurthy, V. *Chem. Commun.* **2005**, 4542.
23. Pattabiraman, M.; Kaanumalle, L. S.; Natarajan, A.; Ramamurthy, V. *Langmuir* **2006**, *22*, 7605.
24. Wang, R.; Yuan, L.; Macartney, D. H. *J. Org. Chem.* **2006**, *71*, 1237.
25. Marquez, C.; Nau, W. M. *Angew. Chem., Int. Ed.* **2001**, *40*, 4387.
26. Jyotirmayee, M.; Nau, W. M. *Angew. Chem., Int. Ed.* **2005**, *44*, 3750.
27. Nau, W. M.; Jyotirmayee, M. *Int. J. Photoenergy* **2005**, *7*, 133.
28. Mohanty, J.; Bhasikuttan, A. C.; Nau, W. M.; Pal, H. *J. Phys. Chem. B* **2006**, *110*, 5132.
29. Wang, R.; Yuan, L.; Macartney, D. H. *Chem. Commun.* **2005**, 5867.
30. Allenmark, S. *Chirality* **2003**, *15*, 409.
31. Scarso, A.; Rebek, J. *Top. Curr. Chem.* **2006**, *265*, 1.
32. Schneider, H. J.; Hacket, F.; Rudiger, H.; Ikeda, H. *Chem. Rev.* **1998**, *98*, 1755.
33. Dodziuk, H.; Kozminski, W.; Ejchart, A. *Chirality* **2004**, *16*, 90.
34. Chankvetadze, B. *Chem. Soc. Rev.* **2004**, *33*, 337.

35. Somogyi, L.; Samu, E.; Huszthy, P.; Lazar, A.; Angyan, J. G.; Surjan, P.; Hollosi, M. *Chirality* **2001**, *13*, 109.
36. Lazar, A.; Angyan, J. G.; Hollosi, M.; Huszthy, P.; Surjan, P. R. *Chirality* **2002**, *14*, 377.
37. Szarvas, S.; Majer, Z.; Huszthy, P.; Vermes, B.; Hollosi, M. *Enantiomer* **2002**, *7*, 241.
38. Kikuchi, Y.; Kobayashi, K.; Aoyama, Y. *J. Am. Chem. Soc.* **1992**, *114*, 1351.
39. Kikuchi, Y.; Aoyama, Y. *Supramol. Chem.* **1996**, *7*, 147.
40. Borovkov, V. V.; Lintuluoto, J. M.; Sugeta, H.; Fujiki, M.; Sugeta, H.; Arakawa, R.; Inoue, Y. *J. Am. Chem. Soc.* **2002**, *124*, 2993.
41. Borovkov, V. V.; Lintuluoto, J. M.; Hembury, G. A.; Sugiura, M.; Fujiki, M.; Arakawa, R.; Inoue, Y. *J. Org. Chem.* **2003**, *68*, 7176.
42. Borovkov, V. V.; Hembury, G. A.; Yamamoto, N.; Inoue, Y. *J. Phys. Chem. A* **2003**, *107*, 8677.
43. Borovkov, V. V.; Fujii, I.; Atsuya, M.; Hembury, G. A.; Tanaka, T.; Ceulemans, A.; Kobayashi, N.; Inoue, Y. *Angew. Chem., Int. Ed.* **2004**, *43*, 5481.
44. Borovkov, V. V.; Hembury, G. A.; Inoue, Y. *J. Org. Chem.* **2005**, *70*, 8743.
45. Rekharsky, M. V.; Yamamura, H.; Inoue, C.; Kawai, M.; Osaka, I.; Arakawa, R.; Shiba, K.; Sato, A.; Ko, Y. H.; Selvapalam, N.; Kim, K.; Inoue, Y. *J. Am. Chem. Soc.* **2006**, *128*, 14871.
46. Day, A.; Arnold, A. P.; Blanch, R. J.; Snushall, B. *J. Org. Chem.* **2001**, *66*, 8094.
47. Frisch, M. J.; Trucks, G. W.; Schlegel, H. B.; Scuseria, G. E.; Robb, M. A.; Cheeseman, J. R.; Montgomery, J. A. Jr.; Vreven, T.; Kudin, N.; Burant, J. C.; Millam, J. M.; Iyengar, S. S.; Tomasi, J.; Barone, V.; Mennucci, B.; Cossi, M.; Scalmani, G.; Rega, N.; Petersson, G. A.; Nakatsuji, H.; Hada, M.; Ehara, M.; Toyota, K.; Fukuda, R.; Hasegawa, J.; Ishida, M.;

Nakajima, T.; Honda, Y.; Kitao, O.; Nakai, H.; Klene, M.; Li, X.; Knox, J. E.; Hratchian, H. P.; Cross, J. B.; Adamo, C.; Jaramillo, J.; Gomperts, R.; Stratmann, R. E.; Yazyev, O.; Austin, A. J.; Cammi, R.; Pomelli, C.; Ochterski, J. W.; Ayala, P. Y.; Morokuma, K.; Voth, G. A.; Salvador, P.; Dannenberg, J. J.; Zakrzewski, V. G.; Dapprich, S.; Daniels, A. D.; Strain, M. C.; Farkas, O.; Malick, D. K.; Rabuck, A. D.; Raghavachari, K.; Foresman, J. B.; Ortiz, J. V.; Cui, Q.; Baboul, A. G.; Clifford, S.; Cioslowski, J.; Stefanov, B. B.; Liu, G.; Liashenko, A.; Piskorz, P.; Komaromi, I.; Martin, R. L.; Fox, D. J.; Keith, T.; Al-Laham, M. A.; Peng, C. Y.; Nanayakkara, A.; Challacombe, M.; Gill, P. M. W.; Johnson, B.; Chen, W.; Wong, M. W.; Gonzalez, C.; Pople, J. A. *Gaussian 03, Revision C.02*, Pittsburgh, PA 2004.

48. Wei, F.; Liu, S. M.; Xu, L.; Cheng, G. Z.; Wu, C. T.; Feng, Y. Q. *Electrophoresis* **2005**, *26*, 2214.

49. Kumata, Y.; Furukawa, I.; Fuene, T. *Bull. Chem. Soc. Jpn.* **1970**, *43*, 3920.

50. Wiberg, K. B.; Vaccaro, P. H.; Cheeseman, J. R. *J. Am. Chem. Soc.* **2003**, *125*, 1888.

51. Huang, W.-H.; Zavalij, P. Y.; Isaacs, L. *Angew. Chem., Int. Ed.* **2007**, *46*, 7425.

Chapter 4

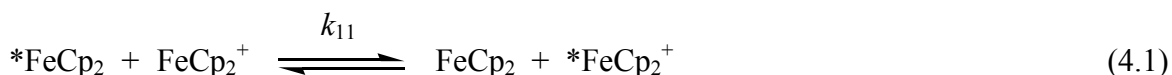
HOST-GUEST COMPLEXATION OF CUCURBIT[7]URIL WITH (TRIMETHYLAMMONIO)METHYLFERROCENE IN AQUEOUS SOLUTION

It has recently been reported that cucurbit[7]uril shows remarkably high affinity for certain guests such as protonated organic amines, viologens, and especially ferrocene derivatives, with the stability constants for the host-guest complexes in the range of 10^9 - 10^{13} M^{-1} in aqueous solution.¹⁻⁸ In this Chapter, the results of an investigation of the effects of host-guest complexation of (trimethylammonio)methylferrocene(+/2+) couple ($FcTMA^{+/2+}$) with CB[7] on the kinetics of its electron self-exchange (using 1H NMR paramagnetic line-broadening measurements) and electron transfer (monitored by stopped-flow techniques) reactions will be described and discussed. The very strong binding between ferrocene guests and the CB[7] host results in slow exchange for the guest on 1H NMR timescale, which make it possible to independently monitor the resonances of both free and bound forms of the reduced ferrocene $FcTMA^+$ in the presence of the paramagnetic $FcTMA^{2+}$ species, such that the rate constants for the possible self-exchange pathways involving the bound and free forms of both the oxidized and reduced forms of the guest can be determined separately. The inclusion of both $FcTMA^+$ and $FcTMA^{2+}$ by CB[7] increases the rate constant of its electron self-exchange reaction from $(2.1 \pm 0.1) \times 10^6 M^{-1} s^{-1}$ (for $FcTMA^{+/2+}$) to $(6.7 \pm 0.7) \times 10^6 M^{-1} s^{-1}$ (for $\{FcTMA \cdot CB[7]\}^{+/2+}$), however, the encapsulation of the reduced form only decreases

the rate constant to $(6 \pm 1) \times 10^5 \text{ M}^{-1} \text{ s}^{-1}$. The electron transfer reactions between FcTMA^+ or hydroxymethylferrocene and the bis(2,6-pyridinedicarboxylato)cobaltate(III) ion (which does not bind to CB[7]) have also been investigated in the absence and the presence of CB[7], in aqueous solution at 25 °C. The encapsulation of the ferrocene guests by CB[7] significantly reduces the rate constant for their oxidation as a result of reduced thermodynamic driving forces and steric hindrance to close approach of the oxidant to the encapsulated ferrocenes.

4.1 Introduction

The electron self-exchange reactions of ferrocene/ferrocenium couples (equation 4.1 for the unsubstituted ferrocene, $\text{FeCp}_2^{0/+}$) have long been of interest in terms of the solvent⁹⁻¹¹ and other medium effects on the kinetics of these processes.¹²⁻¹⁷



Weaver and co-workers found that the self-exchange rate constants for the (trimethylammonio)methylferrocene couple ($\text{FcTMA}^{+/2+}$), determined by ¹H NMR line-broadening experiments, varied somewhat with the nature of the solvent, with k_{ex} ranging from $2.1 \times 10^6 \text{ M}^{-1} \text{ s}^{-1}$ in acetonitrile to $2.3 \times 10^7 \text{ M}^{-1} \text{ s}^{-1}$ in propylene carbonate, compared to a value of $9 \times 10^6 \text{ M}^{-1} \text{ s}^{-1}$ measured in aqueous solution.^{10,11} Hupp and co-workers have reported that, in the presence of the host molecule β -CD, the rate constant for the electron self-exchange reaction of the $\text{FcTMA}^{+/2+}$ couple is decreased 20-50 fold upon inclusion of the reduced form of the compound.¹² The considerably weaker binding of β -CD to the oxidized form of the ferrocene prevented the determination of the rate constant for the symmetrical

electron self-exchange between $\{\text{FcTMA}\cdot\beta\text{-CD}\}^+$ and $\{\text{FcTMA}\cdot\beta\text{-CD}\}^{2+}$. In a related study, they reported that inclusion of the $\text{FcTMA}^{+/2+}$ couple by the anionic *para*-sulfonated calix[6]arene host (*p*-SO₃CX[6]) also affected the rate of electron exchange.¹⁶ In this case, the rate constants were similar when the reduced and oxidized forms were either both unbound ($1.2 \times 10^7 \text{ M}^{-1} \text{ s}^{-1}$) or bound ($1.6 \times 10^7 \text{ M}^{-1} \text{ s}^{-1}$), whereas the transfer of an electron from the unbound reductant to the bound oxidant (followed by rapid host transfer) was considerably faster ($1.3 \times 10^8 \text{ M}^{-1} \text{ s}^{-1}$), because of the favourable electrostatics in the formation of the precursor complex. With both of the hosts, electron transfer in the asymmetrical pathway is accompanied by fast host transfer (from the oxidized to the reduced form with β -CD and the reverse with *p*-SO₃CX[6]).

As was discussed in Chapter 1, the cavity size of CB[7] is comparable to that of β -CD,¹⁷⁻¹⁹ however, the main intermolecular interactions of these two types of hosts with guest molecules are different. Numerous studies reveal that the combined hydrophobic effects are primarily responsible for the stabilization of the inclusion complexes formed between CDs and most organic and organometallic guests.²⁰⁻²⁵ The hydroxyl groups lining the CD cavity openings do not appear to play a large role in the interactions with guest molecules. In contrast to this fact, the interaction forces between CB[n] hosts and guests are mainly of the following two types: (1) the ion-dipole interactions between the carbonyl group lining on the CB[n] portals and positive charge on included guest molecules, and (2) the hydrophobic interaction between organic guests and the inner surface of CB[n].²⁶⁻³⁰ The more restrictive and polar carbonyl portals of the CB[7] have led to the observance of significantly stronger binding interactions with certain guests, such as protonated organic amines and diamines,^{31,32} metal ions³³ and platinum amine complexes,³⁴⁻³⁷ and other organic cations,³⁸⁻⁴¹ compared to

β -CD. This is achieved by combining hydrophobic, ion-dipole, and hydrogen-bonding noncovalent interactions between the guest and the cavity and portals of the cucurbituril host. The carbonyl oxygens on the CB portals are known to be able to interact strongly with metal ions.^{42,43} Ferrocene and substituted ferrocenes, in particular, have recently been found to exhibit remarkably strong binding to CB[7],⁴⁴⁻⁴⁶ with stability constants for the host-guest complexes in the range of 10^9 - 10^{13} M⁻¹ in aqueous solution,^{45,46} compared to 10^3 - 10^4 M⁻¹ for the same guests with β -CD⁴⁷⁻⁴⁹ and 10^4 - 10^5 M⁻¹ with *p*-SO₃CX[6].¹³⁻¹⁶

We have recently shown that encapsulation of the (*E*)-1-ferrocenyl-2-(1-methyl-4-pyridinium)ethylene cation [(*E*)-FcMPE⁺] by CB[7] ($K_{\text{CB}[7]} = (1.3 \pm 0.5) \times 10^{12}$ M⁻¹) prevents indefinitely the normally observed (*E*) \rightarrow (*Z*) photoisomerization ($t_{1/2} \approx 10$ min) in aqueous solution.⁴⁶ Although the encapsulation of the ferrocene portion of the guest increases the reduction potential of the (*E*)-FcMPE^{2+/+} couple by only 30 mV, the rate constant for its outer-sphere chemical oxidation of (*E*)-FcMPE⁺ by the bis(2,6-pyridinedicarboxylato)cobaltate (III) ion ([Co(dipic)₂]⁻) in aqueous solution decreases significantly (from $k_0 = 2.1 \times 10^4$ M⁻¹ s⁻¹ to $k_{\text{CB}[7]} = 1.6 \times 10^2$ M⁻¹ s⁻¹) upon binding of ferrocene to CB[7]. Macartney and co-workers have also reported that the rate constants for the oxidation of the reduced forms of other substituted ferrocenes, such as (trimethylammonio)methylferrocene and ferrocene carboxylic acid, decrease in the presence of cyclodextrin^{50,51} and *p*-sulfonated calixarene⁵² host molecules.

In this chapter, the results of a kinetic study of the electron self-exchange rate constants for the (trimethylammonio)methylferrocene couple (FcTMA^{+ / 2+}), as shown in Figure 4.1, in the absence and presence of CB[7] in aqueous solution, will be discussed. It has recently been determined, by isothermal calorimetry, that the inclusion stability constant

for the reduced form of FcTMA^+ with CB[7] is $(4 \pm 2) \times 10^{12} \text{ M}^{-1}$ in pure water⁴⁵ (a value of $(3.31 \pm 0.62) \times 10^{11} \text{ M}^{-1}$ was determined in D_2O containing 50 mM NaO_2CCD_3 using a ^1H NMR competitive binding method³¹) and that the reduction potential for the $\text{FcTMA}^{2+/+}$ couple is about 110 mV more positive when complexed to CB[7].⁴⁵ In addition to measurements of the electron self-exchange rate constants for the $\text{FcTMA}^{+/2+}$ couple, experiments on the kinetics of the oxidation of FcTMA^+ and hydroxymethylferrocene (FcCH_2OH) by $\text{Co}(\text{dipic})_2^-$ have been carried out in the presence of CB[7]. The effect of CB[7] encapsulation of the ferrocene on the electron-transfer rate constants are compared to those observed previously for the (*E*)- FcMPE^+ complex⁴⁶ and for electron-transfer reactions of substituted ferrocenes in the presence of the β -CD and *p*-sulfonated calixarene hosts in aqueous solution.

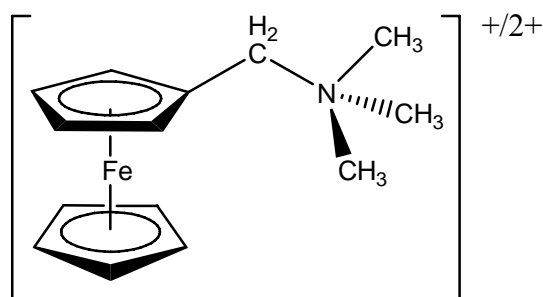


Figure 4.1 The structure of (*trimethylammonio*)methylferrocene($\text{FcTMA}^{+/2+}$) couple.

4.2 Experimental

4.2.1 Material Preparation

Cucurbit[7]uril was prepared and characterized by the method of Day and co-workers.⁵³ (Trimethylammonio)methylferrocene tetrafluoroborate ($[\text{FcTMA}]\text{BF}_4$) was

prepared by methylation of dimethylaminomethylferrocene (Aldrich) using a reported method,⁵⁴ and the oxidized form, [FcTMA](BF₄)₂ ($\lambda_{\text{max}} = 628 \text{ nm}$, $\epsilon = 198 \text{ M}^{-1} \text{ cm}^{-1}$), was prepared by the method of Hupp *et al.*¹² Hydroxymethylferrocene was used as received (Strem Chemicals). The NH₄[Co(dipic)₂] (dipic²⁻ = 2,6-pyridinedicarboxylate) compound was synthesized according to literature methods.⁵⁵

4.2.1.1 (Trimethylammonio)methylferrocene Iodide ([FcTMA]I)

The (trimethylammonio)methylferrocene iodide [Fe(Cp)(C₅H₄CH₂NMe₃)]I (where Cp⁻ is the cyclopentadienyl anion, C₅H₅⁻) was synthesized by methylation of N,N-dimethylaminomethylferrocene with methyl iodide. To a cooled solution of 2.04 mL (13.35 mmol) of N,N-dimethylaminomethylferrocene in 15 mL of absolute methanol was added dropwise a solution of 1.325 mL (20 mmol) of methyl iodide in 15 mL of absolute methanol. The clear solution was refluxed for 5 minutes before 250 mL of diethyl ether was added to produce a precipitate. The resulting precipitate was collected by vacuum filtration and washed with diethyl ether, until the washings were colourless, and then air dried. Yield: 84%, ¹H NMR (in D₂O): δ 4.46 (s, 2H), 4.38 (s, 2H), 4.33 (s, 2H), 4.23 (s, 5H), 2.90 (s, 9H) ppm.

4.2.1.2 (Trimethylammonio)methylferrocene tetrafluoroborate ([FcTMA]BF₄)

As the iodide ion in (trimethylammonio)methylferrocene iodide ([FcTMA]I) is liable to be oxidized in the study of the kinetics of oxidation/reduction reactions, (trimethylammonio)methylferrocene tetrafluoroborate ([FcTMA]BF₄) was prepared and used for all of the measurements and reactions in this chapter. The abbreviation FcTMA⁺, therefore, refers to [FcTMA]BF₄ in this chapter. The [FcTMA]BF₄ was synthesized by

adding aqueous [FcTMA]I (1.0 g in 50 mL water) to a saturated aqueous NH_4BF_4 solution (2.3 g in 5 mL water). The resulting precipitate was washed with cold water, dried and then recrystallized from CH_3CN /ether (dissolve the crude product in minimum amount of CH_3CN , then add diethyl ether dropwise to produce the pure product). Yield: 86%

4.2.1.3 (Trimethylammonio)methylferrocenium tetrafluoroborate {[FcTMA](BF₄)₂}

The oxidized (trimethylammonio)methylferrocenium tetrafluoroborate ([FcTMA](BF₄)₂) was obtained from ([FcTMA]BF₄) (0.138 g, 0.4 mmol) by using benzoquinone (0.043 g, 0.4 mmol) in CH_2Cl_2 (18 mL) as a stoichiometric oxidant under the protection of argon, followed by addition of HBF₄ (48%, 1.0 mL).¹² The resulting blue oily solution was added to 50 mL diethyl ether to produce blue needle-shape crystals. Yield: 73%. Since the product is paramagnetic, characterization with ¹H NMR was not practical. The purity of final product was determined by visible spectroscopy: $A_{628\text{nm}}$ (measured) = 0.0485 using a concentration of 0.25 mM and a cell of 1 cm pathlength. The value of the molar absorptivity coefficient (ϵ) was calculated to be $194 \text{ M}^{-1} \text{ cm}^{-1}$, which is in good agreement with the result ($\epsilon = 198 \text{ M}^{-1} \text{ cm}^{-1}$) reported previously.⁵⁷

4.2.1.4 Ammonium bis(2,6-pyridinedicarboxylato)cobaltate(III)

Ammonium bis(2,6-pyridinedicarboxylato)cobaltate(III) was prepared according to literature method.⁵⁵ Concentrated NH_4OH (200 mL) was added to a solution of 2,6-pyridinedicarboxylic acid (10 g) in 10 mL of water. The mixture was then heated to 60-70 °C, followed by the addition of water (50 mL). The mixture was then taken to dryness and the process repeated once more. The solid was dissolved in 500 mL of warm water while

heating, followed by the addition of a solution of $\text{Co}(\text{NO}_3)_2 \cdot 6\text{H}_2\text{O}$ (8.7 g in 10 mL of water) with stirring, after cooling. Hydrogen peroxide (50 mL of 30% H_2O_2) was then added after one hour, and the resulting mixture was stirred for 3-4 hours at room temperature. The precipitate which resulted was removed by filtration and the filtrate was heated to 60-70 °C with stirring, until the solution became slightly turbid. The solution was cooled and allowed to stand at room temperature for several hours. The final resulting precipitate was filtered and washed thoroughly with ethanol and ether.

4.2.2 Methods and Instruments

4.2.2.1 Kinetic Measurements

The electron-transfer kinetic experiments were performed on an Applied Photophysics SV-MX-17 stopped-flow spectrophotometer, with the temperature maintained at 25.0 ± 0.1 °C using an external temperature bath. The solutions were prepared in distilled water containing 0.10 M NaCl. The second-order rate constants for the oxidation of the ferrocenes by $[\text{Co}(\text{dipic})_2]^-$, in the absence and presence of CB[7], were determined from five to six replicate traces at each concentration of CB[7].

4.2.2.2 ^1H NMR Line Broadening Experiment

^1H NMR spectra of $[\text{FcTMA}]\text{BF}_4$ were obtained on a Bruker AV-400 NMR spectrometer. The ^1H NMR line broadening experiment data were collected on Bruker AV-500 spectrometer in D_2O at 25 °C, with the chemical shifts referenced to the HOD signal internally. A 1:1 ratio of $\{\text{FcTMA} \cdot \text{CB}[7]\}^+$ complex was formed by incubating equal molar (1.0 mM) of $[\text{FcTMA}]\text{BF}_4$ and CB[7] in N_2 -bubbled (for 30 minutes) D_2O for 10 minutes. In

^1H NMR line broadening experiment, 0.70 mL of 1:1 $\{\text{FcTMA}\cdot\text{CB}[7]\}^+$ in D_2O was titrated with consecutive additions of a $[\text{FcTMA}](\text{BF}_4)_2$ solution (.01 mM, 7.07 μL to 8.0 μL), while keeping the total concentration of FcTMA^+ and FcTMA^{2+} constant (1.0 mM). The solutions were thoroughly mixed and allowed to equilibrate for several minutes in the probe (25 $^\circ\text{C}$) before the spectrum was acquired.

4.2.2.3 Cyclic Voltammetry

Cyclic voltammetric measurements on the $\text{FcTMA}^{2+/+}$ couple, in the absence and presence of $\text{CB}[7]$, were recorded using a Bioanalytical Systems CV-1B cyclic voltammeter, attached to a Houston Instrument 100 X-Y recorder with a scan rate of 100mV/s. The working (a glassy carbon) and auxiliary (a platinum wire) electrodes in the sample solutions (1.0 mM FcTMA^+ and $\{\text{FcTMA}\cdot\text{CB}[7]\}^+$ in 0.10 M $\text{NaCl}/\text{H}_2\text{O}$) were separated from the reference electrode (Ag/AgCl , $E^\circ = 0.222$ V vs NHE) by a glass frit. The solutions were purged with argon and thoroughly stirred for 20 minutes before each scan.

4.2.2.4 UV-Visible Spectroscopy

The UV-visible spectra were obtained using a Hewlett-Packard 8452A diode-array and Cary 3 spectrophotometers, interfaced to personal computers and controlled by manufacturer-supplied software. The concentrations of the complexes used for the measurements were usually about 0.10 mM.

4.3 Results and Discussion

4.3.1 Complexation Between CB[7] and FcTMA⁺

The complexation between CB[7] and FcTMA⁺ and the effect of the encapsulation of FcTMA⁺ in the CB[7] cavity on the kinetics of its electron self-exchange reaction and oxidation reaction by Co(dipic)₂⁻ in aqueous solution were investigated by ¹H NMR and ESI-MS spectroscopy. The kinetic measurements of the outer-sphere electron-transfer reactions of the ferrocene by a cobalt(III) complex was undertaken by stopped-flow spectrophotometry.

As shown in Figure 4.2, in the presence of one equivalent of CB[7], the resonances for the methylene group and the cyclopentadienyl rings show significant upfield shifts, indicating the inclusion of both moieties into the hydrophobic cavity, thus optimizing the interaction between the positive charge on the nitrogen atom and the carbonyl lined CB[7] portal. The slightly downfield shift for the resonance of the methyl groups is attributed to the deshielding effect from the carbonyl portal. Two sets of resonances for the guest molecule were observed in the presence of insufficient CB[7], indicating the slow exchange between the free and bound FcTMA⁺ at room temperature on the ¹H NMR timescale. The disappearance of the resonances for free FcTMA⁺ species when one equivalent of CB[7] was added to the solution indicates the formation of 1:1 host-guest inclusion complex.

The formation of a 1:1 {FcTMA•CB[7]}⁺ inclusion complex was also confirmed by the electrospray ionization mass spectrum, in which the peak at $m/z = 1420.7$ represents [CB[7]+FcTMA]⁺, in good agreement with theoretical value for this ion ($m/z = 1420.4$).

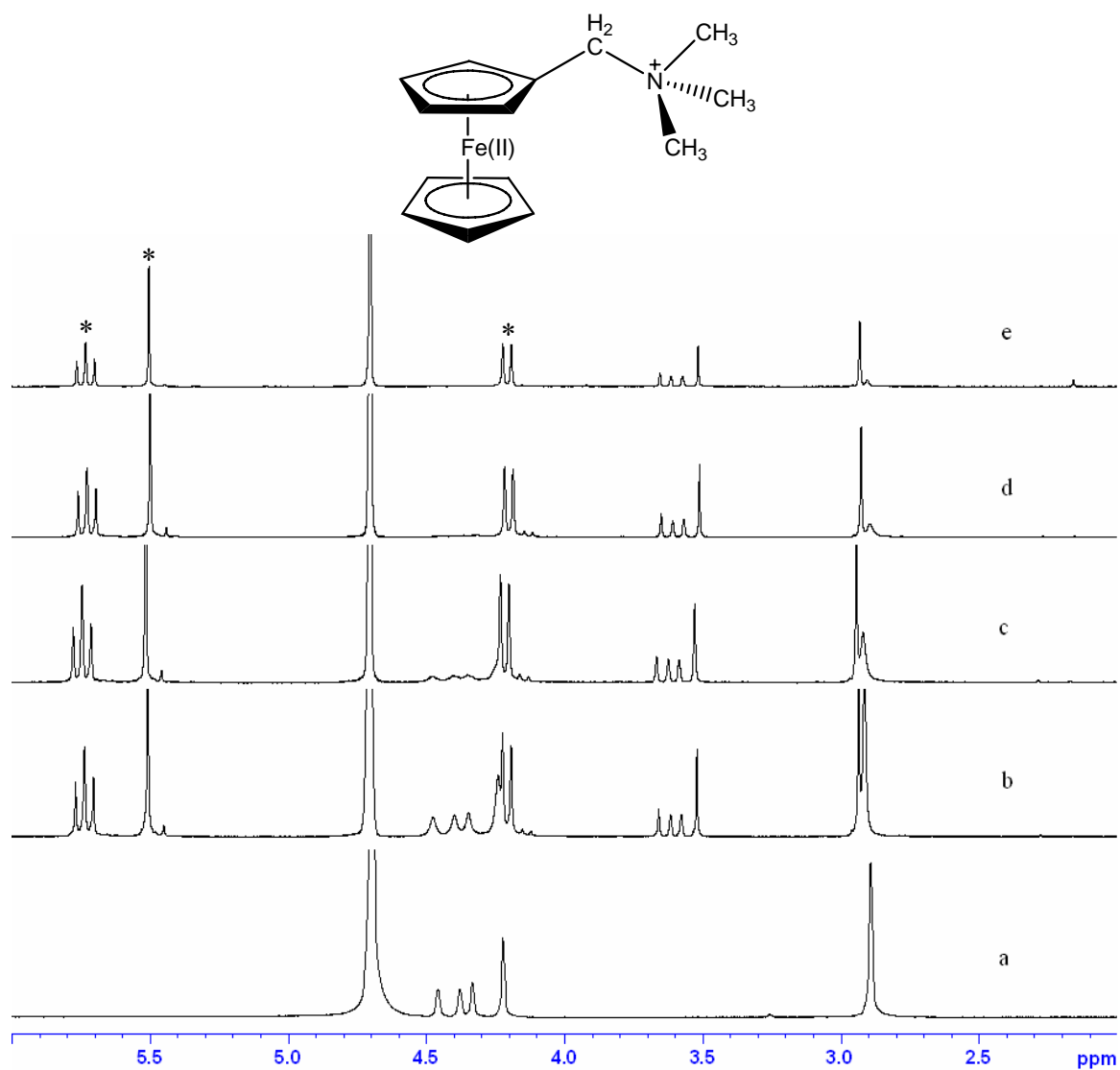


Figure 4.2 ¹H NMR spectra of FcTMA⁺ (1 mM) in the absence and presence of cucurbit[7]uril in D₂O at 25 °C with (a) 0, (b) 0.33, (c) 0.56, (d) 0.89, and (e) 1.12 mM of CB[7] (signals are labeled with *).

4.3.2 Electron Self-Exchange Kinetics

4.3.2.1 Determination of the Self-Exchange Rate Constants

The electron self-exchange reaction of the $\text{FcTMA}^{+/2+}$ couple has previously been studied in the presence of the β -cyclodextrin (β -CD) and *p*-sulfonated calix[6]arene (*p*-SO₃CX[6]) host molecules.^{12,16} With these hosts, the encapsulated FcTMA^+ guest exhibits fast exchange on the ¹H NMR time scale, resulting in proton resonances whose chemical shifts represent the average of the bound $\{\text{FcTMA}\cdot\text{Host}\}^{n+}$ and unbound FcTMA^+ species. However, as shown in Figure 4.2, the binding of FcTMA^+ to CB[7] in D₂O resulted in guest exchange which is slow on the ¹H NMR timescale (500 MHz), indicated by the separate resonances for the unbound and bound guest molecules. The line broadening phenomena resulting from electron self-exchange between FcTMA^+ and added FcTMA^{2+} can therefore be simultaneously monitored for both the bound $\{\text{FcTMA}\cdot\text{CB}[7]\}^+$ and unbound FcTMA^+ . To a 1.0 mM solution of FcTMA^+ in D₂O was added varying amounts of FcTMA^{2+} (from 10 to 80 μM after mixing) while keeping the total $[\text{FcTMA}]^{n+}$ concentration constant. As shown in Figure 4.3, with the addition of FcTMA^{2+} , both sets of resonances were broadened to different degrees. The unsubstituted cyclopentadienyl proton resonance at 3.52 ppm was used for the measurement of peak widths at half height ($W = \Delta\nu_{1/2}$), which were further employed for the determination of observed electron self-exchange rate constant ($k_{\text{ex}}^{\text{obs}}$), when the concentration of CB[7] was relatively low. Due to the much faster broadening process for free FcTMA^+ , the measurement of peak width at half height was not possible with higher CB[7] concentrations (greater than 0.4 equivalents), and thus the methyl proton resonance at 2.92 ppm was used for this measurement. The resonance at 4.48 ppm for the cyclopentadienyl protons adjacent to the substituent was used for the measurement of

broadening of bound FcTMA^+ . The much slower broadening process of the bound FcTMA^+ made the measurement of the peak width at half-maximum height possible and more accurate up to about 1.5 equivalents of CB[7].

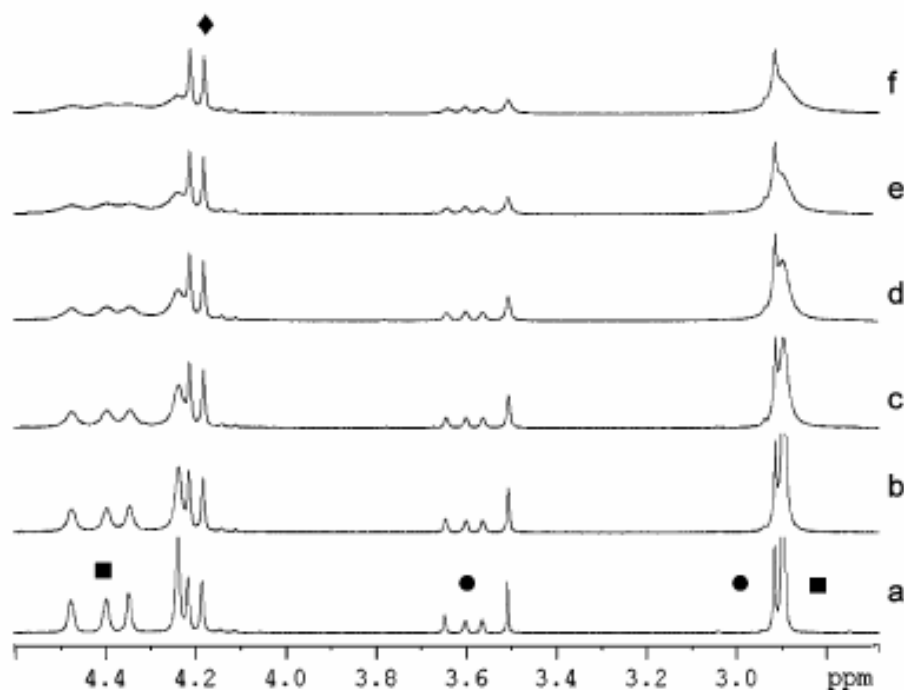


Figure 4.3 ^1H NMR spectra of FcTMA^+ [1.0 mM total, (■) FcTMA^+ and (●) $\{\text{FcTMA}\cdot\text{CB}[7]\}^+$] in the presence of 0.21 mM CB[7] (◆) with increasing concentrations of total FcTMA^{2+} : (a) 0, (b) 10, (c) 20, (d) 30, (e) 40, and (f) 50 μM .

In general, the observed rate constant ($k_{\text{ex}}^{\text{obs}}$) for an electron self-exchange reaction, which is in the slow-exchange region (broadening of the resonances in the presence of the paramagnetic species, but no change in their chemical shifts, were observed at 500 MHz), is given by equation 4.1, where W_{DP} and W_{D} are the line widths of the resonances at half-maximum height, in the presence and absence of the paramagnetic iron(III) species, respectively.

$$k_{\text{ex}}^{\text{obs}} = \frac{\pi (W_{\text{DP}} - W_{\text{D}})}{[\text{FcTMA}^{2+}]_{\text{total}}} \quad (4.1)$$

Figure 4.4 shows the linear dependences of $W_{\text{DP}} - W_{\text{D}}$ on $[\text{FcTMA}^{2+}]_{\text{total}}$ for the FcTMA^+ and $\{\text{FcTMA}\cdot\text{CB}[7]\}^+$ species at various concentrations of $\text{CB}[7]$ at 25 °C, from which a series of the $k_{\text{ex}}^{\text{obs}}$ values can be determined.

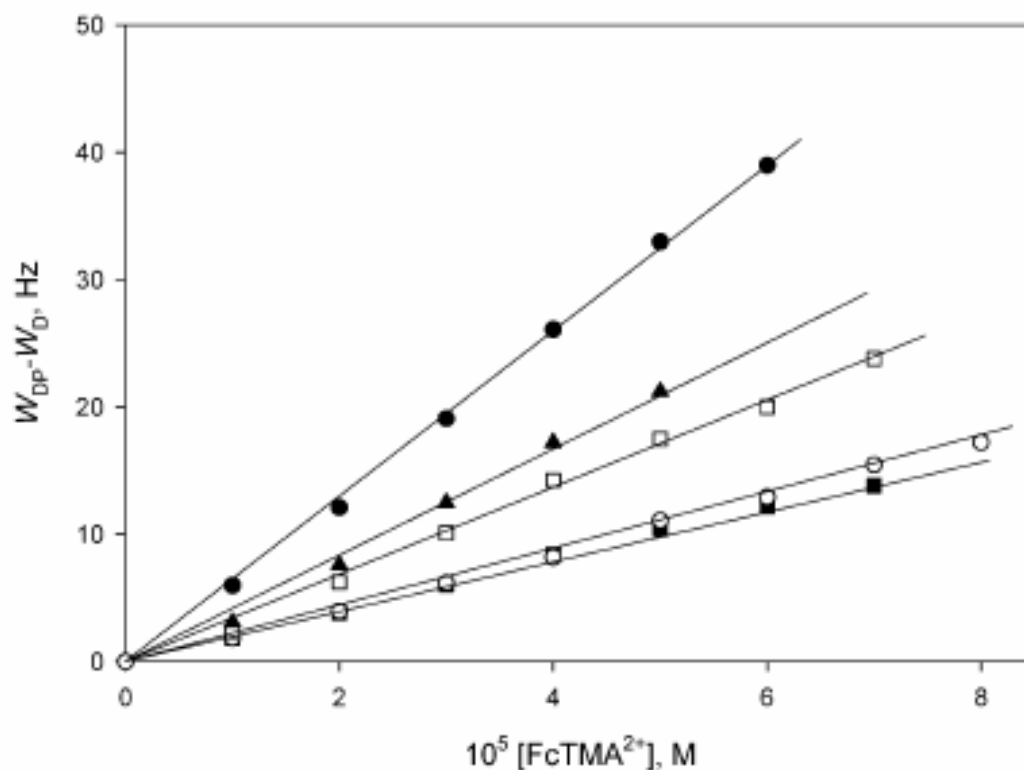


Figure 4.4 Linear dependences of $W_{\text{DP}} - W_{\text{D}}$ on $[\text{FcTMA}^{2+}]_{\text{total}}$ for the Cp ring proton resonance of FcTMA^+ (4.24 ppm) or $\{\text{FcTMA}\cdot\text{CB}[7]\}^+$ (3.52 ppm) at various concentrations of $\text{CB}[7]$ at 25 °C: (●) 0, (■) 0.33, (○) 0.54, (□) 0.77, and (▲) 0.86 mM.

Figure 4.5 shows the possible electron exchange pathways for the $\text{FcTMA}^{+/2+}$ couple in the absence and presence of CB[7] involve symmetric (no thermodynamic driving force) self-exchanges [Figures 4.5(a) and 4.5(c)] and an asymmetric exchange [Figure 4.5(b)], in which one of the two species is bound to CB[7].

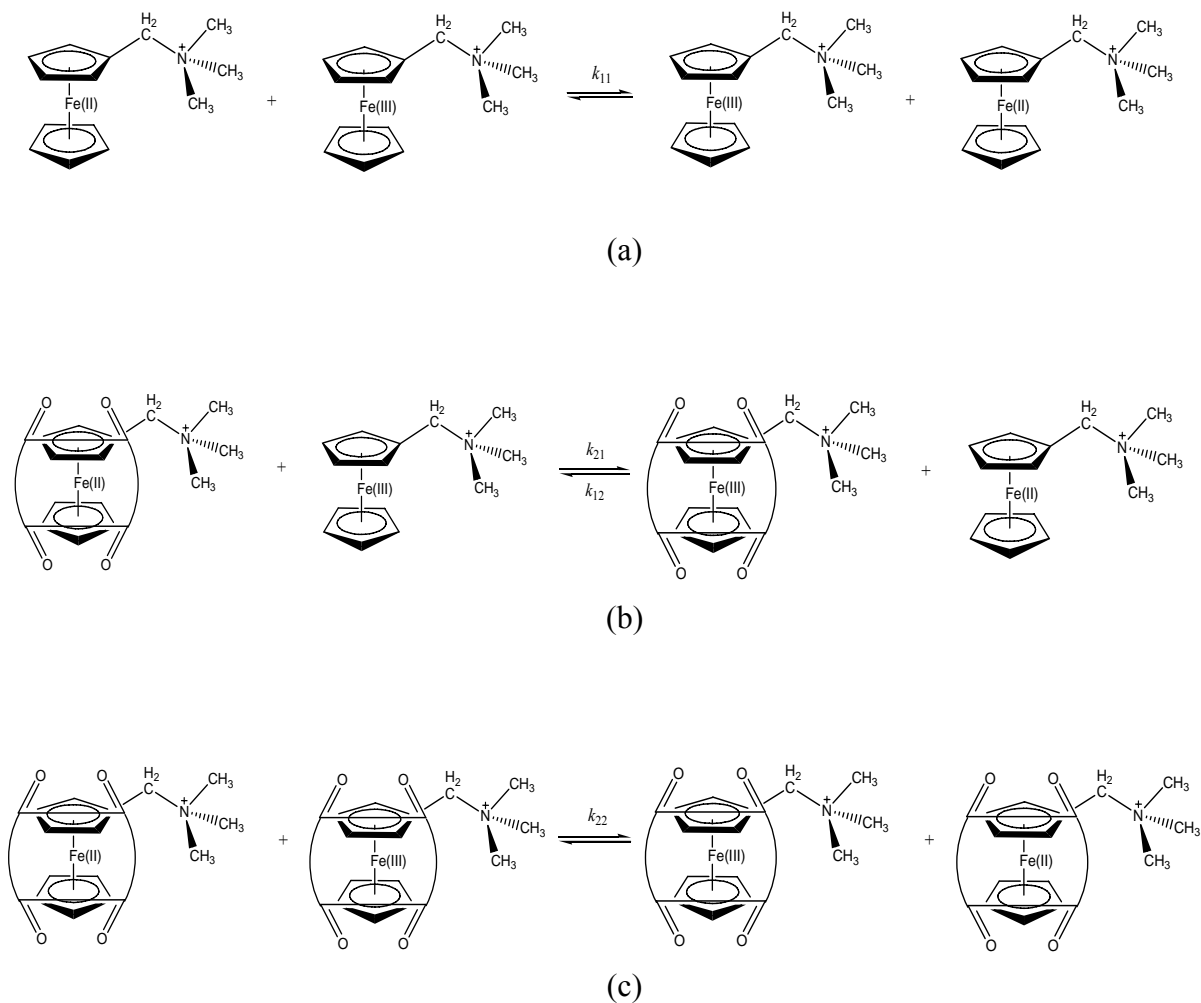


Figure 4.5 The possible pathways of electron self-exchange reactions for the $\text{FcTMA}^{+/2+}$ couple in the absence and presence of CB[7].

The self-exchange rate constant k_{11} for the $\text{FcTMA}^{+/2+}$ couple, in the absence of CB[7] was measured directly by ^1H NMR titration line-broadening experiments (determined by plotting $(W_{\text{DP}} - W_{\text{D}})$ as a function of the concentration of $[\text{FcTMA}]^{2+}$, shown as Figure 4.4), to be $(2.1 \pm 0.1) \times 10^6 \text{ M}^{-1} \text{ s}^{-1}$ at $I \approx 0.002 \text{ M}$ (no added electrolyte). As might be expected for a reaction between complexes with charges of the same sign (+/2+), the self-exchange rate constants reported previously for the $\text{FcTMA}^{+/2+}$ couple are dependent on ionic strength. Weaver reported a rate constant of $9 \times 10^6 \text{ M}^{-1} \text{ s}^{-1}$ at $I \approx 0.03 \text{ M}$ and indicated that it increased to $2.3 \times 10^7 \text{ M}^{-1} \text{ s}^{-1}$ at $I \approx 0.5 \text{ M}$.¹⁰ Hupp *et al.* reported directly measured values of $1.2 \times 10^7 \text{ M}^{-1} \text{ s}^{-1}$ with no added electrolyte (but using slightly higher concentrations of the ferrocene cations than in the present study) and $2.8 \times 10^7 \text{ M}^{-1} \text{ s}^{-1}$ at $I \approx 0.1 \text{ M}$.¹² The value determined in the present study is therefore in line with the previously measured rate constants, considering the difference in ionic strength.

Assuming that the electron-exchange processes are fast compared to the decomplexation rates of the $\{\text{FcTMA}\cdot\text{CB}[7]\}^{n+}$ species, the line broadening observed in the resonances for FcTMA^+ ($k_{\text{ex}}^{\text{unbound}}$) is related to the values of k_{11} and k_{12} , whereas the line broadening in the resonances for $\{\text{FcTMA}\cdot\text{CB}[7]\}^+$ ($k_{\text{ex}}^{\text{bound}}$) depends on the values of k_{21} and k_{22} . The plots of the observed electron-exchange rate constants, $k_{\text{ex}}^{\text{unbound}}$ and $k_{\text{ex}}^{\text{bound}}$, as a function of CB[7] concentration are shown in Figure 4.6. For both the FcTMA^+ and $\{\text{FcTMA}\cdot\text{CB}[7]\}^+$ species, the rate constant increases with increasing CB[7] concentration. The observation of the trend in $k_{\text{ex}}^{\text{unbound}}$ for FcTMA^+ is limited to the lower concentration range (broadening process is too fast for free FcTMA^+ species), whereas the trend in $k_{\text{ex}}^{\text{bound}}$ for $\{\text{FcTMA}\cdot\text{CB}[7]\}^+$ can be observed over a larger range of CB[7] concentration (up to 1.5 equivalent). With one or more equivalents of CB[7] present, the observed exchange rate

constant $k_{\text{ex}}^{\text{bound}}$ is independent of CB[7] concentration, indicating that all the electron exchange process occurs between $\{\text{FcTMA}\cdot\text{CB}[7]\}^+$ and $\{\text{FcTMA}\cdot\text{CB}[7]\}^{2+}$, therefore the rate constant for the $\{\text{FcTMA}\cdot\text{CB}[7]\}^{+/2+}$ couple, k_{22} , was determined by this limit to be $(6.7 \pm 0.7) \times 10^6 \text{ M}^{-1} \text{ s}^{-1}$.

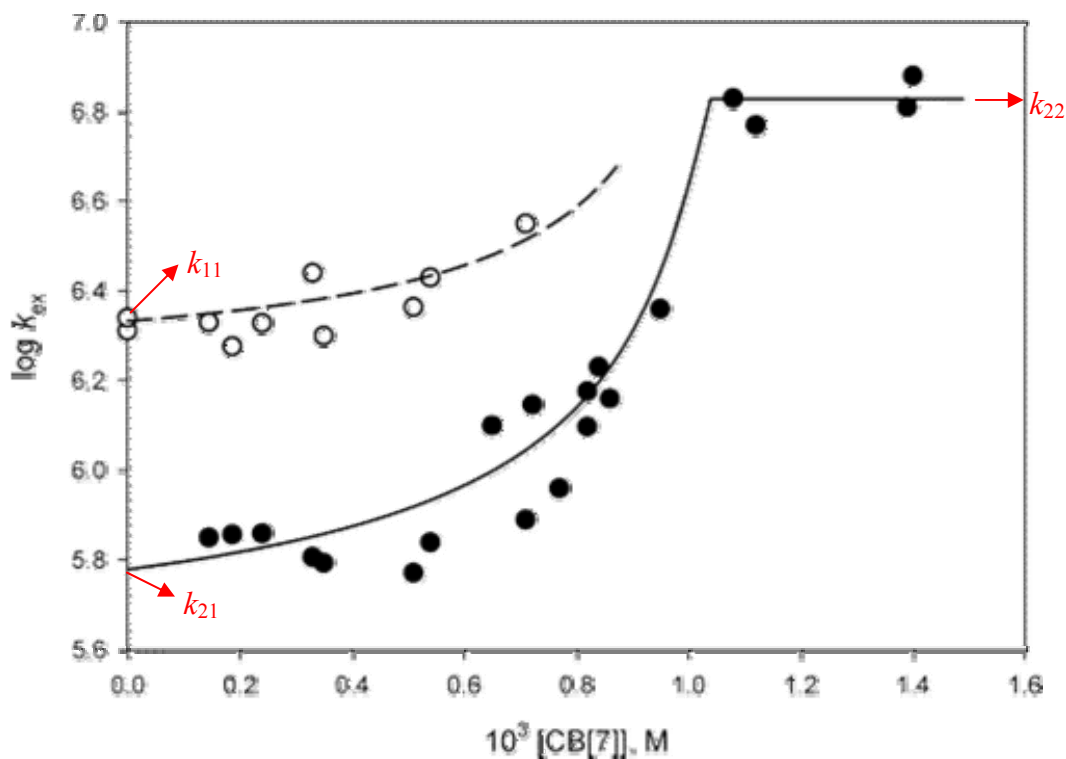


Figure 4.6 Plots of $\log k_{\text{ex}}$ against CB[7] concentration derived from the observed line broadening in the resonances for the (○) FcTMA^+ and (●) $\{\text{FcTMA}\cdot\text{CB}[7]\}^+$ species.

4.3.2.2 Determinations of k_{12} and k_{21}

Cyclic voltammetry (CV) was conducted to study the redox behaviour of FcTMA^+ in the absence and presence of CB[7]. As shown in Figure 4.7, the presence of 1.2 equivalent of CB[7] (1.0 mM FcTMA^+ with 1.2 mM CB[7]) without added electrolyte resulted in a

significant anodic shift (85 mV) in the position of the corresponding $E_{1/2}$ value for $\text{FcTMA}^{2+/+}$ (measured in a solution containing 0.10 M NaCl as an added electrolyte) couple. This change is slightly different from the reported reduction potential value for $\{\text{FcTMA}\cdot\text{CB}[7]\}^{2+/+}$ pair (~110 mV), which was measured in 0.10 M NaCl solution. This difference is attributable to differential ionic strength effects on the binding constants for the $\{\text{FcTMA}\cdot\text{CB}[7]\}^{2+/+}$ species, as observed previously for other CB[7] host-guest complexes.⁴¹

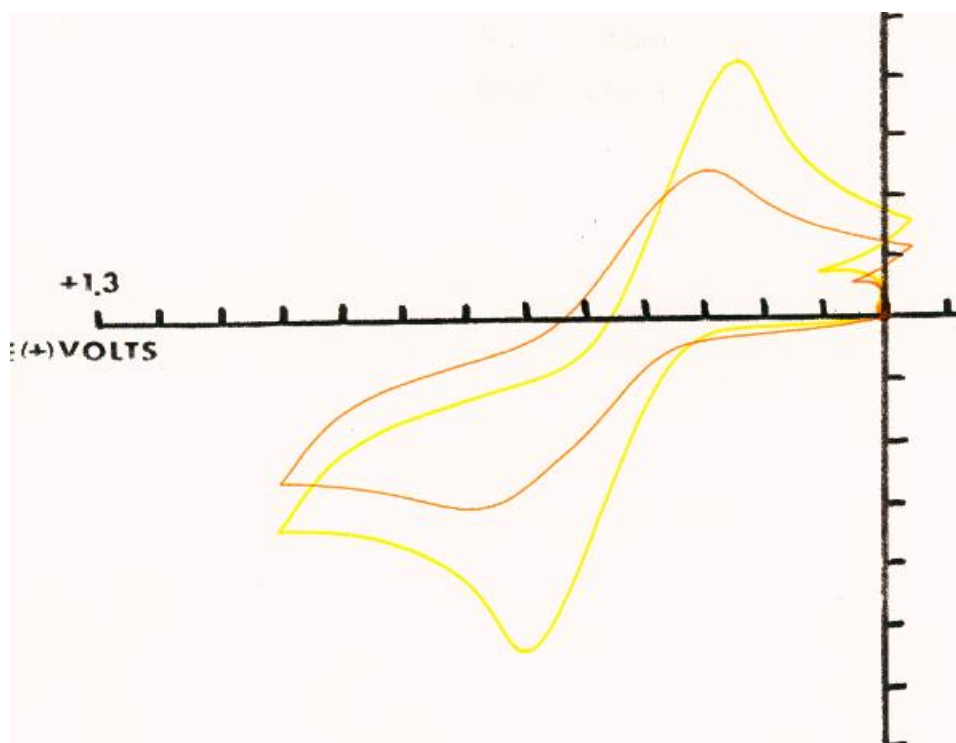


Figure 4.7 Cyclic voltammogram of $\text{FcTMA}^{2+/+}$ (1.0 mM) in the absence (yellow) and presence (orange) of CB[7] host molecule (1.2 equivalent) without added electrolyte at 25 °C.

The anodic shift indicated that the binding of CB[7] to the reduced state (FcTMA^+) is higher relative to that for the oxidized form (FcTMA^{2+}). As a result, the forward process in Figure 4.5(b) would be considerably disfavoured thermodynamically, whereas the reverse

process would be thermodynamically favourable. The stability constant for $\{\text{FcTMA}\cdot\text{CB}[7]\}^{2+}$ can be calculated to be $1.5 \times 10^{11} \text{ M}^{-1}$ using equation 4.2, based on the 85 mV difference in the reduction potentials of bound and unbound couples and the reported stability constant for $\{\text{FcTMA}\cdot\text{CB}[7]\}^+$ ($4 \times 10^{12} \text{ M}^{-1}$),²³ where R is the universal gas constant equal to $8.314 \text{ J K}^{-1} \text{ mol}^{-1}$, T is the temperature in Kelvin (298 K) and F is the Faraday constant, equal to $9.649 \times 10^4 \text{ C mol}^{-1}$.

$$\Delta E^0 = (RT/F) \ln \frac{K_{\text{red}}}{K_{\text{ox}}} \quad (4.2)$$

With the very high stability constant for the $\{\text{FcTMA}\cdot\text{CB}[7]\}^+$ complex, it can be assumed that the equilibrium concentration of $\{\text{FcTMA}\cdot\text{CB}[7]\}^+$ and the total concentration of CB[7] are approximately equal up to the 1:1 equivalence point (1.0 mM). The change in the observed $k_{\text{ex}}^{\text{obs}}$ values with total CB[7] concentration (Figure 4.6) is therefore due to the increasing amounts of the oxidized $\{\text{FcTMA}\cdot\text{CB}[7]\}^{2+}$ as the CB[7] concentration is raised. The expressions for the observed exchange rate constants involving FcTMA^+ ($k_{\text{ex}}^{\text{unbound}}$ which is related to k_{11} and k_{12}) and $\{\text{FcTMA}\cdot\text{CB}[7]\}^+$ ($k_{\text{ex}}^{\text{bound}}$ which is related to k_{21} and k_{22}) are given in equations 4.3 and 4.4, respectively, where $[\text{CB}[7]]_{\text{eq}}$ is the concentration of free cucurbit[7]uril in solution, which can be determined using equation 4.5 by SigmaPlot 7.0 software (method reported by Hupp and coworkers).⁵⁵

$$k_{\text{ex}}^{\text{unbound}} = \frac{k_{11} + k_{12}K_{\text{ox}} [\text{CB}[7]]_{\text{eq}}}{1 + K_{\text{ox}} [\text{CB}[7]]_{\text{eq}}} \quad (4.3)$$

$$k_{\text{ex}}^{\text{bound}} = \frac{k_{21} + k_{22}K_{\text{ox}} [\text{CB}[7]]_{\text{eq}}}{1 + K_{\text{ox}} [\text{CB}[7]]_{\text{eq}}} \quad (4.4)$$

$$[\text{CB}[7]]_{\text{total}} = [\text{CB}[7]]_{\text{eq}} + \frac{K_{\text{red}} [\text{CB}[7]]_{\text{eq}} [\text{FcTMA}^+]_{\text{total}}}{1 + K_{\text{red}} [\text{CB}[7]]_{\text{eq}}} + \frac{K_{\text{ox}} [\text{CB}[7]]_{\text{eq}} [\text{FcTMA}^{2+}]_{\text{total}}}{1 + K_{\text{ox}} [\text{CB}[7]]_{\text{eq}}} \quad (4.5)$$

Using the given values of k_{11} , k_{22} and $K_{\text{ox}} = 1.5 \times 10^{11} \text{ M}^{-1}$ for $\{\text{FcTMA} \cdot \text{CB}[7]\}^{2+}$, the data obtained from NMR line broadening experiments for free and bound species can be fit to equations 4.3 and 4.4 respectively, as shown in Figure 4.6. The solid line represents the fit of measured data to Equation 4.4 for determination of $k_{\text{ex}}^{\text{bound}}$, and the dashed line represents the fit to equation 4.3 to determine $k_{\text{ex}}^{\text{unbound}}$. At the concentrations of CB[7] lower than 1 mM, the rate constant falls off with the decreasing of CB[7] concentration to a limiting value of k_{21} , which is determined to be $(6 \pm 1) \times 10^5 \text{ M}^{-1} \text{ s}^{-1}$ as shown in Figure 4.6. Since the monitoring of the broadening process for free FcTMA^+ on ^1H NMR timescale was limited by the fast process, the estimation of k_{12} value from the data fitting is not applicable. Thus the Marcus theory relationship^{57,58} for electron transfer was used to estimate the values of k_{12} (equation 4.6) and k_{21} (equation 4.7)

$$k_{12} = (k_{11}k_{22}K_{12}f_{12})^{1/2}W_{12} \quad (4.6)$$

$$k_{21} = (k_{11}k_{22}K_{21}f_{21})^{1/2}W_{21} \quad (4.7)$$

where k_{11} and k_{22} are the self-exchange rate constants (Figures 4.5(a) and 4.5(c)), K_{12} is the equilibrium constant ($K_{12} = k_{12}/k_{21}$), f_{12} is a nonlinear correction term, and W_{12} is a collection of work terms, the rate constants can be estimated for k_{12} and k_{21} in the present system with CB[7], using the self-exchange rate constants k_{11} and k_{22} for the $\text{FcTMA}^{+/2+}$ and $\{\text{FcTMA} \cdot \text{CB}[7]\}^{+/2+}$ couples, respectively, and the reduction potential difference of 85 mV

between the $\{\text{FcTMA}\cdot\text{CB}[7]\}^{2+/+}$ and $\text{FcTMA}^{2+/+}$ couples. Assuming that the terms W_{12} (canceling work terms) and f_{12} (small thermodynamic driving force) are close to unity, k_{12} (which equals to $(k_{11}k_{22}K_{12})^{1/2}$) is calculated to be $2.0 \times 10^7 \text{ M}^{-1} \text{ s}^{-1}$, and in the same manner, k_{21} (which equals to $(k_{11}k_{22}/K_{21})^{1/2}$) is calculated to be $7.3 \times 10^5 \text{ M}^{-1} \text{ s}^{-1}$. The k_{21} result is in good agreement with the value of $(6 \pm 1) \times 10^5 \text{ M}^{-1} \text{ s}^{-1}$ determined from the fit of the $k_{\text{ex}}^{\text{bound}}$ data to equation 4.4. The higher value of k_{12} rate constant ($2.0 \times 10^7 \text{ M}^{-1} \text{ s}^{-1}$) supports a trend in $k_{\text{ex}}^{\text{unbound}}$ to higher values with increasing concentrations of CB[7] (dashed line in Figure 4.6).

4.3.2.3 Comparison with Other Hosts

The specific rate constants determined for the FcTMA^{+2+} couple in the presence of cucurbit[7]uril can be compared to the corresponding rate constants in the presence of the β -cyclodextrin and *p*-sulfonated calix[6]arene hosts (data summarized in Table 4.1). For the asymmetric electron-transfer reactions in Figure 4.5(b), the relative rate constants of the observed processes are determined by the direction of favourable thermodynamic driving force for the neutral hosts. For both the CB[7] and β -CD hosts (not observed for *p*-SO₃CX[6]), the reduction potential increases upon inclusion of the reduced ferrocene, and the values of k_{21} are lower than those of k_{11} . In the case of *p*-SO₃CX[6], despite the decrease in the reduction potential upon binding of the oxidized form of the ferrocene, the rate constant k_{12} is greater than k_{11} because of the very favourable electrostatic attraction between FcTMA^+ and the anionic host-guest complex formed with FcTMA^{2+} .²⁵ Neither this pathway (nor that of k_{22}) is observed for β -CD because of its limited solubility and its very low binding constant for FcTMA^{2+} .¹²

Table 4.1 Rate constants (25 °C) for the self-exchange reactions of the $\text{FcTMA}^{+/2+}$ couple (k_{11} , k_{12} , k_{21} , and k_{22}) and the electron-transfer reaction of FcTMA^+ with $\text{Co}(\text{dipic})_2^-$ (k_{Co}^0 and $k_{\text{Co}}^{\text{host}}$) in the presence of CB[7], β -CD, or p - $\text{SO}_3\text{CX}[6]$ in aqueous solution.

parameter	cucurbit[7]uril	β -CD	p -sulfonated calix[6]arene
k_{11} ($\text{M}^{-1}\text{s}^{-1}$)	2.1×10^6 ^a	1.2×10^7 ^b (2.5×10^6) ^b	1.2×10^7 ^c
k_{12} ($\text{M}^{-1}\text{s}^{-1}$)	2×10^7 ^d	not observed	1.3×10^8 ^c
k_{21} ($\text{M}^{-1}\text{s}^{-1}$)	6×10^5 ^a	4.3×10^4 ^b	not observed
k_{22} ($\text{M}^{-1}\text{s}^{-1}$)	6.7×10^6 ^a	not observed	1.6×10^7 ^c
K_{red} (M^{-1})	4×10^{12} ^e	4.8×10^3 ^g	1.1×10^4 ^{hi}
	3.3×10^{11} ^f	4.9×10^3 ^b	8.6×10^3 ^c
K_{red} (M^{-1})	1.5×10^{11} ^j	1.5×10^2 ^g < 20 ^b	5.4×10^4 ^c
ΔE^0 (mV)	+ 110 ^e	+ 80 ^k	- 47 ^c
	+ 85 ^a		- 120 ⁱ
k_{Co}^0 ($\text{M}^{-1}\text{s}^{-1}$)	7.5×10^2 ^l	9.3×10^2 ^g	7.45×10^2 ^h
$k_{\text{Co}}^{\text{host}}$ ($\text{M}^{-1}\text{s}^{-1}$)	3.4×10^{-1} ^l	2.0×10^1 ^g	4.3×10^2 ^h
$k_{\text{Co}}^0/k_{\text{Co}}^{\text{host}}$ ($\text{M}^{-1}\text{s}^{-1}$)	2.2×10^3	4.7×10^1	1.7

Note: ^aThis work, no added electrolyte. ^bReference 12, no added electrolyte. Rate constant in parentheses is a fitted value. ^cReference 16, $I = 0.1$ M. ^dEstimated from Marcus relationship (see text). ^eReference 45, in pure water. ^fReference 31, $I = 0.05$ M. ^gReference 49, $I = 0.10$ M. ^hReference 52, $I = 0.25$ M. ⁱReference 13, $I = 0.05$ M. ^jCalculated from $K_{\text{red}} = 4 \times 10^{12} \text{ M}^{-1}$ (reference 45) and $\Delta E^0 = 85 \text{ mV}$ (see text). ^kReference 48, $I = 0.05$ M. ^lThis work, $I = 0.10$ M.

4.3.2.4 Increase in the Electron Self-Exchange Rate Constant upon Guest Inclusion

After the inclusion of ferrocene moiety into hydrophobic cavity of CB[7], the electron self-exchange rate constant is increased from $k_{11} = 2.1 \times 10^6 \text{ M}^{-1} \text{ s}^{-1}$ to $k_{22} = 6.7 \times 10^6 \text{ M}^{-1} \text{ s}^{-1}$. This 3-fold increase in the electron self-exchange rate constant upon encapsulation is somewhat surprising, as it might be expected that the greater distance for the electron transfer

between the ferrocene groups would result in a reduction in the rate constant. However, it has also been reported that the self-exchange rate constant k_{22} for the $\{\text{FcTMA}\cdot\text{Host}\}^{n/(n+1)}$ -couple is larger (by about 30%) than k_{11} in the presence of the *p*-SO₃CX[6] host,¹⁶ despite the unfavourable repulsions between the anionic self-exchange partners. On the other hand, encapsulations of redox centers⁵⁷⁻⁶⁰ such as ferrocenes,⁶¹⁻⁶⁴ Fe₄S₄ iron-sulfur clusters,^{65,66} and metal tris(bipyridine) complexes⁶⁷⁻⁶⁹ in hemicarcerands and dendrimers have resulted in decreases in the heterogeneous electrochemical electron-transfer rate constants with an increase in the distance between the electrode and the redox center. This was also suggested in a study of dendrimer-encapsulated ferrocenes in which the ferrocene was also encapsulated by cucurbit[7]uril, although rate constants were not reported.⁶⁴

The increases in the self-exchange rate constants for the CB[7]-bound redox couple are likely the net result of several competing factors affecting the magnitude of the electron exchange rate constant k_{ex} ,^{10,11,70} given by the equation:

$$k_{\text{ex}} = K_{\text{p}}\kappa_{\text{el}}\nu_{\text{n}} \exp[-(\Delta G_{\text{in}}^* + \Delta G_{\text{out}}^*)/k_{\text{B}}T] \quad (4.8)$$

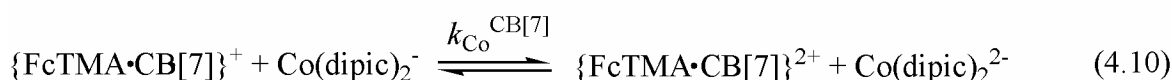
where K_{p} is the effective equilibrium constant for forming the precursor complex (two compounds form certain configurations to facilitate the electron exchange process); κ_{el} is the electronic transmission coefficient; ν_{n} is the nuclear frequency factor; k_{B} is Boltzmann constant and ΔG_{in}^* and ΔG_{out}^* are the inner-sphere and solvent reorganizational energies, respectively. With their measured value of $k_{11} = 9 \times 10^6 \text{ M}^{-1} \text{ s}^{-1}$ ($I = 0.03 \text{ M}$), Weaver and co-workers calculated a value of $\kappa_{\text{el}}\nu_{\text{n}} = 2 \times 10^{11} \text{ s}^{-1}$ for the FcTMA⁺²⁺ couple in water at 25 °C using $K_{\text{p}} = 0.25 \text{ M}^{-1}$ and $\Delta G_{\text{in}}^* + \Delta G_{\text{out}}^* = 5.2 \text{ kcal mol}^{-1}$.

By encapsulating the ferrocene moiety, cucurbit[7]uril forms an outer, second-coordination sphere around the ferrocene, which would prevent FcTMA^+ and FcTMA^{2+} from approaching one another as they would be for the free species. However, at the same time, encapsulation would increase the effective size of these redox reactants. It would be anticipated that preventing the close approach might reduce the electronic transmission coefficient (κ_{el}) between the metal centers somewhat, lowering the rate of electron exchange. However, the increase in the effective radius of ferrocene complex on forming the $\{\text{FcTMA}\cdot\text{CB}[7]\}^{n+}$ species would, however, reduce the energy of solvent reorganization ($\Delta G_{\text{out}}^* \propto 1/r$) required prior to electron transfer. It might also be possible that the positively charged trimethylammoniomethyl substituent on the ferrocene facilitates the docking of one encapsulated ferrocene with the carbonyl-lined portal of the other ferrocene (through ion-dipole interactions), increasing the electron-exchange rate constant through an enhancement in the precursor complex stability constant K_p . In the case of the $\text{FcTMA}^{2+/+}$ couple bound by *p*- $\text{SO}_3\text{CX}[6]$, a similar decrease in the solvent reorganization energy through encapsulation of the ferrocenes might be offset somewhat by the unfavourable repulsions (large decrease in K_p) between the polyanionic host-guest partners in the self-exchange couple.

4.3.3 Electron Transfer Kinetics

The kinetics of the electron-transfer reactions of the FcTMA^+ cation with $[\text{Co}(\text{dipic})_2]^-$ (dipic²⁻ is 2,6-pyridinedicarboxylate), which does not bind to CB[7],⁴⁶ were measured in aqueous solution as a function of CB[7] concentration. Results are also summarized in Table 4.1.

Three stock solutions were made in 0.1 M NaCl/H₂O solution: 12 mL of 5 mM CB[7], 10 mL of 10 mM NH₄Co(dipic)₂ and 50 mL of [FcTMA]BF₄. The pseudo-first-order rate constant k_{obs} was obtained on a stopped-flow spectrophotometer by employing Co(dipic)₂⁻ in a pseudo-first-order excess (2×10^{-3} M) over FcTMA⁺ (2.0×10^{-4} M), the [CB[7]] was varied up to 3.0×10^{-4} M at 25 °C and $I = 0.10$ M. The actual electron transfer rate constant, which is the second-order rate constant (k_1), was then determined by taking into account the concentration of reactants ($k_1 = k_{\text{obs}}/[\text{Co(III)}]$), shown in Table 4.2 as well.



In addition to FcTMA⁺, the other substituted ferrocene employed was the neutral hydroxymethylferrocene (FcCH₂OH) reductant (also summarized in Table 4.2). In the absence of cucurbit[7]uril, the second-order rate constants (k_{Co}^0 , equation 4.9) for the oxidations of FcTMA⁺ and FcCH₂OH by Co(dipic)₂⁻ are determined to be $(7.5 \pm 0.2) \times 10^2$ and $(7.4 \pm 0.2) \times 10^3 \text{ M}^{-1} \text{ s}^{-1}$, respectively. The rate constants decrease linearly with increasing concentration of CB[7], reaching a limiting value ($k_{\text{Co}}^{\text{CB}[7]}$, equation 4.10) at a 1:1 ratio of CB[7] to ferrocene (Figure 4.8), with $k_{\text{Co}}^{\text{CB}[7]} = (3.4 \pm 0.1) \times 10^{-1}$ and $(1.7 \pm 0.2) \times 10^2 \text{ M}^{-1} \text{ s}^{-1}$, for FcTMA⁺ and FcCH₂OH, respectively.

Table 4.2 Rate constants for the oxidation of FcTMA^+ or $\text{Fc}(\text{CH}_2\text{OH})$ (0.20 mM) by $[\text{Co}(\text{dipic})_2]^-$ (2 mM) in the absence and presence of CB[7] at 25 °C and $I = 0.10 \text{ M}$ (NaCl).

CB[7]/[Ferrocene]	FcTMA^+ $k_1 \text{ (M}^{-1} \text{ s}^{-1}\text{)}$	CB[7]/[Ferrocene]	FcTMA^+ $k_1 \text{ (M}^{-1} \text{ s}^{-1}\text{)}$
0.000	3750	0.000	7440
0.200	2660	0.193	6210
0.400	1935	0.385	4740
0.600	1120	0.578	3440
1.600	1.70	0.770	2173
		1.16	179
		1.54	150

This kinetic behaviour was also observed previously in the oxidation of the (*E*)-1-ferrocenyl-2-(1-methyl-4-pyridinium)ethylene cation (FcMPE^+) with $\text{Co}(\text{dipic})_2^-$, where values of $k_{\text{Co}}^0 = (2.1 \pm 0.1) \times 10^4 \text{ M}^{-1} \text{ s}^{-1}$ and $k_{\text{Co}}^{\text{CB}[7]} = (1.6 \pm 0.1) \times 10^2 \text{ M}^{-1} \text{ s}^{-1}$ were determined.⁴⁶ The ratios of the rate constants, $k_{\text{Co}}^0/k_{\text{Co}}^{\text{CB}[7]}$, for the three ferrocene reductants correlate with the difference in the ferrocenium reduction potentials, ΔE^0 , upon inclusion in CB[7]: FcTMA^+ , 2.2×10^3 and 85 mV; FcCH_2OH , 50 and 10 mV;⁴⁵ and FcMPE^+ , 130 and 30 mV.⁴⁶ The greater the increase in the reduction potential for the $\{\text{FcX}\cdot\text{CB}[7]\}^{n+/(n-1)+}$ couple, the greater the rate constant ratio, consistent with the change in the thermodynamic driving force for the reaction. The thermodynamic driving force changes do not account entirely for the decreases in the rate constants for the included reductants, and the remainder is likely steric hindrance of the close approach of the redox reactants when the ferrocene portion of the reductant is included in the CB[7] cavity. These decreases in the electron-

transfer rate constants are observed despite the increase in the electron self-exchange rate constant for the $\{\text{FcX}\cdot\text{CB}[7]\}^{n+/(n-1)+}$ couple (at least in the example examined in the present study).

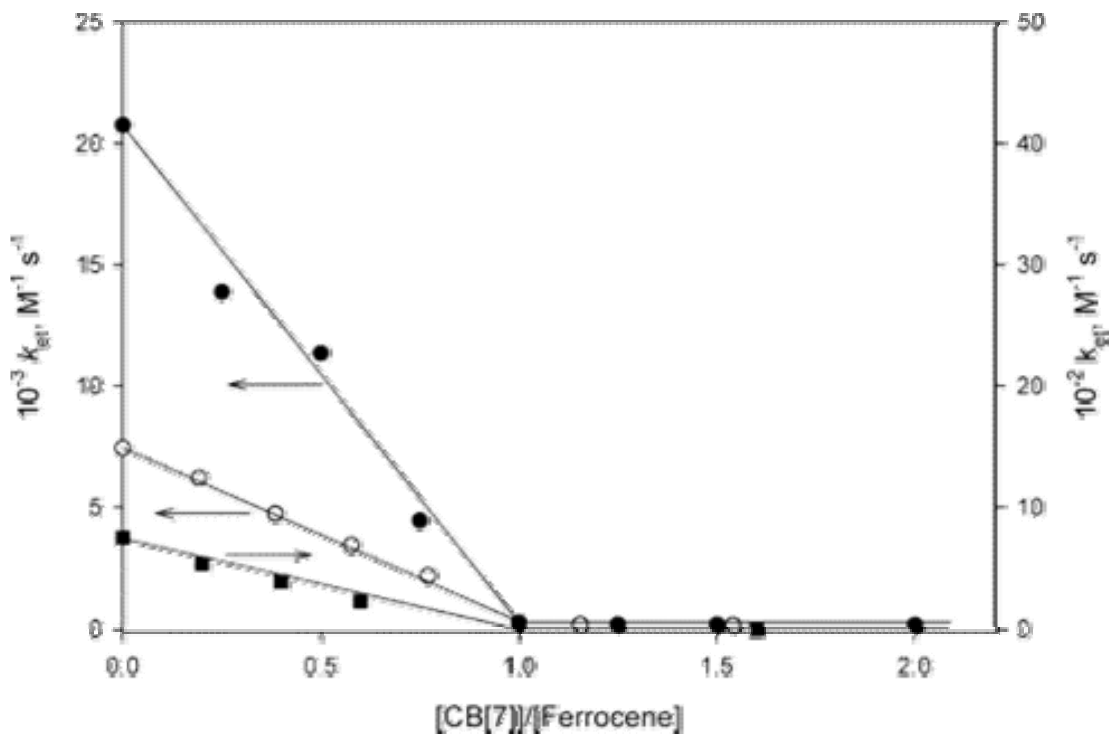


Figure 4.8 Plots of the electron transfer rate constant, k_{et} , against the $[\text{CB}[7]]/[\text{ferrocene}]$ ratio for the oxidation of FcTMA^+ (■), $\text{Fc}(\text{CH}_2\text{OH})$ (○), and FcMPE^+ (●) by $\text{Co}(\text{dipic})_2^-$ in aqueous solution ($I = 0.10 \text{ M}$ (NaCl)) at $25.0 \text{ }^\circ\text{C}$. The data for FcMPE^+ are from reference 32.

The kinetics of the oxidation of FcTMA^+ by $\text{Co}(\text{dipic})_2^-$ in the presence of $\text{CB}[7]$ can also be compared to the behaviour of this redox reaction previously studied in the presence of $\beta\text{-CD}$ ²⁷ and *p*-sulfonated calix[6]arene⁵² (Table 4.1). With each type of host molecule employed, there is a decrease in the rate constant when FcTMA^+ is bound. The extent of the diminution in the electron-transfer rate constant is again dependent on the change in the

reduction potential for the host-guest complex as well as the prevention of the close approach of the oxidant to the encapsulated ferrocene. In the case of the cyclodextrins, the decrease results from an increase in the reduction potential of the ferrocene couple, and both types of host molecule lead to steric hindrance of the close approach of the oxidant to the included reductant. The increase in the reduction potential of the ferrocene couple is due to the much reduced stability constant for the CD inclusion complex with the oxidized form compared to the reduced form of the ferrocene. As a result, the rate constants for the reduction of the oxidized form of the ferrocenes increase somewhat upon their inclusion in the cyclodextrins.^{50,51} In the case of the *p*-sulfonated calixarenes, the oxidized forms of the ferrocenes bind more strongly to the host (by virtue of the increased attraction of the ferrocene cation to the anionic host), lowering the reduction potential. Nevertheless, the rate constants for the oxidation of the ferrocenes by $\text{Co}(\text{dipic})_2^-$ decrease as a result of unfavourable electrostatics between the anionic host-guest complex and $\text{Co}(\text{dipic})_2^-$ and the steric hindrance mentioned above.⁵²

4.4 Summary

The electron self-exchange rate constants for the (trimethylammonio)-methylferrocene(+/2+) couple ($\text{FcTMA}^{+/2+}$) have been measured in the absence and presence of the cucurbit[7]uril (CB[7]) host molecule in aqueous solution, using ^1H NMR line-broadening experiments. The very strong binding of the ferrocene to CB[7] results in slow exchange of the guest on the ^1H NMR time scale, such that resonances for both the free and bound forms of the reduced ferrocene can be observed. The extents of line broadening in the resonances of the two forms of the guest in the presence of the FcTMA^{2+} species can be monitored independently, allowing for the determination of the rate constants for the possible

self-exchange pathways involving the bound and free forms of both the oxidized and reduced members of the redox couple. The encapsulation of both the reduced and oxidized forms of the ferrocene increases the rate constant (25 °C) from $k_{11} = (2.1 \pm 0.1) \times 10^6 \text{ M}^{-1} \text{ s}^{-1}$ (for $\text{FcTMA}^{+/2+}$) to $k_{22} = (6.7 \pm 0.7) \times 10^6 \text{ M}^{-1} \text{ s}^{-1}$ (for $\{\text{FcTMA}\cdot\text{CB}[7]\}^{+/2+}$). The increase in the electron self-exchange rate constants upon inclusion of the reactants, which is also observed previously with the *p*-sulfonated calix[6]arene host molecule, is likely the result of a decrease in the barrier to solvent reorganization, rather than a distance dependence as observed for dendrimer encapsulations. The electron transfer reactions between FcTMA^+ and hydroxymethylferrocene with bis(2,6-pyridinedicarboxylato)cobaltate(III) ion were also investigated, revealing that the binding of FcTMA^+ and hydroxymethylferrocene to CB[7] cavity significantly reduces the rate constants for their oxidations by the bis(2,6-pyridinedicarboxylato)cobaltate(III) ion (which does not bind to CB[7]). This is likely the result of reduced thermodynamic driving forces and steric hindrance to close approach of the oxidant to the encapsulated ferrocenes after encapsulation. Continuing this work, the effects of the encapsulation of CB[7] on other ferrocene derivatives and other metallocenes will be discussed in the next chapter.

References

1. Liu, S.; Ruspic, C.; Mukhopadhyay, P.; Chakrabarti, S.; Zavalij, P. Y.; Isaacs, L. *J. Am. Chem. Soc.* **2005**, *127*, 15959.
2. Wang, R.; Yuan, L.; Macartney, D. H. *Chem. Commun.* **2005**, 5867.
3. Yuan, L.; Wang, R.; Macartney, D. H. *J. Org. Chem.* **2007**, *72*, 4539.
4. Moon, K.; Kaifer, A. E. *Org. Lett.* **2004**, *6*, 185.
5. Nielson, R. M.; Hupp, J. T. *Inorg. Chem.* **1996**, *35*, 1402.
6. Jeon, W. S.; Moon, K.; Park, S. H.; Chun, H.; Ko, Y. H.; Lee, J. Y.; Lee, E. S.; Samal, S.; Selvapalam, N.; Rekharsky, M. V.; Sindelar, V.; Sobransingh, D.; Inoue, Y.; Kaifer, A. E.; Kim, K. *J. Am. Chem. Soc.* **2005**, *127*, 12984.
7. Ong, W.; Kaifer, A. E. *Organometallics* **2003**, *22*, 4181.
8. Nielson, R. M.; Lyon, L. A.; Hupp, J. T. *Inorg. Chem.* **1996**, *35*, 970.
9. Yang, E. S.; Chan, M.-S.; Wahl, A. C. *J. Phys. Chem.* **1980**, *84*, 3094.
10. Nielson, R. M.; McManis, G. E.; Weaver, M. J. *J. Phys. Chem.* **1989**, *93*, 4703.
11. McManis, G. E.; Nielson, R. M.; Gochev, A.; Weaver, M. J. *J. Am. Chem. Soc.* **1989**, *111*, 5533.
12. Nielson, R. M.; Lyon, L. A.; Hupp, J. T. *Inorg. Chem.* **1996**, *35*, 970.
13. Zhang, L.; Macias, A.; Lu, T.; Gordon, J. I.; Gokel, G. W.; Kaifer, A. E. *Chem. Commun.* **1993**, 1017.
14. Zhang, L.; Marcias, A.; Isnin, R. Lu, T.; Gokel, G. W.; Kaifer, A. E. *J. Incl. Phenom. Mol. Recognit. Chem.* **1994**, *19*, 361.
15. Komura, T.; Yamaguchi, T.; Kura, K.; Tanabe, J. *J. Electroanal. Chem.* **2002**, *523*, 126.
16. Nielson, R. M.; Hupp, J. T. *Inorg. Chem.* **1996**, *35*, 1402.

17. Kim, K. *Chem. Soc. Rev.* **2002**, 31, 96.
18. Lee, J. W.; Samal, S.; Kim, H.-J.; Kim, K. *Acc. Chem. Res.* **2003**, 36, 621.
19. Lagona, J.; Mukhopadhyay, P.; Chakrabarti, S.; Isaacs, L. *Angew. Chem., Int. Ed.* **2005**, 44, 4844.
20. Wenz, G. *Angew. Chem., Int. Ed. Engl.* **1994**, 33, 803.
21. Connors, K. A. *Chem. Rev.* **1997**, 97, 1325.
22. Rekharsky, M. V.; Inoue, Y. *Chem. Rev.* **1998**, 98, 1875.
23. Szejtli, J. *Chem. Rev.* **1998**, 98, 1743.
24. Inoue, Y.; Hakushi, T.; Liu, Y.; Tong, L.-H.; Shen, B.-J.; Jin, D.-S. *J. Am. Chem. Soc.* **1993**, 115, 475.
25. Inoue, Y.; Liu, Y.; Tong, L.-H.; Shen, B.-J.; Jin, D.-S. *J. Am. Chem. Soc.* **1993**, 115, 10637.
26. Mock, W. L. In *Comprehensive Supramolecular Chemistry*; Vögtle, F., Ed.; Pergamon: Oxford, **1996**; Vol. 2, p. 447.
27. Cintas, P. *J. Incl. Phenom. Mol. Recognit. Chem.* **1994**, 17, 205.
28. Lee, J. W.; Samal, S.; Selvapalam, N.; Kim, H.-J.; Kim, K. *Acc. Chem. Res.* **2003**, 36, 621.
29. Kim, K.; Kim, H.-J. In *Encyclopedia of Supramolecular Chemistry*; Atwood, S., Ed.; Marcel Dekker Inc.: New York, **2004**; p. 390.
30. Kim, K.; Selvapalam, N.; Oh, D.-H. *J. Incl. Phenom.* **2004**, 50, 31.
31. Liu, S.; Ruspic, C.; Mukhopadhyay, P.; Chakrabarti, S.; Zavalij, P. Y.; Isaacs, L. *J. Am. Chem. Soc.* **2005**, 127, 15959.
32. Wang, R.; Yuan, L.; Macartney, D. H. *Chem. Commun.* **2005**, 5867.

33. Gerasko, O. A.; Samsonenko, D. G.; Fedin, V. P. *Russ. Chem. Rev.* **2002**, *71*, 741.
34. Wheate, N. J.; Day, A. I.; Blanch, R. J.; Arnold, A. P.; Cullinane, C.; Collins, J. G. *Chem. Commun.* **2004**, 1424.
35. Jeon, Y. J.; Kim, S.-Y.; Ko, Y. H.; Sakamoto, S.; Yamaguchi, K.; Kim, K. *Org. Biomol. Chem.* **2005**, *3*, 2122.
36. heate, N. J.; Buck, D. P.; Day, A. I.; Collins, J. G. *Dalton Trans.* **2006**, 451.
37. Bali, M. S.; Buck, D. P.; Coe, A. J.; Day, A. I.; Collins, J. G. *Dalton Trans.* **2006**, 5337.
38. Kim, H.-J.; Jeon, W. S.; Ko, Y. H.; Kim, K. *Proc. Natl. Acad. Sci. USA* **2002**, *99*, 5007.
39. Ong, W.; Gomez-Kaifer, M.; Kaifer, A. E. *Org. Lett.* **2002**, *4*, 1791.
40. Hettiarachchi, D. S. N.; Macartney, D. H. *Can. J. Chem.* **2006**, *84*, 905.
41. Ong, W.; Kaifer, A. E. *J. Org. Chem.* **2004**, *69*, 1383.
42. (a) Mock, W. L.; Shih, N.-Y. *J. Org. Chem.* **1986**, *51*, 4440. (b) Mock, W. L.; Shih, N.-Y. *J. Am. Chem. Soc.* **1988**, *110*, 4706. (c) Mock, W. L.; Shih, N.-Y. *J. Am. Chem. Soc.* **1989**, *111*, 2697. (d) Hoffmann, R.; Knoche, W.; Fenn, C.; Buschmann, H.-J. *J. Chem. Soc., Faraday Trans.* **1994**, *90*, 1507. (e) Jeon, Y.-M.; Kim, J.; Whang, D.; Kim, K. *J. Am. Chem. Soc.* **1996**, *118*, 9790. (f) Whang, D.; Heo, J.; Park, J. H.; Kim, K. *Angew. Chem., Int. Ed. Engl.* **1998**, *37*, 78. (g) Haouaj, M. E.; Luhmer, M.; Ko, Y. H.; Kim, K.; Bartik, K. *J. Chem. Soc., Perkin Trans. 2* **2001**, 804. (h) Haouaj, M. E.; Ko, Y. H.; Luhmer, M.; Kim, K.; Bartik, K. *J. Chem. Soc., Perkin Trans. 2* **2001**, 2104. (i) Marquez, C.; Nau, W. M. *Angew. Chem., Int. Ed.* **2001**, *40*, 3155. (j) Marquez, C.; Hudgins, R. R.; Nau, W. M. *J. Am. Chem. Soc.* **2004**, *126*, 5806.
43. (a) Buschmann, H.-J.; Cleve, E.; Schollmeyer, E. *Inorg. Chim. Acta* **1992**, *193*, 93. (b) Zhang, X. X.; Krakowiak, K. E.; Xue, G.; Bradshaw, J. S.; Izatt, R. M. *Ind. Eng. Chem. Res.*

- 2000**, 39, 3516. (c) Heo, J.; Kim, J.; Whang, D.; Kim, K. *Inorg. Chim. Acta* **2000**, 279, 307.
- (d) Sokolov, M. N.; Virovets, A. V.; Dybtsev, D. N.; Gerasko, O. A.; Fedin, V. P.; Hernandez-Molina, R.; Clegg, W.; Sykes, A. G. *Angew. Chem., Int. Ed.* **2000**, 39, 1659.
44. Ong, W.; Kaifer, A. E. *Organometallics* **2003**, 22, 4181.
45. Jeon, W. S.; Moon, K.; Park, S. H.; Chun, H.; Ko, Y. H.; Lee, J. Y.; Lee, E. S.; Samal, S.; Selvapalam, N.; Rekharsky, M. V.; Sindelar, V.; Sobransingh, D.; Inoue, Y.; Kaifer, A. E.; Kim, K. *J. Am. Chem. Soc.* **2005**, 127, 12984.
46. Wang, R.; Yuan, L.; Macartney, D. H. *Organometallics* **2006**, 25, 1820.
47. Matsue, T.; Evans, D. H.; Osa, T.; Kobayashi, N. *J. Am. Chem. Soc.* **1985**, 107, 179.
48. Isnin, R.; Salam, C.; Kaifer, A. E. *J. Org. Chem.* **1991**, 56, 35.
49. Imonigie, J. A.; Macartney, D. H. *Inorg. Chim. Acta* **1994**, 225, 51.
50. Imonigie, J. A.; Macartney, D. H. *J. Inclusion Phenom. Mol. Recognit. Chem.* **1993**, 15, 195.
51. Macartney, D. H.; Roszak, A. W.; Smith, K. C. *Inorg. Chim. Acta* **1999**, 291, 365.
52. Imonigie, J. A.; Macartney, D. H. *Inorg. React. Mech.* **2006**, 6, 161.
53. Day, A.; Arnold, A. P.; Blanch, R. J.; Snushall, B. *J. Org. Chem.* **2001**, 66, 8094.
54. Lindsay, J. K.; Hauser, C. R. *J. Org. Chem.* **1957**, 22, 355.
55. Mauk, A. D.; Coyle, C. L.; Bordington, E.; Gray, H. B. *J. Am. Chem. Soc.* **1979**, 101, 5054.
56. Imonigie J. A. Ph.D. Thesis, Queen's University, **1994**.
57. Cardona, C. M.; Mendoza, S.; Kaifer, A. E. *Chem. Soc. Rev.* **2000**, 29, 37.
58. Cameron, C. S.; Gorman, C. B. *Adv. Funct. Mater.* **2002**, 12, 17.
59. Niemz, A.; Rotello, V. M. *Acc. Chem. Res.*, **1999**, 32, 44.

60. Kaifer, A. E. *Acc. Chem. Res.*, **1999**, 32, 62.
61. Mendoza, S.; Davidov, P. D.; Kaifer, A. E. *Chem. Eur. J.* **1998**, 4, 864.
62. Cardona, C. M.; Kaifer, A. E. *J. Am. Chem. Soc.* **1998**, 120, 4023.
63. Cardona, C. M.; McCarley, T. D.; Kaifer, A. E. *J. Org. Chem.* **2000**, 65, 1857.
64. Sobransingh, D.; Kaifer, A. E. *Chem. Commun.* **2005**, 5071.
65. Sierzputowska-Gracz, H.; Haney, C. A. *J. Am. Chem. Soc.* **1999**, 121, 9958.
66. Chasse, T. L.; Sachdeva, R.; Li, Q.; Li, Z.; Petrie, R. J.; Gorman, C. B. *J. Am. Chem. Soc.* **2003**, 125, 8250.
67. Newkome, G. R.; Guther, R.; Moorefield, C. N.; Cardullo, F.; Echegoyen, L.; Perez-Cordero, Luftmann, H. *Angew. Chem., Int. Ed. Engl.* **1995**, 34, 2023.
68. Balzani, V.; Campagna, S.; Denti, G.; Juris, A.; Seroni, S.; Venturi, M. *Acc. Chem. Res.* **1998**, 31, 26.
69. Hong, Y.-R.; Gorman, C. B. *Langmuir* **2006**, 22, 10506.
70. Marcus, R. A.; Sutin, N. *Biochim. Biophys. Acta* **1985**, 811, 265.

Chapter 5

HOST-GUEST COMPLEXATION OF CURCUBITURILS WITH BIS(FERROCENE) COMPLEXES AND DIAQUATITANOCENE

Prompted by the results in Chapter 4, the binding behaviour between cucurbiturils hosts with two bis(ferrocene) derivatives ($\text{CpFeC}_5\text{H}_4\text{CH}_2\text{N}(\text{CH}_3)_2\text{CH}_2\text{C}_5\text{H}_4\text{FeCp}^+$ (**1**) and $\text{CpFeC}_5\text{H}_4\text{CH}_2\text{N}(\text{CH}_3)_2(\text{CH}_2)_{12}\text{N}(\text{CH}_3)_2\text{CH}_2\text{C}_5\text{H}_4\text{FeCp}^{2+}$ (**2**)) and bent metallocenes such as diaquatitanocene, have also been investigated. ^1H NMR titration experiments show that only a 1:1 complex was formed between CB[7] host and compound **1**, even with addition of excess host. This can be explained by the short aliphatic chain between the two ferrocene moieties, which will cause significant steric hindrance for two host molecules binding one guest at the same time. However, compound **2**, which has a much longer aliphatic chain between two ferrocene units, forms a 1:1 inclusion complex when less than one equivalent of CB[7] was added, and a 2:1 complex when more CB[7] was introduced to the system. For both guest molecules, the exchanges between free and bound forms were slow on the ^1H NMR timescale, indicated by separate sets of guest proton resonances. The electrochemical properties of the ferrocenes, investigated by cyclic voltammetry, change upon their inclusion in the CB[7] cavity with the half-wave potential ($E_{1/2}$) being shifted 75 and 50 mV more positive for compounds **1** and **2**, respectively, upon encapsulation. The binding constant of compound **1** with CB[7] was determined by a ^1H NMR competition method to be $(2 \pm 1) \times 10^{13} \text{ M}^{-1}$, using (trimethylammonio)methylferrocene as the competitor guest.

The formation of the very stable host-guest complexes of cucurbit[*n*]uril with ferrocenes and the effects of inclusion on the chemical, electrochemical and spectroscopic properties of these guests prompted us to initiate investigations into the formation and properties of host-guest complexes of CB[7] and CB[8] with bent MCp_2X_2 species in aqueous solution. Herein, the complexation of the anti-tumour drug diaquabis(η^5 -cyclopentadienyl)titanium(IV) dication with CB[7] and CB[8] in aqueous solution has been investigated by ^1H NMR titrations, ESI mass spectrometry, cyclic voltammetry, and Gaussian energy-minimization calculations. Unlike the complexation with the “sandwich-shaped” ferrocene, with which CB[7] shows higher affinity than CB[8], the bent titanocene has a preference for the larger CB[8] cavity over that of CB[7]. Upon inclusion into the CB[7] cavity, the half-wave potential $E_{1/2}$ value for the ($\text{Ti}^{4+/3+}$) couple shows a negative shift of 30 mV, indicating that the binding between the CB[7] host and the Ti (IV) guest is more favourable than that with the Ti(III) guest. This is different from what was observed for the ferrocene compound studied in Chapter 4, which exhibits a positive shift upon the inclusion into the CB[7] cavity due to the more favourable binding between CB[7] with the reduced form of ferrocene rather than with the oxidized ferrocenium.

The structure of the host-guest complexes were modelled in the gas-phase from Gaussian calculation (HF/3-21G** basis set), indicating that the titanocene complex is fully encapsulated in the CB[8] cavity, with the cyclopentadienyl rings aligned with the glycoluril units, similar to the inclusion in γ -cyclodextrin, but with a much higher stability constant. The binding constants of the $\{\text{TiCp}_2(\text{H}_2\text{O})_2 \cdot \text{CB}[n]\}^{2+}$ inclusion complexes were determined by ^1H NMR competition methods to be $K_{\text{CB}[7]} = (6.3 \pm 1.0) \times 10^6 \text{ M}^{-1}$ and $K_{\text{CB}[8]} = (2.0 \pm 0.4) \times 10^8 \text{ M}^{-1}$, respectively, by using 1,6-diaminohexane for CB[7] and 1-aminoadamantane for

CB[8], as competing ligands. The inclusions into the CB[n] cavity enhances the thermodynamic stability of titanocene, preventing the cyclopentadienyl rings from dissociating from the titanium upon protonolysis, for up to 7 days at pH = 3.8, compared to the literature report of 90% dissociation after 24 hours for the free titanocene dichloride at pH = 6.1-6.2 in aqueous solution.

5.1 Introduction

CB[7], the most popular member in CB[n] family, has been demonstrated to possess high affinity for ferrocene and substituted ferrocenes in aqueous solution,¹⁻³ with stability constants for the host-guest complexes in the range of 10^9 - 10^{13} M⁻¹,^{2,3} compared to 10^3 - 10^4 M⁻¹ for the same guests with β -CD⁴⁻⁶ and 10^4 - 10^5 M⁻¹ with *p*-SO₃CX[6].⁷⁻¹⁰ We have investigated the effect of inclusion into the CB[7] cavity on the (*E*)→(*Z*) photoisomerization reaction of the (*E*)-1-ferrocenyl-2-(1-methyl-4-pyridinium)ethylene cation ((*E*)-FcMPE⁺) ($K_{\text{CB}[7]} = (1.3 \pm 0.5) \times 10^{12}$ M⁻¹) in aqueous solution, indicating that the encapsulation of CB[7] stabilized the [(*E*)-FcMPE⁺] significantly and inhibited the (*E*)→(*Z*) photoisomerization (normally with a $t_{1/2} \approx 10$ min) dramatically.³ The rate constant for the oxidation of (*E*)-FcMPE⁺ by the bis(2,6-pyridinedicarboxylato)cobaltate(III) ion ([Co(dipic)₂]⁻) was considerably decreased (from $k_0 = 2.1 \times 10^4$ M⁻¹ s⁻¹ to $k_{\text{CB}[7]} = 1.6 \times 10^2$ M⁻¹ s⁻¹) upon binding with CB[7], due to the significant increase of the steric hindrance (CB[n] host adds substantial bulk to the structure) of close approach of the reactants.

In Chapter 4, the effect of encapsulation by CB[7] on the kinetics of electron self-exchange and electron transfer reactions of (trimethylammonio)methylferrocene in aqueous solution have been described.¹¹ The slow exchange between bound and free guest molecule

on the ^1H NMR timescale makes it possible to investigate the electron self-exchange processes separately. The inclusion of both FcTMA^+ and FcTMA^{2+} by $\text{CB}[7]$ increases the rate constant for its electron self-exchange reaction from $(2.1 \pm 0.1) \times 10^6 \text{ M}^{-1} \text{ s}^{-1}$ (for $\text{FcTMA}^{+/2+}$) to $(6.7 \pm 0.7) \times 10^6 \text{ M}^{-1} \text{ s}^{-1}$ (for $\{\text{FcTMA}\cdot\text{CB}[7]\}^{+/2+}$), however, the encapsulation of only the reduced form decreases the rate constant to $(6 \pm 1) \times 10^5 \text{ M}^{-1} \text{ s}^{-1}$. Similar to the behaviour of the guest (*E*)- FcMPE^+ ,¹⁰ the oxidation reactions between FcTMA^+ and hydroxymethylferrocene with bis(2,6-pyridinedicarboxylato)cobaltate(III) ion were slowed down significantly upon their inclusion in the $\text{CB}[7]$ cavity, as a result of reduced thermodynamic driving forces and steric hindrance to close approach of the oxidant to the encapsulated ferrocenes.

It is well known that the metallocene dihalides Cp_2MX_2 (where Cp is cyclopentadienyl ring, M could be Ti, V, Nb, or Mo and X represents F, Cl or Br) possess high anti-tumour activities.¹¹⁻¹⁴ Ever since 1979, when the first non-platinum metal complex, titanocene dichloride (Figure 5.1), was proven to be highly active as an anti-tumour agent in clinical trials, interest in this research field has grown dramatically.^{14a}

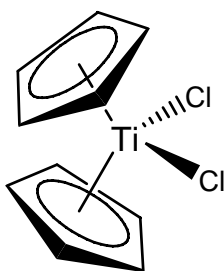
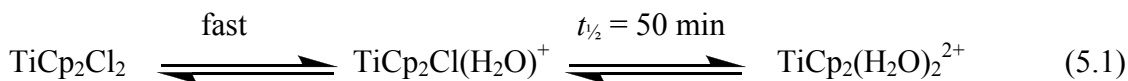


Figure 5.1 Structure of the bent metallocene, titanocene dichloride.

The replacement of the halide ligands by water and the hydrolysis of the Cp rings in titanocene dichloride has been investigated.¹³ The dissociation of the first chloride in water is instantaneous while the half-life for losing the second chloride is approximately 50

minutes (equations 5.1). The coordinated water molecules which replace the chlorides can undergo deprotonation to hydroxide ligands (equation 5.2)



The protonolysis and dissociation of the Cp rings occurs approximately 24 hours after the hydrolysis of the second chloride to yield cyclopentadiene and dicyclopentadiene, as well as an insoluble precipitate which has not been characterized to date. Harding and coworkers have synthesized several substituted titanocene dichloride compounds to improve the stability of titanocene in aqueous solution.¹⁵ Even though complete hydrolysis studies in water have not been carried out, preliminary results suggested that substitution of a methylene bridge on both Cp rings slows down the hydrolysis of Cp rings effectively.

The cucurbit[7]uril and cucurbit[8]uril molecules have been used to form host-guest complexes with mononuclear (*cis*-Pt(NH₃)₂Cl₂ and *cis*-Pt(NH₃)₂(OH₂)Cl⁺), dinuclear (*trans*-[PtCl(NH₃)₂]₂(μ-NH₂(CH₂)₈NH₂)²⁺ and *trans*-[PtCl(NH₃)₂]₂μ-dpzm)²⁺ (dpzm = 4,4'-dipyrazolylmethane)) and trinuclear (*trans*-[*trans*-{PtCl(NH₃)₂]₂-*trans*-{Pt(dpzm)₂(NH₃)₂}]⁴⁺) platinum(II) complexes, which are used as, or are of interest as, anti-tumour agents.¹⁶ While the hydrolyzed Pt(NH₃)₂(OH₂)Cl⁺ appears to bind to the portals of CB[7], the other species are included in the cavities of CB[7] and CB[8]. The inclusions of *trans*-[PtCl(NH₃)₂]₂(μ-NH₂(CH₂)₈NH₂)²⁺ in CB[7] and CB[8] reduces the rate of its reactions with cysteine and glutathione.

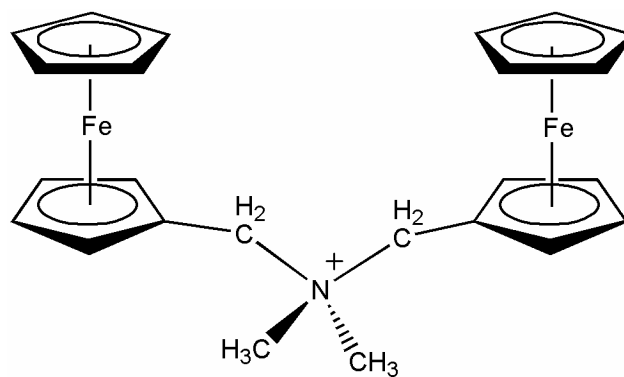
Recently, the formation of host-guest complexes between cyclodextrin host molecules and titanocene dichloride have been investigated by Turel and coworkers.¹⁷ They have concluded from ¹H NMR spectroscopy that the hydrolysis product of TiCp₂Cl₂, TiCp₂(H₂O)Cl⁺, is fully encapsulated in γ -CD ($K_{\gamma\text{-CD}} = 77 \text{ M}^{-1}$), less deeply in β -CD and not at all in α -CD. The complexations of titanocene with CB[7] and CB[8] have been investigated by ¹H NMR titrations, ESI mass spectrometry, and cyclic voltammetry along with gas-phase energy-minimization calculations, prompted by the fact that the inclusion of titanocene dichlorides in the CB[n] host molecules could have an effect on their water solubility, Cp ring protonolysis and cytotoxic properties.

In this chapter, the binding behaviours of two cationic bis(ferrocene) guests **1** and **2** (Figure 5.2) with CB[7] have also been studied by ¹H NMR spectroscopy, ESI mass spectrometry and cyclic voltammetry.

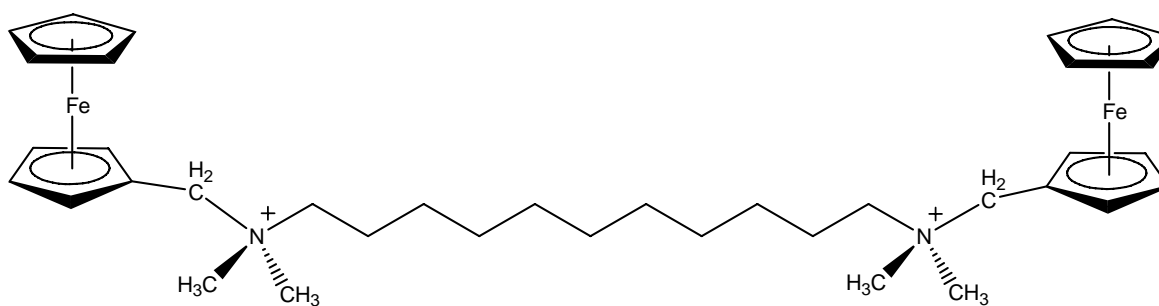
5.2 Experimental

5.2.1 Material Preparation

Titanocene dichloride and cucurbit[8]uril were used as received (Aldrich). Cucurbit[7]uril was prepared and characterized by the method of Day and co-workers, as described in Chapter 3.¹⁸ The bis(ferrocene) compounds [1]Br and [2]I₂ were synthesized according to literature procedures.¹⁹



1



2

Figure 5.2 The structure of the two cationic bis(ferrocene) complexes.

5.2.1.1 Synthesis of compound [1]Br

The compound [1]Br was synthesized by the following method.¹⁹ To a chilled solution of *N,N*-dimethylaminomethylferrocene (12.2 g, 50 mmol) in chloroform (10 mL), 1,2-dibromoethane (3.8 g, 20 mmol) in 30 mL of chloroform was added dropwise while stirring. The mixture was refluxed for two days and then cooled to yield a yellow precipitate. The final product was obtained by recrystallization of the yellow solid from water. Yield:

75%. ^1H NMR (in D_2O): δ 4.43 (s, 4H), 4.37 (s, 4H), 4.23 (s, 4H), 4.20 (s, 10H), 2.64 (s, 6H) ppm. ESI-MS: m/z at 442.0 for $[\text{C}_{24}\text{H}_{28}\text{NFe}_2]^+$ (theoretically $m/z = 442.1$).

5.2.1.2 Synthesis of compound [2]I₂

Compound [2]I₂ was synthesized in a similar manner as described for compound [1]Br.¹⁹ 1,12-Diiodododecane (6.6g, 20 mmol) in 30 mL of chloroform was added dropwise to a chilled solution of *N,N*-dimethylaminomethylferrocene (12.2 g, 50 mmol) in 10 mL of chloroform while stirring, and the mixture was then refluxed for 12 hours. Cooling of the mixture gave a yellow solid, which was subsequently recrystallized from water and then from diethyl ether to give pure compound [2]I₂. Yield: 45%. ^1H NMR (in D_2O): δ 4.42 (s, 4H), 4.36 (s, 4H), 4.30 (s, 4H), 4.21 (s, 10H), 3.02 (t, 4H), 2.81 (s, 12H), 1.66 (m, 4H), 1.22 (m, 16H) ppm. ESI-MS: m/z at 781.2 for $[\text{C}_{38}\text{H}_{58}\text{N}_2\text{Fe}_2\text{I}]^+$ (theoretically $m/z = 781.2$)

5.2.1.3 Assembly of Host-Guest Complexes in Solution

The host-guest complexes were prepared in aqueous solution for ^1H NMR spectral studies by mixing certain ratios of the CB[n] host with the guest molecules in D_2O , bubbling argon through the solutions for at least 20 minutes and then incubating them for approximately one hour at room temperature before acquiring the spectra.

For guest **1**, only the 1:1 complex was formed despite a large excess of CB[7] host, because the central aliphatic chain is not long enough to keep the steric hindrance and repulsive interactions small enough to hold two CB hosts on one molecule at the same time. ^1H NMR: (in D_2O): δ 4.55 (s), 4.36 (s), 4.31 (s) for the free guest and 3.71 (s), 3.58 (s), 3.50 (s), 2.529 (s) ppm for bound guest. Proton resonances are observed at δ 5.72 (d), 5.47 (s) and

4.17 (d) ppm for the CB[7] host. ESI-MS: m/z at 1605.6 for $\{C_{24}H_{28}NFe_2 \cdot CB[7]\}^+$ (theoretically $m/z = 1605.4$)

For guest **2**, both 1:1 and 2:1 host-guest complexes were formed when different relative amounts of CB[7] were added.

1:1 complex: 1H NMR: (in D_2O): δ 4.42 (s), 4.36 (s), 4.30 (s), 4.20 (s), 3.02 (t), 2.81 (s), 1.67 (m) and 1.20 (m) ppm for the free ferrocene end of the guest, and 3.62 (s), 3.54 (s), 3.47 (s), 3.18 (t), 2.74 (s), 1.83 (m) and 1.40 (m) ppm for the bound ferrocene end of the guest. Peaks at δ 5.72 (d), 5.47 (s) and 4.17 (d) ppm are observed for the CB[7] host. ESI-MS: m/z at 1944.32 for $\{C_{38}H_{58}N_2Fe_2I \cdot CB[7]\}^+$ (theoretically $m/z = 1944.58$).

2:1 complex: 1H NMR: (in D_2O): 3.65 (s), 3.56 (s), 3.48 (s), 3.19 (t), 2.76 (s), 1.84 (m), 1.40 (m) and 1.27 (s) ppm for the bound guest and δ 5.72 (d), 5.47 (s) and 4.17 (d) ppm for the CB[7] host. ESI-MS: m/z at 1489.87 for $\{C_{38}H_{58}N_2Fe_2 \cdot 2CB[7]\}^{2+}$ (theoretically $m/z = 1490.01$).

5.2.2 Methods and Instruments

1H NMR spectra were recorded on a Bruker Advance 400 MHz instrument at 25 °C in D_2O . Chemical shifts are given on the δ scale (ppm) and are referenced to the HOD resonance ($\delta = 4.701$ ppm). The solutions for the 1H NMR titration measurements were prepared as follows: 6.0 mL of 1 mM ferrocene derivatives solutions were made and bubbled with Ar gas for 20 minutes and then divided into eight portions to ensure the concentration of the guest molecule was constant for each measurement. Different amounts of CB[7], varying up to 3.5 equivalents, were added. The solutions were sonicated to dissolve completely, bubbled with argon for 30 minutes and incubated for a further 30 minutes before

performing ^1H NMR measurements. The solutions of titanocene in D_2O were bubbled with argon for 30 minutes before the additions of CB[7] or CB[8]. After the addition of CB[7] or CB[8], the solutions containing the host-guest complexes were incubated under argon for six hours before the ^1H NMR measurements, to ensure that the two chlorides were replaced by D_2O . The resonances in the ^1H NMR spectra obtained are for $\text{TiCp}_2(\text{D}_2\text{O})_2^{2+}$ and $\{\text{TiCp}_2(\text{D}_2\text{O})_2\cdot\text{CB}[7]\}^{2+}$, rather than TiCp_2Cl_2 as the guest molecule.

For the competition experiments to determine the host-guest stability constant, a solution of CB[7] with diaquatitanocene and the competitor (hexamethylenediamine dihydrochloride) in a ratio of 1:3.2:1.4 was prepared, and incubated for one hour before the ^1H NMR spectra measurement was obtained. For CB[8], 1-aminoadamantane dihydrochloride was used as the competitor and a ratio of 1:1:1 was employed.

Electrospray ionization mass spectra were obtained on a Waters 2Q Single Quadrupole MS spectrometer, equipped with an ESI/APCI multiprobe, to confirm the formation of the host-guest complexes. Solutions were prepared in distilled water and measurements were performed after a one hour incubation at room temperature for each solution.

Cyclic voltammetry measurements on the bis(ferrocene) complexes and diaquatitanocene, in the absence and presence of the CB[n] hosts, were collected using a Bioanalytical Systems CV-1B cyclic voltammeter, attached to a Houston Instrument 100 X-Y recorder. The reference electrode was Ag/AgCl, while the working and auxiliary electrodes were platinum button and platinum wire electrodes, respectively.

The energy-minimized structures of the $\{\text{TiCp}_2(\text{H}_2\text{O})_2\cdot\text{CB}[n]\}^{2+}$ were calculated using Gaussian 03 programs (HF/3-21G** basis set), as described in Chapter 3.

5.3 Results and Discussion

5.3.1 Complexation of Bis(ferrocenes) with Cucurbit[7]uril

The complexation of compound **1** by CB[7] was monitored by ^1H NMR titration experiments at room temperature in D_2O solution. As shown in Figure 5.3, upon the addition of insufficient CB[7], the resonances for Cp rings and methylene groups were partially shifted upfield to 3.71, 3.58 and 3.50 ppm, indicating the inclusion of Cp rings and methylene groups into the hydrophobic cavity and the slow exchange between the free and bound forms. Meanwhile, the signal for methyl groups on the nitrogen atoms experienced an upfield shift as well (from 2.64 to 2.53 ppm), which is different from what had been expected. Normally, the CB[7] includes the Cp rings and the methylene portion, leaving one of the carbonyl portals interacting with the positive charge on nitrogen atom; the resonances for methyl groups on the nitrogen atom will be affected by the electronegative oxygen atoms of the carbonyl portal and experience downfield shifts.²⁰⁻²² Thus in this case, the unusual upfield shifts of the methyl groups indicated that they were bent back towards the included Cp ring portion to optimize the hydrophobic interaction with the cavity. The cavity of CB[7] is large enough to contain the ferrocene unit and the methyl groups as well. No 2:1 complex formation was observed, even with up to 3.5 equivalents of added CB[7], according to the resonances in the ^1H NMR spectra (there are still resonances for the free Cp unit). That can be explained by the structural characteristics of the guest, in which two ferrocene units are connected by a short aliphatic chain, bearing the positive charge. The repulsive interactions between the carbonyl portals of two adjacent CB[7] hosts, which would have to come in close proximity in order to form the 2:1 complex with two CB[n] hosts on the two ferrocenes, would make its formation thermodynamically unfavourable.

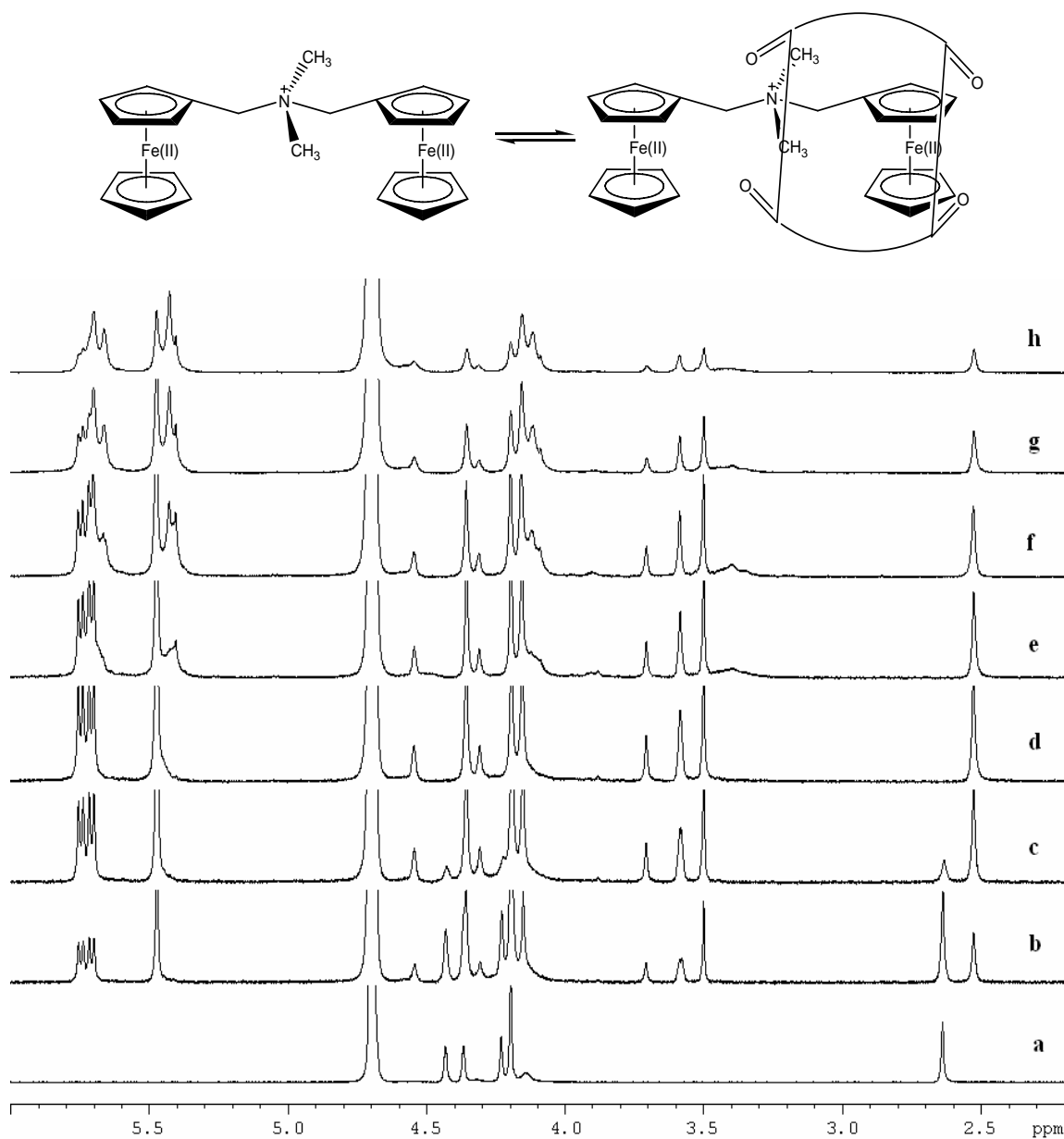


Figure 5.3 ¹H NMR spectra (400 MHz) of compound **1** (1.0 mM) in the absence and presence of (a) 0; (b) 0.42; (c) 0.85; (d) 1.26; (e) 1.65; (f) 2.24; (g) 2.8 and (h) 3.53 mM of CB[7] in D₂O at 25 °C.

(Trimethylammonio)methylferrocene, whose binding constant with CB[7] was reported to be $(4 \pm 2) \times 10^{12} \text{ M}^{-1}$,¹¹ was used as competitor to determine the stability constant

of the formed 1:1 complex in D₂O at room temperature. Figure 5.4 shows the spectra of the solution with 1:1:3 (compound 1:CB[7]:FcTMA⁺) in D₂O. Using the method described in Chapter 3 (competing method to determine binding constant), the stability constant was calculated to be $(2 \pm 1) \times 10^{13} \text{ M}^{-1}$ by monitoring the resonances for bound and unbound forms of methyl groups of both guest, which have different chemical shifts in the ¹H NMR spectra. The formation of this 1:1 complex was confirmed by the results of the ESI mass spectrum, in which a peak at $m/z = 1605.6$ for $\{\text{C}_{24}\text{H}_{28}\text{NFe}_2 \cdot \text{CB}[7]\}^+$ was observed, in good agreement with the theoretical value of $m/z = 1605.4$.

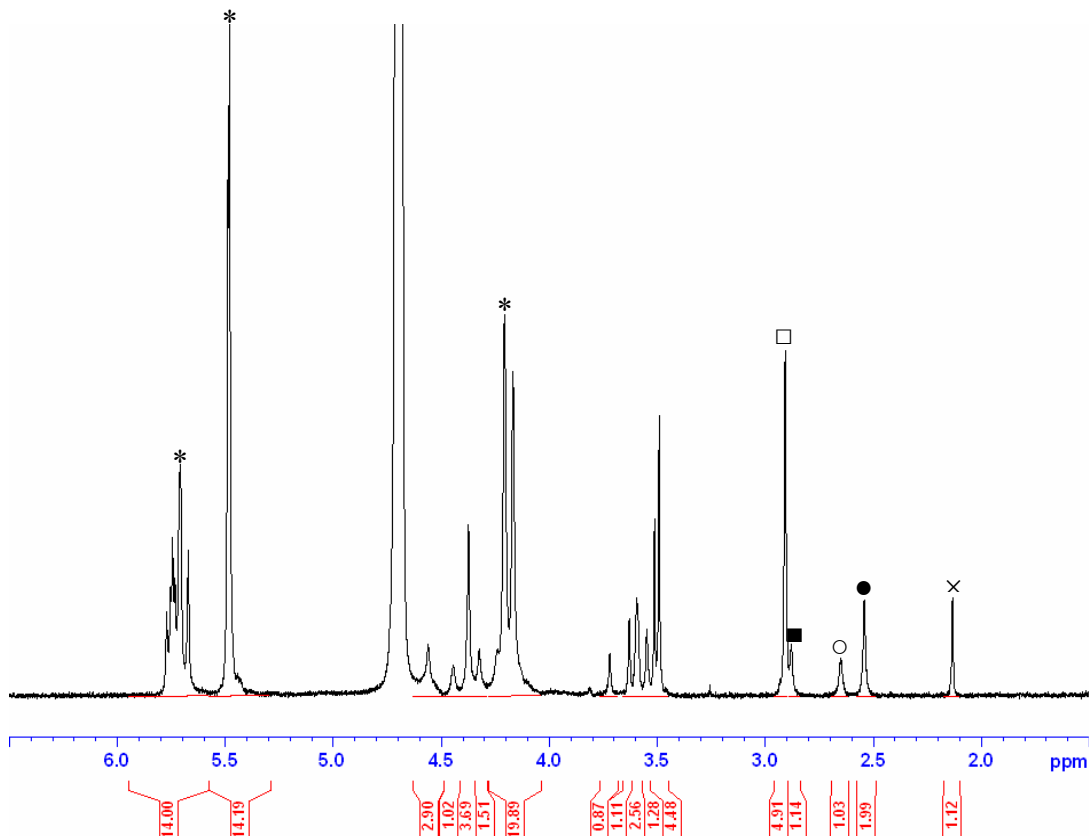


Figure 5.4 ¹H NMR spectra (400 MHz) of the solution containing compound **1** (1.0 mM), FcTMA⁺ (3.0 mM) and CB[7] (1.0 mM) in D₂O at 25 °C, which was used to determine the inclusion constant of compound **1** into CB[7]. (* CB[7]; o free compound **1**; • bound compound **1**; □ free competitor; ■ bound competitor; × impurity from CB[7])

The complexation behaviour of compound **2** with CB[7] was also investigated by monitoring the resonance changes in NMR spectra, which were obtained by measuring solutions of compound **2** with different amount of CB[7] in D₂O at room temperature, as shown in Figure 5.5. In the presence of less than one equivalent of CB[7], the resonances for Cp rings and methylene (4.42, 4.36, 4.30 and 4.21 ppm), as well as the resonance for methyl groups (2.81 ppm), experienced significant upfield shifts, which is similar to what was observed in the case of compound **1**. However, the signals of the α , β , γ and other aliphatic protons on the central chain show obvious downfield shifts, caused by the deshielding interactions with the carbonyl groups lined on the CB[7] portals. Resonances for both the free and bound ferrocene units were observed due to the slow exchange between these two forms on the ¹H NMR timescale. When more than one equivalent of CB[7] was added, the resonances for the unbound ferrocene end of the guest disappeared gradually (up to 2.3 equivalents, at which point the resonances for the free species disappeared completely, as shown in Figure 5.5 (f)) and at the same time the resonances for the bound species became more intense, indicating the inclusion of the second ferrocene unit in the CB[7] cavity, forming a 2:1 host-guest complex. The overlap of the signal of compound **2** with those of the competing guest, (trimethylammonio)methylferrocene, prevents the determination of the binding constant by using this guest as a competitor.

Cyclic voltammetry, which can be used to characterize electro-active species which can not be detected via NMR or IR spectroscopies,²³⁻²⁵ has been used to monitor the changes in the electrochemical properties upon the inclusions of compounds **1** and **2** in the hydrophobic cavity of the CB[7] host.

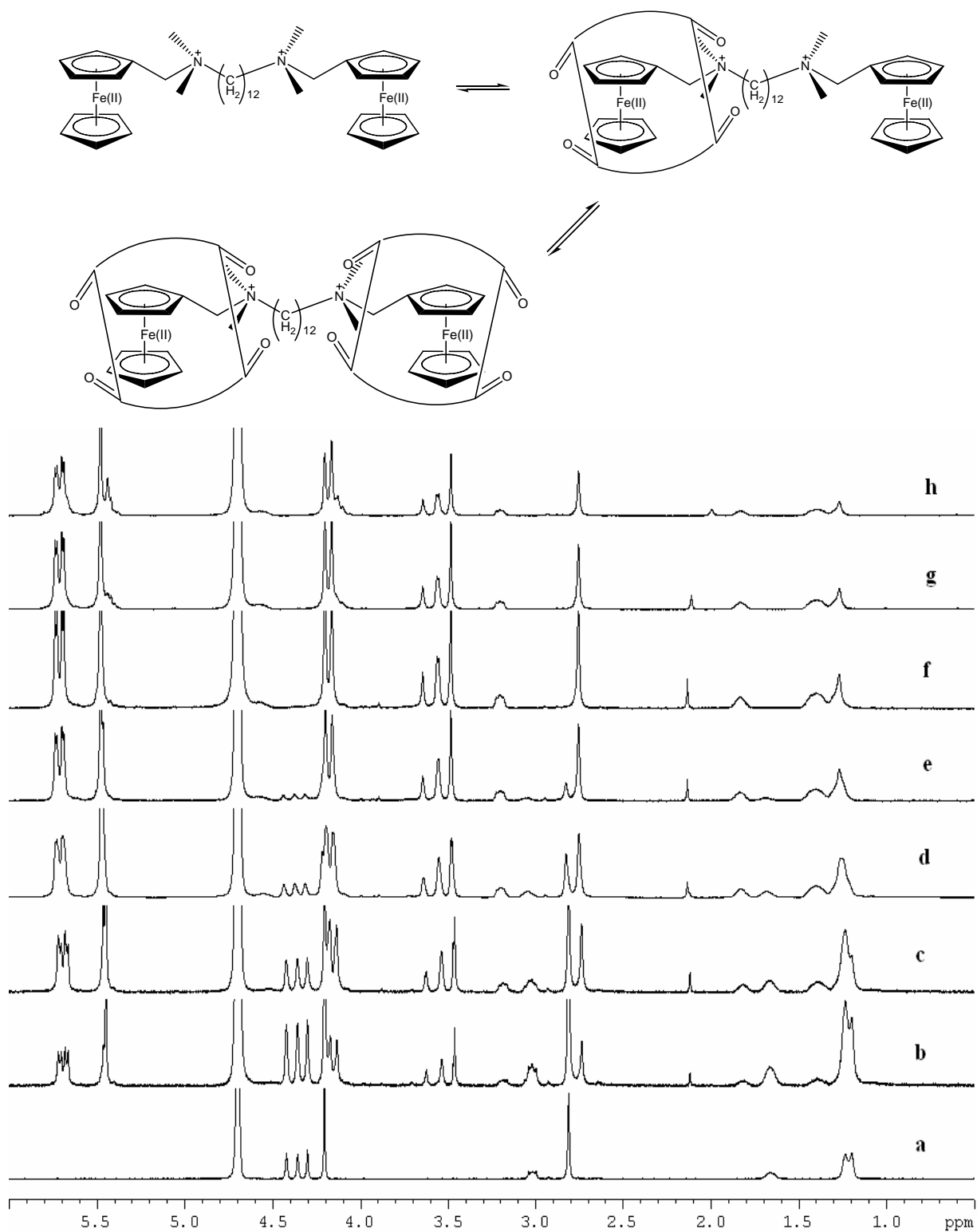


Figure 5.5 ¹H NMR spectra (400 MHz) of compound 2 (1mM) in the absence and presence of (a) 0; (b) 0.37; (c) 0.77; (d) 1.18; (e) 1.55; (f) 2.33; (g) 2.64 and (h) 3.43 mM of CB[7] in D₂O at 25 °C.

As shown in Figures 5.6 and 5.7, the half-wave potential $E_{1/2}$ for both **1** and **2** are shifted to more positive values by 75 mV and 50 mV, respectively, suggesting the more favourable binding between the CB[7] host with the reduced forms of both guest molecules. In Figure 5.6, two half-wave potentials were observed, which correspond to the two iron centers in the two ferrocene units. In the presence of 0.8 equivalents of CB[7], the more positive wave appears to split into two waves, corresponding to the binding of one of the two ferrocenes, while the other remains unbound, while the more negative peak corresponds to the remaining unbound guest. Upon the addition of 1.6 equivalents, all of compound **1** is bound with one CB[7] host.

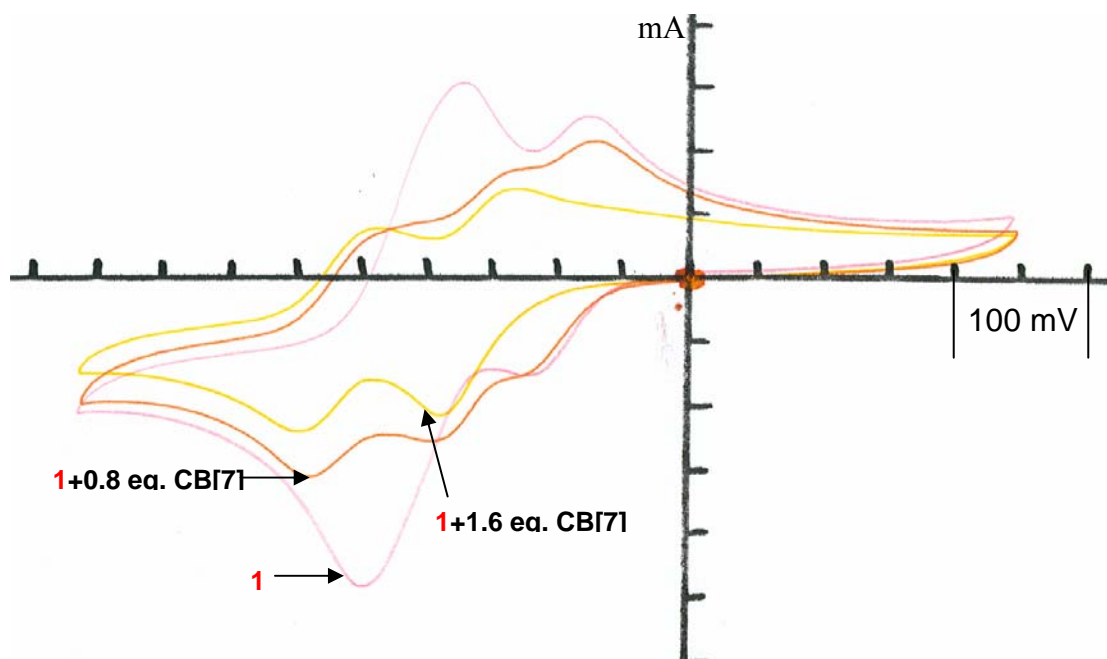


Figure 5.6 Cyclic voltammograms of compound **1** (1 mM) in the absence and presence of 0.8 and 1.6 mM CB[7] in 0.1 M NaCl aqueous solution at room temperature, using a glassy carbon as working electrode, Ag/AgCl as the reference electrode and platinum wire as the auxiliary electrode.

In Figure 5.7, addition of CB[7] to a solution of **2** results in an increase in the reduction potential of the ferrocene units (which act independently) by about 50 mV, consistent with what is observed with other substituted ferrocenes.

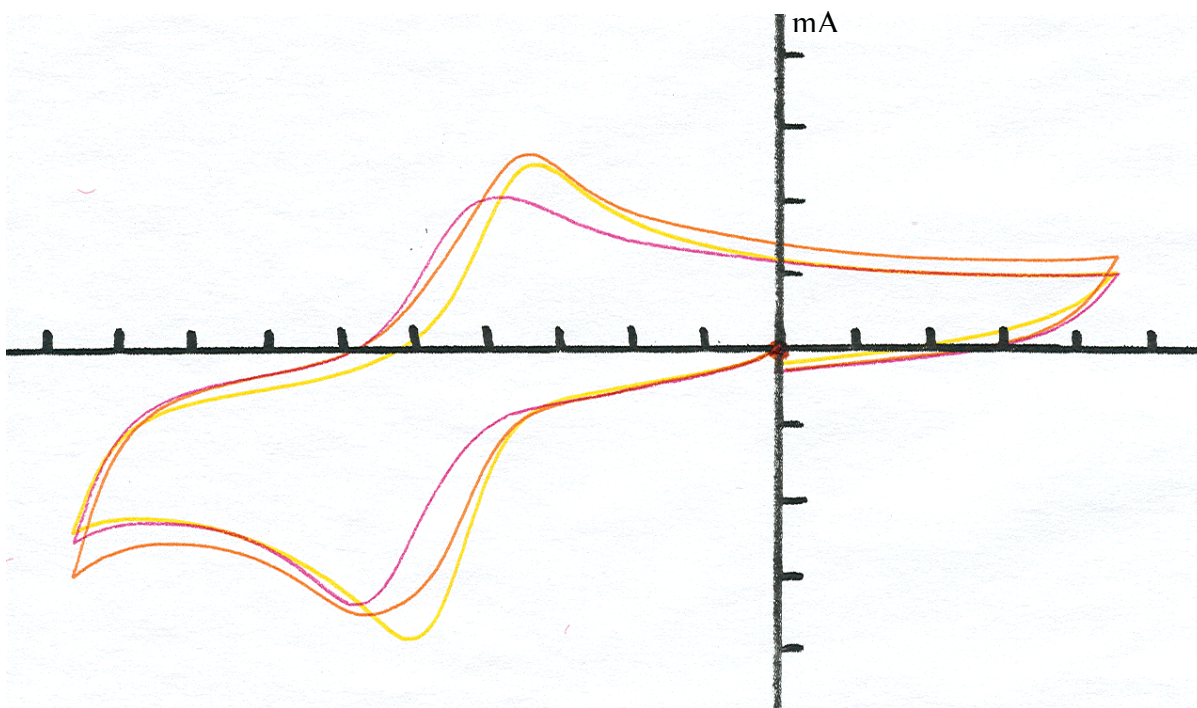


Figure 5.7 Cyclic voltammograms of compound **2** (1.0 mM) in the absence (yellow) and presence of 0.8 (orange) and 1.6 mM (red) CB[7] in 0.10 M NaCl aqueous solution at room temperature. (Scale is 50 mV/cm)

5.3.2 Complexation of Diaquatitanocene with CB[7]

Titanocenes have drawn considerable attention in the past two decades due to their anti-tumour activities.¹¹⁻¹⁵ Their inclusion in host molecules may affect their physical properties such as solubility and thermodynamic stability, which might be utilized in studies of their anti-tumour behaviour.¹⁷ Herein, the binding properties of a bent titanocene, the diaquabis(η^5 -cyclopentadienyl)titanium(IV) dication, with the CB[7] host molecule in

aqueous solution have been investigated. First, the formation of host-guest complex was monitored by ^1H NMR spectroscopy, as shown in Figure 5.8. The addition of CB[7] to an aqueous solution of $\text{TiCp}_2(\text{D}_2\text{O})_2^{2+}$, formed from the rapid hydrolysis of TiCp_2Cl_2 , results in a broadening and upfield shift of the 6.54 ppm resonance of the Cp ring protons. As the ratio of TiCp_2Cl_2 to CB[7] approaches 1:1, the resonance begins to sharpen again and reaches a final position at 5.83 ppm. The large upfield shift ($\Delta\delta = -0.71$ ppm) results from the shielding afforded guest Cp protons located in the CB[n] cavity.

The broadening and chemical shift behaviour for the CB[7] inclusion is consistent with intermediate exchange on the ^1H NMR timescale.²⁶⁻²⁸ As shown in Figure 5.9, a frequency difference of 324 Hz in the bound and free guest resonances, indicates an exchange rate of $< 720 \text{ s}^{-1}$. With systems of moderately fast exchange and unequal populations of free (P_f) and bound (P_b) guests, the resonance position is not the fully averaged mole fraction value ($\delta_{\text{obs}} = P_f\delta_f + P_b\delta_b$), but rather is shifted towards the species with the higher mole fraction.²⁶⁻²⁸ As a result, a plot of $\Delta\delta_{\text{obs}}$ as a function of the [host]/[guest] ratio has a sigmoidal shape, rather than the exponential shape normally observed with faster exchange processes.

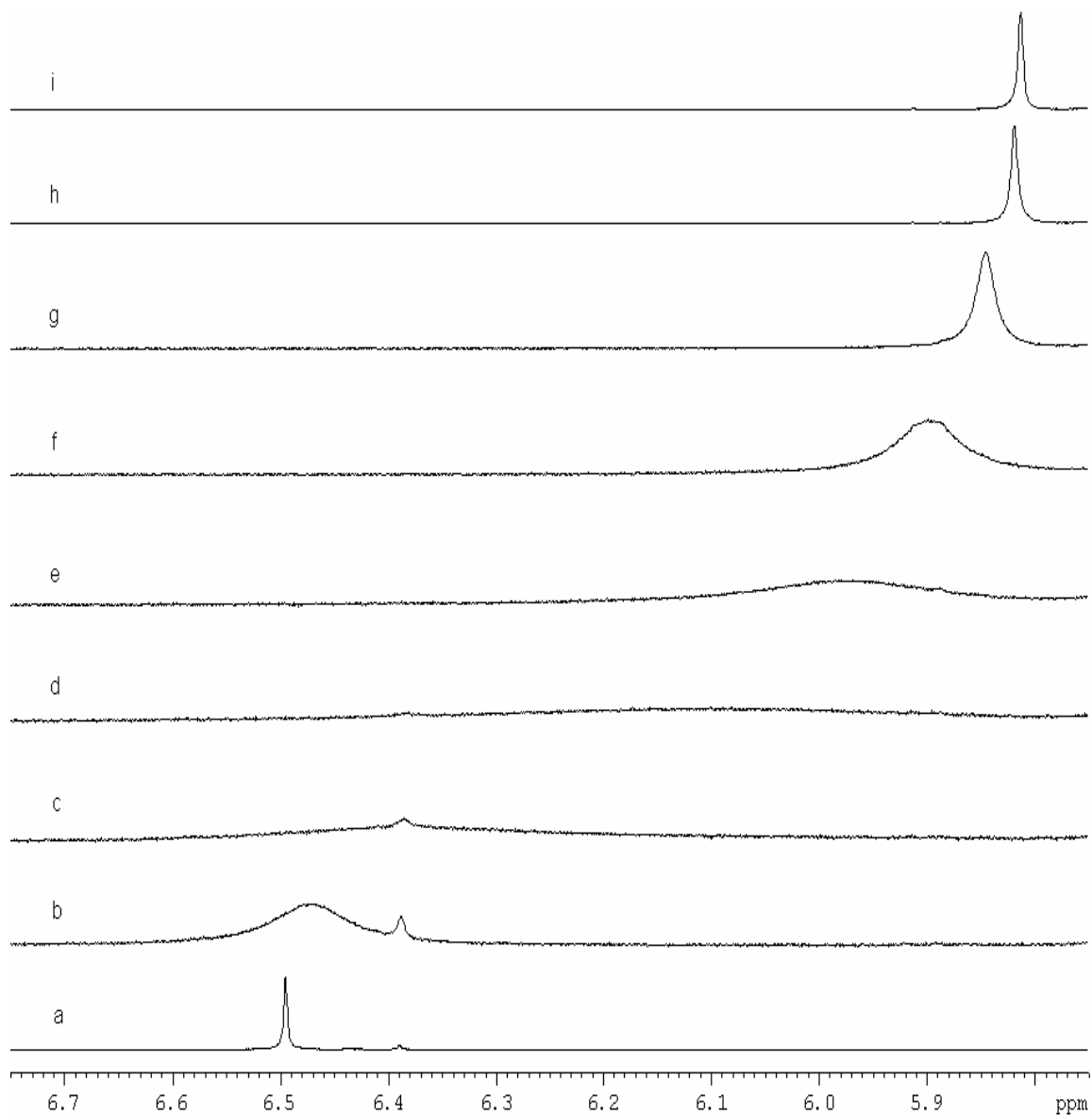


Figure 5.8 ^1H NMR spectra (400 MHz) of $\text{TiCp}_2(\text{D}_2\text{O})_2^{2+}$ (1.0 mM) in the absence and presence of: (a) 0, (b) 0.26, (c) 0.56, (d) 0.84, (e) 1.08, (f) 1.30, (g) 1.39, (h) 1.85, and (i) 2.42 mM CB[7] in D_2O at 25 °C.

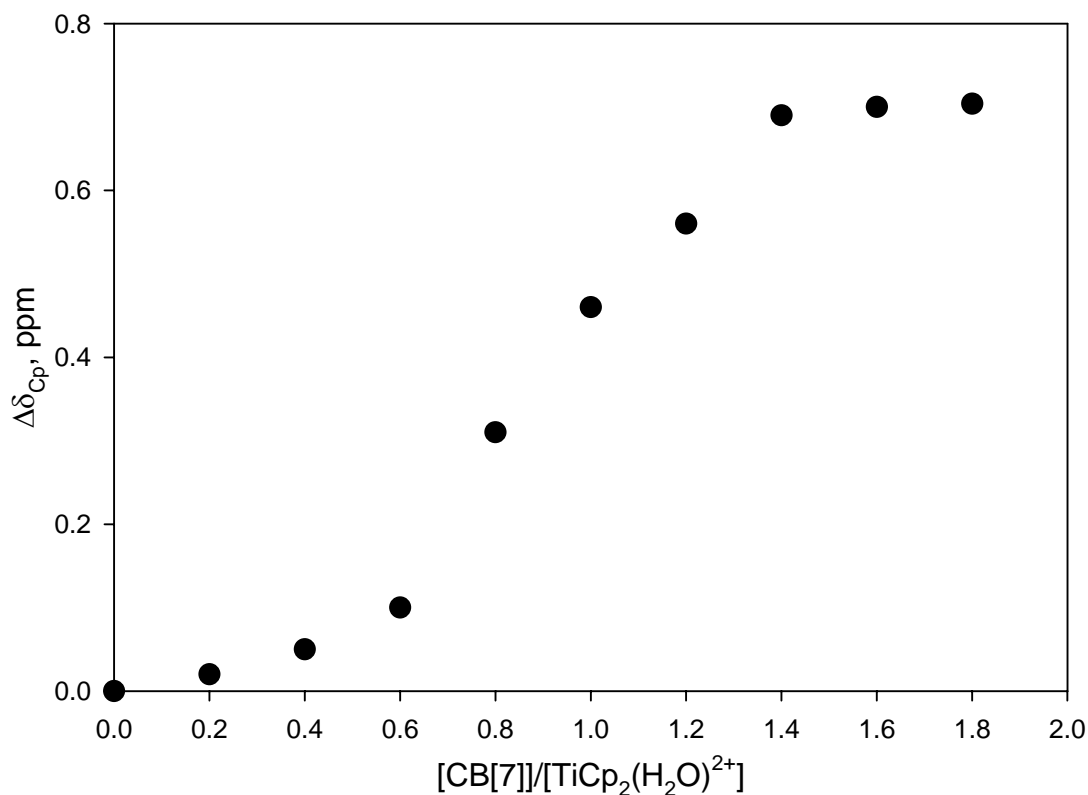


Figure 5.9 Plot of $\Delta\delta_{obs}$ against the host/guest ratio for the inclusion of CB[7] by the $TiCp_2(D_2O)_2^{2+}$ complex in D_2O .

The binding constant of $\{TiCp_2(D_2O)_2 \cdot CB[7]\}^{2+}$ complex was determined by 1H NMR competition studies, using hexamethylenediamine dihydrochloride ($K_{CB[7]} = (8.97 \pm 1.43) \times 10^7 M^{-1}$)³¹ as a competitor to be $(6.3 \pm 1.0) \times 10^6 M^{-1}$. A solution of CB[7] with the titanocene and the competitor in the ratio of 1:3.2:1.4 was used to perform the calculation. The 1H NMR spectra was shown in Figure 5.10, the value of $K_{relative}$ was determined by the equation as follows:

$$K_{\text{relative}} = \frac{K_{\text{Ti}\cdot\text{CB}[7]}}{K_{\text{competitor}\cdot\text{CB}[7]}} = \frac{[\text{Ti}\cdot\text{CB}[7]] [\text{Competitor}]_{\text{free}}}{[\text{Competitor}\cdot\text{CB}[7]] [\text{Ti}]_{\text{free}}} \quad (5.3)$$

where the parameters needed for equation 5.3 can be determined by the given total concentrations of the host and the guest, as well as the integrations for bound and free species (refer to Chapter 3 for calculation details).

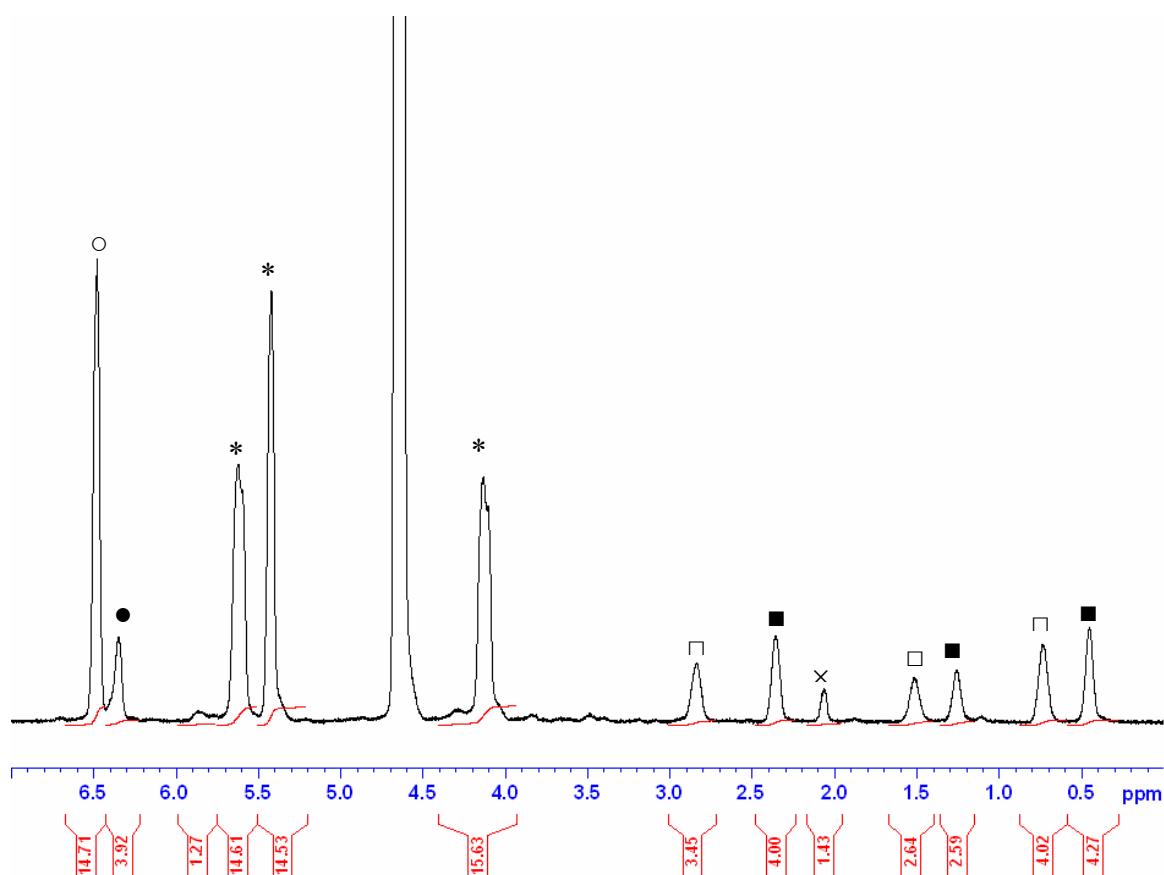


Figure 5.10 ^1H NMR spectra (400 MHz) of the solution containing diaquatitanocene, the competitor and CB[7] in a ratio of 3.2:1.4:1 in D_2O at 25 °C, which was used to determine the inclusion constant of diaquatitanocene with CB[7], by a competition method. (* CB[7]; o free compound 1; • bound compound 1; □ free competitor; ■ bound competitor; x impurity from CB[7])

The effect on molecular property of the guest upon the inclusion into CB cavity was also characterized by cyclic voltammetry, as shown in Figure 5.11. The $\text{TiCp}_2(\text{H}_2\text{O})_2^{2+}$ undergoes an irreversible one-electron reduction with a reduction potential of -450 mV in aqueous solution. A slight negative shift (30 mV) in the reduction potential was observed for Ti(IV)/Ti(III) couple upon the binding with 1.2 equivalent of CB[7]. With several ferrocene complexes, a positive shift in the (Fe(III)/Fe(II)) potential in the presence of CB[7] was observed, which is associated with a reduction in the stability constant of the oxidized ferrocene complex.³²⁻³⁵ With the titanocene complex, the decrease in the reduction potential is related to an increase in the stability constant for the Ti(IV) complex compared to Ti(III) complex.

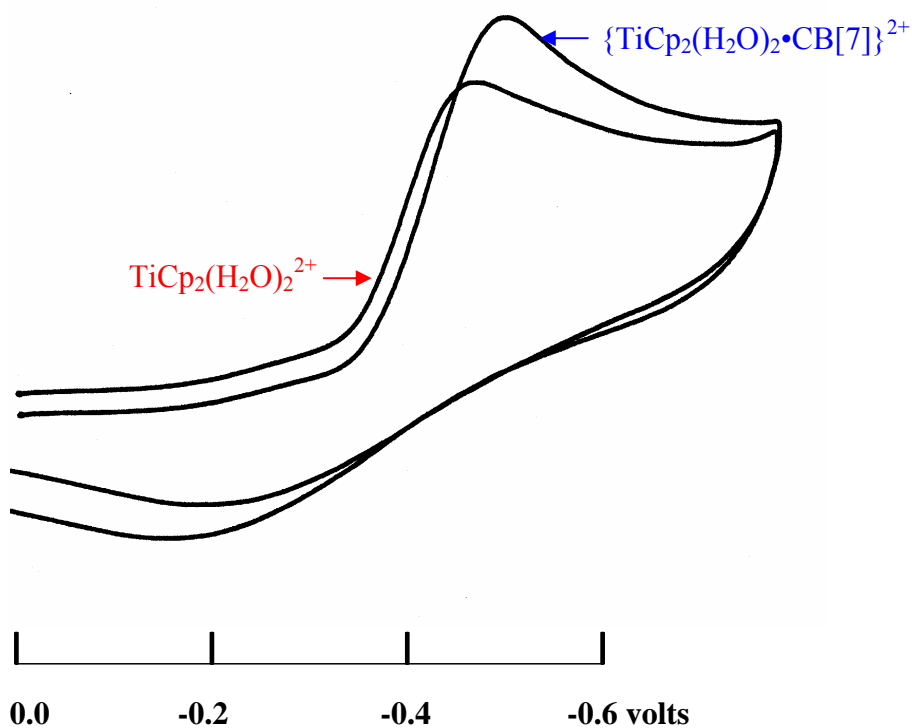


Figure 5.11 Cyclic voltammograms of $\text{TiCp}_2(\text{H}_2\text{O})_2^{2+}$ (1.0 mM) in the absence and presence of 1.2 mM CB[7] in aqueous solution (containing 0.10 M NaNO_3) at room temperature.

5.3.3 Complexation of Titanocene with CB[8]

A similar investigation for the binding process of titanocene with CB[8] has been carried out using ^1H NMR spectroscopy and ESI mass spectrometry. A cyclic voltammetry study was not possible due to the low solubility of CB[8] in aqueous solution. Figure 5.12 shows the result of the ^1H NMR titration, in which the guest exchange process is slower compared to that of CB[7], as at intermediate ratios of CB[8] to Ti, the resonances for both the bound and free $\text{TiCp}_2(\text{D}_2\text{O})_2^{2+}$ species are observed (Figures 5.12 (c) and (d)). Upon the addition of CB[8], the resonances for the Cp rings first broadened and shifted upfield and then sharpened to finish at 5.79 ppm with excess CB[8] added, similar to the result obtained in the case of CB[7]. The formation of the 1:1 complex was confirmed by ESI mass spectrometry, with m/z at 780.18 for the $\{\text{TiCp}_2(\text{H}_2\text{O})_2 \cdot \text{CB}[8] + \text{H}_2\text{O}\}^{2+}$ species, in good agreement of theoretical value of 780.23.

The binding constant of $\{\text{TiCp}_2(\text{D}_2\text{O})_2 \cdot \text{CB}[8]\}^{2+}$ complex was also determined by a ^1H NMR competition study (spectrum is shown in Figure 5.13), using 1-aminoadamantane [$K_{\text{CB}[8]} = (8.19 \pm 1.75) \times 10^8 \text{ M}^{-1}$]²⁹ as the competitor guest, to be $(1.97 \pm 0.42) \times 10^8 \text{ M}^{-1}$, in the similar manner to the determination of $K_{\text{Ti} \cdot \text{CB}[7]}$. Unlike the binding between the competitor with CB[7], which exhibits slow exchange on the ^1H NMR timescale, the binding between the 1-aminoadamantane competitor with CB[8] exhibits fast exchange process on the ^1H NMR timescale, thus the ratio of bound and free species can not be obtained directly from Figure 5.13, instead it is determined by the ^1H NMR titration data of 1-aminoadamantane with CB[8]. However, the same equation (Equation 5.3) was used for the calculation of K_{relative} .

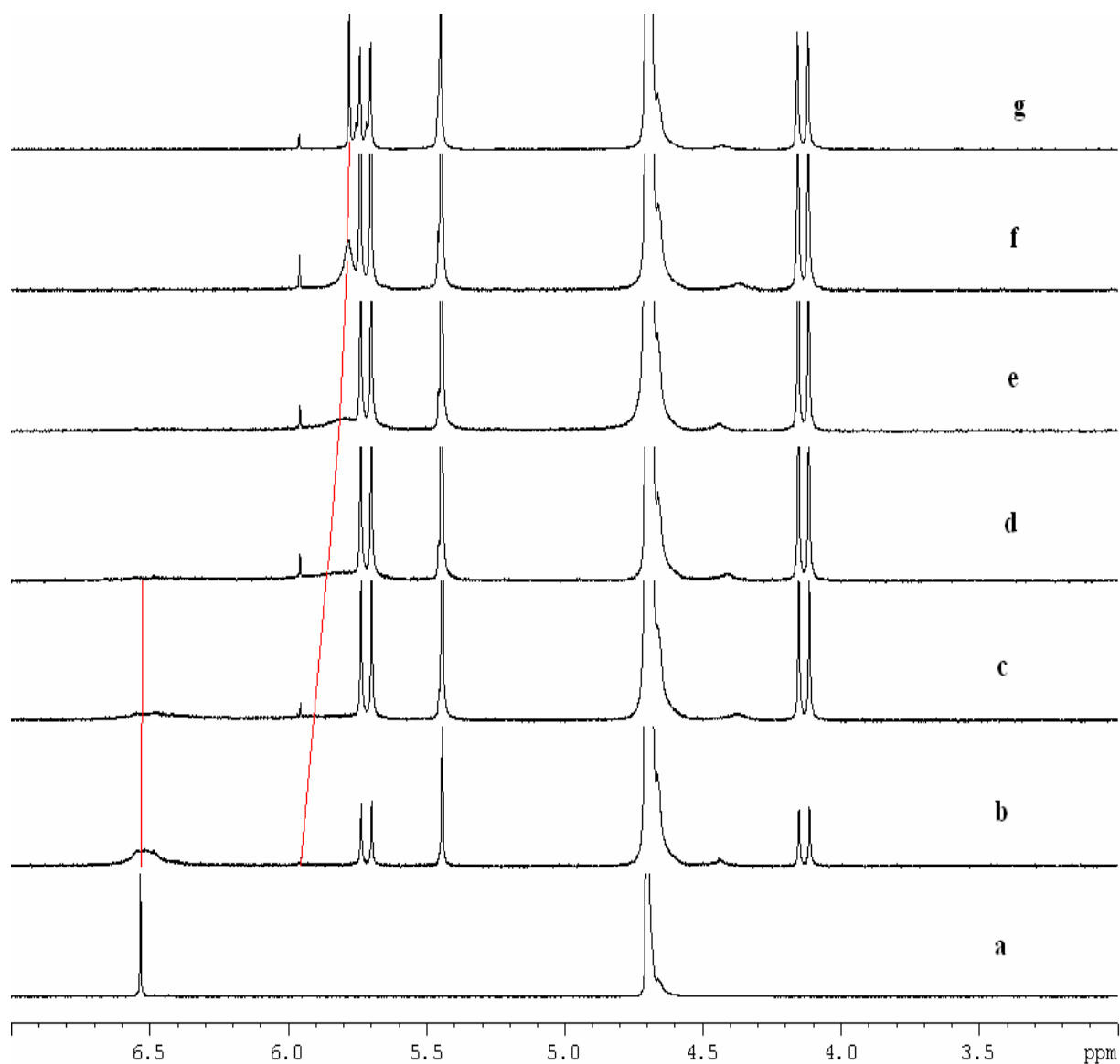


Figure 5.12 ¹H NMR spectra (400 MHz) of TiCp₂(D₂O)₂²⁺ (1mM) in the absence and presence of: (a) 0, (b) 0.31, (c) 0.70, (d) 0.85, (e) 1.0 (f) 1.13, and (g) 1.36 mM of CB[8] in D₂O at 25 °C. [Note: The calculation of values for (e) from NMR spectra is not applicable due to the almost flat resonances, however from the original weight, the ratio of host to guest were determined to be 1.0].

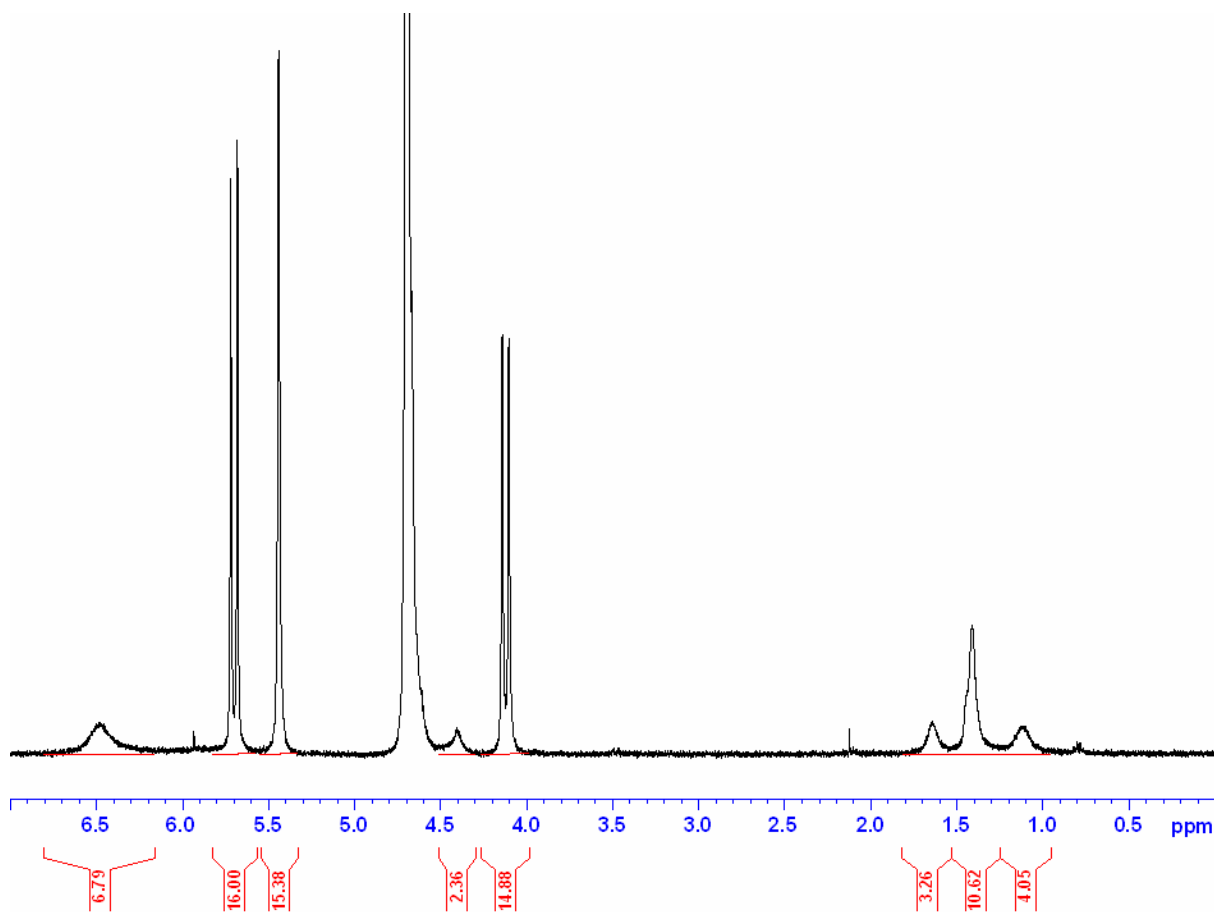


Figure 5.13 ¹H NMR spectra (400 MHz) of the solution containing diaquatitanocene, the protonated 1-aminoadamantane competitor and CB[8] in a ratio of 1:1:1 in D₂O at 25 °C, used to determine the inclusion constant of TiCp₂(D₂O)₂²⁺ with CB[8] by the NMR competition method.

5.3.4 Comparison of the Effects of Complexation with CB[7] and CB[8]

Contrary to the higher binding constants determined for ferrocenes with CB[7],¹⁻³ compared with CB[8]²⁹ ($K_{\text{CB}[7]} = (3.31 \pm 0.62) \times 10^{11}$ and $K_{\text{CB}[8]} = (3.12 \pm 0.80) \times 10^9 \text{ M}^{-1}$

for (trimethylammonio)methylferrocene, for example), the bent metallocenes prefer the larger CB[8] cavity, presumably as a result of the larger effective radius of the guests because of the bent orientation of the two Cp rings, along with the presence of the two aqua ligands.

The structures of the host-guest complexes were modelled in the gas-phase from energy-minimization calculations (HF-/3-21G** basis set), as shown in Figure 5.14. For the $\{\text{TiCp}_2(\text{H}_2\text{O})_2 \cdot \text{CB}[8]\}^{2+}$ complex in Figure 5.14(b), the diaquatitanocene dication is fully encapsulated in the CB[8] cavity, with the Cp rings aligned with the glycoluril units. A similar inclusion in γ -cyclodextrin has been predicted from spectroscopic and theoretical calculations, although the stability constant (77 M^{-1}) is 8 orders of magnitude lower than determined herein for inclusion in a similarly sized CB[8] cavity.

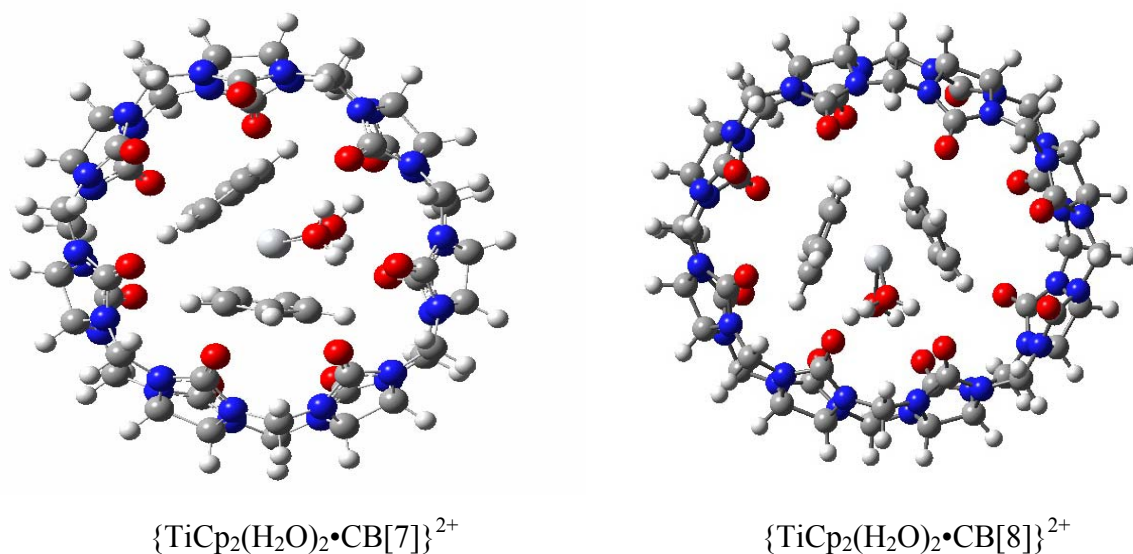


Figure 5.14 The energy-minimized gas-phase structure of the (a) $\{\text{TiCp}_2(\text{H}_2\text{O})_2 \cdot \text{CB}[7]\}^{2+}$ and (b) $\{\text{TiCp}_2(\text{H}_2\text{O})_2 \cdot \text{CB}[8]\}^{2+}$ host-guest complex (HF/3-21G** basis set).

The effects of the inclusions of the $\text{TiCp}_2(\text{H}_2\text{O})_2^{2+}$ complex into the CB[7] and CB[8] cavities on the rate of the cyclopentadienyl protonolysis (to form $\text{C}_5\text{H}_5\text{D}$) were investigated

at pH 4 by ^1H NMR spectroscopy. Since the cyclopentadiene released from these complexes was found to experience rapid deuterium exchange in the deuterated solvent, the detection of it by ^1H NMR spectroscopy is applicable.¹³ Preliminary data shows that the protonolysis of Cp rings, indicated by the disappearance of the Cp resonance, was slowed from 5.5 hrs for free titanocene, to 7 days for the diaquatitanocene included by the CB[n] hosts. Further work needs to be done to further investigate of the effects of inclusion on the chemical and spectroscopic properties of the diaquatitanocene (and other bent metallocenes), as well as their stability in solution (hydrolysis processes).

5.4 Summary

In this chapter, the binding behaviours of CB[n] hosts with two bis(ferrocene) guests, and with the anti-tumour agent $\text{TiCp}_2(\text{H}_2\text{O})_2^{2+}$, based on the results obtained from ^1H NMR spectroscopy, ESI mass spectrometry and cyclic voltammetry, have been discussed. The two bis(ferrocene) compounds show different binding properties with CB[7] due to their different central chain lengths. When the aliphatic chain between the two ferrocenes units is short (compound **1**), only a 1:1 complex is formed even with a large excess of the host due to the steric hindrance and repulsive interactions between carbonyl groups on adjacent CB[7] molecules. Both the 1:1 and 2:1 complexes were observed in the case of compound **2**, which possesses a central chain (dodecamethylene) long enough to separate two CB[7] hosts present on the two ferrocene groups of the guest at the same time. Compared with the traditional “sandwich-shaped” ferrocene, the anti-tumour agent $\text{TiCp}_2(\text{H}_2\text{O})_2^{2+}$ possesses a bent metallocene structure. This compound can form 1:1 complexes with both CB[7] and CB[8] in aqueous solution, with large stability constants. The effects of the inclusion in the

host cavity on the electrochemical properties of these guests revealed that the half wave potential experienced positive shifts for the bis(ferrocene) cations and a negative shift for the diaquatitanocene dication. These results suggest that the host molecules can form more stable complex with the reduced forms of ferrocene (iron(II)) and the oxidized form of the titanocene (Ti(IV)). For the diaquatitanocene, preliminary results show that the inclusion in the host cavity can decrease the tendency of the Cp ring to become hydrolyzed, increasing the stability of the titanocene in aqueous solution, which could be a valuable feature in clinical trials of anti-tumour titanocene candidates.

References

1. Ong, W.; Kaifer, A. E. *Organometallics* **2003**, *22*, 4181.
2. Jeon, W. S.; Moon, K.; Park, S. H.; Chun, H.; Ko, Y. H.; Lee, J. Y.; Lee, E. S.; Samal, S.; Selvapalam, N.; Rekharsky, M. V.; Sindelar, V.; Sobransingh, D.; Inoue, Y.; Kaifer, A. E.; Kim, K. *J. Am. Chem. Soc.* **2005**, *127*, 12984.
3. Wang, R.; Yuan, L.; Macartney, D. H. *Organometallics* **2006**, *25*, 1820.
4. Matsue, T.; Evans, D. H.; Osa, T.; Kobayashi, N. *J. Am. Chem. Soc.* **1985**, *107*, 179.
5. Isnin, R.; Salam, C.; Kaifer, A. E. *J. Org. Chem.* **1991**, *56*, 35.
6. Imonigie, J. A.; Macartney, D. H. *Inorg. Chim. Acta* **1994**, *225*, 51.
7. Zhang, L.; Macias, A.; Lu, T.; Gordon, J. I.; Gokel, G. W.; Kaifer, A. E. *Chem. Commun.* **1993**, 1017.
8. Zhang, L.; Marcias, A.; Isnin, R.; Lu, T.; Gokel, G. W.; Kaifer, A. E. *J. Incl. Phenom. Mol. Recognit. Chem.* **1994**, *19*, 361.
9. Komura, T.; Yamaguchi, T.; Kura, K.; Tanabe, J. *J. Electroanal. Chem.* **2002**, *523*, 126.
10. Nielson, R. M.; Hupp, J. T. *Inorg. Chem.* **1996**, *35*, 1402.
11. Yuan, L.; Macartney, D. H. *J. Phys. Chem. B* **2007**, *111*, 6949.
12. Köpf-Maier, P.: 'Metal complexes in cancer chemotherapy', in Keppler, B. K. (ed.), *Antitumour Metallocenes*, VCH, Weinheim, 1993, pp. 261–296.
13. Toney, J. H.; Marks, T. J. *J. Am. Chem. Soc.* **1985**, *107*, 947.
14. (a) Köpf, H.; Köpf-Maier, P. *Angew. Chem., Int. Ed. Engl.* **1979**, *18*, 477. (b) Köpf-Maier, P.; Hesse, B.; Köpf, H. *J. Cancer Res. Clin. Oncol.* **1980**, *96*, 43.
15. Mokdsi, G.; Harding, M. M. *J. Organometal. Chem* **1998**, *565*, 29.

16. (a) Wheate, N. J.; Day, A. I.; Blanch, R. J.; Arnold, A. P.; Cullinane, C.; Collins, J. G. *Chem. Commun.* **2004**, 1424. (b) Wheate, N. J.; Buck, D. P.; Day, A. I.; Collins, J. P. *Dalton Trans.*, **2006**, 451. (c) M. S. Bali, M. S.; Buck, D. P.; Coe, A. J.; Day, A. I. Collins, J. G. *Dalton Trans.*, **2006**, 5337. (d) Kemp, S.; Wheate, N. J.; Wang, S.; Collins, G. J.; Ralph, S. F.; Day, A. I.; Higgins, V. J.; Aldrich-Wright, J. R. *J. Biol. Inorg. Chem.* **2007**, *12*, 969.
17. Turel, I.; Demsar, A.; Kosmrlj, J. *J. Inclu. Phen. Macro. Chem.* **1999**, *35*, 595.
18. Day, A.; Arnold, A. P.; Blanch, R. J.; Snushall, B. *J. Org. Chem.* **2001**, *66*, 8094.
19. Macartney, D. H.; Roszak, A. W.; Smith, K. C. *Inorg. Chim. Acta* **1999**, *291*, 365.
20. Yuan, L.; Wang, R.; Macartney, D. H. *J. Org. Chem.* **2007**, *72*, 4539.
21. Yuan, L.; Wang, R.; Macartney, D. H. *Tetrahedron: Asymmetry* **2007**, *18*, 483.
22. Wang, R.; Yuan, L.; Macartney, D. H. *Chem. Commun.* **2005**, 5867.
23. Bott, A. W. *Current Separations* **1991**, *10*, 139.
24. Haque, I. U.; Sadaf, S.; Fatima, G. *ECS Transactions* **2007**, *6*, 79.
25. Tustin, G. J.; Lafitte, V. G. H.; Banks, C. E.; Jones, T. G. J.; Smith, R. B.; Davis, J.; Lawrence, N. S. *J. Organometal. Chem.* **2007**, *692*, 5173.
26. Bain, A. D. *Prog. Nucl. Magn. Reson. Spectr.* **2003**, *43*, 63
27. London, R. E. *J. Magn. Reson. A* **1993**, *104*, 190.
28. Feeney, J.; Batchelor, J. G.; Albrand, J. P.; Roberts, G. C. K. *J. Magn. Reson.* **1979**, *33*, 519.
29. Liu, S.; Ruspic, C.; Mukhopadhyay, P.; Chakrabarti, S.; Zavalij, P. Y.; Isaacs, L. *J. Am. Chem. Soc.* **2005**, *127*, 15959.

Chapter 6

CONCLUSIONS AND SUGGESTIONS FOR FUTURE WORK

6.1 Conclusions

The research projects in this thesis have been focused on the investigation of the changes in the chemical, electrochemical and spectroscopic properties of a variety of guest molecules upon the inclusion into the hydrophobic cavities of members of the cucurbit[n]uril host family.

The host-guest complexation behaviours of several types of guest molecules with CB[n] hosts in this thesis have been discussed. Initially, a tetracationic bis(viologen) guest $\text{CH}_3\text{bpy}(\text{CH}_2)_6\text{bpyCH}_3^{4+}$ was synthesized and employed to investigate the relative binding behaviours of CB[6] and CB[7], based on the different binding site preferences due to the sizes of the host cavity and portals.¹ As might be expected, with the smaller cavity size, CB[6] resides on the central aliphatic chain of the guest, forming a 1:1 [2]pseudorotaxane complex. With CB[7], however, more interesting binding behaviours were revealed. When less than one equivalent of CB[7] host is added, a 1:1 complex is formed with CB[7] including the central aliphatic chain, similar to what was observed in the case of CB[6]. When excess CB[7] is added, the 1:1 complex is converted into a 2:1 [3]pseudorotaxane complex with both CB[7] hosts residing on the two separated viologen units. Since the inclusion of both the central chain and an adjacent viologen unit at the same time is not favourable, due to the steric and electrostatic repulsive interactions between the carbonyl portals on the CB[7] molecules, the CB[7] which was initially on the central aliphatic chain,

is forced to give up its inclusion of the central chain and move on to the other viologen group when the second CB[7] is introduced to the system.

The effect of host-guest complexation on the chiroptic properties of a set of chiral enantiomeric guests, protonated (*S*)- and (*R*)-*N*-benzyl-1-(1-naphthyl)ethylamine, was investigated in terms of the changes in the molar optical rotation and the circular dichroism (CD) spectra of the chiral guests upon the binding with the achiral CB[7] host.² Spectral evidence supports the formation of a 1:1 complex with CB[7], with inclusion of the benzyl, rather than the naphthyl moiety of the guests. The five-fold increase in molar optical rotation and significant changes in the CD spectra may be explained by some degree of steric restriction in the rotation of the naphthyl chromophore of the guest about chiral center, upon the inclusion of benzyl unit into the host cavity.

The effects of the host-guest complexation of substituted ferrocenes, notably (trimethylammonio)methylferrocene, with CB[7] on the kinetics of their electron self-exchange and electron transfer reactions have been investigated³ and compared the behaviour in the presence of other related macrocyclic hosts such as β -cyclodextrin and *p*-sulfonatedcalix[6]arene. The unique feature about ferrocene-CB[7] guest-host system is that the slow exchange of the ferrocene from the CB[7] on the ¹H NMR timescale makes it possible to monitor the electron self-exchange process for both the bound and unbound species independently, such that the rate constants for the possible self-exchange pathways involving the bound and free forms of both the oxidized and reduced forms of the guest can be determined separately. The electron self-exchange rate constant increased when both the reduced and oxidized forms are encapsulated by CB[7] host compared to the free redox couple, and decreased when only the reduced form was included in CB[7]. The electron

transfer reactions between two substituted ferrocenes with the bis(2,6-pyridinedicarboxylato)cobaltate(III) ion (which does not bind to CB[7]) were also investigated in the absence and the presence of CB[7] in aqueous solution at 25 °C. The encapsulation of ferrocene guests by CB[7] significantly reduces the rate constant for their oxidation, as a result of reduced thermodynamic driving forces and steric hindrance to close approach of the oxidant to the encapsulated ferrocenes.

Prompted by the results obtained for (trimethylammonio)methylferrocene, the binding behaviour of two cationic bis(ferrocene) derivatives, $\text{CpFeC}_5\text{H}_4\text{CH}_2\text{N}(\text{CH}_3)_2\text{CH}_2\text{C}_5\text{H}_4\text{FeCp}^+$ and $\text{CpFeC}_5\text{H}_4\text{CH}_2\text{N}(\text{CH}_3)_2(\text{CH}_2)_{12}(\text{CH}_3)_2\text{NCH}_2\text{C}_5\text{H}_4\text{FeCp}^{2+}$, with CB[7] were also investigated, revealing that the nature and the length of central linker between two ferrocene units has significant effects on their binding behaviours with CB[7]. The former monocationic guest, with a shorter linker, can only form a 1:1 complex with CB[7], even in the presence of excess host, as the repulsive electrostatic interactions between the carbonyl groups on the portals of adjacent hosts will not allow two CB[7] molecules to reside on the guest molecule simultaneously. However, the latter bis(ferrocene) with the much longer aliphatic chain between two ferrocene units forms both 1:1 (with insufficient host) and 2:1 (in the presence of excess host) host-guest complexes. The electrochemical change of both guests upon the inclusion into CB[7] cavity were also investigated by cyclic voltammetry, indicating that the half wave potentials ($E_{1/2}$) were shifted to more positive potentials, due to the more favourable binding of host to the reduced forms of the guests, as expected. Further studies using other linkers between the ferrocenes are planned.

The complexation of a bent metallocene, diaquatitanocene, with CB[7] and CB[8] were also investigated by ^1H NMR, ESI-MS and cyclic voltammetry.⁴ The exchange between free and bound titanocene was found to be intermediate on NMR scale, indicated by the extreme broadening of the Cp resonances in the present of insufficient CB host. Contrasting to the ferrocenes, whose binding to CB[7] is stronger, the bent titanocene shows higher affinity to CB[8], presumably as a result of the larger effective radius of the guest. Cyclic voltammetry shows that the half wave potential of $\text{Ti}^{4+/3+}$ was shifted to 30 mV more negative, which was also different from that of ferrocene. This result suggests that the CB hosts prefer to bind the oxidized form of titanocene rather than the reduced form. The inclusion into hydrophobic cavity of the CB host could have effect on the physical properties of this anti-tumour drug such as cytotoxicity and solubility, which might be utilized in clinical trails.

In summary, the investigations of the host-guest complex formations between the cucurbit[n]uril ($n = 6, 7, \text{ and } 8$) hosts and a variety of organic and organometallic guests have demonstrated that significant changes in the chemical, electrochemical and spectroscopic properties of the guest molecules may occur upon their inclusion into the CB[n] cavities, with non-covalent interactions with the carbonyl-lined portals. The examples we have illustrated in this thesis may lead to expansions in the applications of CB[n] host molecules in the fields of catalysis, molecular sensing and molecular machine/switch construction.

6.2 Suggestions for Future Work

The understanding of behaviours of the various host-guest systems investigated with the cucurbit[n]uril host family in this thesis may be applied to future work with related guest

molecules. The work on the tetracationic bis(viologen) guest molecule is being extended to other extended guest systems in which it may be possible to accommodate CB[7] in adjacent regions of the molecule by extending the components to reduce the steric and electrostatic repulsions. An undergraduate student has synthesized an analog of the tetracationic guest described in Chapter 2, in which the 4,4'-bipyridine group is replaced by a *trans*-1,2-bis(4,4-bipyridyl)ethylene group (Figure 6.1). Preliminary ^1H NMR spectral evidence suggests that three CB[7] host molecules may be accommodated on this extended guest molecule. The introduction of the ethylene group also allows for investigations of the effects of CB[7] inclusion on *trans-cis* photoisomerization processes.

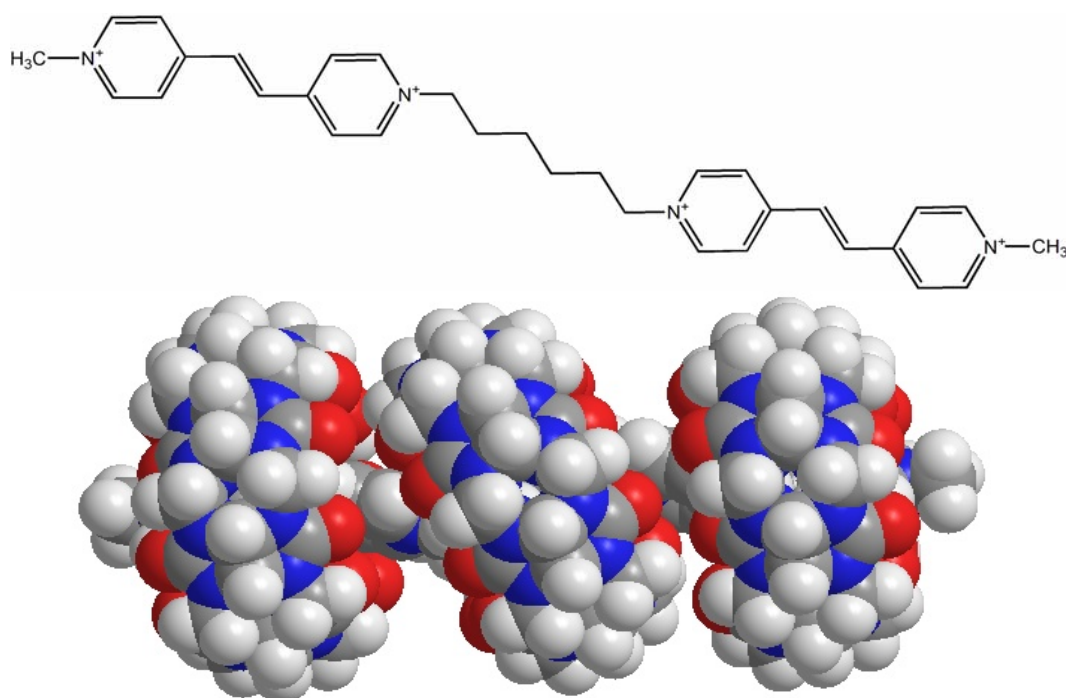
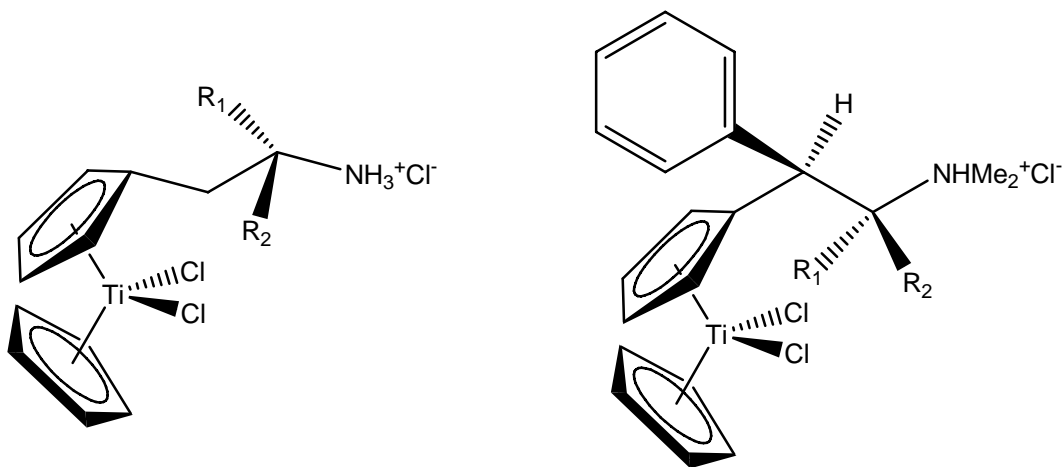


Figure 6.1 Structures of the $\text{CH}_3\text{bpe}(\text{CH}_2)_6\text{bpeCH}_3^{4+}$ tetracation (top) and the proposed $\{\text{CH}_3\text{bpe}(\text{CH}_2)_6\text{bpeCH}_3 \cdot 3\text{CB}[7]\}^{4+}$ complex (bottom).

The investigation of complexation of CB hosts with titanocene will be extended to a more comprehensive study for more anti-tumour drugs, such as those whose structures are shown below (Figure 6.2),^{5,6} and other bent metallocenes, such as analogous diaquamolybdocenes.



S: $R_1 = \text{H}; R_2 = \text{CH}_3$
R: $R_2 = \text{CH}_3; R_1 = \text{H}$

Figure 6.2 Two examples of chiral substituted titanocene dichloride complexes.

Preliminary results indicate that the diaquamolybdocene exhibits a high affinity towards CB[8] ($K_{\text{CB}[8]}$ is estimated to be about 10^{10} M^{-1} by a ^1H NMR competition method). The molybdocene is more susceptible to dimerization and loss of the Cp rings,⁷ and has been observed to catalyze the oxidation of cucurbit[n]urils in aerobic solutions.⁸ More detailed research about the stabilization of the coordinated Cp rings from protonolysis and dissociation, upon the inclusion in CB[n] cavities, will need to be conducted.

References

1. Yuan, L.; Wang, R.; Macartney, D.H. *J. Org. Chem.* **2007**, *72*, 4539.
2. Yuan, L.; Wang, R.; Macartney, D.H. *Tetrahedron: Asymmetry* **2007**, *18*, 483.
3. Yuan, L.; Macartney, D.H. *J. Phys. Chem. B* **2007**, *111*, 6949.
4. Yuan, L.; Macartney, D.H. *J. Chem. Soc., Dalton Trans.*, to be submitted for publication.
5. Potter, G. D.; Baird, M. C.; Cole, S. P. C. *J. Organometal. Chem.* **2007**, *692*, 3508.
6. Potter, G. D.; Baird, M. C.; Chan, M.; Cole, S. P. C. *Inorg. Chem. Commun.* **2006**, *9*, 1114.
7. Balzarek, C.; Weakley, T. J. R.; Kuo, L. Y.; Tyler, D. R. *Organometallics*, **2000**, *19*, 2927.
8. A. I. Day, private communication to D. H. Macartney, August 2007.